JOAQUIN - JOINT AIR QUALITY INITIATIVE

Work Package 1 Action 1 and 3

Monitoring of ultrafine particles and black carbon

FINAL REPORT

November 2015

Investing in Opportunities

This project has received European Regional Development Funding through INTERREG IV B.

INTERREG IVB

To be cited as:

Joaquin (2015). Monitoring of ultrafine particles and black carbon. Joint Air Quality Initiative, Work Package 1 Action 1 and 3. Flanders Environment Agency, Aalst. Available at http://www.joaquin.eu.

Jeroen Staelens[a], Jelle Hofman[a], Gerard Kos[b], Ernie Weijers[b], Sarkawt Hama[c], Harald Helmink[d], Tiphaine Delaunay[e], Kirsty Smallbone[f], Christine Matheeussen[a], Rebecca Cordell[c], Kevin P. Wyche[f], Marieke Dijkema[d], Paul S. Monks[c], Edward Roekens[a]

[a] Flanders Environment Agency (VMM), Department Air, Environment and Communication, Belgium
[b] Energy research Centre of the Netherlands (ECN), Department of Air Quality, the Netherlands
[c] University of Leicester, Department of Chemistry, United Kingdom
[d] atmo Nord-Pas-de-Calais, France
[e] Public Health Service of Amsterdam, Department of Air Quality, the Netherlands
[f] University of Brighton, School of Environment and Technology, Brighton

Summary

This report describes 2-year long measurements of ultrafine particles (UFP) and black carbon (BC) at four monitoring stations and a mobile trailer in the North-West European region. The study was carried out as part of the Joint Air Quality Initiative (Joaquin project, Work Package 1 Action 1 and 3).

Background
Epidemiological studies attribute the most important health impacts of air pollution to particulate matter (PM), although it is still unclear which specific particle properties (such as size and chemical composition) or sources are most relevant to health effects. Current air quality legislation on PM is focused on the mass concentration of airborne particles (expressed in µg/m^3). However, there are indications that other metrics are also relevant to human health. There is for example considerable interest in particles with an aerodynamic diameter smaller than 0.1 µm (ultrafine particles, UFP). Ultrafine particles contribute little to the PM mass concentration in ambient air, but have high number concentrations (expressed in particles/cm^3). The negative health impacts of UFP have been shown by toxicological studies, but epidemiological evidence is still scarce due to the limited number of UFP monitoring sites and long-term studies. As UFP measurements are not included in policy-oriented air quality monitoring programmes, one of the aims of the Joaquin project was to set up a long-term UFP monitoring network in different cities in NW Europe.

Aims
The main objectives were:

- To evaluate the feasibility of long-term UFP measurements in air quality monitoring networks.
- To gain a better understanding of the spatiotemporal variation in UFP number concentration and size distribution in urban environments.
- To assess the added value of UFP data compared to more commonly measured parameters such as BC and nitrogen oxides (NO_x).

To do so, it was important to assess the comparative usefulness and reliability of different instruments, to harmonize the instrumental operation within the network, to assure the quality and comparability of the data gathered, to investigate the temporal and intra-urban spatial variation of UFP and to investigate the relationships between UFP, traffic and other traffic-related air pollutants.

Methods
From April 2013 to March 2015, UFP were continuously measured at an urban background site in four cities in NW-Europe (Amsterdam, Antwerp, Leicester and London). Results are available for 1-2 years, depending on the site. At all sites the total particle number concentration (TNC) was measured with a water-based condensation particle counter (TSI 3783, particles in the range of 7-1000 nm) and BC with a MAAP (Thermo 5012). Information on the particle size distribution was obtained by a scanning mobility particle sizer (SMPS, Grimm 5420/L-DMA, 10-1000 nm) in Amsterdam and Antwerp and by a differential mobility analyser with corona discharger and electrometer (TSI 3031, 20-200 nm) in Leicester and London. Instrument comparability was assessed by an initial measurement campaign at one site and follow-up comparisons at each of the four sites using a mobile trailer equipped with the same instruments as the monitoring stations. The trailer was also used for short-term campaigns (2-4 weeks) at a second urban background site in Amsterdam, Antwerp and Leicester.

Results
Over the span of the reported period, data coverage of the UFP instruments was reasonable (81-84% at the 30-min level) but below that of more commonly used NO_x and PM monitoring equipment. The comparability of the instruments was good for each type of instrument, but TNC was underestimated by the size-resolved devices (SMPS, TSI 3031) compared with the particle counters.

Results showed a traffic-related diurnal variation of UFP, BC and NO_2 with distinct morning and evening peaks on weekdays, coinciding with traffic rush hours. In the weekends only an evening peak could be observed. For all monitoring sites, the highest monthly-averaged concentrations were found in the cold season (September to March), likely due to meteorological conditions. The site in Antwerp showed the highest UFP, BC and NO_2 concentrations, which can be explained by its proximity (30 m) to a traffic-intensive road.

At all sites BC and NO_2 were correlated with the TNC and size-specific particle number concentration (PNC), but the relationships depended on the site and season, likely reflecting differences in local site and traffic characteristics and meteorological effects. The relationships between UFP and BC/NO_x confirm that vehicle engines are an important source of UFP in urban environments. Nevertheless, the relationship was weakest during summer, which may be due to non-traffic-emitted UFP, for example originating from new particle formation. For the monitoring site in Amsterdam, relations between the typical traffic-related pollutants and UFP were weaker. Therefore, road traffic may not be the dominant source of UFP at this site, for example due to the presence of a low emission zone in Amsterdam and/or other sources that contribute significantly to the measured UFP concentrations. The relative UFP size distribution was quite similar for all sites, with the highest particle numbers in the 30-50 nm size class. The 10-20 nm particle size class (only measured in Antwerp and Amsterdam) showed a higher relative contribution in Amsterdam and persisted through the day and during the weekend, suggesting a non-traffic related UFP source for this site.

The spatial variation in TNC between the sites was evaluated using coefficients of divergence (COD) and Spearman rank correlation coefficients. This suggested that TNC is not covarying well at the regional level and that much of the variation in UFP is due to local factors. An increased association (smaller COD and larger correlation) was obtained for increasing particle sizes. Therefore larger particles tend to be more uniform, which may indicate the regional nature of these aerosols. The spatial variation within a city was investigated by simultaneous mobile trailer measurements at a second site in Amsterdam, Antwerp and Leicester and by two intra-urban campaigns in Antwerp. The UFP concentrations within a city generally covaried over time, although meaningful intra-urban differences between the sites were observed, depending on the considered particle size class. This can be explained by an overall urban contribution mostly originating from traffic emissions that follow a similar behaviour in time but differ in quantity, depending on the distance to and intensity of these emissions source. In addition, specific local sources may affect a single site. On average, the largest variation in TNC between the monitoring station and the trailer site was observed in Antwerp (38%), followed by Amsterdam (24%) and Leicester (20%). While the spatial variation in particle mass concentration is relatively low over an urban region, this is not the case for particle numbers.

Polar plots of the PNC as a function of wind direction and wind speed indicated site-dependent UFP sources. For Antwerp the highest UFP concentrations were obtained for low wind speeds coming from the south, pointing at the main road near the site. For Amsterdam, a clear increase in TNC due to increases in the PNC of 10-20 and 20-30 nm particles was observed during strong SW winds. In combination with the high and continuous 10-20 nm contribution through the day and the weekends and the weaker relationships between UFP and BC/NO_x, this suggests an influence of Schiphol airport on UFP measured at a distance of 8 km in Amsterdam. For the site in Leicester, the polar plots and diurnal patterns indicate that the main road is contributing significantly to the local UFP concentrations. For the site in London, the PNC seemed rather independent from the wind direction.

Conclusions

While UFP sizing instruments represent feasible additions to air quality monitoring networks, to obtain the best data coverage more maintenance and expertise may be required than for traditional monitors. Care should be taken to minimize particle losses due to air sampling. An SMPS provides the most comprehensive data coverage over the largest range of particle sizes. The TSI 3031 monitor appears to provide reliable data mostly in the mid (30-200 nm) size range. Total particle counters can offer a cheaper, simpler yet still reliable solution if particle size fractionation is not required. Size-resolved measurements, however, offer more information on the type, origin and transformation processes of atmospheric aerosols.

The obtained time series provide important insights into the spatiotemporal variation of total and size-resolved UFP in urban environments. The degree of correlation between UFP and other traffic-related pollutants shows that traffic is a significant, but not exclusive, UFP source at all the sites investigated. Due to the short atmospheric lifetime of UFP and their strong dependence on local sources, total and size-specific PNC can vary meaningfully on short spatial and temporal scales. Therefore, UFP monitoring at a single site may not be indicative of the actual exposure in the communities surrounding the site. This pleads for thoughtful consideration when selecting urban background stations for UFP measurements in heterogeneous urban environments. To more accurately estimate human exposure and subsequent health impacts of UFP, measurements and/or modelling on finer spatial scales is valuable.

Table of contents

List of abbreviations and terminology

#/cm^3	Number of particles per cubic centimeter of air. Unit of measure that indicates the number concentration of particles in the air
µg/m^3	Microgram (millionth of a gram) per cubic meter of air. Unit of measure that indicates the mass concentration of a pollutant in the air
AD1	Air quality monitoring site 'Vondelpark' (Amsterdam, the Netherlands)
AD2	Air quality monitoring site 'Nieuwendammerdijk' (Amsterdam, the Netherlands)
AP1	Air quality monitoring site 'Borgerhout' (Antwerp, Belgium)
AP2	Air quality monitoring site 'Stadspark' (Antwerp, Belgium)
BC	Black carbon, a component of PM. It is formed through the incomplete combustion of fossil fuels, biofuel and biomass. It is an indicator of soot. Black carbon is determined by an optical method
COPD	Chronic obstructive pulmonary disease
EC	Elemental carbon. Elemental carbon is determined by a thermo-optical method
ECN	Energy research Centre of the Netherlands
EPC	Environmental particle counter; TSI model 3783
ESG	Environmental Scientifics Group
GGD	Municipal Health Service (*Geneeskundige en Gezondheidsdienst*)
INERIS	*Institut National de l'Environnement industriel et des RISques*
ISSeP	*Institut scientifique de service public*
Joaquin	Joint Air Quality Initiative, an EU cooperation project supported by INTERREG IVB NWE
LDSA	Lung-deposited surface area concentration of particles (µm^2/cm^3)
LE1	Air quality monitoring site 'Leicester University' (Leicester, United Kingdom)
LE2	Air quality monitoring site 'Brookfield' (Leicester, United Kingdom)
LL1	Air quality monitoring site 'Lille-Fives' (Lille, France)
LO1	Air quality monitoring site 'Eltham' (London, United Kingdom)
MAAP	Multiangle absorption photometer (MAAP Thermo Scientific model 5012)
NO	Nitrogen oxide
NO_2	Nitrogen dioxide
NO_x	Nitrogen oxides
NSAM	Nanoparticle surface area monitor; TSI model 3550
O_3	Ozone
O_3	Ozone
OC	Organic carbon
P	Air pressure
PM	Particulate matter
PM_{10}	Particles smaller than 10 µm. PM_{10} are the particles that pass a size-selective inlet with an efficiency limit of 50% for an aerodynamic diameter of 10 µm
$PM_{2.5}$	Particles smaller than 2.5 µm. $PM_{2.5}$ are the particles that pass a size-selective inlet with an efficiency limit of 50% for an aerodynamic diameter of 2.5 µm
PNC	(Size-specific) Particle number concentration (#/cm^3)
Polar plot	A polar plot shows the mean concentration of a pollutant as a function of wind direction and wind speed
RH	Relative humidity (in %)
ROS	Reactive oxygen species
SMPS	Scanning mobility particle sizer spectrometer. In this report SMPS is used to indicate instrument Grimm SMPS+C 5420 with L-DMA;
SOP	Standard operating procedure
SO_x	
T	Ambient air temperature
TNC	Total number concentration of particles (#/cm^3)
UFP	Ultrafine particles, or particles smaller than 100 nm (= 0.1 µm)
UFPM	Ultrafine particle monitor; TSI model 3031
VITO	Flemish Institute for Technological Research
VMM	Flanders Environment Agency (*Vlaamse Milieumaatschappij*)
VOC	Volatile organic compound
WD	Wind direction

WS	Wind speed
WZ1	Air quality monitoring site 'Wijk aan Zee' (Wijk aan Zee, the Netherlands)
$\mu m^2/cm^3$	Surface area of particles in square micrometer per cubic centimeter of air. Unit of measure that indicates the surface area concentration of particles in the air

1 Introduction

This report describes 2-year long air quality measurements at several monitoring stations and a mobile station (trailer) in NW Europe, focusing on ultrafine particles (UFP) and black carbon (BC). The study was carried out as part of the Joint Air Quality Initiative (Joaquin), Work Package 1 Action 1 and 3.

1.1 Joint Air Quality Initiative

Joaquin (Joint Air Quality Initiative) is an EU cooperation project supported by the INTERREG IVB Northwest-Europe programme (www.nweurope.eu). The aim of the project is to support health-oriented air quality policies in Europe. To achieve this, the project provides policy makers with the necessary evidence on the current local and/or regional situation by measuring emerging health-relevant parameters, provides them with best-practice measures that can be taken and motivates them to adapt and strengthen their current air quality policies.

The project partnership and their observers cooperate on 3 different topics:

1. **Work package 1: Capacity building**
The project wants to translate the science of new and emerging health-relevant pollutants in to practice, to obtain data and information on the current local and/or regional situations and to improve the collective understanding of air pollution and its impact on citizens' health. This will result in health-relevant information that is crucial to increase the capacity of air quality experts, authorities and public health professionals in order to facilitate and provide the motivation for better air quality policies.

2. **Work package 2: Measures**
The project also wants to help decision makers to find specific solutions within this adapted framework by identifying, piloting and evaluating the most efficient and cost-effective measures to reduce exposure to health-relevant pollutants. This will lead to a ranking of measures which will enable decision makers at various levels to adapt their current policies and/or action plans.

3. **Work package 3: Dissemination and communication**
Finally, the project will further develop the support base for policy changes by involving an extended stakeholder consultation process during the lifetime of the project and by raising the awareness of the general public on the health effects of air pollution. This will result in an improved relationship between the involved policy levels, stakeholder groups and the general public on the necessity of health-relevant policies and clean air in day-to-day life.

1.2 Work package 1: Capacity building

The overall aim of Joaquin work package 1 is novel knowledge gathering of emerging health-pertinent pollutants for the future protection of human health and sustainable development.

Current EU air quality legislation is centred on monitoring, limiting & reducing mass concentrations of airborne particles. However, recent toxicological and epidemiological research argues that other particle metrics may constitute better links to health endpoints than mass concentration. For instance, the potential of inhaled ultrafine particles (UFPs), which are able to penetrate deeply into the respiratory system and cause inflammation, is believed to be significant in causing illness. So far, information on the number, size and distribution of such emerging pollutants in Europe is limited and air quality experts and health professionals are unable to identify UFP pollution sources, adapt their current policies and re-define appropriate mitigation measures to protect citizens' health. Before action can be taken to mitigate against those pollutants that have the greatest impact on public health, we must first understand the nature of the problem.

This work package aims to enhance our understanding of novel, health-relevant air pollution and its sources within the Northwest-Europe hotspot zone, with specific focus on emerging health-relevant pollutants. We aim to acquire data and information on the current local/regional situations, which we will use to improve our knowledge of more air pollutants and their impacts on citizens.

Work package 1 consists of 4 actions:

1. Setup and operation of a transnational next-generation "**Watchdog network**" for health-relevant pollution parameters.
2. Health-relevant **source characterization of particulate matter**: identifying air pollution sources and composition of particulate matter (PM_{10}) and elucidating the links between pollution and human health.
3. **Mobile pollution monitoring** to validate, expansion and publicising of the NWE Watchdog Network Infrastructure
4. Creation of the North West European **air pollution observatory** and information centre

Together, these actions will result in the acquisition and dissemination of health-relevant information and tools necessary for air quality experts (authorities/public health professionals) for development and implementation of future policies and pollution reduction measures.

In this report we focus on the continuous air quality measurements of action 1 and 3. The filter-based PM_{10} measurements of action 2 and 3 are described elsewhere (Joaquin 2015).

1.3 Description of WP1A1 - continuous air quality monitoring

Action 1 of work package 1 (WP1A1) is entitled 'Setup and operation of a next-generation "Watchdog network" for health-relevant pollution parameters'. It focuses on the development and implementation of novel air quality monitoring infrastructure for pollutants associated with the most dangerous aspects of air pollution on human health. In four cities in NWE Europe, cutting edge instrumentation is used to measure airborne concentrations of black carbon (BC) and the number concentration and size distribution of UFP. The monitors will be located at sites where statutory air quality parameters are measured such as nitrogen oxide (NO_x) concentrations and the mass concentration of particulate matter (PM).

1.3.1 Context

Current EU air quality legislation is centred on monitoring, limiting and reducing mass concentrations of airborne particles. However, there is increasing evidence that other particle metrics constitute better links to some health outcomes (e.g. chronic obstructive pulmonary disease (COPD), heart disease, etc.) than mass concentration.

Recent toxicological and epidemiological research argues that more emphasis should be placed on particle characteristics such as the composition (e.g. elemental/black/organic carbon) and number concentration, particularly for UFP, which are able to penetrate deeply in to the human respiratory system and are believed to be responsible for causing numerous negative health effects. Also, the inflammatory potency of inhaled particles is now known to be a highly important health-relevant measurement. However, despite its clear importance, information on these emerging indicators is very scarce in the NWE region.

1.3.2 Aims

With this action a new monitoring infrastructure will be established that aims to implement a common measurement standard and a comprehensive comparison of these alternative indicators between the involved Member States. This includes an assessment of the correlation of UFP indicators to particle mass concentration measurements that are made as standard.

The infrastructure will constitute a health-focused air quality monitoring network in the NWE region, providing truly health-relevant information, which will be crucial for improving our understanding of pollution exposure and sources and for protecting citizens' health and NWE's economy. This knowledge could provide a scientific foundation for future studies in the area of human epidemiology and could be used as a basis for setting future emission and air quality standards based on particle number.

1.3.3 Subactions

To achieve this goal, a new monitoring infrastructure is constructed (part of a NWE air quality observatory and complementary to the existing EU network), comprising four monitoring stations in Antwerp, Amsterdam, Leicester and London. With this infrastructure continuous measurements of UFP number and size distribution and of black carbon concentrations are made.

As a first step, the instrumental approaches used for UFP monitoring were assessed. From literature review and a laboratory test, an evaluation was made of commercially available UFP devices in order to choose the appropriate instrumentation and methodology to measure particle number concentration and size distribution under routine measuring network conditions.

Based on the evaluation, the three following monitors were selected for UFP monitoring:

- Grimm SMPS 5420 with L-DMA
- TSI UFP monitor 3031
- TSI EPC 3783

In addition, the MAAP (Thermo model) 5012 has been purchased in order to measure the concentration of BC. The above instruments were installed at all the Joaquin UFP monitoring sites.

We made and used standard operating procedures (SOP) for the chosen instrumentation to avoid different monitoring circumstances at different locations (monitoring artefacts, e.g. inlet systems, maintenance frequency etc.). Furthermore, all instruments were compared before applying them for monitoring. As part of the evaluation of alternative exposure metrics that reflect particle toxicity, information on surface area concentration will be considered as one of the health-relevant parameters that contribute towards developing understanding of particle characteristics. The use of direct-reading instruments for surface area concentration was evaluated against alternative methods to estimate surface area concentration based on size selective particle number measurements.

1.4 Description of WP1A3 - mobile pollution monitoring

Action 3 of work package 1 (WP1A3) is entitled: “Validation and expansion of the NWE “Watchdog Network” for health-pertinent pollution parameters with mobile monitoring”. A mobile station (ECN trailer, Figure 1.1) has been equipped with identical instruments and acted as a (fifth) reference site in each of the four cities participating in the UFP measurements of the Joaquin project (Antwerp, Amsterdam, Leicester, London). In this Joaquin monitoring network, cutting edge instrumentation is applied to measure airborne concentrations of BC and the number concentration and size distribution of UFP. Dedicated monitoring campaigns were carried at the fixed sites (WP1A1) out to ensure the quality and comparability of the experimental data gathered in the network.

Figure 1.1: Trailer of ECN used for mobile air quality monitoring and public awareness raising.

Furthermore this action aimed to increase the coverage of the network. As such, the trailer has been located at a second urban background site in 3 of the 4 UFP monitoring cities (Amsterdam, Antwerp and Leicester). Finally the action also contributed to help raising public awareness. The trailer has been liveried with Joaquin corporate colors and devices in order to raise awareness of the project and the air quality problem (link to WP3A10). This took place during several public events in each of the Joaquin cities, synchronized with the mobile monitoring campaigns.

1.4.1 Context

There is increasing evidence that other particle metrics (like BC and UFP) constitute better links to some adverse health effects. The shift towards better, more health relevant, air quality policies and mitigation strategies will only occur if there is enough credible evidence to drive the changes. Part of this evidence will be provided within the Joaquin project and will be derived from the "Watchdog network" (WP1A1). To assure the quality and comparativeness of the data collected in this network, a harmonized operation (and data acquisition) is imperative. In addition, there is a need to understand the geographical coverage offered by the spatially constrained fixed network sites and to provide access to other locations.

1.4.2 Aims

1. To assure the quality and comparability of the data gathered in the Joaquin monitoring infrastructure "Watchdog network" (link to WP1A1).
2. To harmonize the instrumental operation within the network (link to WP1A1, WP1A2 and WP1A4).
3. To equip a mobile trailer identically to the fixed monitoring infrastructure for the purpose of data validation and support of the Network.
4. To produce technical documents containing standard operational protocols (SOP) for each of the instrumental device in the Network to ensure similar handling by operators.
5. To enable an additional monitoring site to complement the fixed network (link to WP1A1) in order to determine the spatial representativeness of each Joaquin site.
6. To enable a reference station to carry out source apportionment for each fixed site (link to WP1A2).
7. To write an expert opinion on the measurement of UFPs in routine monitoring networks.

1.4.3 Subactions

1. Assessing the various instrumental approaches used for UFP monitoring. To this purpose commercially available UFP devices are compared in the ECN laboratory on performance, accuracy, stability and operation. This is part of the evaluation process preceding the purchase of the appropriate instrumentation and design of methodology to measure particle number concentration and size distribution under routine measuring conditions.
2. Furnishing a mobile trailer with identical instruments as those used in the fixed infrastructure. With the trailer UFP number and size distribution and BC will be measured in real-time during dedicated campaigns at each of the four Joaquin UFP monitoring stations.
3. Writing standard operating procedures (SOP) for the chosen instrumentation.
4. Checking the performance of instruments at the Joaquin experimental sites to detect artefacts due to e.g. inlet systems, maintenance, operational handling, differences in flows etc. If any serious deviation is detected further action will be undertaken to determine the reason why and corrections are made.
5. Using the experimental data to carry out a comparison study for the UFP and BC measuring devices.
6. Comparing each of the monitoring sites with the second relevant location, usually a less traffic exposed urban background site, to study the spatial representativity of the statutory site.
7. Supplying the data gathered in the mobile monitoring campaigns to WP1A4 for inclusion in the observatory data base and for advanced data analysis.
8. Advice on how to monitor UFP in a multiple site network and possible harmonization.

2 Materials and methods

2.1 Overview of sampling sites and periods

2.1.1 Sites

In the Joaquin project, air quality was measured in six cities in NW Europe (Figure 2.1):

- Amsterdam and Wijk aan Zee (The Netherlands);
- Antwerp (Belgium);
- Leicester and London (United Kingdom);
- Lille (France).

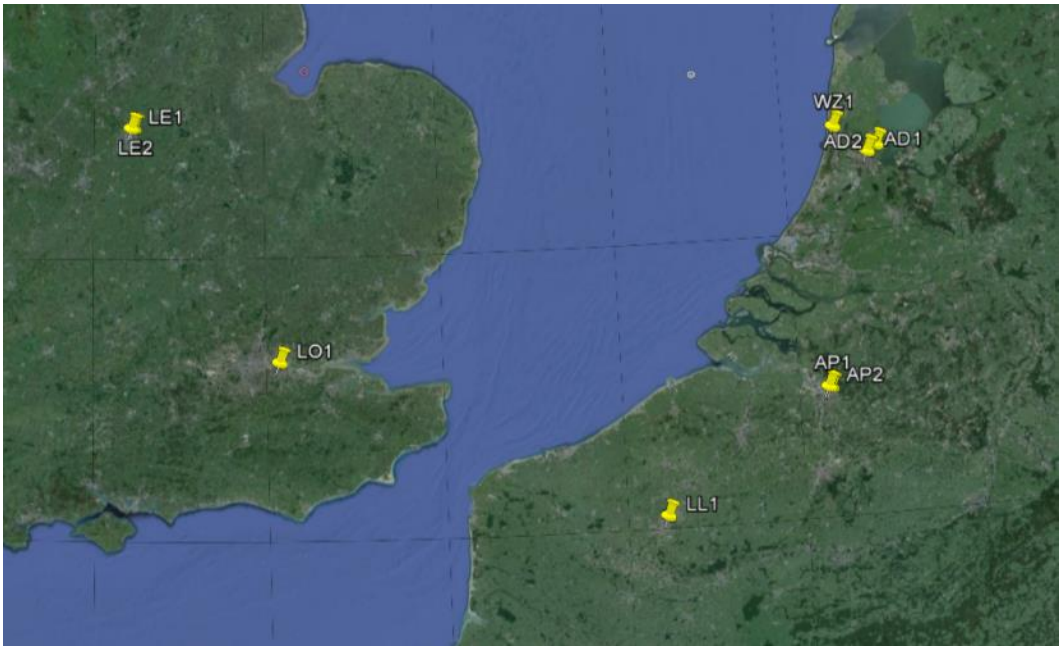

Figure 2.1: Overview of Joaquin sampling sites in NW Europe.

Table 2.1 gives an overview of the sampling sites. In each city continuous air quality measurements were carried out in a long-term air quality monitoring station. In Amsterdam, Antwerp and Leicester there were additional measurements at a second site. This resulted in a total of nine Joaquin sampling sites.

Table 2.1: Overview of Joaquin sampling sites.

City	Site code	Site name	Street	Coordinates	
				Latitude	Longitude
Amsterdam	AD1	Vondelpark	Overtoom	52°21’35" N	4°51'59" E
	AD2	Nieuwendammerdijk	Nieuwendammerdijk	52°23'21" N	4°56'38" E
Antwerp	AP1	Borgerhout	Plantin en Moretuslei	51°12’35” N	4°25’55” E
	AP2	Stadspark	Rubenslei	51'12'48" N	4°24'51" E
Leicester	LE1	Leicester University	Welford and University Road	52°37'12" N	1°07'38" W
	LE2	Brookfiled	London Road	52°37'15" N	1°06'32" W
Lille	LL1	Lille-Fives	rue du Vieux Moulin	50°37'41" N	3°05'25" E
London	LO1	Eltham	Bexley Road	51°27'09" N	0°04'14" E
Wijk aan Zee	WZ1	Wijk aan Zee	Burgemeester Rothestraat	52°49'40" N	4°60’23“ E

For the sampling sites, the two letters abbreviate the city, e.g. "AD" for Amsterdam. This is followed by a number indicating the site (1 = permanent UFP site, 2 = extra site).

Results from the permanent air quality stations are referred to by "S", e.g. "AD1S" indicate results from the instruments installed in Vondelpark station in Amsterdam. Results from instruments in the trailer are referred to by suffix "T", e.g. "AD1T" indicates data from the instruments in the trailer when it was next to the permanent Vondelpark station.

In the city of Antwerp, air quality measurements were additionally carried out at six extra sites:

- one site for the initial comparison of the UFP instruments;
- three sites to study the intra-urban variation of UFP;
- two sites to study the gradient of UFP near the road.

These UFP campaigns in Antwerp have already been reported elsewhere, and we refer to the reports by VITO and VMM for more details on the sites, methods and results. This report only summarizes the main conclusions of these studies.

2.1.2 Periods

Measurements of UFP (particle number concentration and size distribution), BC and NO_x were carried out in Amsterdam, Antwerp, Leicester and London. Data collection started in April 2013 (Amsterdam, Antwerp), November 2013 (Leicester) and April 2014 (London). This report discusses results up to March 2015, hence covering a period of 1 to 2 years depending on the site.

The composition of PM_{10} was determined in Amsterdam, Antwerp, Leicester, Lille and Wijk aan Zee. Filter sampling of PM_{10} was carried out from April 2013 to May 2014 (14 months), except for Lille where data collection started in June 2013 (12 months).

Table 2.2: Overview of measurement periods of (ultra)fine particles and/or PM_{10} composition per city.

City	Ultrafine particles	PM_{10} composition	Arrival of trailer (no. of weeks)	
	Site 1	Site 1	Site 1	Site 2
Amsterdam	Apr 2013 - Mar 2015	Apr 2013 - May 2014	Apr 2013 (7)	May 2013 (2)
Antwerp	Apr 2013 - Mar 2015	Apr 2013 - May 2014	Sep 2013 (4)	Oct 2013 (4)
Leicester	*Nov 2013* - Mar 2015	Apr 2013 - May 2014	Mar 2014 (5)	Apr 2014 (6)
Lille	-	*Jun 2013* - May 2014	-	-
London	*Apr 2014* - Mar 2015	-	Jun 2014 (4)	-
Wijk aan Zee	-	Apr 2013 - May 2014	-	-

Note: dates in *italic* indicate a deviating start of the measurements.

To check the stability and comparability of the air quality monitors, a mobile trailer of ECN was equipped to sample UFP, BC and PM_{10} visited each of the permanent air quality monitoring stations. The UFP and BC monitors and PM_{10} sampler were identical as for the permanent Joaquin stations.

The main aim was to check the stability and comparability of the air quality monitors as well as a surveillance of the handling of instruments at the Joaquin sites. The trailer measurements were carried out during 4-7 weeks adjacent to the permanent stations in Amsterdam, Antwerp, Leicester and London (site codes AD1, AP1, LE1 and LO1).

Furthermore, to extend spatial coverage, trailer measurements were carried out during 2-6 weeks at a second urban background site in Amsterdam, Antwerp and Leicester (sites AD2, AP2 and LE2).

This report deals with the continuous air quality measurements, focussing on UFP and BC. The filter-based PM_{10} mass and composition is discussed elsewhere (Joaquin 2015).

2.1.3 Air quality monitors

Table 2.3 summarizes the availability of monitors for UFP, BC, NOx and PM_{10} per site. Measurements at sites AD2, AP2 and LE2 were carried out with the devices in the trailer.

Table 2.3: Overview of instrument types per sampling site (variable measured).

Site code	EPC (NC)	UFPM (NC, Distr.)	NSAM (Surface)	SMPS (NC, Distr.)	MAAP (BC)	NO_x (NO, NO_2)	PM_{10} (Mass)	PM_{10} (Comp.)
AD1	x			x	x	x	x	x
AP1	x			x	x	x	x	x
LE1	x	x	x		x	x	x	x
LL1						x	x	x
LO1	x	x			x	x	x	
WZ1						x	x	x
Trailer at AD1, AD2, AP1, AP2, LE1, LE2, LO1	x	x		x	x		x	x
Total	5	3	1	3	5	6	7	6

Note: At LE1, LO1 and in the trailer the EPC and UFPM were connected to one sampling system. NC = particle number concentration, Distr. = particle size distribution, BC = black carbon; Comp. = composition.

2.2 Site description

This section shortly describes the Joaquin air quality sampling sites, focussing on the immediate vicinity of the sites. Annex 1 gives a more detailed description, including maps of the site locations and information on potential (regional) air pollution sources.

Table 2.4 summarizes the distance to the main street and the traffic intensity per sampling site. No traffic data are available for LL1 and WZ1.

Table 2.4: Distance to main street and traffic intensity per sampling site.

City	Site code	Site name	Distance to main street (m)	Traffic intensity[a] (vehicles/day)
Amsterdam	AD1	Vondelpark	64	17000
	AD2	Nieuwendammerdijk	20	<300
Antwerp	AP1	Borgerhout	30	29500
	AP2	Stadspark	45	7800
Leicester	LE1	Leicester University	140	22500
	LE2	Brookfiled	150	20500
Lille	LL1	Lille-Fives	35	n.a.
London	LO1	Eltham	60	16500
Wijk aan Zee	WZ1	Wijk aan Zee	70	n.a.

[a] Mean traffic intensity at the nearest main street: time period and reference see site descriptions.

2.2.1 Amsterdam (the Netherlands)

2.2.1.1 Vondelpark (AD1)

The Joaquin sampling site in Amsterdam is an urban background station of the air quality monitoring network of GGD Amsterdam (Figure 2.2). The station is located at the northern edge of the public park 'Vondelpark.

At a distance of 64 m to the north there is a main road (Overtoom) with a mean traffic intensity of about 17000 vehicles/day (http://www.verkeersprognoses.amsterdam.nl for 2015). The Overtoom road has two lanes, one in each direction plus two bus/tram lanes in the centre of the road and has relatively high buildings on both sides ('street canyon'). Between the site and the Overtoom there is a six-storey building. A small passage connects the Overtoom with the site. The measuring station is located in the courtyard of a revalidation centre. The site is close to tennis courts and a public park (in the south). The gravel tennis court can be a source of coarse dust particles. In the Vondelpark, barbecue activities are allowed at specific locations, except during dry periods.

Figure 2.2: Detail of the location of site AD1 (Amsterdam Vondelpark).

2.2.1.2 Nieuwendammerdijk (AD2)

The temporary Joaquin site AD2 is an urban background station of the air quality monitoring network of GGD Amsterdam (Figure 2.3). The station is located at Nieuwendammerdijk, at a distance of about 6.2 km from site AD1.

The nearest road (Nieuwendammerdijk) is at a distance of 20 m and is only used by local residents. The traffic intensity will be less than 300 vehicles per day (http://www.verkeersprognoses.amsterdam.nl for 2015). Site AD2 is a typical background location surrounded by grass fields without any specific sources nearby. Further to the south is a water connection to the North Sea used by inland shipping vessels and sea vessels for bulk transportation.

Figure 2.3: Detail of the location of site AD2 (Amsterdam Nieuwendammerdijk).

2.2.2 Antwerp (Belgium)

2.2.2.1 Borgerhout (AP1)

The Joaquin sampling site in Antwerp is an urban background station that is part of the VMM air quality monitoring network. The station is located in Borgerhout. It is located 30 m from a major access road (Figure 2.4). The road is east-west orientated and has four lanes (two in each direction). There is a bus stop in front of the entrance to AP1. In February and October 2013, the mean traffic intensity

was 32000 vehicles on week days and 23500 vehicles in the weekend, or a time-weighted average of 29500 vehicles/day (VMM 2014).

Figure 2.4: Detail of the location of site AP1 (Antwerp Borgerhout).

2.2.2.2 Stadspark (AP2)

Site AP2 is a temporary sampling location in a public park with mainly deciduous trees (Figure 2.5). Site AP2 is located at a distance of 1.3 km to the northwest from site AP1.The closest road to site AP2, at distance of 45 m, is the Rubenslei with 2x1 lanes. In February and October 2013, the mean traffic intensity at the Rubenslei was 8500 vehicles on week days and 6000 vehicles in the weekend or a time-weighted average of 7800 vehicles/day.

Parallel to the Rubenslei there is a busier road (Frankrijklei). This road has 2x3 lanes plus 2 central bus and tram lines. Traffic intensity data are not available for this road. Site AP2 is located further away from the main ring road around Antwerp than AP1, but it is closer to the River Scheldt (1.5 km in western direction).

Figure 2.5: Detail of the location of site AP2 (Antwerp Stadspark).

2.2.2.3 Six extra sites in Antwerp

Next to AP1 (Borgerhout) and AP2 (Stadspark), within the Joaquin project the UFP number concentration and size distribution have been measured at six extra sites in Antwerp. An initial instrument comparison was carried out at an urban background site in Wilrijk (Vuurkruisenplein) in December 2012 and January 2013. The site is described by Frijns et al. (2013a).

In February 2013, UFP measurements were carried out seven sites in Antwerp: the sites AP1 and AP2 described above, two sites near site AP1, a suburban site (Frederik Van Eedenplein), an urban street

canyon site (Turnhoutsebaan) and a ring road site (Noordersingel). In October 2013, measurements occurred at four sites in Antwerp: AP1, AP2, the suburban site and the ring road site. These sites are described by VMM (2014).

2.2.3 Leicester (United Kingdom)

2.2.3.1 Leicester University (LE1)

The Joaquin sampling site in Leicester is an urban background station of the AURN network. The station is located near Welford Road (Figure 2.6) on the campus of the University of Leicester. The nearest road is the University Road (20 m NW). The nearest main road is Welford Road (140 m S-SW) with 2x1 lanes. According to traffic counts by the Department for Transport, the traffic intensity on the Wellington Road was about 22500 vehicles/day in 2013.

Figure 2.6: Detail of the location of site LE1 (Leicester University).

2.2.3.2 Brookfield (LE2)

The temporary Joaquin site LE2 in Leicester is an urban background site in Brookfield, at a distance of about 1.2 km east from LE1. The trailer was located on a large and frequently-used parking lot (Figure 2.7. The nearest roads are Ashfield Road (90 m in the north) and Holmfield Road (90 m south). The nearest main road is London Road, at 190 m west of LE2. According to traffic counts by the Department for Transport, the traffic intensity on London Road was about 20500 vehicles/day in 2013.

Figure 2.7: Detail of the location of site LE2 (Leicester Brookfield).

2.2.4 Lille-Fives (LL1, Lille, France)

The Joaquin sampling site in Lille (LL1) is an urban background site that is part of the air quality monitoring network of atmo Nord-Pas-de-Calais. The station is located on the campus of a school (Groupe Scolaire Lakanal) in Lille-Fives (Figure 2.8). The nearest road is at 35 m (rue du Vieux Moulin). This is a local street with 2x1 lanes that is located east, south-east and south of the site. No traffic data is available for this street.

Figure 2.8: Detail of the location of site LL1 (Lille-Fives).

2.2.5 Eltham (LO1, London, United Kingdom)

The Joaquin sampling site in London (LO1) is an urban background station that is part of the Defra Air Quality Network. The station is located in Eltham, a suburban district of South East London, in a building on the grounds of an environmental education centre (Figure 2.9). The surroundings consist of a mixture of habitats including trees, areas of grass, ponds, a golf course and housing. The University of Greenwich is opposite the site.

The nearest road (A210 Bexley Road) is approximately 60 m to the south of the site. The A210 is a feeder road into and out of the centre of London and a local high street for the neighbourhood with a lively shopping area. According to traffic counts by the Department for Transport, the annual traffic intensity on the A210 is about 16500 vehicles/day.

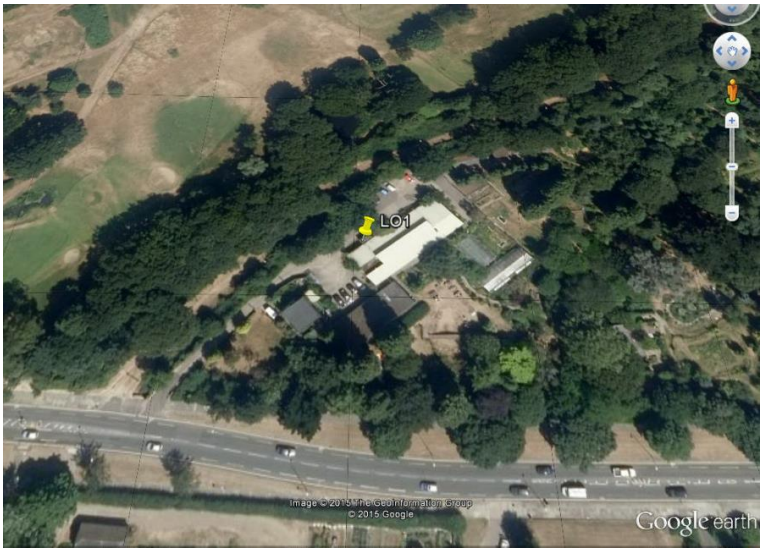

Figure 2.9: Detail of the location of LO1 (London Eltham).

2.2.6 Wijk aan Zee (WZ1, the Netherlands)

The Joaquin sampling site in Wijk aan Zee (WZ1) is an industrial monitoring site of Province North Holland, located approximately 30 km west from Amsterdam. Site WZ1 is at the north side of a parking lot used by visitors of a camping site (Banjaert). Residences of Wijk aan Zee inhabitants are present at a distance of approximately 40 m. The nearest road (Burgemeester Rothestraat) is at a distance of 70-80 m to the south and west. The nearest main road (Verlengde Voorstraat) is at 175 m (Figure 2.10).

Figure 2.10: Detail of the location of WZ1 (Wijk aan Zee).

2.3 Instrument description

This section describes the main instruments used within the Joaquin project for measuring:

- Particle number concentration, size distribution and/or surface area
- Black carbon
- Nitrogen oxides

Table 2.5 summarizes relevant specifications of the ultrafine particle monitors and the (standard) settings used within the Joaquin project.

Table 2.5: Instrument specifications (ultrafine particle instruments only)

	EPC TSI 3783	UFPM TSI 3031	SMPS Grimm 5420/L-DMA	NSAM TSI 3550
Size range				
Lower size (nm)	7	20	10	10
Upper size (nm)	1000	~800 with TSI 3031200 system	1084	1000 (by cyclone)
Size classes				
Number	1	6	45	1
Range per class	7 nm - < 3 µm	20-30, 30-50, 50-70, 70-100, 100-200, >200 nm		Alveolar
Accuracy (according to manufacturer)	±10% at 10^6 particles/cm^3	Not given	Not given Systematic error of CPC is <5%	± 20% for 20-200nm range
Sample time	1 min	10 min	10 min	1 min
Inlet flow rate (L/min)	3.0	5.0	0.3	2.5
Sample flow rate (L/min)	0.12	4.0	0.3	1.5
Radioactive source	-	-	^{85}Kr (185 MBq)	-
Working fluid	Water	-	Butanol	-

2.3.1 EPC (TSI 3783)

In the stations in Amsterdam, Antwerp, Leicester and London (AD1S, AP1S, LE1S and LO1S) and in the mobile trailer, the particle number concentration was measured with a water-based condensation particle counter (CPC) (TSI model 3783; Figure 2.11). This instrument is also called Environmental Particle Counter (EPC).

Figure 2.11: Condensation particle counter TSI 3783.

Its operation principle is illustrated in Figure 2.12. The aerosol sample is pulled through a conditioner that is saturated with water vapour and then passes to a warmer growth section with thermodynamic 'supersaturation' conditions. As a result, the small particles act as condensation nuclei and grow into micron size droplets, which are detected individually by a light pulse when passing through a laser beam.

As the EPC uses water as condensation liquid, this mode of operation differs slightly from the more common butanol-based CPCs. When an alcohol is used as condensation liquid, after the conditioning phase particles pass through a condenser region (10°C). In a water-based CPC, in contrast, after conditioning the particles pass through a warmer "growth tube" (60°C).

The EPC can be used with a high-flow (3 L/min) or low-flow (0.6 L/min) inlet. The aerosol flow rate is 0.12 L/min. Based on the initial tests, we used the high-flow mode to minimize particle losses during the sampling. The response time (95%) is < 3 s (high-flow) or <5 s (low-flow). The averaging interval can be set from 1 to 60 s. Most partners recorded the particle number at 1-min resolution.

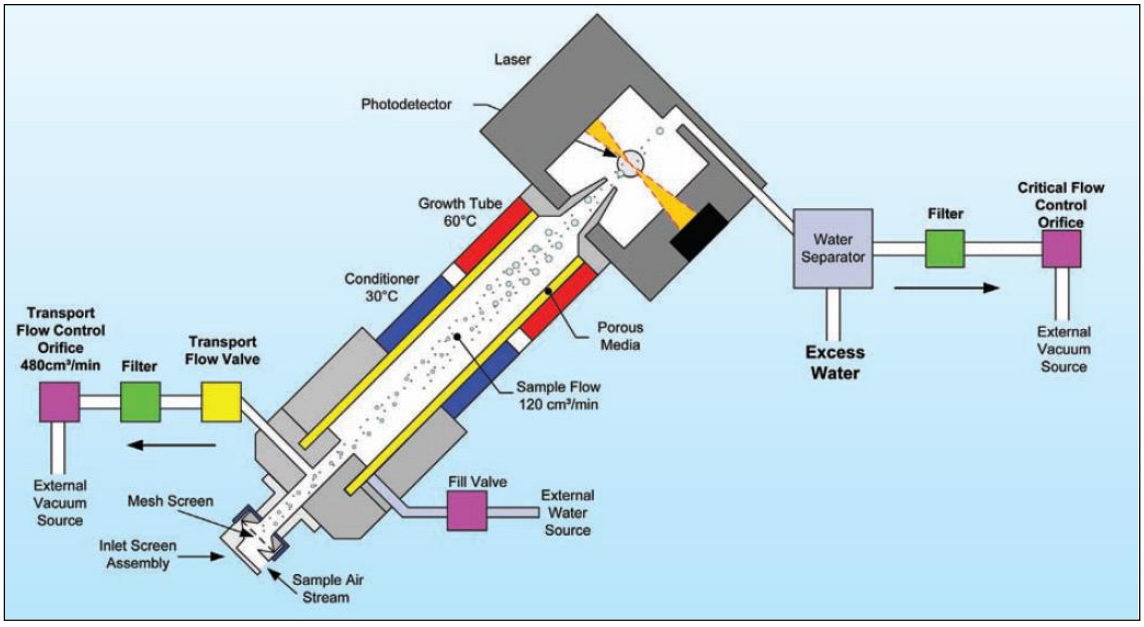

Figure 2.12: Schematic of condensation particle counter TSI 3738.

2.3.2 UFPM (TSI 3031)

In the stations in Leicester and London (LE1S, LO1S) and in the trailer, the particle size distribution was measured by UFP monitor TSI model 3031 (Figure 2.13).

Figure 2.13: UFP monitor TSI 3031.

The operational principle is based on diffusion charging of particles, followed by size segregation within a differential mobility analyser (DMA) and detection of the aerosol via an electrometer. The flow schematic is shown in Figure 2.14.

An aerosol sample is drawn into the instrument continuously at a rate of 5.0 L/min. Within the instrument, the aerosol sample mixes in an equalization tank to smooth out short-term fluctuations in the aerosol sample and then passes on to the diffusion charger, a "Corona-Jet" charger.

The main components of the UFP monitor are:
- Diffusion charger: unipolar corona charger, with counter flow diffusion charging (after flow splitting)
- Differential mobility analyzer (DMA): size classification by stepwise change in DMA voltage. More information on differential mobility analysis is given in section 2.3.3)
- Faraday cup electrometer: current allows detection of particle concentration per size class

The TSI 3031 UFPM needs no working fluid or radioactive source.

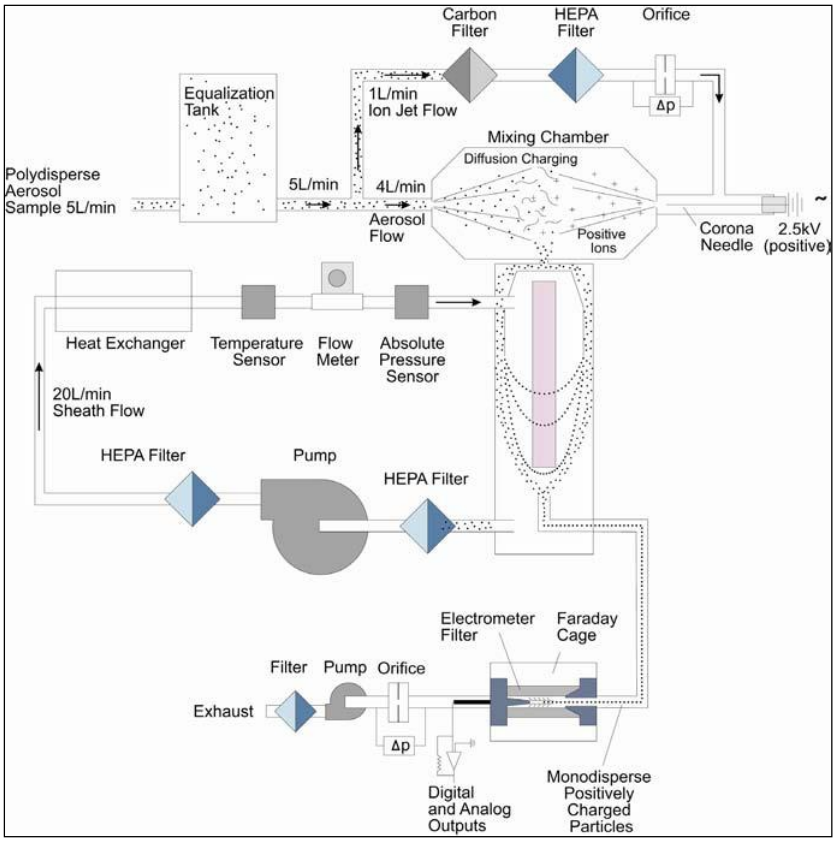

Figure 2.14: Flow schematic of UFP monitor TSI 3031.

Sampling intervals are 7.5, 10 or 15 min. In the Joaquin project a sampling interval of 10 min was used. The UFP monitor software corrects for diffusion losses due to the sampling system, but there is no correction for multiple charging of particles.

Note that ISO 15900:2009 states that “Unipolar charging …. leads to both a higher fraction of multiply-charged particles and higher charge levels on these particles. This has the adverse effect of reducing the size resolution of the differential electrical mobility classifier”.

2.3.3 SMPS (Grimm 5420/L-DMA)

In the stations in Amsterdam and Antwerp (AD1S, AP1S) and in the trailer, the particle size distribution was measured by a scanning mobility particle sizer spectrometer (Grimm SMPS+C 5420 with L-DMA; Figure 2.15).

Figure 2.15: Grimm SMPS+C 5420 (right) with L-DMA (left).

An SMPS is actually a cylindrical capacitor: two flows enter the DMA (Figure 2.15; left), the particle-free sheath air and the aerosol flow containing charged particles. By knowing the dimensions of the DMA, one can calculate the voltage between the electrodes to transport particles with a certain electrical mobility to a small slit in the centre rod of the capacitor. A flow carrying particles with nearly the same electrical mobility is then sucked through this small slit. The number concentration of this sample aerosol (particles with the same electrical mobility) is finally counted in a CPC (Figure 2.15; right).

The main components of the Grimm SMPS are:
- Neutralizer: ^{85}Kr source, 185 MBq, obtained from Eckert & Ziegler (Grimm normally uses ^{241}Am);
- DMA: Vienna type L-DMA (~50 cm long), with up to 255 size channels per scan;
- CPC: butanol-based condensation particle counter.

The flow rate of the CPC is 0.3 L/min. To measure a 10-1100 nm range, the sheath air flow rate is 3 L/min. A complete particle sizing scan for 32 channels can be done in 5 min. In the Joaquin project a scan time of 10 min was used to measure the particle concentration in 45 size classes by stepping the voltage downwards.

The software corrects for internal diffusion losses and multiple charging. For comparability between data sets, the ambient aerosol is kept at low relative humidity (RH) by a Nafion dryer in the inlet system (see section 2.3.7 for more information on the sampling and drying systems). However such a drying system leads also to extra losses of the smallest particles (starting at sizes of below approximately 70 nm). Although in Joaquin these losses were calculated and corrected for, the losses might have been higher, as could be derived from field tests

2.3.4 NSAM (TSI 3550)

In the station in Leicester (LE1S), particle surface area deposition in the lung region was measured by a nanoparticle surface area monitor (NSAM, TSI model 3550; Figure 2.16).

Figure 2.16: Nanoparticle surface area monitor TSI 3550.

The NSAM was originally developed by Fissan et al. (2007).

The NSAM operational principle is based on diffusion charging of particles, followed by detection of the charged aerosol using an electrometer (Figure 2.17). The instrument can be switched between sampling for the tracheobronchial (TB) and alveolar (A) fractions of the total aerosol by changing the ion trap voltage. The ion trap essentially acts as a size-selective sampler for the electrometer. The inlet flow rate is 2.5 L/min, of which 1.5 L/min is used as aerosol flow rate.

The NSAM does not measure the total surface area of airborne particles. The instrument was designed to report the surface area of particles (reported as $\mu m^2/cm^3$) deposited in the tracheobronchial (TB) or alveolar (A) regions of the lung. The calculations are made for a reference worker as predicted by human lung deposition models published by the International Commission on Radiological Protection (ICRP, 1995) (Figure 2.18). In Leicester the NSAM was set to measure the alveolar LDSA at a 1-min time resolution.

The NSAM detects particles ranging in size from 20 to 1000 nm, however, it measures only up to 400 nm with high precision (Asbach et al. 2009). According to Asbach et al. (2009), particle hygroscopicity may cause the lung deposition curves to change significantly, a factor which is not taken into account by this monitor.

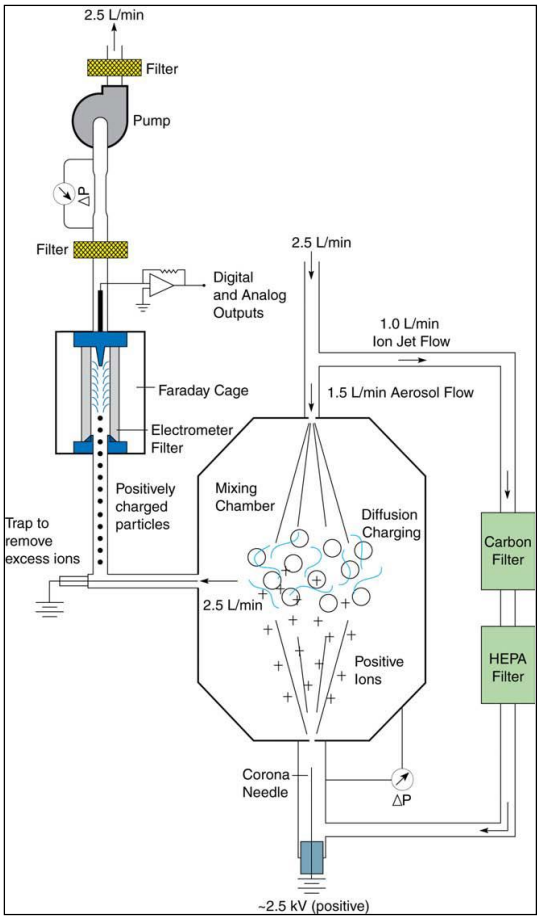

Figure 2.17: Flow schematic of NSAM TSI 3550.

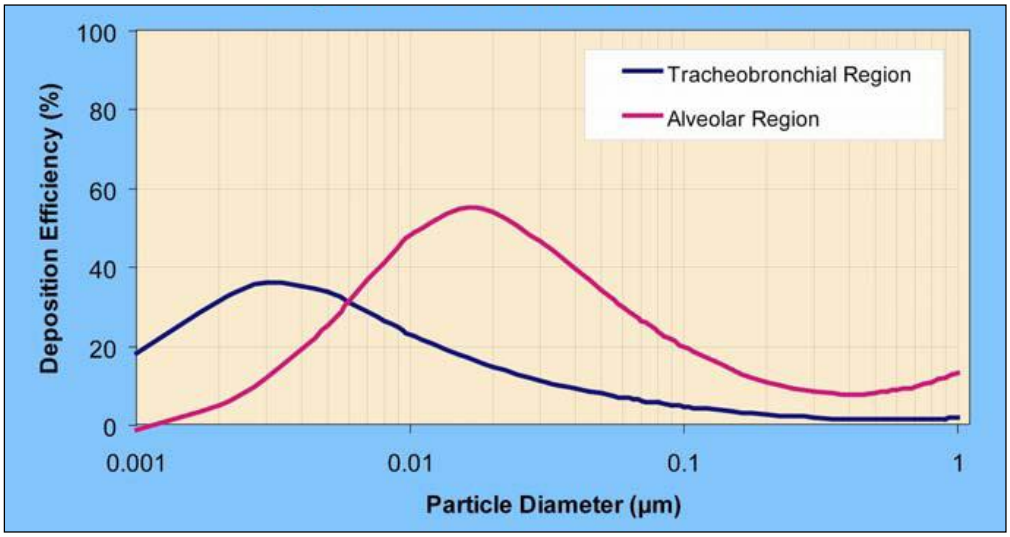

Figure 2.18: Curves for tracheobronchial and alveolar lung deposition for a reference worker.

More information on the NSAM can be found in the TSI application note on measuring nanoparticle exposure (note NSAM-001) and in e.g. Asbach et al. (2009).

2.3.5 MAAP (Thermo Scientific 5012)

In the stations in Amsterdam, Antwerp, Leicester and London (AD1S, AP1S, LE1S and LO1S) and in the trailer, the BC concentration was measured with a multiangle absorption photometer (MAAP Thermo Scientific model 5012; Figure 2.19).

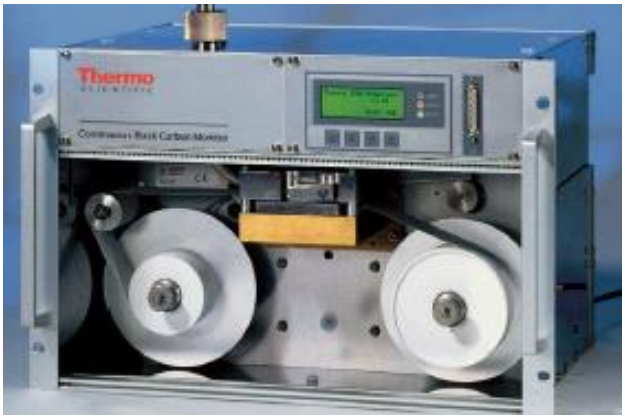

Figure 2.19: Multiangle absorption photometer Thermo Scientific 5012.

The MAAP determines the BC content of aerosols by simultaneous measurement of optical absorption and scattering of light by the particles collected on the filter tape (glass fiber type GF10). Within the detection chamber a 670-nm visible light source is aimed towards the deposited aerosol and filter tape matrix (Figure 2.20). The light transmitted into the forward hemisphere and reflected into the back hemisphere is measured by a series of photo-detectors. During sample accumulation the light beam is attenuated from an initial reference reading from a clean filter spot. More information on the principle of the MAAP is given by Petzold et al. (2002).

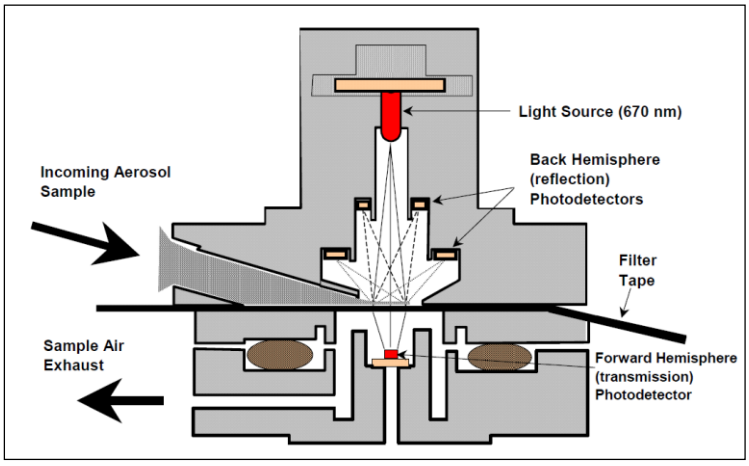

Figure 2.20: MAAP 5012 detection chamber.

2.3.6 NO_x monitors

In the stations in Antwerp, Leicester and Lille (AP1S, LE1S, LL1S), nitrogen oxides were measured by a Thermo 42i NO-NO_2-NO_x monitor (Figure 2.21). This monitor uses chemiluminescence technology to measure the amount of nitrogen oxides in the air. It has a single chamber, single photomultiplier tube design that cycles between the NO and NO_x modes.

Figure 2.21: NO-NO_2-NO_x monitors: TS 42i (left) and API 200A (right).

In the station in Amsterdam (AD1S) an API 200A analyzer was used (Figure 2.21), which is also a chemiluminescent NO-NO_2-NO_x analyzer. In the station in London (LO1S) the NOx monitor was an ML 2041 chemiluminescence analyser.

2.3.7 Sampling systems

2.3.7.1 TSI (EPC and UFPM)

The UFPM is normally equipped with an Environmental Sampling System (TSI 3031200; Figure 2.22) to provide the monitor with dry ambient aerosol. It consists of a standard PM_{10} inlet and a sharp-cut PM_1 cyclone to remove large particles that may contaminate the monitor.

Essential is also the Nafion dryer, which conditions the sample to lower RH to avoid humidity effects on the particle size and behaviour. It has also a disadvantage: it removes a certain amount of nano-sized particles due to diffusion losses in the PermaPure system. In recent studies by ECN and other organizations dealing with UFP number measurements losses up to 40% were noted (unpublished results). Further research is necessary to assess the implications.

The recommended flow rate is 16.7 L/min at the PM_{10} inlet. According to TSI, the particle transmission efficiency (with the given flow rates) is 82% at 25 nm, 87% at 40 nm, 93% at 60 nm, 97% at 150 nm and 100% at 300 nm.

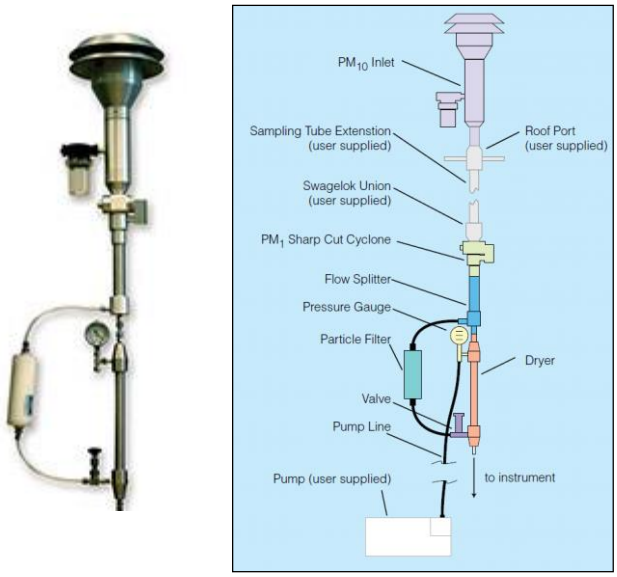

Figure 2.22: Photo and schematic drawing of TSI 3031200 Environmental Sampling System.

The CPCs in the stations in Amsterdam and Antwerp (AD1S, AP1S) were individually connected to one environmental sampling system. In the stations in Leicester and London (LE1S, LO1S) and in the trailer, two TSI instruments (CPC and UFPM) were connected to one TSI sampling system.

2.3.7.2 Grimm SMPS

For comparability between data sets, also for the SMPS the ambient aerosol is kept at low RH by a Nafion dryer in the inlet system. However such a drying system leads to extra losses of the smallest particles (starting at sizes of below approximately 70 nm). Although in this project the losses were calculated and corrected for, the losses might have been higher, as could be derived from field tests

The SMPS devices in the Amsterdam and Antwerp stations (AP1S and AD1S) were connected to an individual Grimm sampling system with TSP sampling pipe, including a Nafion dryer and sensors for temperature, relative humidity and pressure.

The length of the Grimm sampling pipe is 1.5 m. The inlet flow rate is 1.2 L/min, of which 0.3 L/min is used by the SMPS.

2.3.7.3 MAAP

Two types of different sampling systems were used, depending on the station. In the stations in Amsterdam and Antwerp (AD1S, AP1S) and in the trailer a Thermo Scientific TSP inlet was used. In the station in Leicester (LE1S) initially a TSP inlet was used, which was replaced by a $PM_{2.5}$ inlet on 03/03/2014. In the monitoring station in London (LO1S) there was a $PM_{2.5}$ inlet.

2.4 Continuous air quality measurements

2.4.1 Vondelpark monitoring station (AD1S)

Air quality measurements in station AD1S started in 1998 and are funded by Amsterdam's Municipality. Particle number monitoring in the framework of the Joaquin project started in April 2013.

In addition to the parameters mentioned in Table 2.6, currently also CO (Thermo 49i) and O3 (Thermo 48c) are measured. The instruments are hosted in a Portakabin cabin (Portakabin ltd, Huntington York, UK). The inlet heights are at 3.2 to 3.6 m above ground level.

GGD Amsterdam is using the Iséo-XR data acquisition system with a general time base of 60 min. For the particle number and size distribution data 30-min data are available.

Table 2.6: Overview of continuous air quality monitors per variable and sampling site.

Site code	TNC	Size distr.	Surface	BC	NO_x	PM_{10}	$PM_{2.5}$
AD1	EPC	SMPS	SMPS	MAAP	API200A	BAM1020	BAM1020
AP1	EPC	SMPS	SMPS	MAAP	TS42i	ESM / Fidas[b]	ESM / Fidas[c]
LE1	EPC	UFPM	NSAM[a]	MAAP	TS42i, Teledyne	-	TEOM-FDMS
LL1	-	-	-	-	Megatec 42i	TEOM-FDMS	TEOM-FDMS
LO1	EPC	UFPM	-	MAAP	ML2010	TEOM-FDMS	TEOM-FDM
WZ1	-	-	-	-	API200A	BAM1020	BAM1020
Trailer at AD1, AD2, AP1, AP2, LE1, LE2, LO1	EPC	SMPS, UFPM	SMPS	MAAP	-	-	-

Note: At LE1, LO1 and in the trailer the EPC and UFPM were connected to one sampling system. TNC = total particle number concentration, Size distrib. = particle size distribution, BC = black carbon.
[a] Lung-deposited surface area; [b] PM_{10} by ESM until end of 2014, then by Fidas; [c] $PM_{2.5}$ by ESM until August 2014, then by Fidas; [d] Leckel from 14/08/2013 on.

2.4.2 Borgerhout monitoring station (AP1S)

The measurements in station AP1S are carried out by the Flemish Environment Agency (VMM), funded by the Flemish government. The measurements started in the 1980s. Particle number monitoring started in February 2013.

In addition to the parameters mentioned in Table 2.6, also SO_2 (Thermo 43i), CO (API300), O3 (API40E) and BTEX (benzene, ethylbenzene, toluene, mp-xylene, o-xylene; BTX Chromatosud 1000) are currently measured in AP1S. The inlets of the monitors are approximately at 4.6 m height. The inlets of the CPC and SMPS are slightly lower because of the fixed lengths of the sampling tubes.

Until the summer of 2014, PM was monitored by four continuous monitors (ESM FH62 I-R with PM_{10} inlet, ESM FH62 I-R with $PM_{2.5}$ inlet, BAM 1020 with $PM_{2.5}$ inlet and Grimm EDM 365 with TSP inlet). The data of the two ESM instruments were used to report PM_{10} and $PM_{2.5}$ mass concentrations. Since August 2014, PM_{10} and $PM_{2.5}$ are measured by another type of monitor (Palas Fidas 200). The ESM PM_{10} sampler has been in use until end of 2014, so that simultaneous PM_{10} measurements are available during 4 months. In addition, two Leckel samplers, one with a PM_{10} inlet and one with a $PM_{2.5}$ inlet, are used for gravimetric PM determination from August 2014 to March 2015.

Next to the main road (5 m from the Plantin en Moretuslei) VMM operates a second air quality station in Borgerhout (traffic station) where measurements of BC (MAAP 5012), NO_x (Thermo 42i) and PM_{10} and $PM_{2.5}$ (Palas Fidas 200) are carried out.

2.4.3 Leicester University monitoring station (LE1S)

The air quality measurements in station LE1S are carried out by Bureau Veritas and the University of Leicester. The station was built in 2013 and is replacing the Leicester Centre station (52°37'53" N, 1°07'59" W). Monitoring of BC and NO_x at the LE1 site started in April 2013, with monitors built in a mobile trailer. From October 2013 on, BC, NO_x and particle numbers are measured with monitors installed in the new station. In addition to the parameters mentioned in Table 2.6, O_3 (Thermo 49i) is also measured.

2.4.4 Lille-Fives monitoring station (LL1S)

The air quality measurements in station LL1S are carried out by atmo Nord-Pas-de-Calais since 1995. The monitoring station participated in the Joaquin project for WP1A2 only. Ultrafine particles were not monitored.

2.4.5 Eltham monitoring station (LO1S)

The air quality measurements in station LO1S are carried out by Kings College London, Ricardo-AEA and the University of Brighton. Particle number monitoring started in April 2014. In addition to the variables in Table 2.6, also SO_2 (AF-21M), O_3 (ML2010) and 29 different hydrocarbons (Hewlett-Packard GC-MS) are measured.

2.4.6 Wijk aan Zee monitoring station (WZ1S)

The air quality measurements in station WZ1S are carried out by GGD Amsterdam since 1998, funded by Province North Holland. The monitoring station participated in the Joaquin project for WP1A2 only. Next to the variables in Table 2.6, also CO (Thermo 48c), SO_2 (Thermo 43i) and H_2S (Thermo 450i) are measured. The instruments are hosted in a Portakabin cabin (Portakabin ltd, Huntington York, UK).

2.5 Meteorological measurements

Table 2.7 summarizes the availability of meteorological data for each Joaquin monitoring station. At most stations, ambient air temperature (T), relative humidity (RH) and air pressure (P) were locally measured. Radiation (Rad) and precipitation (Prec) were available from other stations in the region. During its operation at the various sites, the trailer recorded its own meteorological data (WS, WD, T).

Table 2.7: Overview of meteorological data avaible per monitoring station.

Station	Local variables	Regional variables	Regional site
AD1S	T, RH, P	T, RH, P, WS, WD, Rad, Prec	Schiphol (9 km)
AP1S	T, RH, P (WS, WD)	T, RH, WS, WD, Rad, Prec	Luchtbal (5 km)
LE1S	T, RH, P, WS, WD, Rad (> Oct 2014)	T, P, WS, WD, Rad, Prec	Groby road Traffic Island
LL1S		T, RH, P, WS, WD (10 m)	Sequedin (7 km)
LO1S	T*, RH$, P*, WS, WD, Rad*, Prec*	T, WS, WD	Different sites in the region
WZ1S	-	WS, WD	IJmuiden (4 km)

* Data measured at Barking and Dagenham - Rush Green
$ Data measured at Bexley - Belvedere West

For the interpretation of air quality measurements, wind speed (WS) and wind direction (WD) are the most relevant meteorological parameters. The availability of locally measured wind data varied by site. It should also be noted that wind speed and direction measured locally at low heights can be affected

by local buildings, so that some local measurements may not reflect larger scale air transportation processes.

For most stations, also more regional wind data were available, i.e. wind measurements thought to represent the wind conditions for a wider region (measured at a height of 30 m or more).

For the stations in Amsterdam, Antwerp and Wijk aan Zee, regional wind data were used:
- For AD1S, the regional meteo site was Schiphol airport (52°18'39" N, 4°46'12" E)
- For AP1S, the regional meteo site was VMM station Luchtbal (51°15'40" N, 4°25'28" E)
- For WZ1S, the regional meteo site was IJmuiden (52°27'41" N, 4°34'18" E)

In the station in Leicester (LE1S), local meteorological measurement started in October 2014 on. Until then, data are available for the station at Groby road Traffic Island (52°39'08" N, 1°10'34" W) (data collection since 1997, sensors at 2 and 8 m height).

Meteorological data used for the station in Lille (LL1S) were measured at Sequedin (50°37'04" N, 2°59'23" E), at a distance of 7 km of LL1S. Meteo variables were measured at 10 m height.

For the station in London (LO1S), local wind measurements were available throughout the sampling period. For LO1S also regional results were available for T, WS and WD: a 'typical' meteorological data set representing London, which is a composite of data from several instruments co-located with air pollution monitoring sites.

The location of the meteorological sites is shown in the maps in Annex 1.

2.6 Analysis of continuous air quality data

2.6.1 Data validation and diffusion loss correction

All data were screened for irregularities. Continuous air quality data collected during instrument errors or maintenance were removed from the analysis.

For ultrafine particles, particle losses to the surface of the sampling system and the measuring device can occur via diffusion. Therefore sampling pipes are kept as short as possible and laminar flow conditions are aimed for. Nevertheless, meaningful diffusional losses during sampling and measurement occur for particles <100 µm, so that diffusion correction factors should be applied. For the results of the Grimm SMPS and UFP monitor 3031, the diffusion correction factors used were manufacturer factors integrated into the instruments algorithms, after which an additional correction was done using factors based on the simplified expression formula for cylindrical pipes by Hinds (1999). No other instrument corrections were applied.

2.6.2 Processing and analysis of half-hourly data

All data were aggregated to the half-hourly level for further analysis. The threshold to retain the data was 75% availability at the half-hourly level. For the comparison of the size distribution data between all the sites, data were aggregated to the following size classes: <20, 20-30, 30-50, 50-70, 70-100, 100-200 and >200 nm. The data were aggregated to the hourly level to calculate diurnal patterns.

Boxplots, single linear regression plots and Pearson correlation coefficients were used to compare sites, periods and pollutants. In the regressions an intercept as well as regressions forced through the origin, i.e. with a zero intercept, were used. We considered the regressions through the origin as most representative to evaluate differences in temporal variability.

The Pearson correlation coefficient (r) is a standard method used to evaluate the (linear) relationship between paired data points. The correlation can vary from 0 (no correlation, independent data points) to ±1, indicating perfect positive or negative correlation. The correlation helps to determine what fraction of the number concentrations at any particular site can be explained by the concentrations simultaneously measured at the other sites. A limitation of Pearson correlations, however, is that

perfect correlation can be observed between two sites where the concentrations vary by a consistent factor. In other words high correlations between paired sites would only imply uniform temporal variation. Therefore, calculating r alone does not necessarily provide sufficient information to characterize the variability between sites.

Another useful method to characterize the spatial variability between site pairs is using the so-called coefficient of divergence (COD), which is defined as:

$$\mathrm{COD}_{jk} = \sqrt{\frac{1}{n}\sum_{i=1}^{n}\left(\frac{x_{ij} - x_{ik}}{x_{ij} + x_{ik}}\right)^2}$$

Where *x* and *y* represent the considered instruments, C_i is the simultaneous half-hourly UFP number concentration and *n* is the total number of half-hourly measurements.

where j and k are two sites, x_{ij} and x_{ik} represent the i_{th} concentration for a given sampling period at j and k, respectively, and n is the number of simultaneous observations. The COD for a given pair of sites can vary from 0, when concentrations are identical at both sites, to 1, when concentrations are highly different. So a low COD indicates a high level of homogeneity in concentrations between site pairs, and a high COD the opposite. The COD therefore specifically addresses the limitation to the correlation described above. A COD value larger than 0.2 can be considered heterogeneous (Wilson et al. 2005). In the present study CODs were calculated at the half-hourly or hourly level to determine the variability between different sites.

The Spearman rank correlation (r_s) is a nonparametric measure to evaluate the relationship between paired data points. This is a method generally applied for distributions that deviate from the normal/Gaussian distribution. The correlation can vary from 0 (no correlation, independent data points) to ±1, indicating perfect positive or negative correlation. The correlation helps to determine what fraction of the number concentrations at any particular site can be explained by the concentrations simultaneously measured at the other sites. A limitation of Spearman rank correlations, however, is that perfect correlation can be observed between two sites where the concentrations vary by a consistent factor. In other words high correlations between paired sites would only imply uniform temporal variation. Therefore, calculating r_s alone does not necessarily provide sufficient information to characterize the variability between sites.

The effect of wind on air quality measurements is multidimensional as both the wind speed and wind direction have to be considered. To show the experienced wind field, a traditional wind rose plot is applied which plots wind speed and direction by different intervals. The pollution rose applies the same plot structure but substitutes other measurements, most commonly a pollutant time series, for wind speed. Hereby, it is important to note that wind speed is disregarded from the plot (only wind direction and pollutant concentration is shown). To include all wind speed effects on pollutants concentration, a polar plot can be applied which plots the pollutant concentration in polar coordinates showing concentration by wind speed and direction. Mean concentrations are calculated for wind speed-direction 'bins' and generalized additive model (GAM) smoothed.

The analyses were carried using Microsoft Excel and R software (R Development Core Team, 2014), in particular the package *openair* (Carslaw and Ropkins, 2012, 2015).

3 Results of the preparation phase

3.1 Literature review, laboratory test and purchase of UFP instruments

As a first step, the instrumental approaches used for UFP monitoring were assessed. From literature review and a laboratory test, an evaluation was made of commercially available UFP devices in order to choose the appropriate instrumentation and methodology to measure particle number concentration and size distribution under routine measuring network conditions.

In 2012, based on this evaluation three different types of monitors were purchased for measuring UFP: a Grimm SMPS 5420 with L-DMA (further called SMPS), a TSI UFP monitor 3031 (UFPM) and a TSI EPC 3783 (EPC). In addition, monitors for BC and NOx were purchased when not yet available in the monitoring stations. The instruments are described in detail in section 2.3.

To avoid different monitoring circumstances at the different locations (monitoring artefacts, e.g. inlet systems, maintenance frequency, etc.), standard operating procedures (SOP) were made and used for the chosen instrumentation. Furthermore, the instruments were compared before setup at the different monitoring stations (see 3.2).

3.2 Initial comparison of UFP instruments (Dec 2012 - Jan 2013, Antwerp)

Before installing these instruments in monitoring stations across the NWE region, the instruments were compared at an urban background site in Antwerp (Vuurkruisenplein, Wilrijk; Dec 2012 - Jan 2013). The site, methods and results of this comparison are described in detail by Frijns et al. (2013a).

In Dec 2012, the UFPM of UoB, to be used at the monitoring station in London (LO1, Eltham) was not yet available. Therefore, another UFPM belonging to VITO was used in this comparison study. In addition to the instruments that were used in the rest of the Joaquin project, another type of SMPS belonging to ISSeP was compared in the study.

The instrument comparison was used to decide on the best setup and settings of the instruments. E.g. for the EPC it was found that changing low flow (0.6 L/min) to high flow (3 L/min) gave higher efficiencies. Furthermore, the inlet screen assembly was found to increase diffusion losses due to the fitted screen and sharp edges. The assembly was therefore removed and conductive tubing was fitted instead when using an ESS with PM_{10} and PM_1 pre-separator.

The conclusions of this comparison of three types of UFP instruments (EPC, SMPS, UFPM) were:

- All EPCs en SMPSs differed less than 10%, except the UoL EPC (13 %). The setup of UoL used a combined sample flow for 3 instruments using a flow splitter which probably resulted in more particle losses than was corrected for. Therefore in the monitoring station in LE1 a different setup was used, with 2 instruments instead of 3 instruments connected to one ESS;
- All EPCs en SMPSs were strongly correlated;
- The total number concentration measured with the UFPM differed less than 10% from the reference (ECN), but not for some individual size channels (20-30 nm for UoL and VITO, 30-50 nm for UoL, >200 nm for VITO);
- The UFPMs were strongly correlated (R^2 >0.9) except for the size channel >200 nm;
- The correlation between the ECN EPC and ECN SMPS/UFPM (all reference instruments) was strong, the EPC total number concentrations were about 20% higher compared to the SMPS and 24% higher compared to the UFPM;
- The correlation between the ECN UFPM and ECN SMPS was strong, the total number concentrations were comparable;
- The ISSeP SMPS connected to the ISSeP sampling system gave 3% higher total particle number concentrations than the ECN SMPS. The difference was very small. The total particle number concentrations measured with the EPC connected to the ISSeP sampling system where 25% higher compared to the reference (ECN) systems, probably due to the differences in the sampling system;

Overall, it was concluded that the EPC, SMPS and UFPM instruments could reliably be used at the different monitoring sites, without intra-instrument correction.

4 Trailer measurements adjacent to the four WP1A1 monitoring stations

4.1 Quality checks and SOPs

4.1.1 Flow checks

Flows were measured as part of the regular quality checks during the mobile campaigns. They were found to be rather equal as can be seen in Table 4.1.

Table 4.1: Results of quality checks during the Joaquin mobile campaigns.

	EPC	EPC	ESS	MAAP	UFPM	Remarks
	Total	**Aerosol**	**EPC+UFPM**	**sample**	**sample**	
	(l/min)	(l/min)	(l/min)	(l/min)	(l/min)	
ECN	3.09	0.607	16.9	16.9	5.15	All flows std to
GGD	3.01	0.605	16.7	16.7	NA	21.1 C and 1013 hPa
ECN	3.11	0.607	16.8	16.9	5.08	
VMM	3.19	0.604	17.6	17.9	NA	
ECN	3.12	0.607	16.5	16.9	5.15	
UoL	3.19	0.592	11.5	13.6	5.04	Found at Apr 5, 2013
UoL			16.7	16.7		Changed to at Apr 5
ECN	3.12	0.607	16.6	16.9	5.15	
UoB	3.33	0.620	16.9	16.5	5.20	

All flows were measured with a TSI flowmeter 4043 E (standard 21.1 °C and 1013 hPa). Only the lowest flow (aerosol EPC) was measured with a TSI 4140 D (same standard). Accuracies were 2% or 0.05 l/min and 2% or 0.05 l/min, respectively.

Mostly, the flows were in good agreement. One large deviation was encountered during the start of the measuring campaign at Leicester. This was solved rather quickly and data taken before 3 March 2014 might have been collected with deteriorated flows.

4.1.2 Control of the sizing measurements

During the visits of the mobile station at the fixed stations the sizing equipment of the partners was checked with monodisperse polystyrene Latex aerosol. Two sizes (73 nm and 269 nm) were used to check the performance of either the UFPM or the SMPS. The calibration took place with a so-called constant output atomizer of TSI. None of the checked instruments showed deviations. An example of the sizing by a SMPS at one of the sites can be found in the Figure 4.1 and Figure 4.2.

4.1.3 Maintenance and SOPs

It was agreed that during the measuring campaigns the maintenance as described in the manufacturer's manuals would be followed. All monitoring systems of TSI (UFPM and EPC) had to be equipped with ESS inlet systems. All monitoring was performed after Nafion drying of the aerosol, except for the MAAP (BC monitoring).

The EPC had to be used without inlet screen assembly (bug screen) and at a flow of 3 l/min. The aerosol flow remained at 0.6 l/min. The SOP and maintenance had further to be performed according to the descriptions in the interim report of VITO by Frijns and van Laer (2013). The same applies for the SOPs and maintenance of the SMPS and UFPM. The SOP and maintenance of the Leckel SEQ 47/50 was described by VMM (2012) and is explained in more detail by Joaquin 2015).

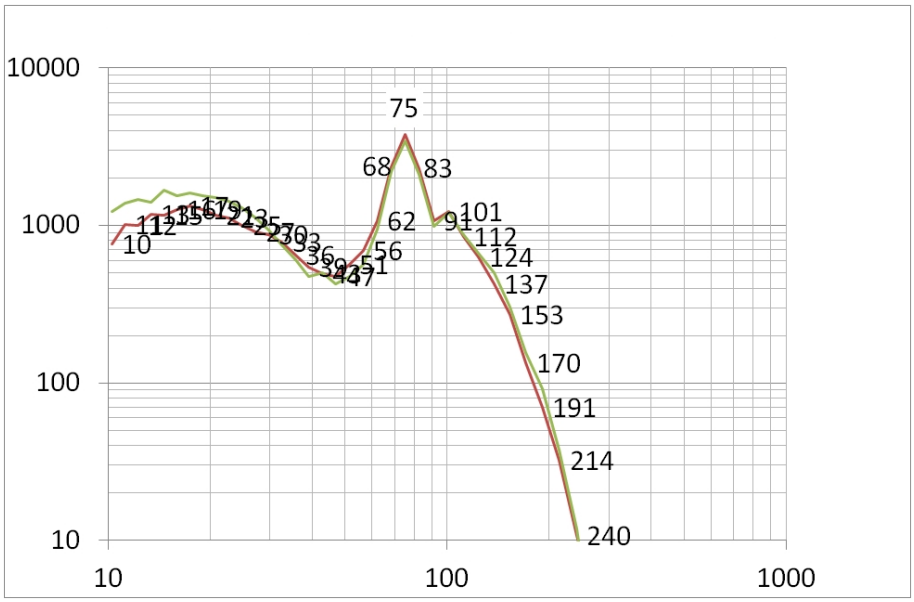

Figure 4.1: The sizing of PSL of 73 nm by the SMPS of VMM at the start of the campaign at Antwerp.

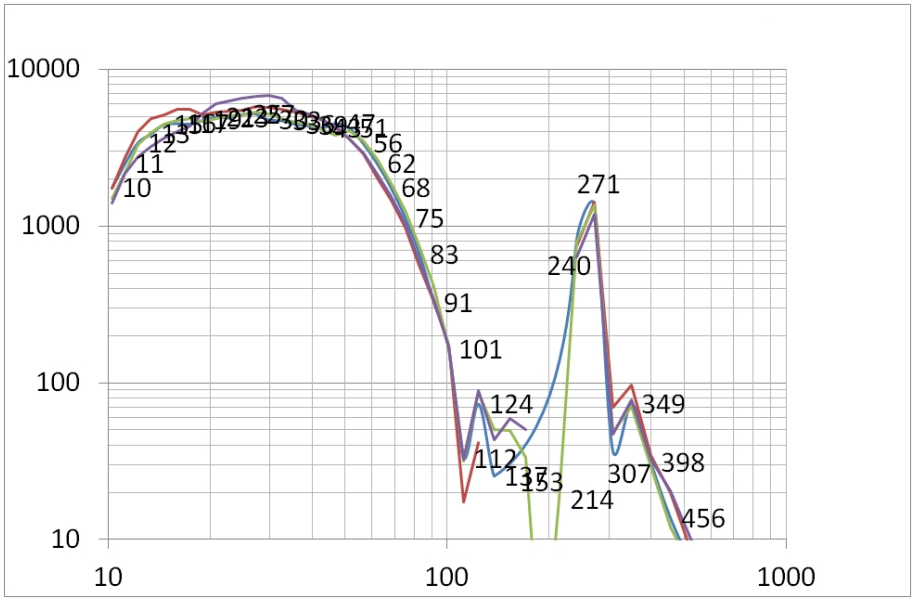

Figure 4.2: The sizing of PSL of 269 nm by the SMPS of VMM at the start of the campaign at Antwerp.

Finally a short description of the main issues faced and solved during the mobile campaigns and site visits:

- Amsterdam: slider vane pumps of GGD without filters (9 to 16 April 2013) during start comparison, ECN closer to exhausts, higher values of BC and PNC in trailer than in the monitoring station (AP1S), all pumps equipped with filters after 16 April 2013.
- Antwerp: ECN-SMPS detoriated, slowly decreasing PNC, problem solved by Grimm. New comparison at the fixed site (AP1) was necessary and has been performed later on.
- Amsterdam and Antwerp: poor comparability of ECN-SMPS and ECN-UFPM. In February 2014 'ghost' counts were discovered during a long run with a HEPA filter. Also discovered: crumbled O-ring in the DMA during disassembling and servicing, debris found down in the cylinder of the DMA: solved by replacing O-ring and cleaning and update of software by TOPAS (manufacturer of the UFPM of TSI).
- Leicester: flows of ESS and MAAP far too low. Thermistor of the MAAP broken, solved. Both problems solved at start campaign with mobile trailer.

- New Eltham: large difference between PN of UFPMs, not obvious during the mobile during campaign, but later discovered during data handling. Can be solved with algorithms as correlations of (SMPS EPC UFPM)/ECN and (EPC UFPM)/UoB are good (see section 4.3).

4.2 EPC

The Environmental Particle Counters (EPCs) installed at the four permanent Joaquin sites have been compared with the EPC in the ECN trailer (EPC ECN) in order to find deviations in the operation. The ECN EPC acted as the reference instrument. Every EPC was operated following the predefined procedure (SOP). The EPC data presented have not been corrected for diffusion losses.

The comparison was done during the following campaigns:
- AD1 (Amsterdam Vondelpark, GGD): 17 April - 14 May 2013 (25 days, 2 days off)
- AP1 (Antwerp Borgerhout, VMM): 9 September - 7 October 2013 (all 26 days)
- LE1 (Leicester AURN, UoL): 10 March - 4 April 2014 (23 days, 1 day off)
- LO1 (London Eltham, UoB): 4 June 2014 - 30 June 2014 (23 days, 2 days off)

4.2.1 Time series EPC

Time series of half-hourly total number concentrations (TNC) as measured during the four campaigns are shown below (Figure 4.3) as well as daily averages (Figure 4.4).

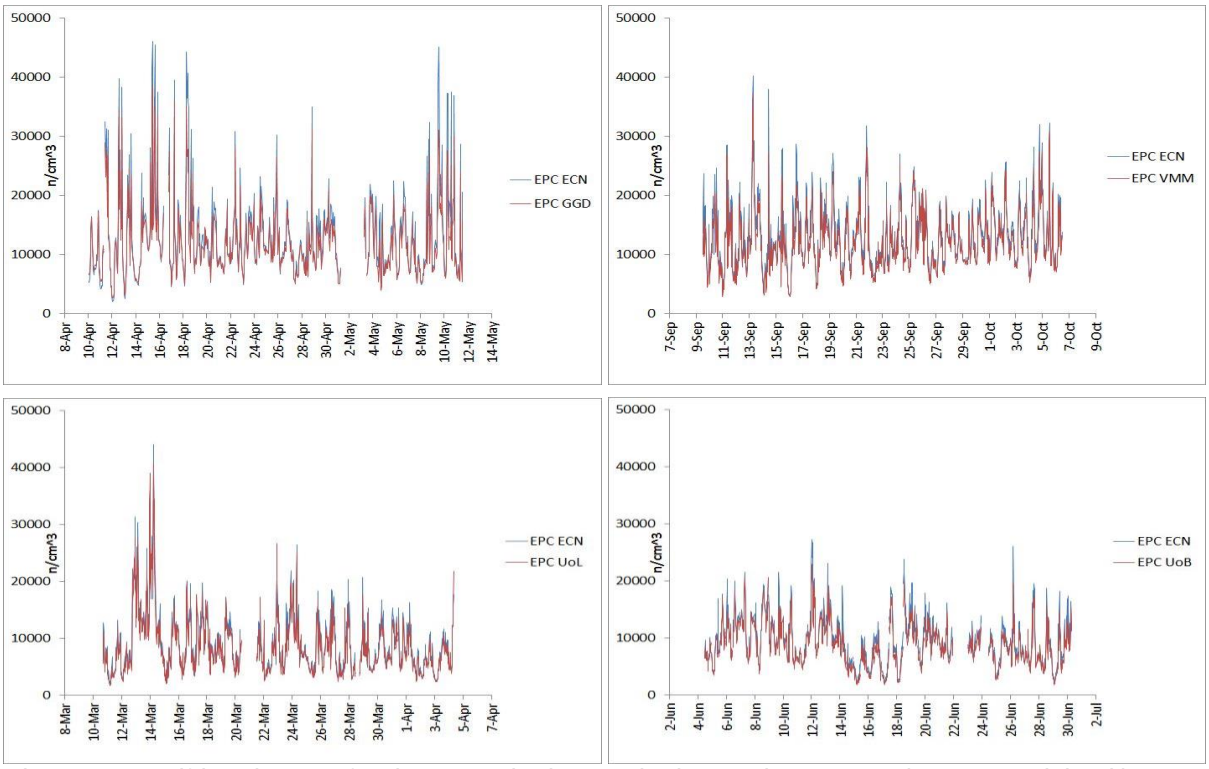

Figure 4.3: Half-hourly TNC for the EPCs in the monitoring stations AD1S (GGD, Vondelpark), AP1S (VMM, Borgerhout), LE1S (UoL, Leicester University) and LO1S (UoB, Eltham) compared to the EPC in the trailer (EPC ECN, reference instrument).

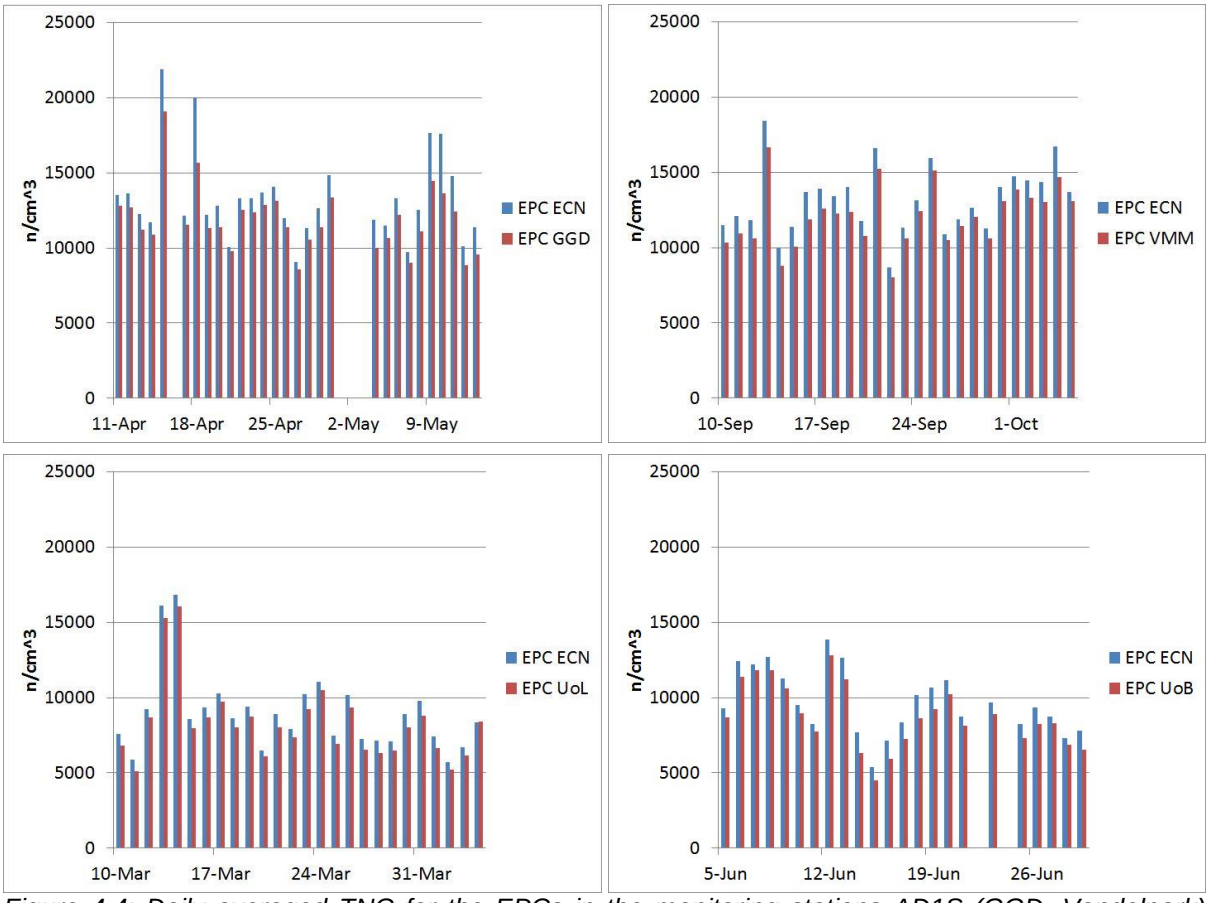

Figure 4.4: Daily averaged TNC for the EPCs in the monitoring stations AD1S (GGD, Vondelpark), AP1S (VMM, Borgerhout), LE1S (UoL, Leicester University) and LO1S (UoB, Eltham) compared to the EPC in the trailer (EPC ECN, reference instrument).

4.2.2 Scatterplots EPC

The half-hourly average values were also used to create correlation plots. Figure 3.3 shows the corresponding scatterplots for the four fixed monitoring stations.

4.2.3 Summarizing remarks EPC

Table 4.2 summarizes the respective coefficients of determination (= R^2) and regression coefficients (= slope of the regression). The values are obtained for linear regressions (forced through the origin) between the ECN EPC and the other EPCs as shown in the scatterplots. Regression coefficients are always equal or more than 0.87.

Table 4.2: Coefficient of determination (R^2) and regression coefficient for linear regressions between the ECN EPC in the trailer and the EPCs in the monitoring stations.

City (responsible)	Mobile trailer		Initial comparison[a]	
	R^2	Regression coefficient	R^2	Regression coefficient
Amsterdam (GGD)	0.95	0.87	0.99	0.93
Antwerp (VMM)	0.97	0.91	0.99	0.94
Leicester (UoL)	0.94	0.92	0.99	0.88
London (UoB)	0.94	0.89	NA	NA
Wilrijk (VITO)			0.99	0.97

[a] Comparison in Dec 2012 - Jan 2013 (Frijns et al. 2013a)

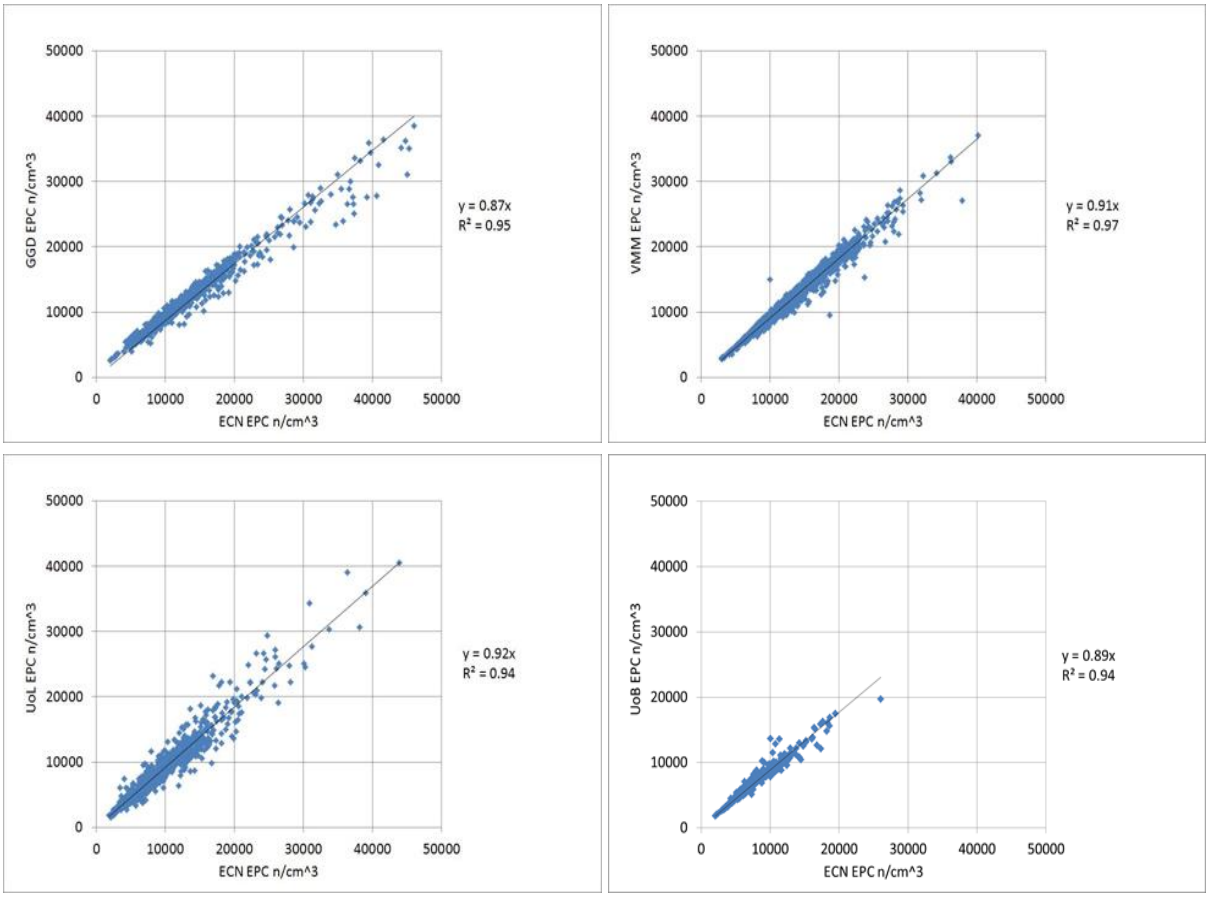

Figure 4.5: Scatterplots (half-hourly concentrations) of the EPCs in the monitoring stations AD1S (GGD, Vondelpark), AP1S (VMM, Borgerhout), LE1S (UoL, Leicester University) and LO1S (UoB, Eltham) versus to the EPC in the trailer (EPC ECN, reference instrument).

For the sake of comparison, results of the initial instrument comparison at Vuurkruisenplein (Frijns et al. 2013a) have been added to this table. During that period the measurements were performed with all units at one location (see also section 3.2). The EPC of UoL was not yet available at that time.

The concentration averages for each campaign are shown in Figure 4.6. Note that the concentrations in this figure cannot be compared directly between the four sites, since the campaigns took not place simultaneously.

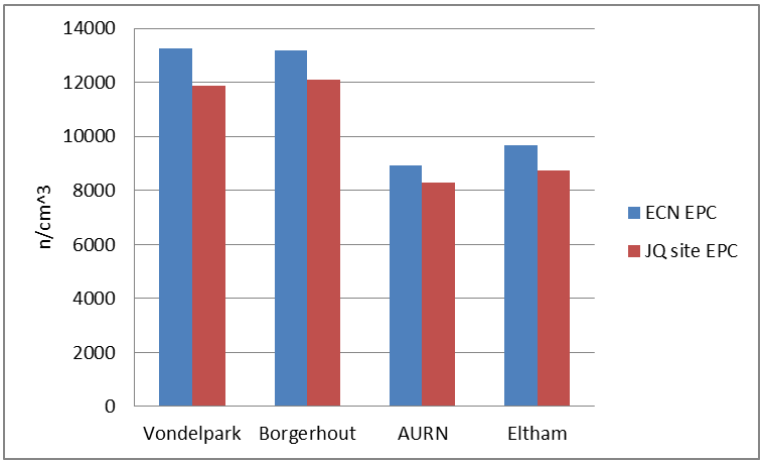

Figure 4.6: Total number concentrations during the mobile campaigns at AD1 (Vondelpark), AP1 (Borgerhout), LE1 (AURN) and LO1 (Eltham) measured by the EPC in the mobile trailer (ECN EPC) and the monitoring station (JQ site EPC).

The time series and scatterplots presented above clearly demonstrate the rather close correspondence with the ECN EPC in terms of accuracy (absolute value) and precision (correlation). Coefficients of determination (R^2) are 0.94 or higher and indeed indicate a high precision, which was expected from previous studies such as the initial comparison by Frijns et al. (2013a).

It is further shown that the ECN EPC systematically measures slightly higher particle numbers in each of the campaigns. Roughly, the difference is in the order of +10%.There is no clear explanation for this observation. Because all partners monitored according to the same SOP, there should be another (technical) reason for the difference in concentration levels. Aerosol flows of the EPCs were equal within 10%, so this does not explain the difference. Also differences in flows through the ESS per site (as a consequence of more monitors being connected) are not the reason, as in Leicester and London there are also two instruments (EPC using 3 L/min and UFP-3031 using 5 L/min) connected to one ESS, identical to the setup of the ECN trailer. It is therefore suggested that differences in electronics or software versions are the only possible cause.

4.3 SMPS and UFPM

At four monitoring sites we compared either SMPS (Grimm GmbH Germany) with SMPS or UFP-3031 (further UFPM, TSI-Topas) with UFPM. In two of the four campaigns SMPS versus SMPS data were compared and in the other two campaigns we compared UFPM with UFPM data. The sampling sites and periods are described in chapter 2.

In Amsterdam and Antwerp only SMPS devices were applied and in at Leicester and Eltham UFPMs were installed. The reason for the different set-up was that the UK partners foresaw problems working with instruments that need a radioactive source for the measuring process (as is the case using an SMPS).

The comparison was done during the following campaigns:
- AD1 SMPS (Amsterdam Vondelpark, GGD): 17 April - 13 May 2013 (26 days, 2 days off)
- AP1 FSSP (Antwerp Borgerhout, VMM): 4 Nov - 18 Nov 2013 (13 days)
- LE1 UFPM (Leicester AURN, UoL): 4 March - 4 April 2014 (27 days, 3 days off)
- LO1 UFPM (London Eltham, UoB): 2 June 2014 - 27 June 2014 (23 days 2 days off)

The aerosol spectra the instruments can determine are different: SMPS measures in 45 size classes, starting at 10 nm and ending at about 1000 nm. These classes are divided in almost equal logarithmic steps. The UFPM has less resolution regarding the size classes (5 only) and also the range differs: from 20 nm as lower cut-off up to 200 nm as largest diameter to be classified. However a last “oversized” class is abundant that arbitrarily ends at 500 or 800 nm (depending on the manufacturer's documentation). This size class >200 nm should be considered as indicative only and it attributes only very little to the overall number concentrations as this is almost completely ruled by sizes below 200 nm.

4.3.1 Time series SMPS/UFPM

The SMPS and UFPM time series collected during the four mobile campaigns are shown below for half-hourly averaged number concentrations. It concerns the total particle number derived from the cumulated concentrations of the spectra (Figure 4.7). Also shown are the daily averages (Figure 4.8) and scatterplots (Figure 4.10). All the aggregated figures show first two plots of SMPS versus SMPS data and then two plots of UFPM versus UFPM data.

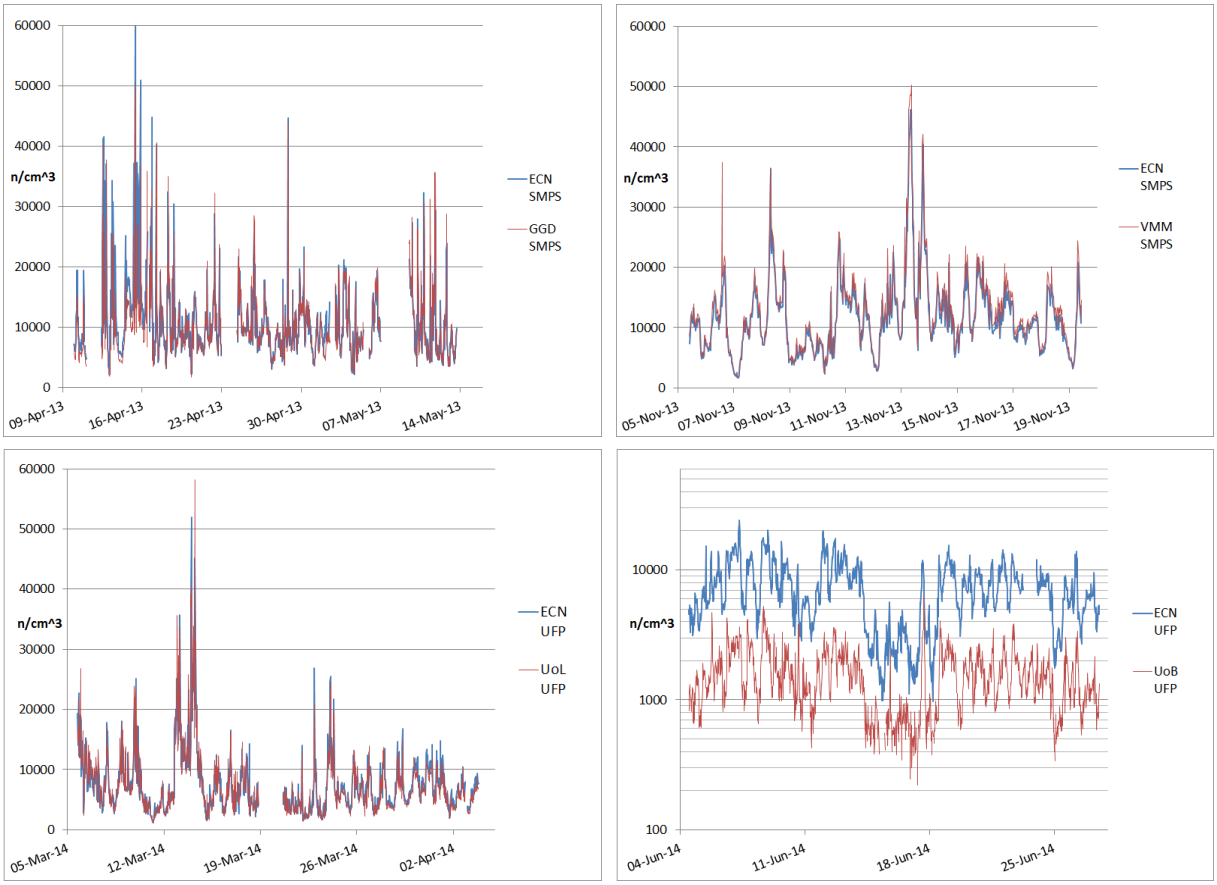

Figure 4.7: Half-hourly number concentrations for the SMPSs in the monitoring stations AD1S (GGD, Vondelpark) and AP1S (VMM, Borgerhout) and for the UFPM in the monitoring stations LE1S (UoL, Leicester University) and LO1S (UoB, Eltham) compared to the instruments in the trailer (ECN SMPS or ECN UFPM, reference instrument).

For the first three sites the comparability as can be seen from the time series alone is rather good. But, as can easily be seen in the last figure, UFPMs had very different totalized numbers at New Eltham (LO1). This concerns the UFPM ran by the University of Brighton (UoB) that is consequently lower than the UFPM of ECN (situated in the mobile trailer). More precise analyses revealed that the difference was very constant, also per size class, and thus this might support the suggestion to correct all the data with the factors found per channel, not only for the period of comparison but also for the periods before and after.

During the meeting in Paris in March 2015, the UoB mentioned that they had the intention to compare this instrument again at the end of the Joaquin measuring period, now with an UFPM from and in cooperation with TSI subsidiary in the UK. Thus more precise correctional algorithms might be established if eventual slight changes of performance of the instrument towards the end of the total measuring period would have occurred. At the end of the Joaquin measuring period, and in consultation with Topas and TSI, it was concluded by UoB to correct the anomalous data by means of the SMPS measurements of the ECN trailer during the comparison campaign, as the trailer data consisted of longest time series for comparison. From the simultaneous trailer measurements, size-channel specific correction factors were derived to correct the UFPM data. There is always a time-shift between the two size-resolved measurements (UFPM and SMPS) due to the scanning differences of the individual particle size classes. Therefore, the data was compared on hourly or daily base and not per measurement (10 minutes in this case). The results of the comparisons on daily base are shown in Figure 4.9.

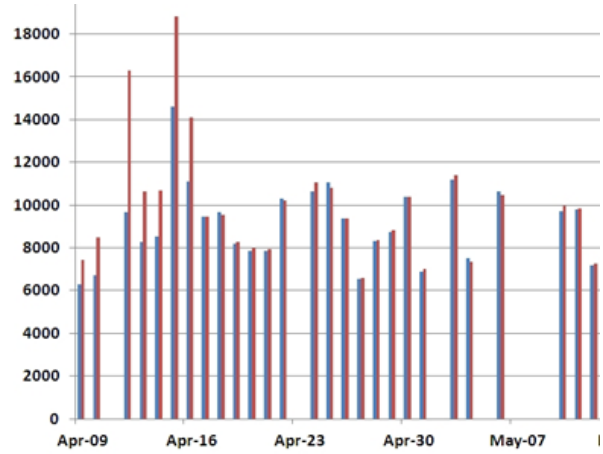

AD1, SMPS of ECN (red) and GGD (blue)

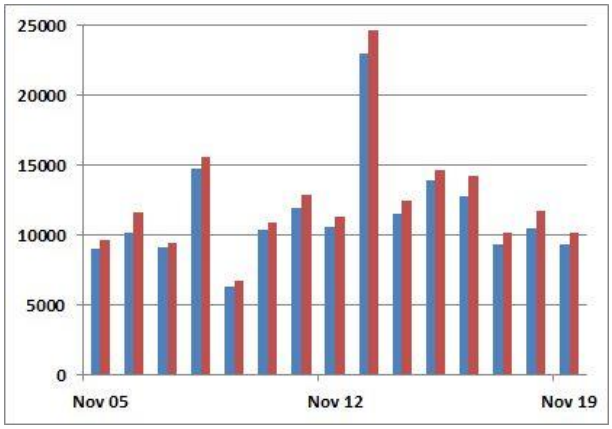

AP1, SMPS of ECN (red) and VMM (blue)

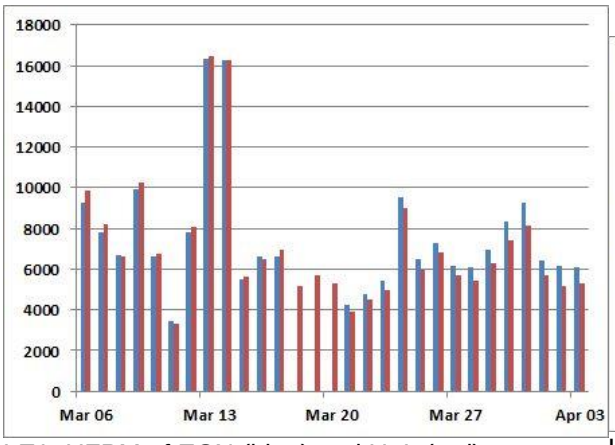

LE1, UFPM of ECN (blue) and UoL (red)

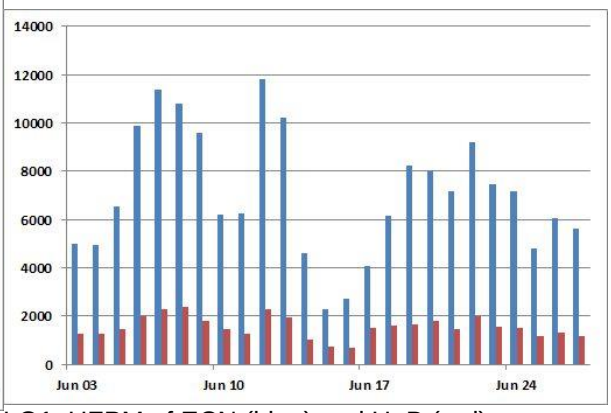

LO1, UFPM of ECN (blue) and UoB (red)

Figure 4.8: Daily averaged number concentrations for the SMPSs in the monitoring stations AD1S (GGD, Vondelpark) and AP1S (VMM, Borgerhout) and for the UFPM in the monitoring stations LE1S (UoL, Leicester University) and LO1S (UoB, Eltham) compared to the instruments in the trailer (ECN SMPS or ECN UFPM, reference instruments).

Only the last channel suffers from poor comparability (R^2 = 0.05) but the others channels have consistent comparability (R^2 > 0.79). The regressions are (Figure 4.9):

- 20-30 nm $UFPM_{trailer} = 0.1949 \cdot UFPM_{station} + 25.4$
- 30-50 nm $UFPM_{trailer} = 0.1479 \cdot UFPM_{station} + 95.6$
- 50-70 nm $UFPM_{trailer} = 0.1355 \cdot UFPM_{station} + 41.1$
- 70-100 nm $UFPM_{trailer} = 0.1213 \cdot UFPM_{station} + 34.1$
- 100-200 nm $UFPM_{trailer} = 0.1520 \cdot UFPM_{station} + 7.8$

Therefore, the particle number concentrations measured by the UFPM in station LO1S were corrected using size channel-specific correction factors based on the above relationships. To evaluate the (corrected) UFPM time series for LO1S, 5-day and monthly correlations with the TNC quantified by the EPC were calculated and also a count of the number of NaNs reported by the UFPM was evaluated.

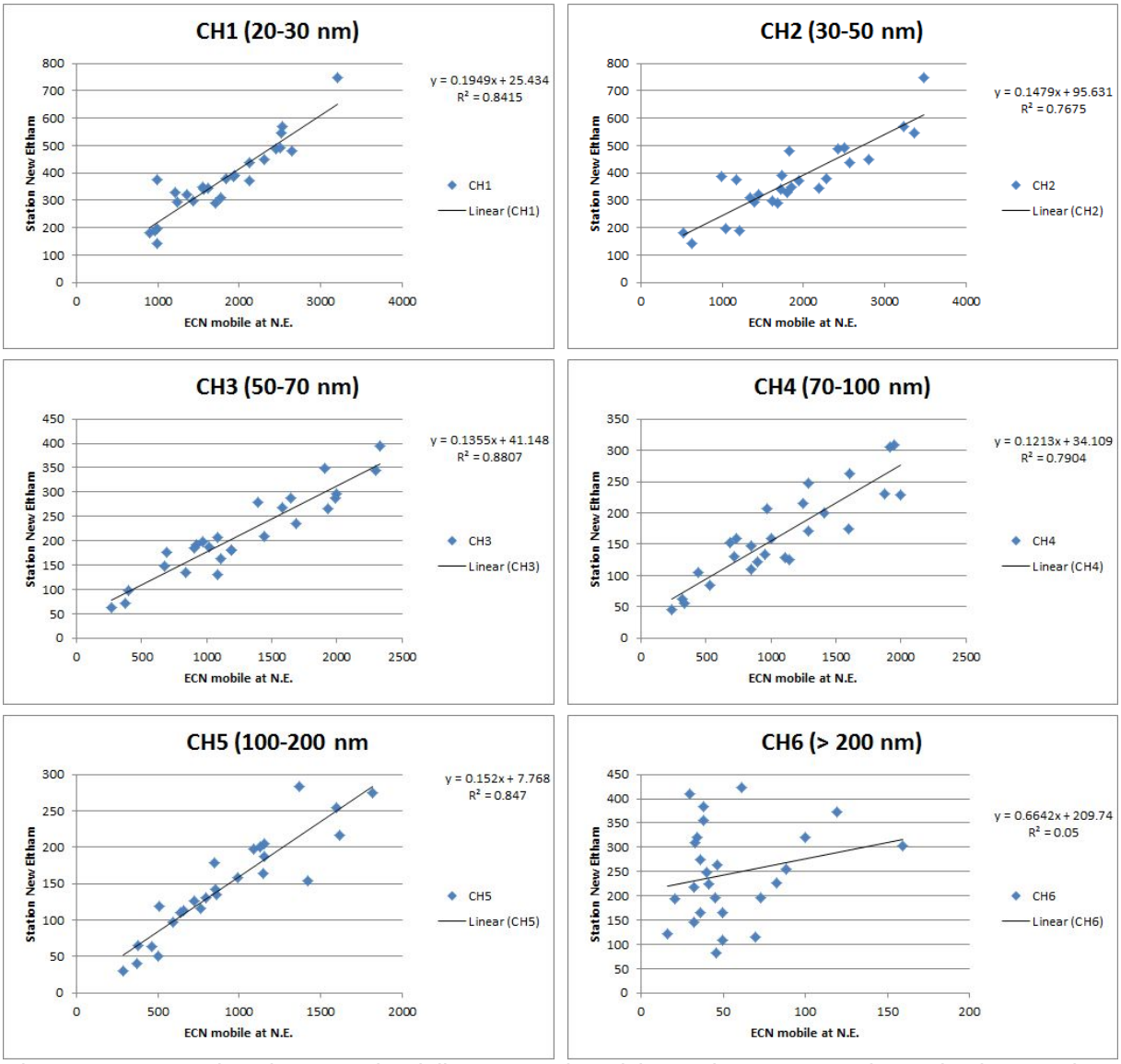

Figure 4.9: Comparison between the daily-averaged particle number concentrations, simultaneously quantified by the UFPM at the fixed LO1S site (New Eltham) and the UFPM in the ECN trailer (ECN mobile at New Eltham).

4.3.2 Scatterplots SMPS/UFPM

Daily or half-hourly average values were used to create correlation plots. Again, the SMPS or UFPM in the mobile station of ECN was selected as the reference instrument. Figure 4.10 shows the corresponding scatterplots for the 4 monitoring stations.

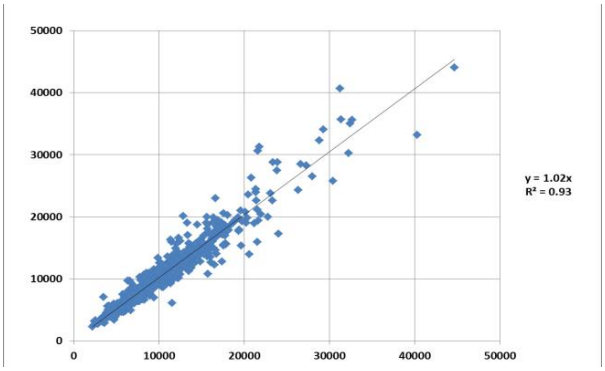

AD1, SMPS GGD vs. SMPS ECN

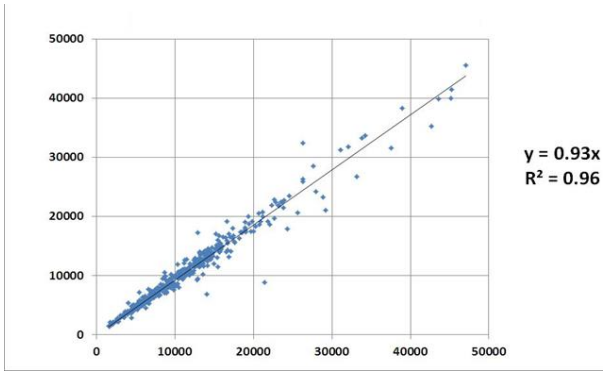

AP1, SMPS VMM vs. SMPS ECN

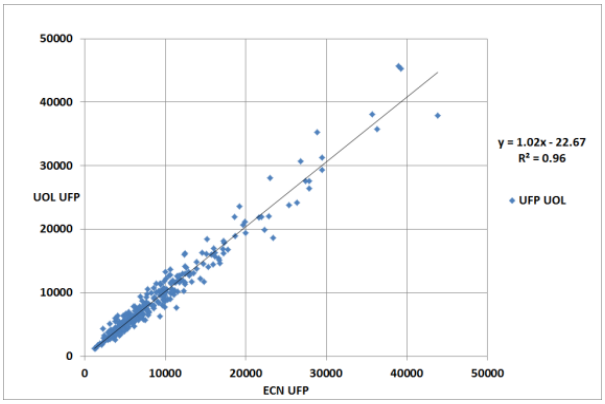

LE1, UFPM UoL vs. UFPM of ECN

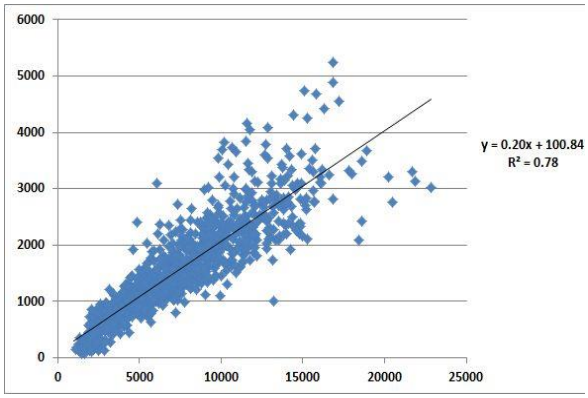

LO1, UFPM UoB vs. UFPM ECN

Figure 4.10: Scatterplots (half-hourly number concentrations) for the SMPSs in the monitoring stations AD1S (GGD, Vondelpark) and AP1S (VMM, Borgerhout) and for the UFPM in the monitoring stations LE1S (UoL, Leicester University) and LO1S (UoB, Eltham) compared to the instruments in the trailer (ECN SMPS or ECN UFPM, reference instruments).

4.3.3 Association between individual particle size classes (SMPS/UFPM)

To evaluate the association between the individual particle size classes, the trailer measurements were compared to the fixed site measurements for the periods in which the trailer was located next to the fixed monitoring sites. For each location, particle number concentrations of the same instrument type were compared (SMPS for Antwerp and Amsterdam, UFPM for Leicester and London). Spearman rank correlations and COD were calculated (Table 4.3) to evaluate the association between the aggregated size classes (10-20, 20-30, 30-50, 50-70, 70-100 and 100-200 nm).

Table 4.3 indicates fairly good agreement (COD = 0.13 to 0.29 and r_s = 0.8 to 0.95) between the fixed and trailer instruments for all sites, except for Amsterdam. For Amsterdam, at first considerable lower associations (COD = 0.30 to 0.34 and r_s = 0.74 to 0.78; not shown) were found between the trailer SMPS and the fixed site SMPS. This is due to the issues encountered in the trailer campaign in Amsterdam, described in section 4.1.3. The slider vane pumps of the fixed site had no filters at the start of the comparison (9 to 16 April). As the ECN trailer was closer to exhausts, higher values of BC and PN were obtained for the trailer measurements compared to the fixed site. All pumps were equipped with filters after 16 April 2013, which resulted in a better association. This can already be observed from the daily-averaged number concentrations in Figure 4.2. Indeed, when the data from 9-16 April was excluded, associations were much better (COD = 0.09 to 0.18 and r_s = 0.83 to 0.97; see Table 4.3) and comparable to the other sites.

Overall, the associations increased with increasing particle size (Table 4.3), which might be due to the short-lived nature of small-sized UFP, resulting in higher spatiotemporal variation, compared to the larger particles.

Table 4.3: Coefficients of divergence (COD) and Spearman rank correlations (r_s) between the size-resolved UFP instruments of the fixed site and the co-located ECN trailer for Amsterdam (SMPS), Antwerp (SMPS), Leicester (UFPM) and London (UFPM).

Size class	Amsterdam		Antwerp		Leicester		London*	
	COD	r_s	COD	r_s	COD	r_s	COD	r_s
10-20 nm	0.18	0.88	0.17	0.82	-	-	-	-
20- 30 nm	0.16	0.83	0.16	0.82	0.2	0.84	0.29	0.8
30-50 nm	0.12	0.87	0.14	0.85	0.16	0.85	0.17	0.86
50-70 nm	0.10	0.93	0.14	0.86	0.16	0.89	0.21	0.85
70-100 nm	0.10	0.96	0.14	0.91	0.15	0.92	0.2	0.82
100-200 nm	0.09	0.97	0.13	0.93	0.14	0.95	0.23	0.86

* Corrected number concentrations (see section 3.2.3.1).

4.3.4 Summarizing remarks SMPS/UFPM

The time series and scatterplots above clearly demonstrate a close correspondence with the sizing instruments in the mobile station of ECN in terms of accuracy (absolute value) and precision (correlation). However, for the UFPM measurements of UoB at New Eltham only the correlation is satisfactory, but absolute values differ a lot. This discrepancy made it necessary to check all the channels separately. By deriving a correction algorithm per size channel these data were corrected to fit the data as they were gathered by ECN during the comparison period (see section 4.3).

Table 4.4: Coefficient of determination (R^2) and regression coefficient for linear regressions between the SMPS/UPM in the trailer and the SMPS/UFPM in the monitoring stations.

Site	City (responsible)	Instrument	R^2	Regression coefficient
AD1	Amsterdam (GGD)	SMPS	0.98	1.00
AP1	Antwerp (VMM)	SMPS	0.96	0.93
LE1	Leicester (UoL)	UFPM	0.96	1.02
LO1	London (UoB)	UFPM	0.90	0.16

Table 4.4 summarizes the respective correlation and regression coefficients. Except for New Eltham, as explained, coefficients of determination (R^2) are 0.96 or higher indicating a very strong correlation. Regression coefficients for three stations are larger than 0.93 and around 1 even representing good comparability, but the poor agreement of the comparison at New Eltham is easily derived from the regression coefficient of only 0.16 and emphasizes once again that these data need significant corrections. However, daily averages were in good agreement and could be used for a correction of the UFPM data at Eltham. From the figures and table above it can be deducted that the spectra of the SMPS at Amsterdam and Antwerp agree well. The same applies for the size segregated concentrations of the UFPM in Leicester. The deviations (half-hourly) observed at New Eltham could be explained by local emissions at the parking lot nearby. However, daily averages were in good agreement and could be used for a correction of the UFPM data at New Eltham.

4.4 MAAP

The Multi Angle Absorption Photometers (MAAP) operated at the four permanent Joaquin sites have been compared with the MAAP in the ECN trailer (ECN MAAP). The MAAPs were operated following the same procedure. The comparison was done during the same campaigns as mentioned for the EPC, except at Leicester where the EPC was temporarily not available (see section 4.2).

4.4.1 Time series MAAP

Time series for the MAAP instruments collected during the four mobile campaigns are given below for half-hourly black carbon concentrations (Figure 4.11) and daily averages (Figure 4.12).

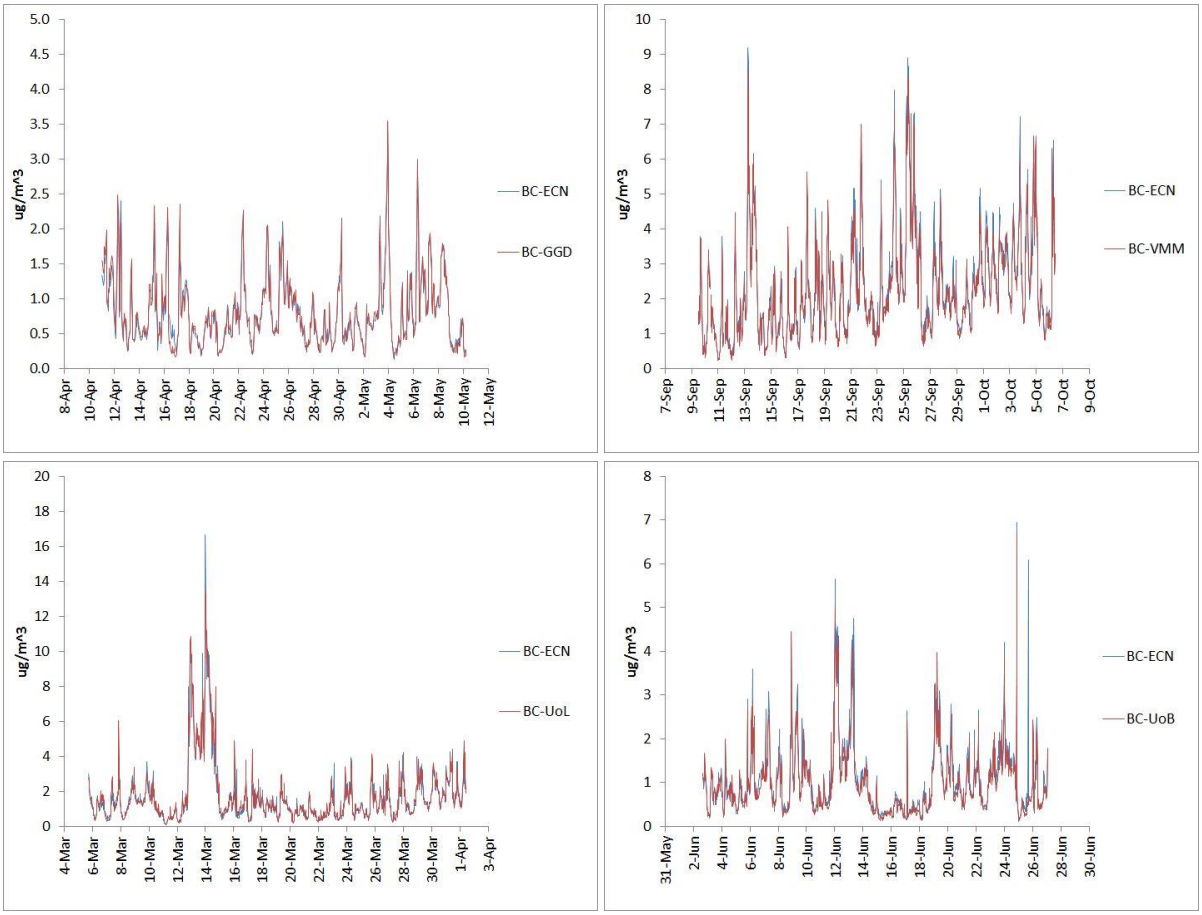

Figure 4.11: Half-hourly black carbon concentrations for the MAAPs in the monitoring stations AD1S (GGD, Vondelpark), AP1S (VMM, Borgerhout), LE1S (UoL, Leicester University) and LO1S (UoB, Eltham) compared to the reference MAAP in the trailer (ECN). Note the different vertical scaling.

Figure 4.12: Daily averaged black carbon concentrations for the MAAPs in the monitoring stations AD1S (GGD, Vondelpark), AP1S (VMM, Borgerhout), LE1S (UoL, Leicester University) and LO1S (UoB, Eltham) compared to the reference MAAP in the trailer (ECN).

4.4.2 Scatterplots MAAP

The half-hourly average values were also used to create correlation plots. Again, the ECN MAAP was selected as the reference instrument. Figure 4.13 shows the corresponding scatterplots for each monitoring station with BC measurements.

4.4.3 Summarizing remarks MAAP

Even more than was the case for the EPCs, the time series and scatterplots for the MAAP data sets shown above demonstrate the very close correspondence between the various instruments. Table 4.5 summarizes the respective correlation and regression coefficients. Coefficients of determination (R^2) are equal to or above 0.93 and regression coefficients are between 0.94 and 1.01.

Note that the ECN MAAP measures mean BC concentrations equally high (Amsterdam AD1, Leicester LE1) or slightly lower (Antwerp AP1, London LO1) than the MAAPs in the fixed monitoring stations. In Antwerp the mean lower BC value in the station than in the trailer may be due to the closer distance of the trailer to the main road.

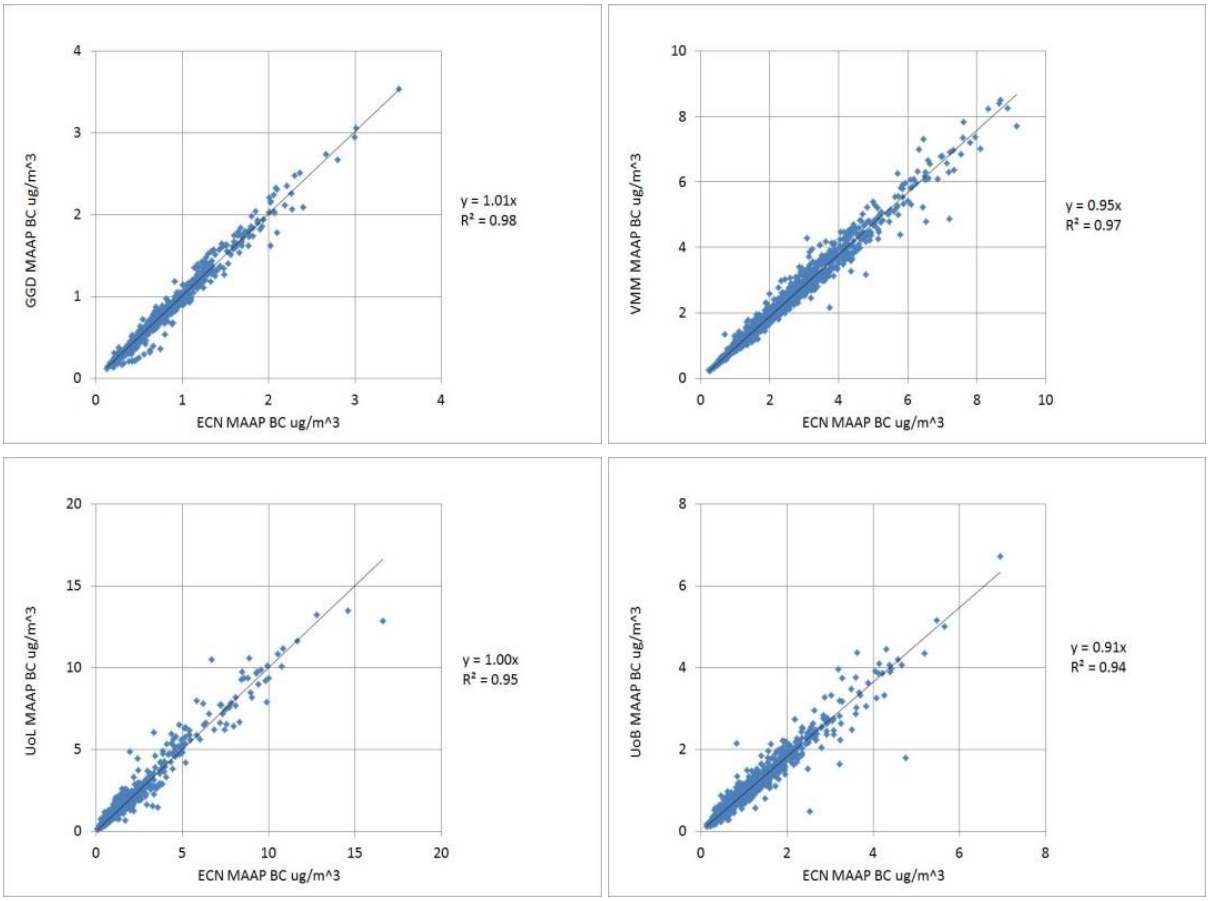

Figure 4.13: Scatterplots (half-hourly concentrations) of the MAAPs in the monitoring stations AD1S (GGD, Vondelpark), AP1S (VMM, Borgerhout), LE1S (UoL, Leicester University) and LO1S (UoB, Eltham) versus the MAAP in the trailer (ECN, reference instrument).

Table 4.5: Coefficient of determination (R^2) and regression coefficient for linear regressions between the MAAP in the trailer and the MAAPs in the monitoring stations.

Site	City (responsible)	R^2	Regression coefficient
AD1	Amsterdam (GGD)	0.98	1.01
AP1	Antwerp (VMM)	0.97	0.95
LE1	Leicester (UoL)	0.95	1.00
LO1	London (UoB)	0.94	0.91

5 UFP results for the WP1A1 monitoring stations

5.1 General data overview

Half-hourly air quality and meteorological data were collected for the entire sampling period, from April 2013 to March 2015. An overview of the availability of the air quality data is given in Table 5.1. Data coverage for all fixed Joaquin monitoring stations (AD1S, AP1S, LE1S, LO1S, LL1S and WZ1S) was between 67 and 98% for the common air pollutants (PM_{10}, $PM_{2.5}$, NO_2 and NO) (except for PM_{10}, which was not monitored in Leicester) (Table 5.1). Total particle number concentration (TNC), particle size distribution (PNC) and black carbon (BC) were sampled in Amsterdam, Antwerp, Leicester and London. These variables showed the lowest data coverage (27-50%) for London due to the late start of the measurements (April 2014), and problems with the PNC measurements with the UFPM, as explained before (section 4.3). Accounting for the later start in Leicester and London, the average data coverage for the six sites is 84% for TNC and 81% for PNC, which is comparable to the more usually monitored pollutants like NO_2 (92%), PM_{10} (94%) and $PM_{2.5}$ (90%).

Table 5.2 and Table 5.3 give the range (25% quartile, mean, 75% quartile and maximum) of the half-hourly-averaged and hourly-averaged air pollutants for all fixed Joaquin monitoring stations.

At the start of the multi-site data analysis a clear deviation was observed for the size-specific particle number concentrations measured at the station in London. The data of the UPFM in LO1S showed consistently lower particle counts (correlation in temporal behaviour, but with a constant factor ~4 offset) throughout the entire sampling period, even though the total particle concentration (TNC), measured by the EPC, was of the same order of magnitude as at the other monitoring sites (Table 5.2). The TSI 3031 instrument was revised by the manufacturer (TSI and Topas) to evaluate the possibility for derivation of calibration factors to correct the obtained time series of data.

Eventually the entire size-resolved UFP time series was corrected using calibration factors derived by ECN, based on the half-hourly UFP measurements of the Grimm SMPS during the co-location of the ECN trailer in London (from 2/6/2014 to 27/6/2014, see section 3.2.3.1). To evaluate the (corrected) UFPM time series,5-day and monthly correlations with the TNC quantified by the EPC were calculated and also a count of the number of NaNs reported by the UFPM was evaluated. When the UFPM stopped tracking the EPC TNC and the NaN count increased above the baseline level, it was decided to make a break in the data. This point was 01/01/2015; before this the data can be considered fully ratified, after this point it is considered unratified. Therefore, all further analyses for London are based on the corrected UFPM data before 01/01/2015.

Table 5.1: Half-hourly air quality data availability for all fixed Joaquin monitoring stations (AD1S, AP1S, LE1S, LL1S, LO1S and WZ1S) during the considered sampling period (April 2013 to December 2014). Data availability is evaluated for PM_{10}, $PM_{2.5}$, NO_2, NO, BC, total particle number concentration (TNC) and size-specific particle number concentration (PNC).

Station	Start	Stop	Observations	PM_{10}		$PM_{2,5}$		NO_2		NO		BC		TNC		PNC		Total availability
			#	NA's	%	NA's	%	NA's	%	NA's	%	NA's	%	NA's	%	NA's	%	%
Amsterdam (AD1S)	01/04/2013	31/03/2015	35040	848	**98**	1074	**97**	1698	**95**	1698	**95**	240	**99**	6034	**83**	9660	**72**	**91**
Antwerp (AP1S)	01/04/2013	31/03/2015	35040	3287	**91**	2560	**93**	2478	**93**	2478	**93**	734	**98**	4583	**87**	5765	**84**	**91**
Leicester (LE1S)	01/04/2013	31/03/2015	35040	-	**-**	11008	**69**	5014	**86**	5008	**86**	4849	**86**	13500	**61**	12731	**64**	**75**
London (LO1S)	01/04/2013	31/03/2015	35040	2600	**93**	11634	**67**	6814	**81**	6786	**81**	17678	**50**	24881	**29**	25451	**27**	**61**
Lille (LL1S)	01/04/2013	31/03/2015	35040	1076	**97**	2712	**92**	645	**98**	940	**97**	-	**-**	-	**-**	-	**-**	**96**
Wijk aan Zee (WZ1S)	01/04/2013	31/03/2015	35040	836	**98**	1030	**97**	1032	**97**	1032	**97**	-	**-**	-	**-**	-	**-**	**97**

Note:
- TNC and PNC measurements in LE1S started in Oct 2013
- TNC, PNC and BC measurements in LO1S started in Apr 2014

Table 5.2: Overview of half-hourly and hourly air quality data (PM_{10}, $PM_{2.5}$, NO_2, NO, BC and TNC) for the considered sampling period in the fixed Joaquin monitoring stations (AD1S, AP1S, LE1S, LL1S, LO1S and WZ1S).

	Half-hourly						Hourly					
	Amsterdam	Antwerp	Leicester	London	Lille	Wijk aan Zee	Amsterdam	Antwerp	Leicester	London	Lille	Wijk aan Zee
PM_{10} (µg/m^3)												
25% quartile	12.24	15.00	-	11.30	12.50	14.54	12.24	15.62	-	11.35	12.78	14.54
mean	20.64	25.99	-	18.64	22.35	25.80	20.64	25.96	-	18.67	22.75	25.80
75% quartile	25.21	32.50	-	22.50	28.00	32.57	25.21	31.88	-	22.45	28.75	32.57
max	227.50	176.25	-	122.50	437.50	258.40	227.50	162.70	-	120.65	316.75	258.40
$PM_{2.5}$ (µg/m^3)												
25% quartile	6.82	7.00	6.70	6.10	8.00	6.82	6.82	7.00	6.70	6.10	8.13	6.82
mean	14.24	16.17	13.47	13.00	16.32	15.40	14.24	16.15	13.47	13.00	16.75	15.40
75% quartile	17.66	20.47	16.70	15.90	20.50	20.26	17.66	20.47	16.70	15.90	21.00	20.26
max	225.30	145.00	181.00	90.40	357.00	191.00	225.30	144.00	181.00	90.40	256.00	191.00
NO_2 (µg/m^3)												
25% quartile	14.00	24.00	14.20	9.20	12.50	5.80	14.00	24.50	14.50	9.20	13.15	5.80
mean	25.49	41.37	27.13	20.63	23.12	20.63	25.49	41.33	27.13	20.63	24.08	20.63
75% quartile	34.00	55.00	36.20	28.60	30.65	32.00	34.00	54.50	36.10	28.60	32.15	32.00
max	107.00	242.00	117.80	105.70	229.50	99.00	107.00	233.50	110.75	105.70	112.50	99.00
NO (µg/m^3)												
25% quartile	0.40	2.00	1.80	1.30	1.00	0.00	0.40	2.00	1.90	1.30	1.15	0.00
mean	4.89	17.56	11.07	6.60	7.95	6.92	4.89	17.53	11.07	6.60	8.65	6.92
75% quartile	4.00	18.00	10.60	4.90	7.10	5.00	4.00	18.50	10.85	4.90	7.69	5.00
max	230.03	784.00	540.00	321.10	475.50	291.00	230.03	656.00	429.15	321.10	403.50	291.00
BC (µg/m^3)												
25% quartile	0.49	1.11	0.61	0.52	-	-	0.49	1.12	0.63	0.53	-	-
mean	1.01	2.36	1.40	1.22	-	-	1.01	2.36	1.40	1.22	-	-
75% quartile	1.29	3.00	1.70	1.49	-	-	1.29	3.00	1.71	1.50	-	-
max	9.56	19.52	16.05	12.13	-	-	9.56	18.68	16.04	11.89	-	-
TNC (#/cm^3)												
25% quartile	5889	8713	4760	5230	-	-	5956	8799	4840	5297	-	-
mean	9070	13481	8623	8353	-	-	9067	13480	8624	8353	-	-
75% quartile	10952	16538	10916	10506	-	-	11000	16502	10931	10477	-	-
max	76549	76170	63481	45155	-	-	58411	72223	60413	39511	-	-

Table 5.3: Overview of half-hourly and hourly size specific particle number concentrations (# cm^{-3}) for the considered sampling period and the fixed Joaquin monitoring stations (AD1S, AP1S, LE1S, LO1S, LL1S and WZ1S). All size-resolved UFP data of London (*) was corrected with calibration factors provided by ECN.

	Half-hourly						Hourly					
	Amsterdam	Antwerp	Leicester	London	Lille	Wijk aan Zee	Amsterdam	Antwerp	Leicester	London*	Lille	Wijk aan Zee
PNC 10-20 nm (#/cm^3)												
25% quartile	1125	1327	-	-	-	-	1154	1361	-	-	-	-
mean	2592	2468	-	-	-	-	2593	2467	-	-	-	-
75% quartile	2956	3093	-	-	-	-	2991	3109	-	-	-	-
max	56575	35412	-	-	-	-	29500	23645	-	-	-	-
PNC 20-30 nm (#/cm^3)												
25% quartile	805	974	755	475*	-	-	820	998	778	501*	-	-
mean	1552	1709	1541	1007*	-	-	1551	1709	1541	1016*	-	-
75% quartile	1773	2112	2001	1191*	-	-	1780	2114	2001	1194*	-	-
max	39199	19634	13795	29072*	-	-	20310	14250	13724	24103*	-	-
PNC 30-50 nm (#/cm^3)												
25% quartile	1031	1278	891	811*	-	-	1052	1302	920	841*	-	-
mean	1773	2195	1774	1539*	-	-	1771	2195	1774	1557*	-	-
75% quartile	2163	2704	2227	1946*	-	-	2164	2702	2231	1962*	-	-
max	19756	26669	16641	22534*			18518	21470	13213	20818*		
PNC 50-70 nm (#/cm^3)												
25% quartile	537	717	594	426*	-	-	545	722	616	443*	-	-
mean	950	1267	1247	809*	-	-	949	1267	1248	820*	-	-
75% quartile	1215	1598	1539	1042*	-	-	1213	1593	1550	1054*	-	-
max	8907	15387	14614	8959*	-	-	5266	9427	12369	6033*	-	-
PNC 70-100 nm (#/cm^3)												
25% quartile	362	553	504	400*	-	-	366	560	521	418*	-	-
mean	759	1063	1112	776*	-	-	758	1063	1112	787*	-	-
75% quartile	1026	1382	1363	1012*	-	-	1027	1384	1365	1025*	-	-
max	5546	5765	17444	10074*	-	-	5502	8891	14602	5908*	-	-
PNC 100-200 nm (#/cm^3)												
25% quartile	363	604	447	319*	-	-	367	612	461	341*	-	-
mean	807	1182	1010	711*	-	-	807	1183	1010	722*	-	-
75% quartile	1069	1531	1233	936*	-	-	1067	1535	1239	951*	-	-
max	20116	11903	19702	12707*	-	-	10646	11602	16005	7751*	-	-

As shown in Figure 5.1, the considered monitoring sites have comparable concentration variability. Nevertheless, the Antwerp monitoring site shows much higher concentrations for the traffic-related pollutants (NO_2, BC and TNC). This can probably be explained by its proximity (30 m) to a traffic-intensive access road (Plantin en Moretuslei). In February and October 2013, the mean traffic intensity was 32000 vehicles on week days and 23500 vehicles in the weekend, or a time-weighted average of 29500 vehicles/day (VMM 2014).

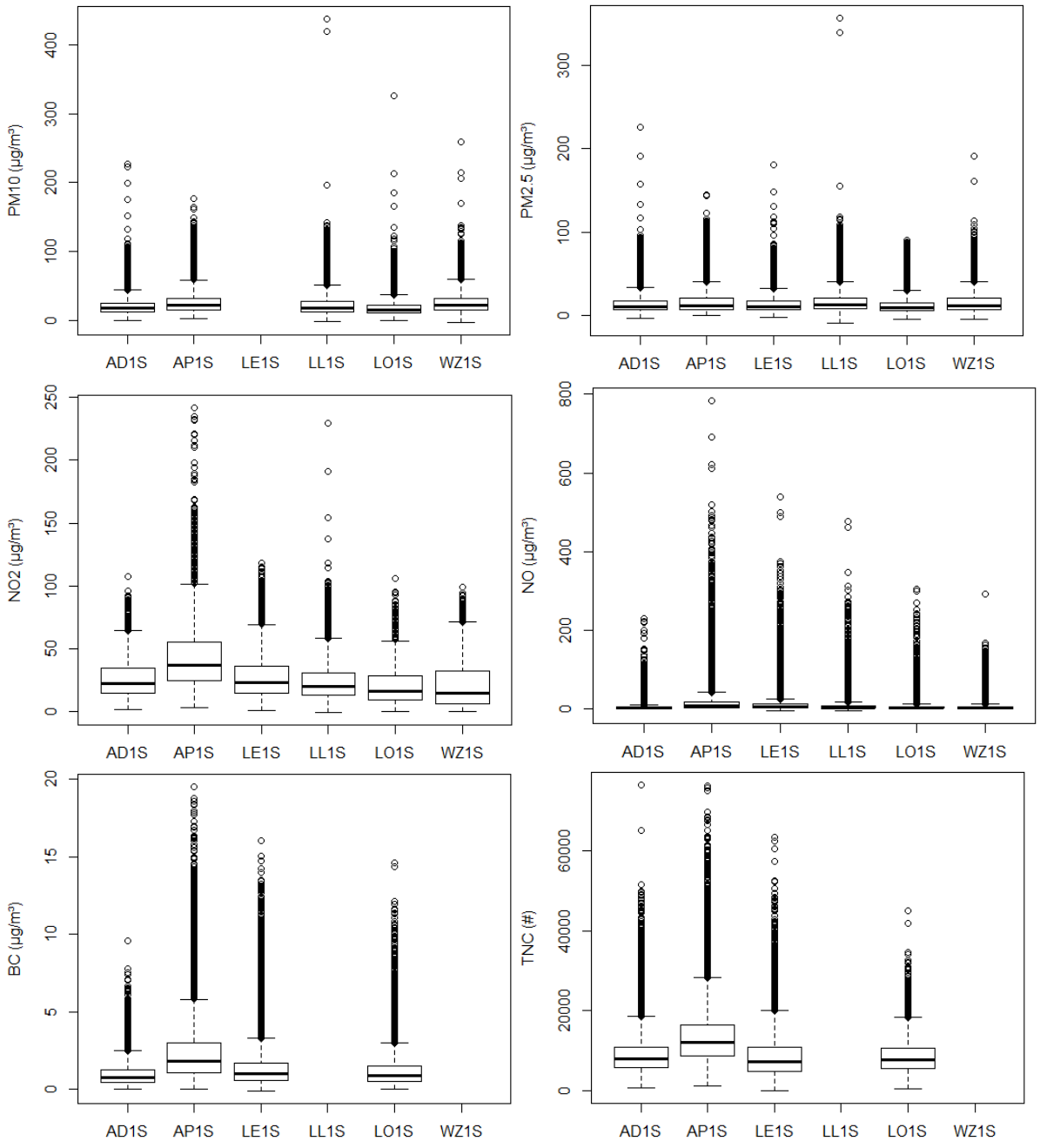

Figure 5.1: Boxplots of PM_{10}, $PM_{2.5}$, NO_2, NO, BC and TNC for the considered monitoring period and all fixed Joaquin stations (AD1S, AP1S, LE1S, LL1S, LO1S and WZ1S).

Figure 5.2 demonstrates the daily averaged pollutant concentrations (75% half-hourly data threshold) for all considered monitoring sites during the envisaged monitoring period (from 1 April 2013 to 31 March 2015). Please note that UFP (TNC and size-resolved) and BC measurements were only conducted in the stations in Amsterdam (AD1S), Antwerp (AP1S), Leicester (LO1S) and London (LO1S). Moreover, size-resolved UFP measurements in Leicester and London were not obtained in

the smallest particle size range (10-20 nm) due to size range restrictions of the applied UFPM instruments (20-500 nm).

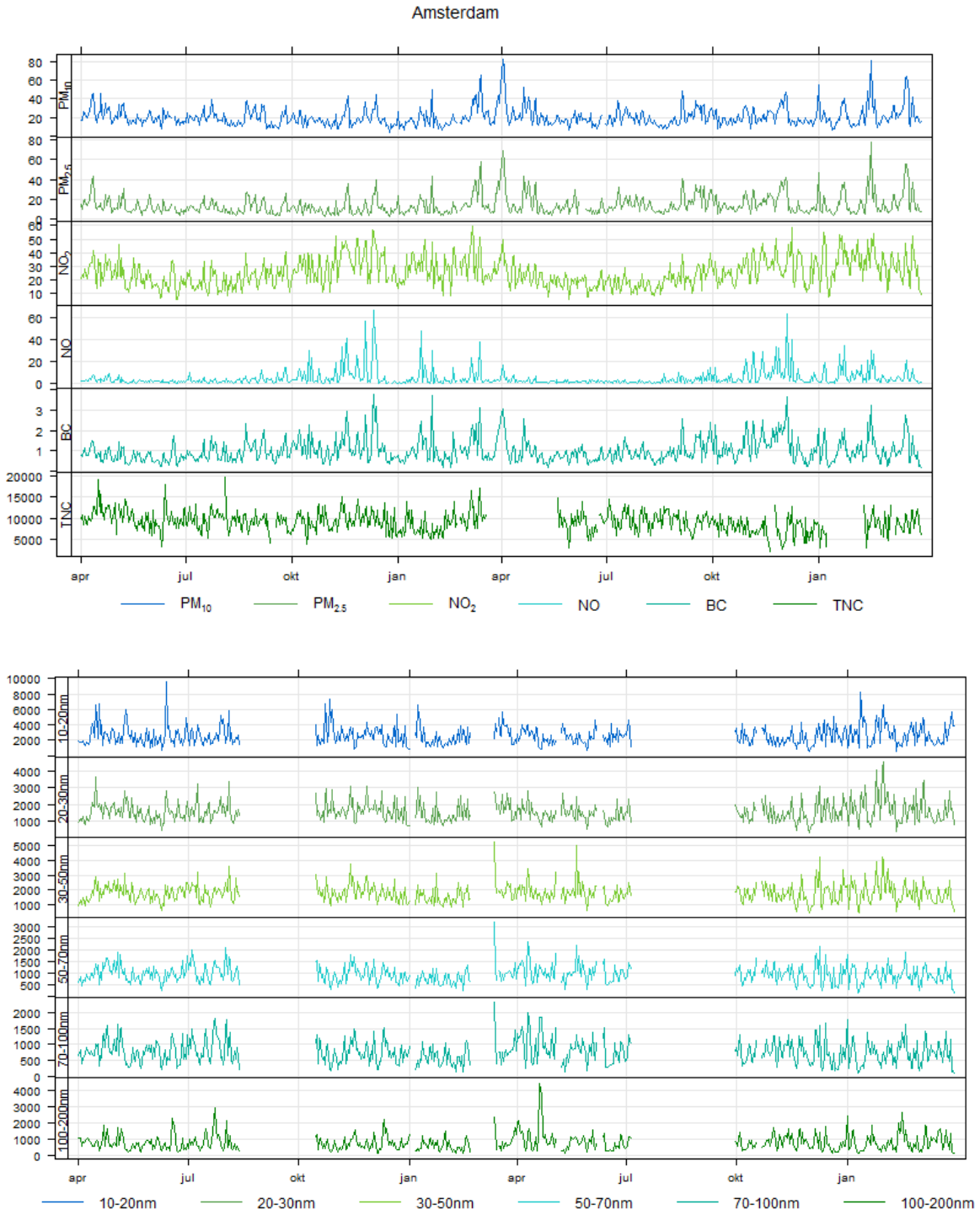

Figure 5.2: Daily averaged (75% half-hourly data threshold) concentrations of PM_{10}, $PM_{2.5}$, NO_2, NO, BC, TNC (upper) and size-resolved UFP (lower) during the envisaged monitoring period (April 2013 - March 2015) in Amsterdam, the Netherlands (AD1S).

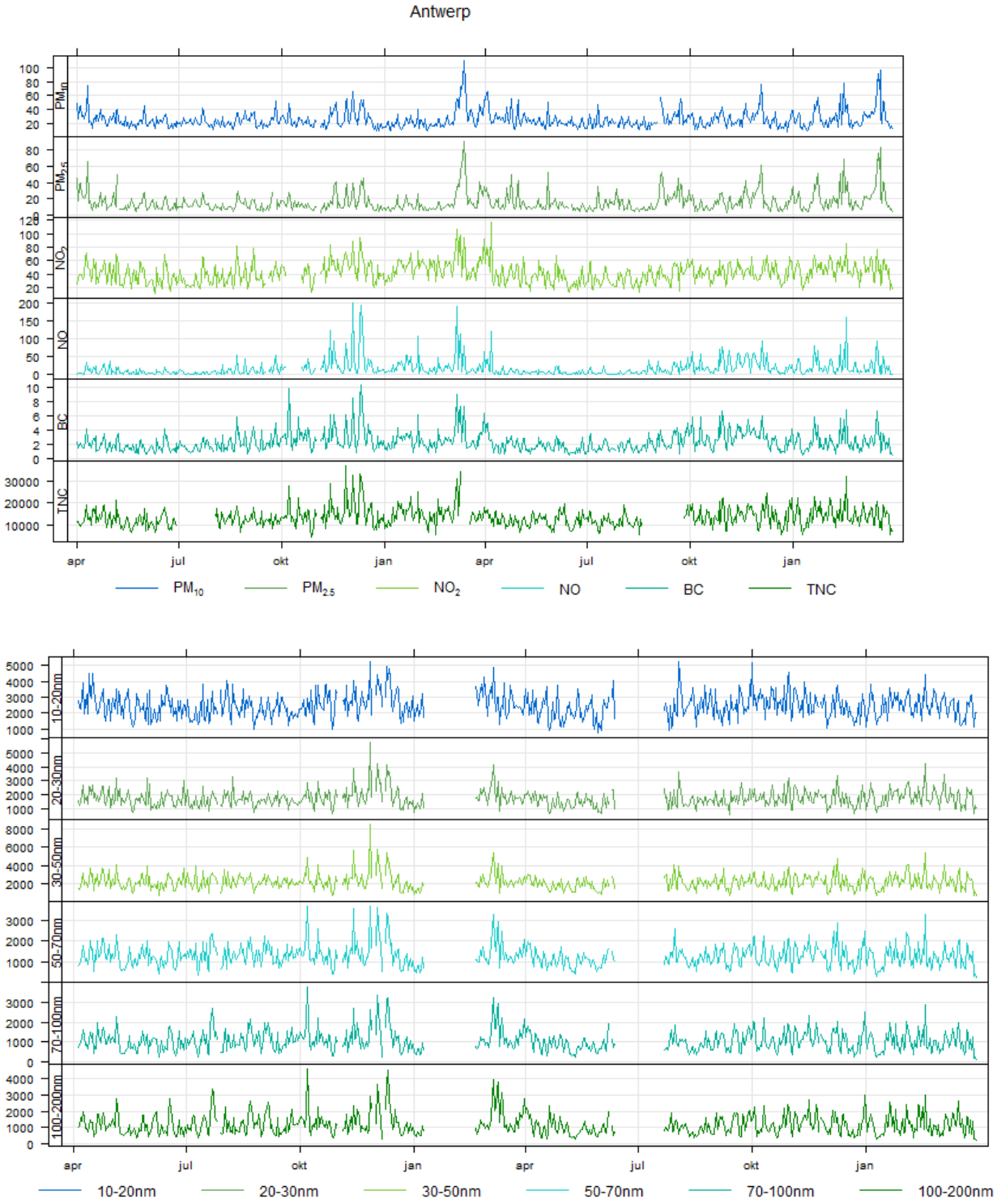

Figure 5.3: Daily averaged (75% half-hourly data threshold) concentrations of PM_{10}, $PM_{2.5}$, NO_2, NO, BC, TNC (upper) and size-resolved UFP (lower) during the envisaged monitoring period (April 2013 - March 2015) in Antwerp, Belgium (AP1S).

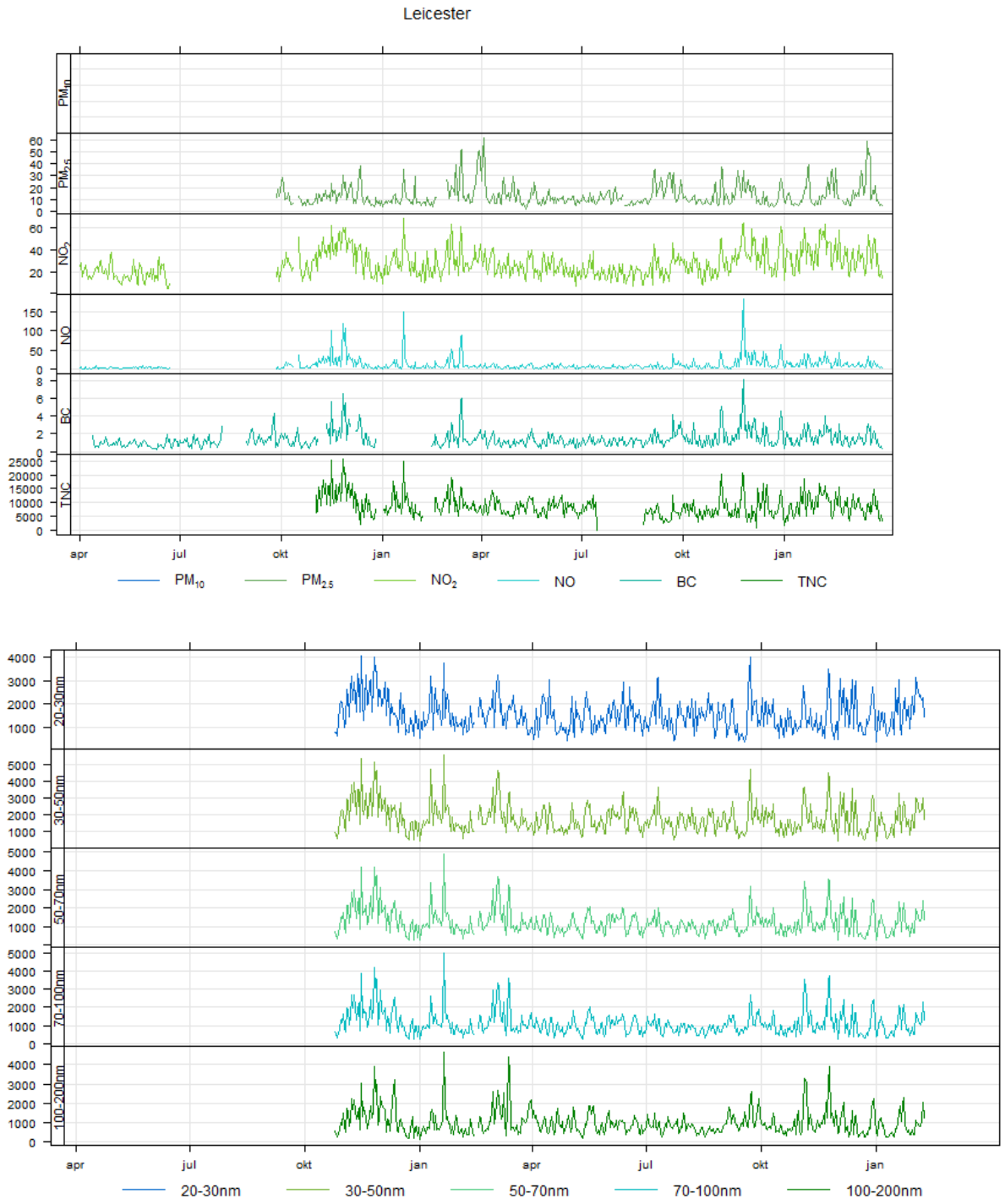

Figure 5.4: Daily averaged (75% half-hourly data threshold) concentrations of PM_{10}, $PM_{2.5}$, NO_2, NO, BC, TNC (upper) and size-resolved UFP (lower) during the envisaged monitoring period (April 2013 - March 2015) in Leicester, UK (LE1S).

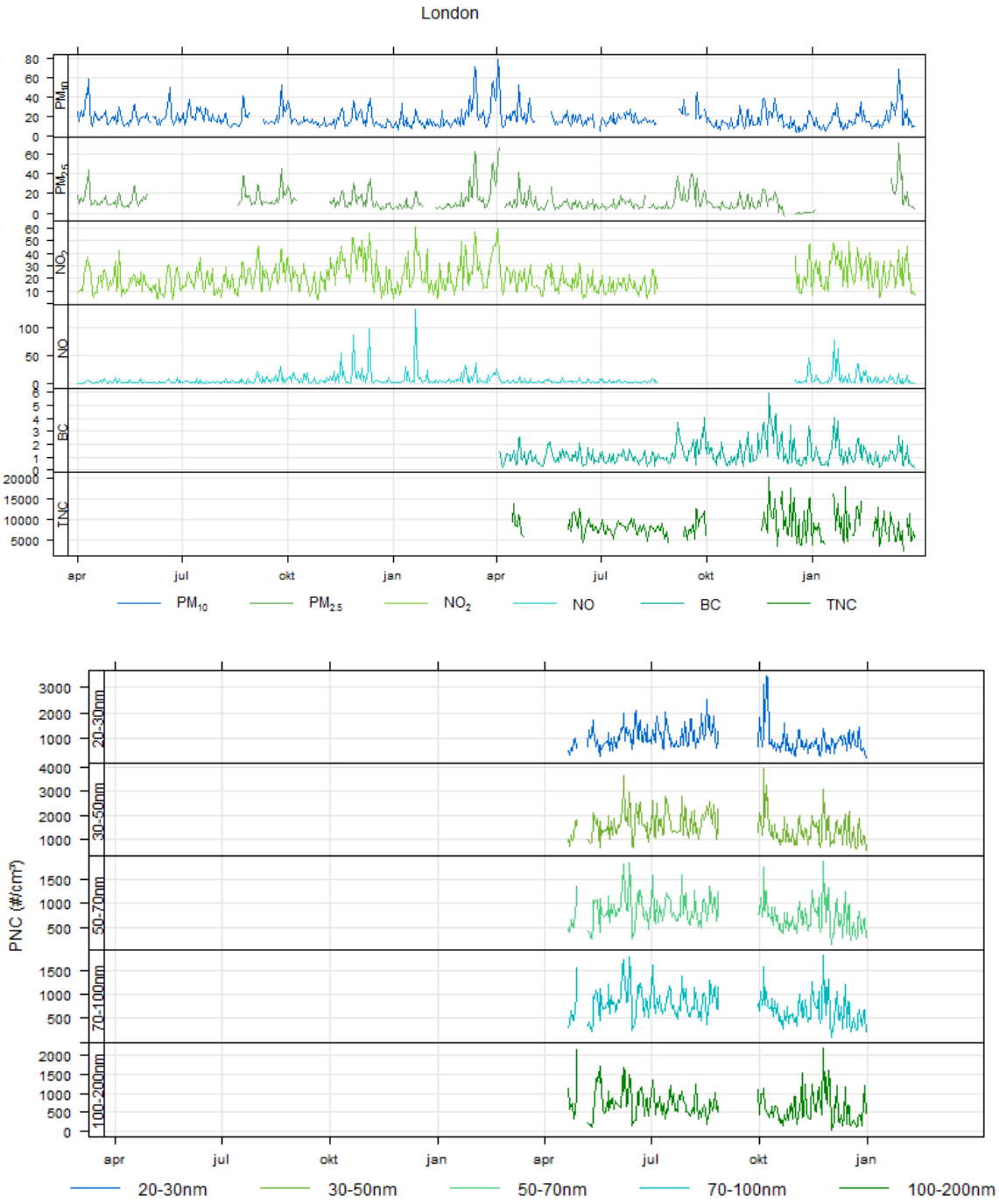

Figure 5.5: Daily averaged (75% half-hourly data threshold) concentrations of PM_{10}, $PM_{2.5}$, NO_2, NO, BC, TNC (upper) and size-resolved UFP (lower) during the envisaged monitoring period (April 2013 - March 2015) in London, UK (LO1S).

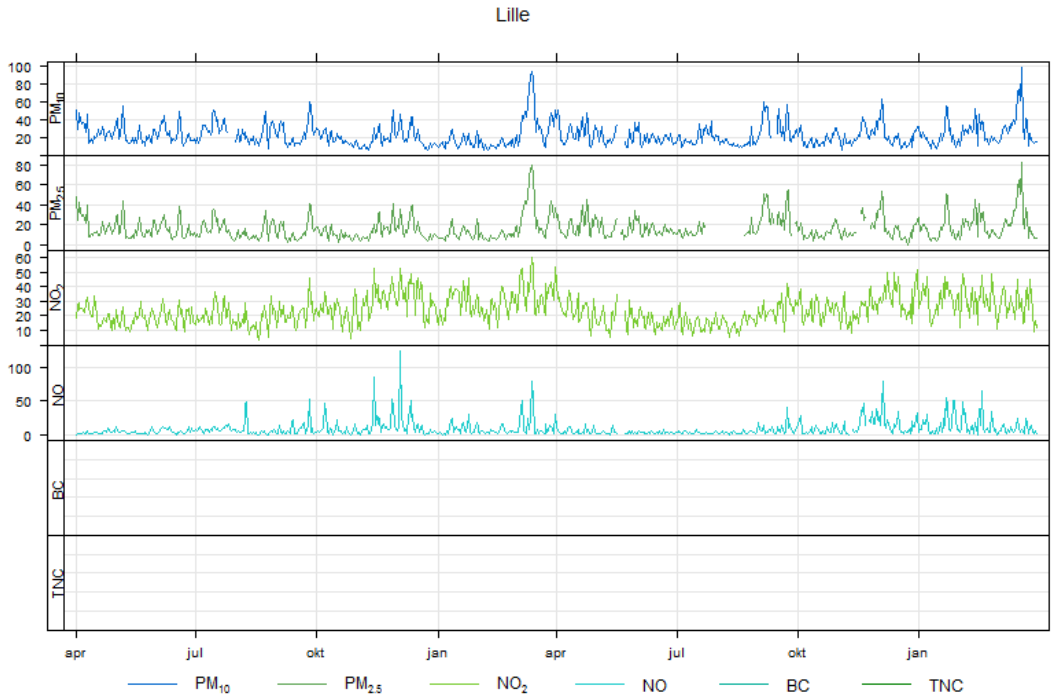

Figure 5.6: Daily averaged (75% half-hourly data threshold) concentrations of PM_{10}, $PM_{2.5}$, NO_2, NO, BC, TNC during the envisaged monitoring period (April 2013 - March 2015) in Lille, France (LL1S).

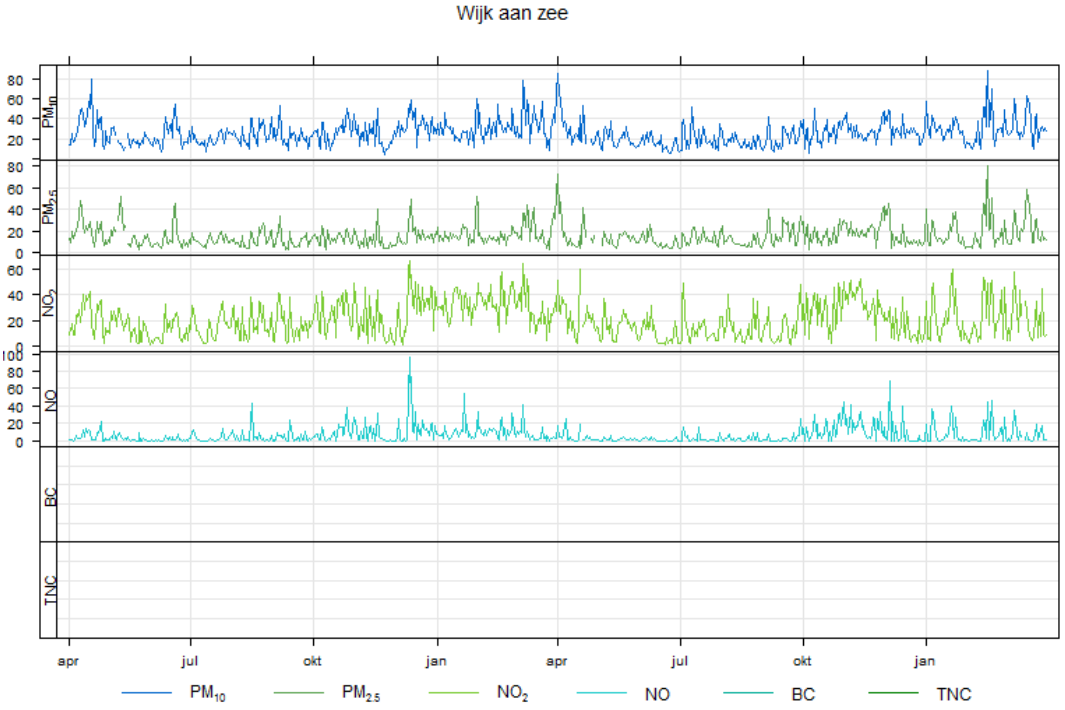

Figure 5.7: Daily averaged (75% half-hourly data threshold) concentrations of PM_{10}, $PM_{2.5}$, NO_2, NO, BC, TNC during the envisaged monitoring period (April 2013 - March 2015) in Wijk aan Zee, the Netherlands (WZ1S).

5.2 Specific UFP events

The temporal variation for the UFP concentrations throughout the Joaquin monitoring period (Figure 5.2 to Figure 5.5) shows distinct higher or lower concentrations on specific days. To explain these pollution events, information on specific dates/events (e.g. car free day, fireworks, bonfires, …) that might have influenced atmospheric pollutant concentrations was collected for Amsterdam, Antwerp,

Leicester and London. Based on expert knowledge, a list of potential pollution events was compiled (Table 5.4) and compared to the measured UFP concentrations. Also days with PM_{10} exceedances (>50 µg m^{-3}) at the fixed monitoring sites (see Annex 2) were included in Table 5.4. As no PM_{10} measurements were available for the Leicester site (LE1S), days with $PM_{2.5}$ exceedances (>25 µg m^{-3}) were used instead (Annex 2).

Table 5.4: List of events in Amsterdam, Antwerp, London and Leicester that might influence the measured concentrations of ultrafine particles within the considered cities.

Leicester

	Date	Name	Description
1	06/05/2013	Bank holiday	Reduced traffic, increased barbeques
2	27/05/2013	Bank holiday	Reduced traffic, increased barbeques
3	26/08/2013	Bank holiday	Reduced traffic, increased barbeques
4	1-2/10/2013	>25 µg/m³	>25 µg/m³ $PM_{2.5}$
5	2-3/11/2013	Guy Fawkes Night	Fireworks & bonfires
6	3-7/11/2013	Diwali	Fireworks
7	05/11/2013	Guy Fawkes Night	Fireworks & bonfires
8	26/11/2013	>25 µg/m³	>25 µg/m³ $PM_{2.5}$
9	11-12/12/2013	>25 µg/m³	>25 µg/m³ PM+
10	25-26/12/13	Bank holiday	Reduced traffic
11	31/12/2013	New Year's Eve	Fireworks
12	20/01/2014	>25 µg/m³	>25 µg/m³ $PM_{2.5}$
13	30/01/2014	>25 µg/m³	>25 µg/m³ $PM_{2.5}$
14	8-9/03/2014	>25 µg/m³	>25 µg/m³ $PM_{2.5}$
15	28-31/03/2014	>25 µg/m³	>25 µg/m³ $PM_{2.5}$
16	1-4/04/2014	>25 µg/m³	>25 µg/m³ $PM_{2.5}$
17	18/04/2014	Bank holiday	Reduced traffic, increased barbeques
18	21/04/2014	Bank holiday	Reduced traffic, increased barbeques
19	29/04/2014	>25 µg/m³	>25 µg/m³ $PM_{2.5}$
20	05/05/2014	Bank holiday	Reduced traffic, increased barbeques
21	5-6/09/2014	>25 µg/m³	>25 µg/m³ $PM_{2.5}$
22	11/09/2014	>25 µg/m³	>25 µg/m³ $PM_{2.5}$
23	17-19/9/2014	>25 µg/m³	>25 µg/m³ $PM_{2.5}$
24	22-23/09/2014	>25 µg/m³	>25 µg/m³ $PM_{2.5}$
25	29/09/2014	>25 µg/m³	>25 µg/m³ $PM_{2.5}$
26	1-2/11/2014	Guy Fawkes Night	Fireworks & bonfires
27	05/11/2014	Guy Fawkes Night	Fireworks & bonfires
28	5-6/11/2014	>25 µg/m³	>25 µg/m³ $PM_{2.5}$
29	20-21/11/2014	>25 µg/m³	>25 µg/m³ $PM_{2.5}$
30	23-27/11/2014	Diwali	Fireworks
31	25/11/2014	>25 µg/m³	>25 µg/m³ $PM_{2.5}$
32	29/11/2014	>25 µg/m³	>25 µg/m³ $PM_{2.5}$
33	29/12/2014	>25 µg/m³	>25 µg/m³ $PM_{2.5}$
34	31/12/2014	New Year's Eve	Fireworks
35	22-23/1/2015	>25 µg/m³	>25 µg/m³ $PM_{2.5}$
36	09/02/2015	>25 µg/m³	>25 µg/m³ $PM_{2.5}$
37	12-14/02/2015	>25 µg/m³	>25 µg/m³ $PM_{2.5}$
38	17/02/2015	>25 µg/m³	>25 µg/m³ $PM_{2.5}$
39	12-13/03/2015	>25 µg/m³	>25 µg/m³ $PM_{2.5}$
40	16-20/03/2015	>25 µg/m³	>25 µg/m³ $PM_{2.5}$

Antwerp

	Date	Name	Description
1	10/04/2013	>50µg/m³	>50 µg/m³ PM_{10}
2	15/09/2013	Autoluwe zondag	Carfree day
3	14/11/2013	>50µg/m³	>50 µg/m³ PM_{10}
4	24/11/2013	>50µg/m³	>50 µg/m³ PM_{10}
5	03/12/2013	>50µg/m³	>50 µg/m³ PM_{10}
6	11/12/2013	>50µg/m³	>50 µg/m³ PM_{10}
7	13/12/2013	>50µg/m³	>50 µg/m³ PM_{10}
8	31/12/2013	New year's eve	Fireworks
9	11/01/2014	Christmas bonfires	Bonfires Linkeroever
10	06/03/2014	>50µg/m³	>50 µg/m³ PM_{10}
11	07/03/2014	>50µg/m³	>50 µg/m³ PM_{10}
12	10/03/2014	>70 µg/m³	>70 µg/m³ PM_{10}
13	11/03/2014	>70 µg/m³	>70 µg/m³ PM_{10}
14	12/03/2014	>70 µg/m³	>70 µg/m³ PM_{10}
15	13/03/2014	SMOG event	SMOG alert
16	14/03/2014	SMOG event	SMOG alert
17	31/03/2014	>50µg/m³	>50 µg/m³ PM_{10}
18	1-3/04/2014	>50µg/m³	>50 µg/m³ PM_{10}
19	24/04/2014	>50µg/m³	>50 µg/m³ PM_{10}
20	30/04/2014	>50µg/m³	>50 µg/m³ PM_{10}
21	14/09/2014	Car-free day	Car-free day
22	02/12/2014	>50µg/m³	>50 µg/m³ PM_{10}
23	4-5/12/2014	>50µg/m³	>50 µg/m³ PM_{10}
24	31/12/2014	New year's eve	Fireworks
25	10/01/2015	Christmas bonfires	Bonfires Linkeroever
26	23/01/2015	>50µg/m³	>50 µg/m³ PM_{10}
27	12-13/02/2015	>50µg/m³	>50 µg/m³ PM_{10}
28	16/02/2015	>50µg/m³	>50 µg/m³ PM_{10}
29	17/03/2015	>70 µg/m³	>70 µg/m³ PM_{10}
30	18/03/2015	>70 µg/m³	>70 µg/m³ PM_{10}
31	19/03/2015	>70 µg/m³	>70 µg/m³ PM_{10}
32	20/03/2015	>70 µg/m³	>70 µg/m³ PM_{10}
33	23/03/2015	>50µg/m³	>50 µg/m³ PM_{10}

Amsterdam

	Date	Name	Description
1	31/12/2013	New year's eve	Fireworks
2	13-14/03/2014	>50 µg/m³	>50 µg/m³ PM_{10}
3	31/03/2014	>50 µg/m³	>50 µg/m³ PM_{10}
4	1-3/04/2014	>50 µg/m³	>50 µg/m³ PM_{10}
5	19/04/2014	>50 µg/m³	>50 µg/m³ PM_{10}
6	20/04/2014	Eastern	Wood burning (from eastern part of the Netherlands and Germany)
7	21/04/2014	Eastern	Wood burning (from eastern part of the Netherlands and Germany)
8	09/10/2014	Incident	Incident at Tata Steel, release of SO_2, CO and PM
9	10/10/2014	Incident	Incident at Tata Steel, release of SO_2, CO and PM
10	31/12/2014	New year's eve	Fireworks
11	01/01/2015	>50 µg/m³	>50 µg/m³ PM_{10}
12	15-16/02/2015	>50 µg/m³	>50 µg/m³ PM_{10}
13	17-19/03/2015	>50 µg/m³	>50 µg/m³ PM_{10}

London

	Date	Name	Description
1	10/04/2013	>50µg/m³	>50 µg/m³ PM_{10}
2	24/09/2013	Pollution episode	Pollution episode
3	25/09/2013	>50µg/m³	>50 µg/m³ PM_{10}
4	26/09/2013	Pollution episode	High PM episode
5	31/12/2013	New year's eve	Fireworks
6	12/03/2014	Pollution episode	Pollution episode
7	13/03/2014	>50µg/m³	>50 µg/m³ PM_{10}
8	14/03/2014	>50µg/m³	>50 µg/m³ PM_{10}
9	28/03/2014	>50µg/m³	>50 µg/m³ PM_{10}
10	29/03/2014	>50µg/m³	>50 µg/m³ PM_{10}
11	2-3/04/2014	>50µg/m³	>50 µg/m³ PM_{10}
12	31/12/2014	New year's eve	Fireworks
13	17/03/2015	>50µg/m³	>50 µg/m³ PM_{10}

A marked increase in PM_{10} and $PM_{2.5}$ can be observed during events with fireworks (e.g. new year's eve) with similar concentration peaks in total UFP numbers (TNC), most clearly observed in the larger particle size classes (>100 nm for Antwerp, >50 nm for Amsterdam). Most significant peaks are observed for Antwerp and Amsterdam which might be due to the respective distance of the monitoring sites to the fireworks event locations (± 3 km for Antwerp and Amsterdam, compared to ±16 km for London), and the fact that, aside from a few fireworks at private events, no large firework event is

organised in Leicester. In Leicester, fireworks and bonfires are traditionally organised in November, during Diwali and Guy Fawkes Night.

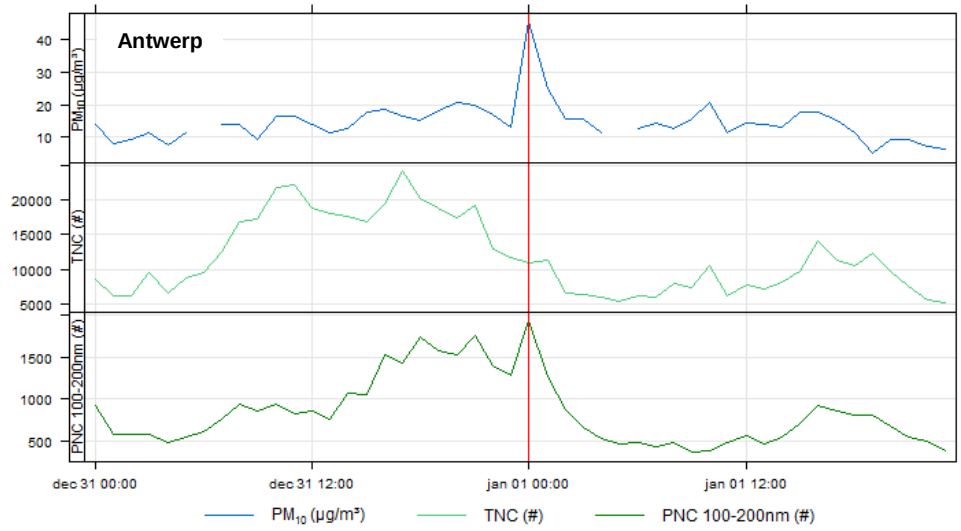

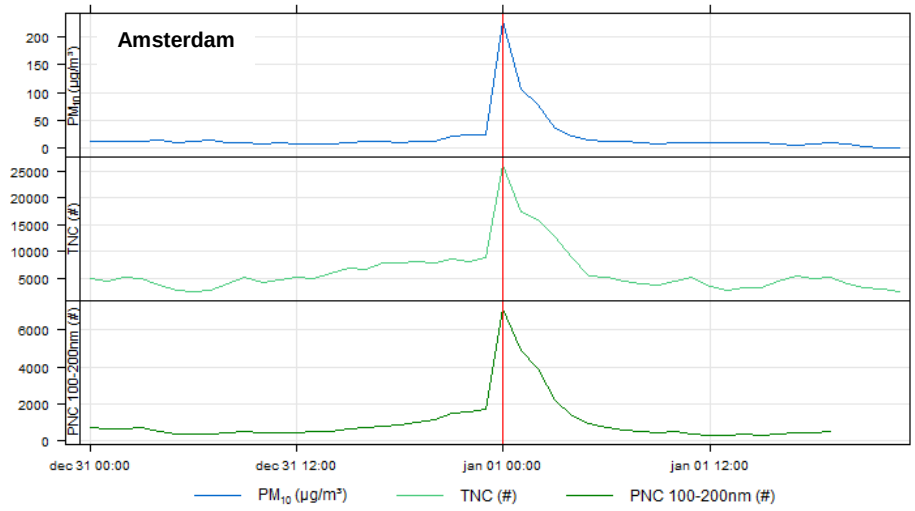

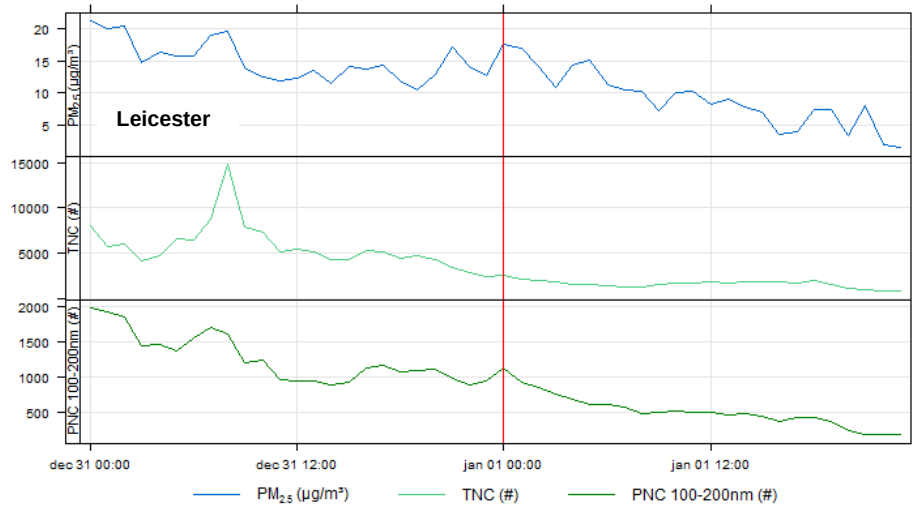

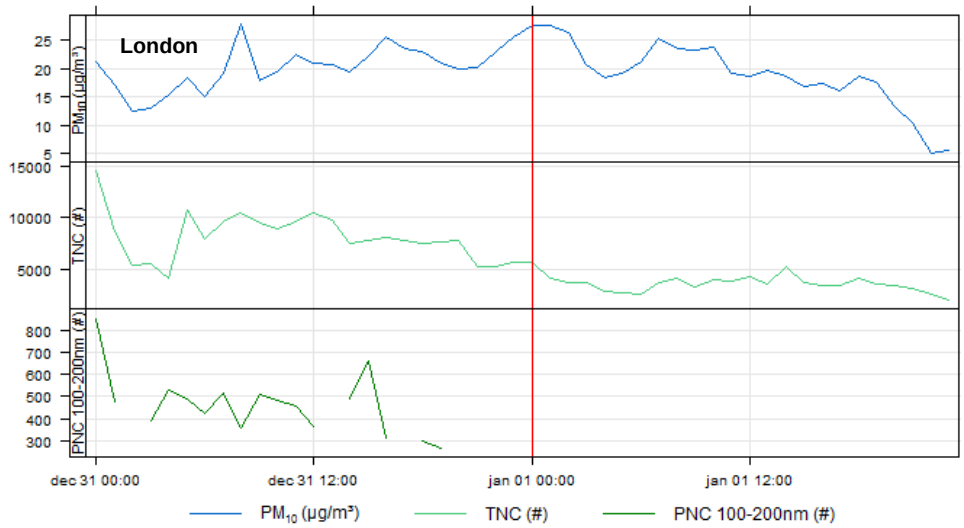

Figure 5.8: PM (µg/m³), total (TNC, #/cm³) and size-resolved (PNC, 100-200 nm, #/cm³) UFP concentrations during New Year's Eve in Antwerp (upper: 2013-2014), Amsterdam (2013-2014), Leicester (2014-2015) and London (2014-2015). The vertical red line denotes the New Year's eve event.

Christmas tree bonfires in Antwerpen on 11 January 2014 and 10 January 2015 seem to correspond with concentration peaks for PM and UFP. Most profound concentration peaks are found for the 100-200 nm particle size class.

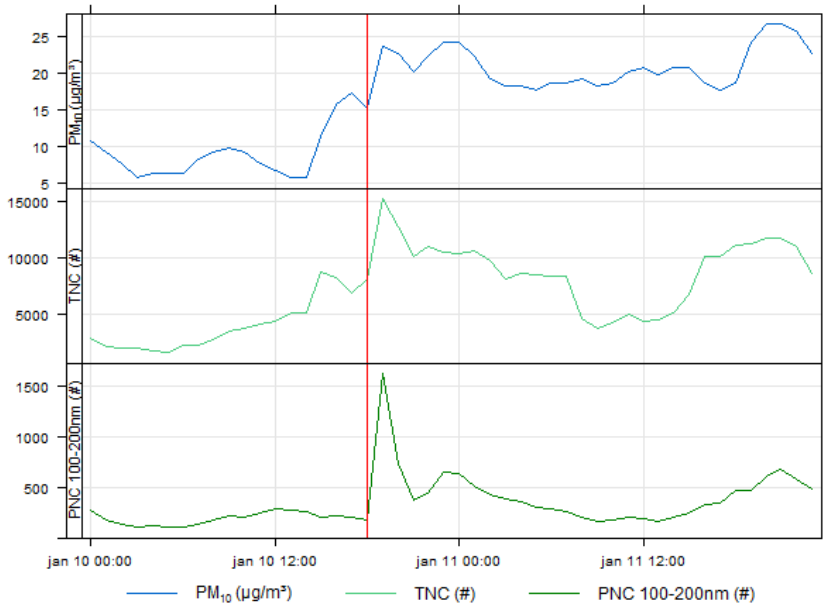

Figure 5.9: PM_{10} (µg/m³), total (TNC, #/cm³) and size-resolved (PNC, 100-200 nm, #/cm³) UFP concentrations measured at the Antwerp monitoring station (AP1S) during the 2015 Christmas tree bonfires in Antwerp. The vertical red line denotes the start of the bonfire event (10 January 2015, 19:00).

No clear effects of Christmas holidays or car-free days on ambient PM or UFP concentrations could be observed for Antwerp. For Leicester, specific events associated with bonfires or fireworks (Diwali, Guy Fawkes Night, …) showed distinct concentration peaks in $PM_{2.5}$ and larger UFP size classes (Figure 5.10). Diwali is a 5-day Hindu festival, celebrated at many places, but Leicester has one of the biggest outside of India. Diwali events are organised in the vicinity of Abbey Park, located at about 3 km from the Leicester monitoring site.

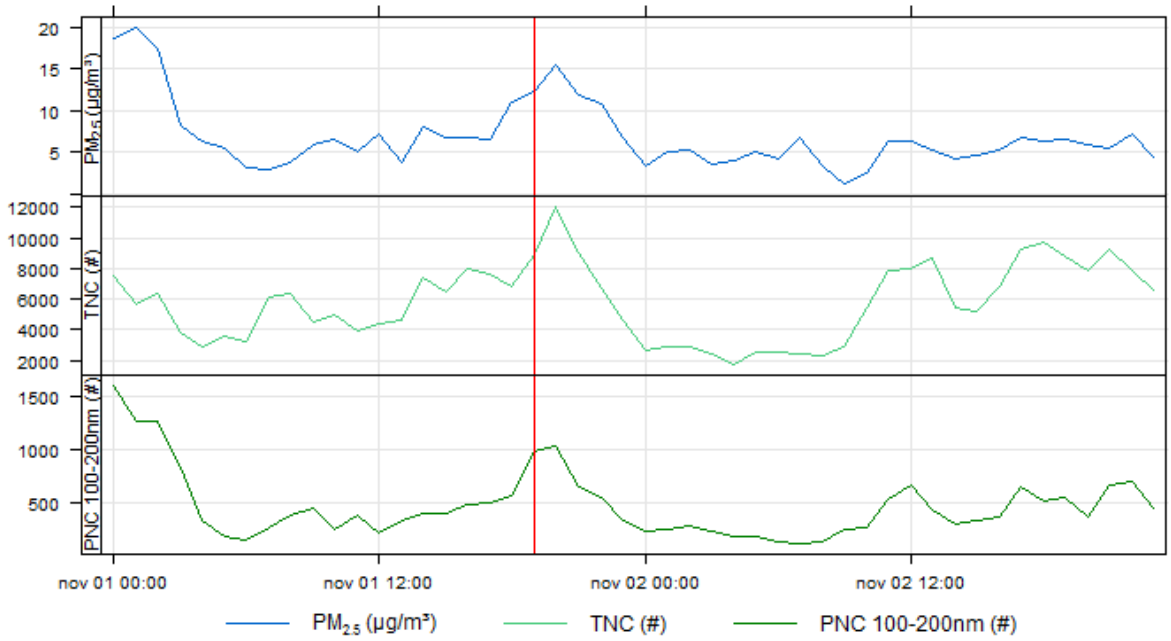

Figure 5.10: *PM_{10} (µg/m³), total (TNC, #/cm³) and size-resolved (PNC, 100-200 nm, #/cm³) UFP concentrations measured at the Leicester monitoring station (LE1S) during the Diwali event. The vertical red line denotes the start of fireworks during the event "Abbey park Bonfire and fireworks display" (1 November 2014, 20:00).*

Also pollution episodes (e.g. SMOG periods in Flanders) with marked increases in PM_{10}, NO_2 or $PM_{2.5}$ concentrations seem to be reflected in UFP peaks in the larger or median particle size classes. This already suggests that the considered pollutants will be related (see section 5.6).

5.3 Total number concentration: comparison of EPC versus SMPS or UFPM

For the four UFP monitoring stations (AD1S, AP1S, LE1S and LO1S), the particle number concentration was quantified using the EPC (TSI 3783) for total number concentration between 7-1000 nm (#/cm³) on the one hand and the Grimm SMPS or UFPM (TSI 3031) for the size-resolved particle number concentration. The Grimm SMPS (10-1000 nm) was used in Amsterdam and Antwerp while the UFPM (20-800 nm) was applied in Leicester and London.

In order to compare the total number concentration of the EPC against the size-resolved monitors (SMPS and UFPM), the measured TNC was plotted against the sum of the concentrations of all size bins of respectively the Grimm SMPS (Amsterdam and Antwerp) or the UFPM (Leicester and London) (Figure 5.11). The relation between the EPC and the size-resolved instruments was evaluated by calculating the coefficients of divergence (COD) and Spearman Rank correlation coefficients (r_s) for all considered monitoring sites (Table 5.5).

Table 5.5: Coefficient of divergence (COD) and Spearman rank correlation coefficients (r_s) between the half-hourly total number concentration quantified by the EPC and the size-resolved instruments, for all individual monitoring sites.

Station	City	COD	Spearman rank (r_s)
AD1S	Amsterdam	0.10	0.93
AP1S	Antwerp	0.17	0.96
LE1S	London	0.33	0.68
LO1S	Leicester	0.21	0.85

The correlation analysis provides information on the overall trend in association between the instruments, while the COD analysis shows differences in absolute concentrations. More information and the definition of the COD can be found in section 2.6.2.

Table 5.5 shows that the best associations (low COD and high r_s) are obtained between the SMPS and EPC instruments in the stations in Amsterdam and Antwerp. The observed COD and r_s differences can be explained by the sampling range of the individual instruments. While the SMPS quantifies >10 nm particles, the UFPM only samples particles larger than 20 nm, resulting in much less particle counts. As smaller-sized particles are fairly short-lived and thus determine much of the temporal variation in particle number concentration, part of the temporal variation will be underestimated when not quantified by the UFPM. This most likely explains the weaker correlation coefficients for London and Leicester. Lowest association is obtained for London (COD = 0.33, r_s = 0.68) which might be due to the shorter monitoring period and the applied calibration factors.

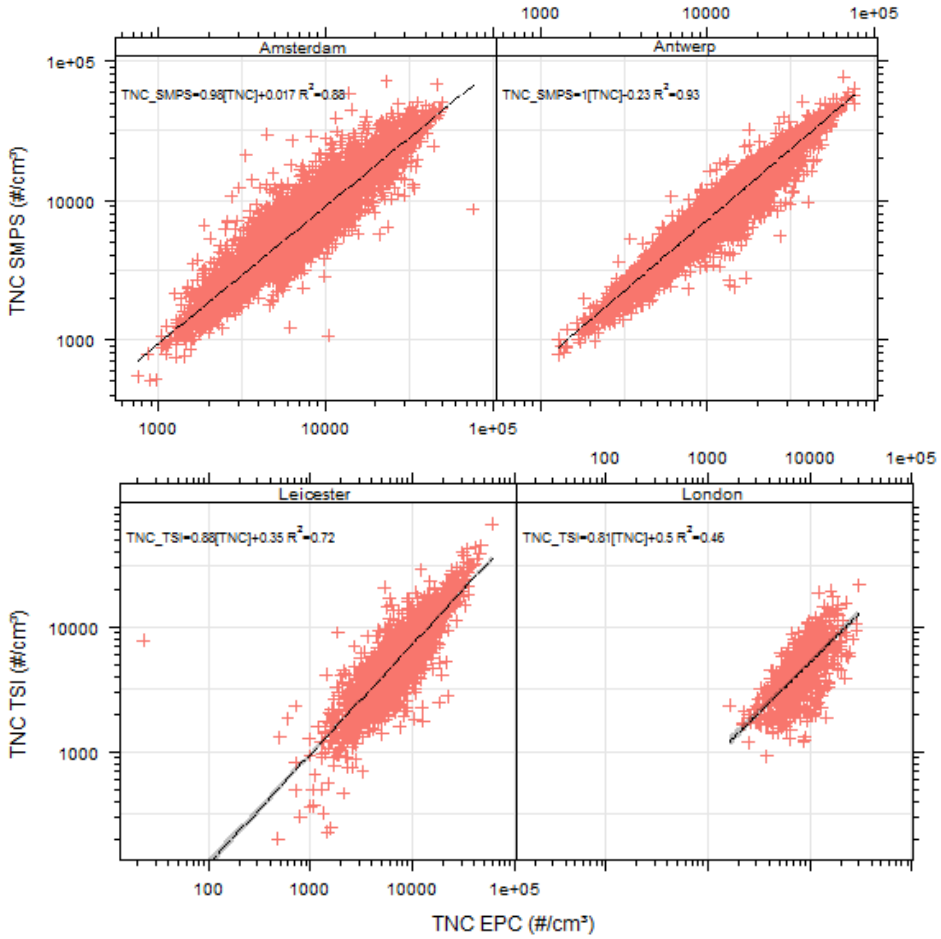

Figure 5.11: Comparison of the TNC measured by the EPC (TSI 3783) and the TNC obtained by the size-resolved UFP instruments (Grimm SMPS for Amsterdam and Antwerp and UFPM (TSI 3031) for Leicester and London).

The scatterplots in Figure 5.11 illustrate that the TNC of the size-resolved instruments is always lower than the TNC measured by the EPC. Based on the regression coefficients forced through the origin (not shown), the TNC according to the size-resolved instruments was 8% (Amsterdam), 26% (Antwerp), 23% (Leicester), and 46% (London) lower than with the EPC. Except for London, this corresponds with previous findings during the initial instrument comparison (Frijns et al. 2013a), where the TNC measured by the size-resolved monitors (UFPM and Grimm SMPS) were respectively 24% and 20% lower than the TNC measured by the EPC. The higher EPC number concentrations could be explained by a lower minimal detectable particle size (EPC: 7 nm, SMPS: 10 nm, UFPM: 20 nm), diffusion losses and (unaccounted) losses during the particle sizing process by the instruments. The difference in minimal detectable particle size will have a significant influence in environments where a nucleation mode is frequently present (Frijns et al. 2013a).

5.4 Spatial variation of the UFP size distributions

In further analyses, the 45 size bins of the Grimm SMPS were aggregated to the size bins of the UFPM for comparison purposes. Nevertheless, we also looked at the individual size classes for the SMPS monitoring sites (AD1S and AP1S). Comparing the mean UFP size distribution for Amsterdam and Antwerp (Figure 5.12) reveals a general unimodal distribution with different maxima for each city, at around 22 nm for Amsterdam and 40 nm for Antwerp. This might be an indication of different source contributions for both cities or a different distance to the UFP emission source (e.g. road) which can also alter the UFP size distribution due to so-called "aging" of the particles in time (VMM 2014, Zhu et al. 2002).

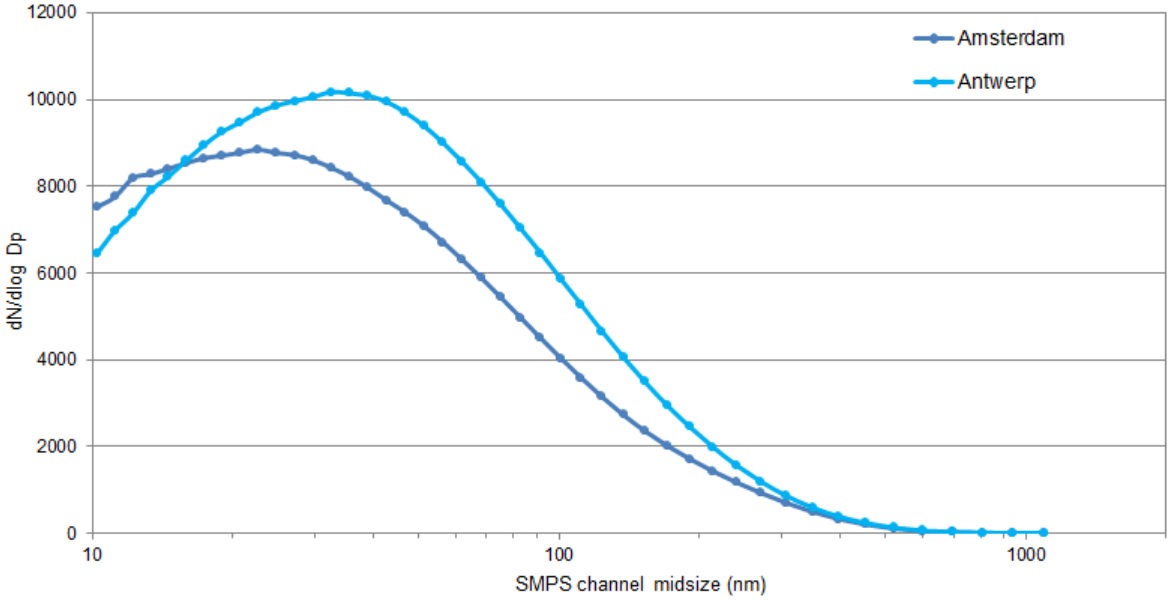

Figure 5.12: Normalized (dN/dlog Dp) UFP size distributions using 45 size bins of the SMPS. Size distributions are averaged over the entire monitoring period in Amsterdam (AD1S) and Antwerp (AP1S).

For the next analyses, particle number concentrations in the 45 size classes in Amsterdam and Antwerp were aggregated to the six particle size classes of the UFPM (10-20, 20-30, 30-50, 50-70, 70-100 and 100-200 nm) for comparison purposes. Average UFP size distributions for each monitoring site are shown in Figure 5.13. For Leicester and London, no particle numbers for the smallest particle size range are available due to smaller sampling range of the available sizing instrument (UFPM).

Figure 5.13 indicates that the overall UFP size distribution is relatively similar at the four monitoring stations. The smallest size class (10-20 nm, only measured in Antwerp and Amsterdam) seemed to be relatively more important in Amsterdam (where 10-20 nm particles contributed 30% of the 10-200 nm particles) than in Antwerp (25%), although the difference was small.

The TNC measured by the EPC was properly quantified for each city and, as discussed before, showed the highest average particle numbers in Antwerp, followed by Amsterdam, London and Leicester (Figure 5.13). The high TNC for Antwerp can be explained by the location of the monitoring site, situated at about 30 m from a very busy thoroughfare of Antwerp.

As SMPS measurements were conducted in the trailer when it was located at the fixed monitoring sites in Antwerp (AP1T), Amsterdam (AD1T), Leicester (LE1T) and London (LO1T), detailed size distributions (45 size bins) could be plotted for each site to compare the size distributions in more detail (Figure 5.14).It should be noted, however, that this figure is based on short (3-4 weeks) and non-simultaneous monitoring periods of the trailer at these sites (see section 2.1 for an overview). Nevertheless, similar patterns as described above can be observed. Antwerp is clearly dominating in particle numbers, Amsterdam has a relatively higher contribution of smaller-sized UFP (10-20 nm) and Leicester and London have comparable particle number concentrations. In contrast to Figure 5.13,

significantly higher particle number concentrations are observed for Amsterdam than for Leicester and London, and Leicester shows a very broad particle number peak between 22 and 75 nm.

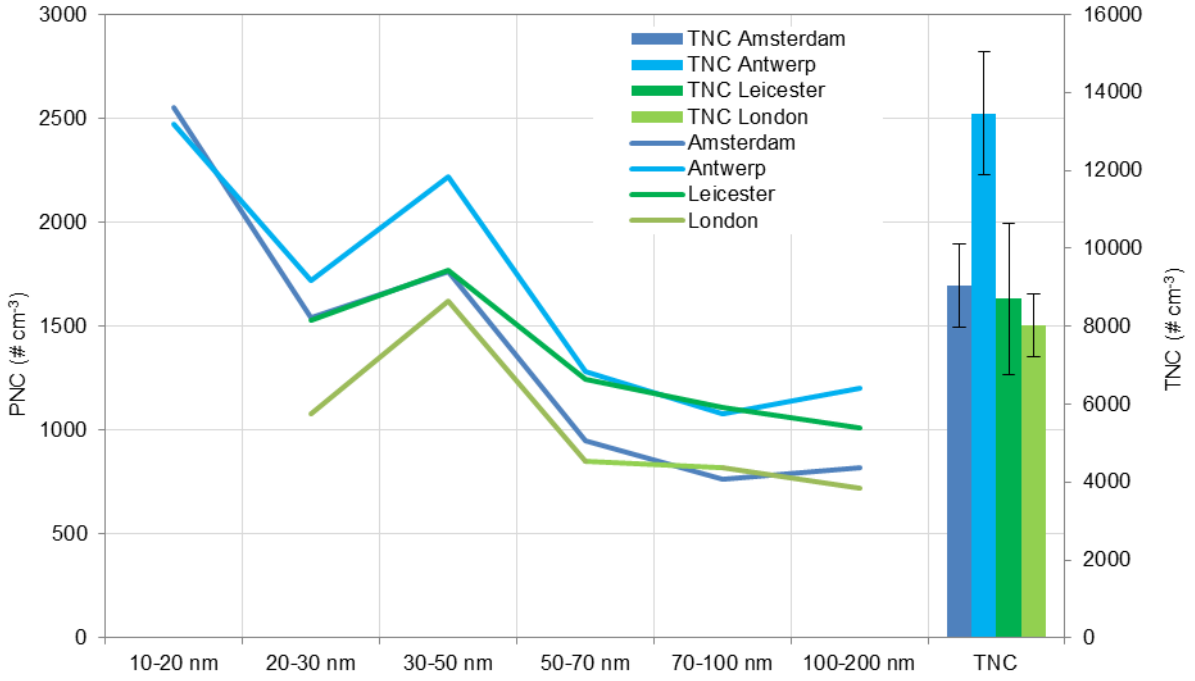

Figure 5.13: Average size-resolved (lines) and total (bars) particle number concentrations for Amsterdam (AD1S), Antwerp (AP1S), Leicester (LE1S) and London (LO1S).

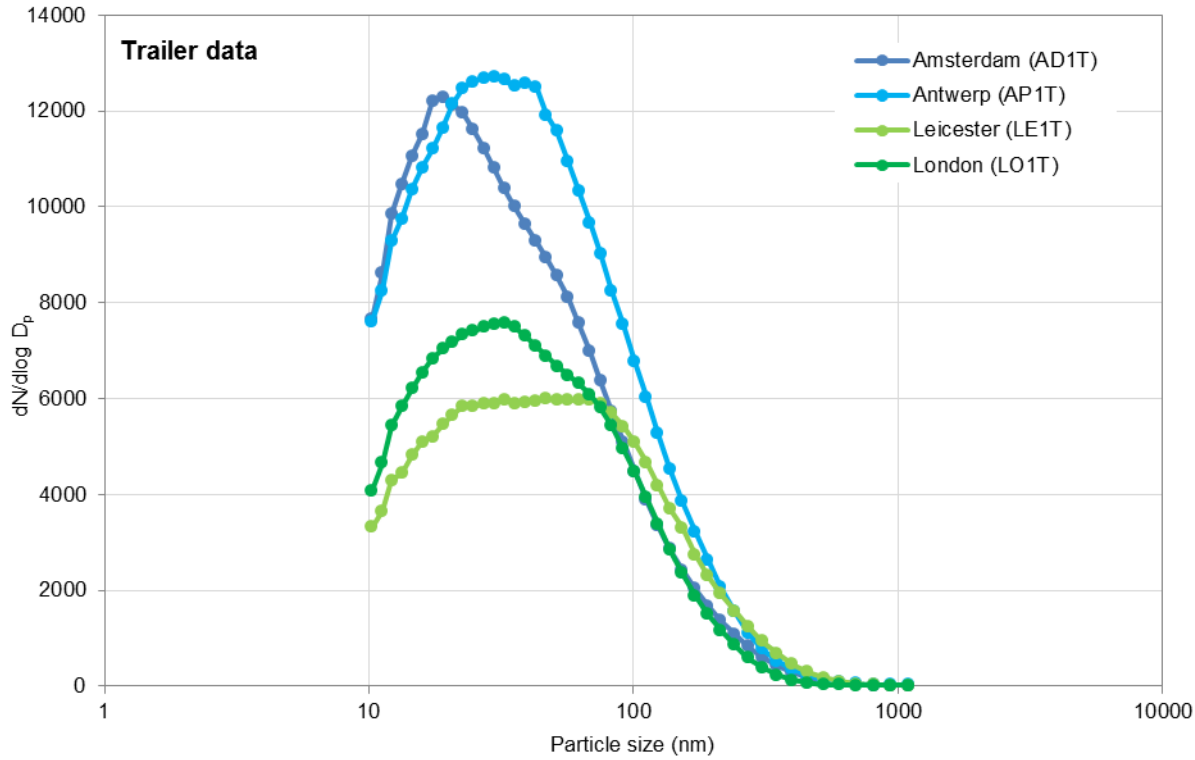

Figure 5.14: Normalized (dN/dlog D_p) UFP size distributions for Amsterdam (AD1T), Antwerp (AP1T), Leicester (LE1T) and London (LO1T), based on SMPS measurements (45 size bins). Data of short and non-simultaneous monitoring periods (see section 2.1 for the exact dates).

The spatial variation in TNC was evaluated by calculating the coefficients of divergence (COD) and Spearman rank correlation coefficients (r_s) between pairs of the considered monitoring sites. Looking

at the COD and correlation results in Table 5.6, most variation in TNC is observed between the monitoring sites in Antwerp and Leicester (COD = 0.37, r_s = 0.30), while the best agreement in TNC was found between Leicester and London (COD = 0.28, r_s = 0.50). This is not surprising, as London and Leicester are most closely located to one another. Overall, correlations are fairly low (≤0.5) indicating that TNC is not covarying well at the regional level of NW Europe and that much of the variation in TNC is due to more local factors.

Table 5.6: Coefficients of determination (COD, left) and Spearman rank correlations (r_s, right) of the half-hourly total particle number concentration (TNC) between the respective monitoring sites.

COD TNC (#/cm^3)

	Antwerp	Amsterdam	Leicester	London
Antwerp	0.00	0.32	0.37	0.33
Amsterdam	0.32	0.00	0.32	0.29
Leicester	0.37	0.32	0.00	0.28
London	0.33	0.29	0.28	0.00

Spearman rank (r_s) TNC (#/cm^3)

	Antwerp	Amsterdam	Leicester	London
Antwerp	1	0.37	0.30	0.38
Amsterdam	0.37	1	0.31	0.28
Leicester	0.30	0.31	1	0.50
London	0.38	0.28	0.50	1

From the COD and correlation coefficients of the individual size classes (Table 5.7), an increased association (smaller COD and larger correlation) is obtained with increasing particle size. Therefore larger particles tend to be more uniform, which may be indicate the regional nature of these aerosols. This was also observed in former studies, e.g. Krudysz et al. (2009).

Table 5.7: Coefficients of determination (COD, left) and Spearman Rank correlations (r_s, right) of the half-hourly size-resolved particle number concentrations between the respective monitoring sites.Only for Antwerp and Amsterdam,10-20 nm size class measurements were available (SMPS).

COD 10-20 nm (#/cm^3)

	Antwerp	Amsterdam	Leicester	London
Antwerp	0.00	0.36	NA	NA
Amsterdam	0.36	0.00	NA	NA
Leicester	NA	NA	NA	NA
London	NA	NA	NA	NA

Spearman rank (r_S) 10-20 nm #/cm^3)

	Antwerp	Amsterdam	Leicester	London
Antwerp	1.00	0.37	NA	NA
Amsterdam	0.37	1.00	NA	NA
Leicester	NA	NA	NA	NA
London	NA	NA	NA	NA

COD 20-30 nm #/cm^3)

	Antwerp	Amsterdam	Leicester	London
Antwerp	0.00	0.33	0.35	0.44
Amsterdam	0.33	0.00	0.36	0.42
Leicester	0.35	0.36	0.00	0.40
London	0.44	0.42	0.40	0.00

Spearman rank (r_S) 20-30 nm #/cm^3)

	Antwerp	Amsterdam	Leicester	London
Antwerp	1.00	0.36	0.31	0.11
Amsterdam	0.36	1.00	0.29	0.17
Leicester	0.31	0.29	1.00	0.34
London	0.11	0.17	0.34	1.00

COD 30-50 nm (#/cm^3)

	Antwerp	Amsterdam	Leicester	London
Antwerp	0.00	0.31	0.35	0.37
Amsterdam	0.31	0.00	0.35	0.35
Leicester	0.35	0.35	0.00	0.32
London	0.37	0.35	0.32	0.00

Spearman rank (r_S) 30-50 nm (#/cm^3)

	Antwerp	Amsterdam	Leicester	London
Antwerp	1.00	0.38	0.35	0.17
Amsterdam	0.38	1.00	0.25	0.15
Leicester	0.35	0.25	1.00	0.35
London	0.17	0.15	0.35	1.00

COD 50-70 nm (# cm^{-3})

	Antwerp	Amsterdam	Leicester	London
Antwerp	0.00	0.30	0.34	0.39
Amsterdam	0.30	0.00	0.38	0.36
Leicester	0.34	0.38	0.00	0.35
London	0.39	0.36	0.35	0.00

Spearman rank (r_S) 50-70 nm (#/cm^3)

	Antwerp	Amsterdam	Leicester	London
Antwerp	1.00	0.48	0.39	0.21
Amsterdam	0.48	1.00	0.27	0.18
Leicester	0.39	0.27	1.00	0.38
London	0.21	0.18	0.38	1.00

COD 70-100 nm (#/cm^3)

	Antwerp	Amsterdam	Leicester	London
Antwerp	0.00	0.32	0.35	0.38
Amsterdam	0.32	0.00	0.41	0.37
Leicester	0.35	0.41	0.00	0.35
London	0.38	0.37	0.35	0.00

Spearman Rank (r_S) 70-100 nm (#/cm^3)

	Antwerp	Amsterdam	Leicester	London
Antwerp	1.00	0.60	0.39	0.17
Amsterdam	0.60	1.00	0.31	0.18
Leicester	0.39	0.31	1.00	0.36
London	0.17	0.18	0.36	1.00

COD 100-200 nm (#/cm^3)

	Antwerp	Amsterdam	Leicester	London
Antwerp	0.00	0.32	0.36	0.44
Amsterdam	0.32	0.00	0.38	0.40
Leicester	0.36	0.38	0.00	0.36
London	0.44	0.40	0.36	0.00

Spearman rank (r_S) 100-200 nm (#/cm^3)

	Antwerp	Amsterdam	Leicester	London
Antwerp	1.00	0.66	0.42	0.27
Amsterdam	0.66	1.00	0.38	0.28
Leicester	0.42	0.38	1.00	0.48
London	0.27	0.28	0.48	1.00

5.5 Temporal variation of BC, total number concentration and size distribution

5.5.1 Black carbon

Looking at the temporal variation of BC at three time-scales (monthly, daily and hourly averages), different temporal effects can be observed (Figure 5.15). Please note that the y-axis is not starting at zero in this figure and in the following temporal variation plots.

First of all, BC concentrations show a traffic-related diurnal variation with distinct morning and evening peaks on week days. On week days, the morning peaks are higher but shorter compared to the evening peaks that are lower but take longer. In the weekends, the traffic rush hour peaks are less pronounced and almost negligible for morning hours. The site in Antwerp shows the highest overall BC concentration and highest peaks, which is probably due to the meaningful exposure to traffic from the Plantin en Moretuslei. Lowest BC concentrations are measured in Amsterdam, while higher and comparable concentrations are observed in Leicester and London. The rush hour peaks in Amsterdam appear slightly shifted in time (later) compared to the other monitoring sites.

In Antwerp and Amsterdam, daily-averaged BC concentrations seem to build up through the week (Mon-Thu for Antwerp and Mon-Fri for Amsterdam) and are reduced throughout the weekends. Highest monthly-averaged BC concentrations are observed during the winter months (September-March), which may be due to meteorological conditions (e.g. temperature and mixing layer height).

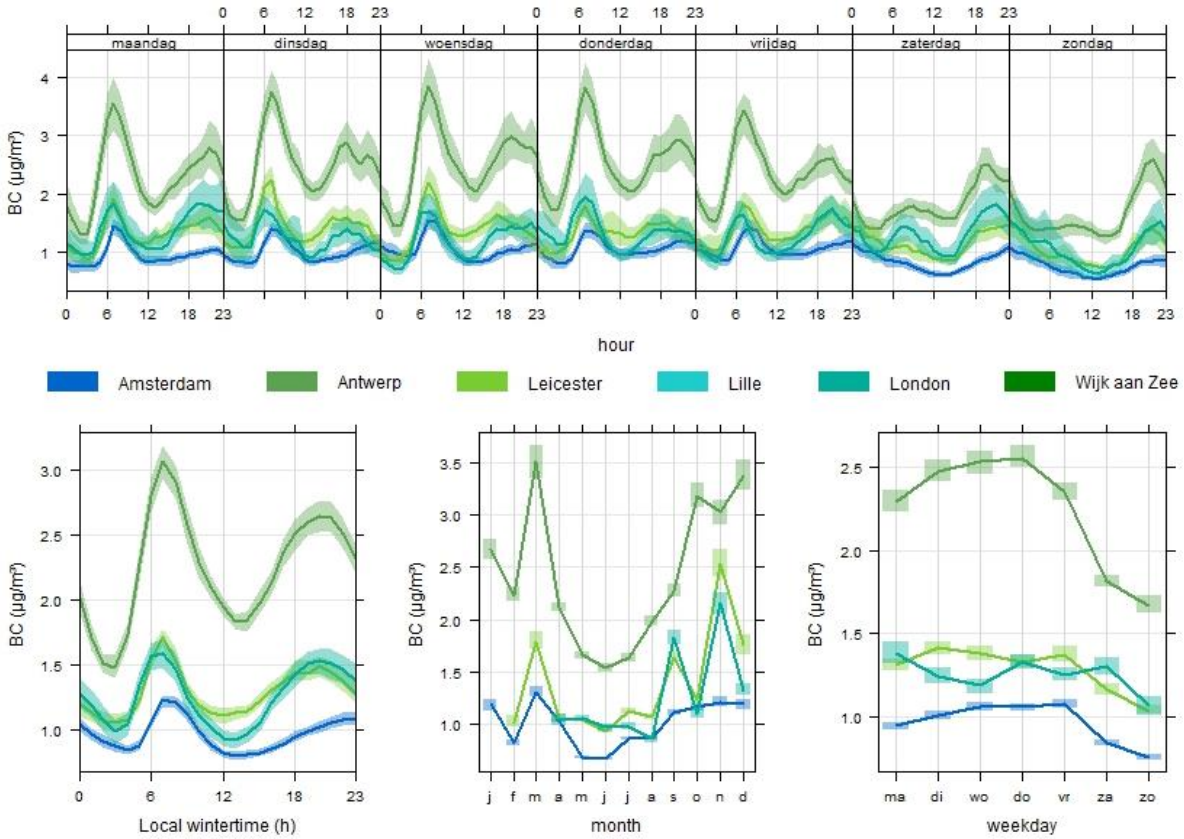

Figure 5.15: Temporal variation of BC (µg m^{-3}) for the considered monitoring stations (AD1S, AP1S, LE1S and LO1S) at three different time scales (monthly, daily and hourly averages).The coloured zone represents the 95% confidence interval.

5.5.2 Total particle number concentration (TNC)

Evaluating the temporal variation of the TNC for the considered monitoring sites (Figure 5.16), comparable effects as described for BC can be observed. Total number concentrations show a traffic-

related diurnal variation with morning and evening peaks. Morning peaks are more strongly pronounced than the evening peaks, except during weekends. For all sites, the TNC increases throughout week days and decreases in the weekends and highest monthly-averaged concentrations are obtained during winter months (September-March).

Antwerp shows the highest TNC, in correspondence with the findings for BC. However, for Amsterdam contrasting results as for BC are found, since the hourly, daily and monthly mean TNC is higher in Amsterdam than in Leicester and London. This suggests the presence of UFP sources in Amsterdam which are not contributing to BC.

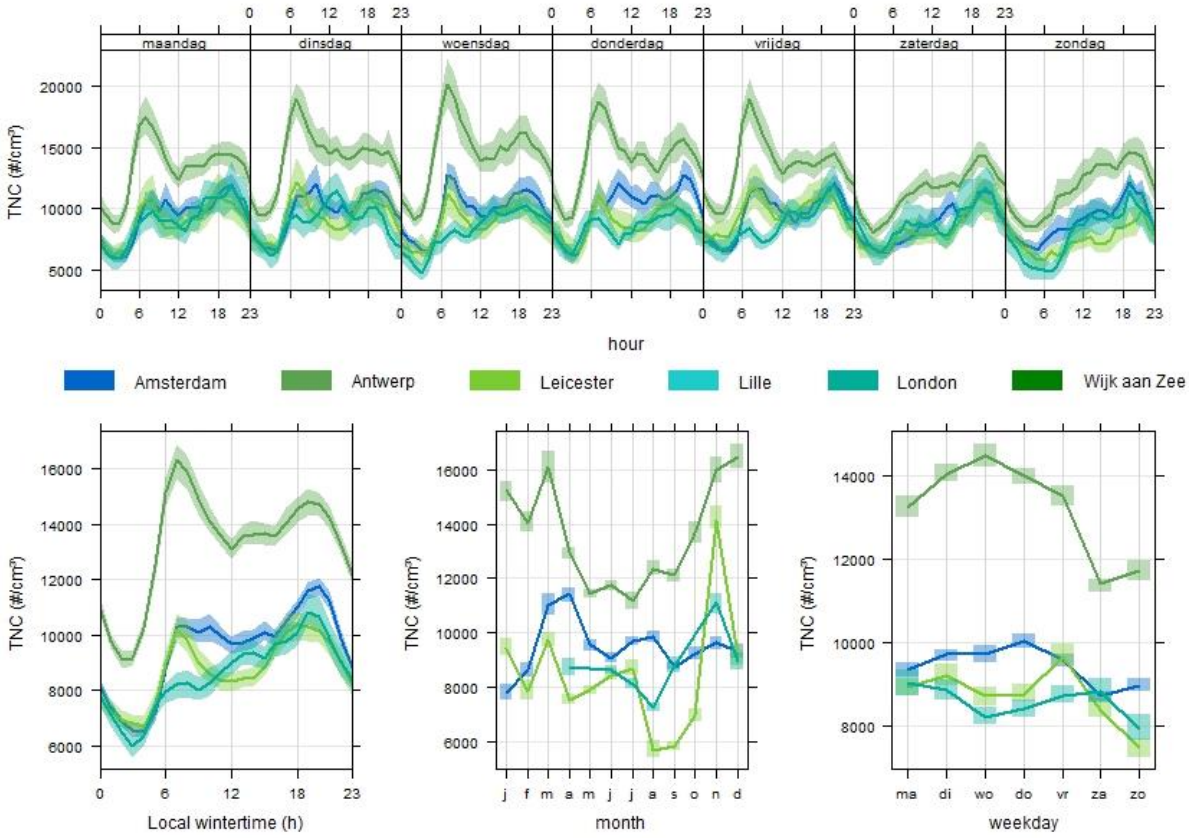

Figure 5.16: Temporal variation of total particle number concentration (# cm^{-3}) for the considered monitoring stations (AD1S, AP1S, LE1S and LO1S) at three different time scales (monthly, daily and hourly averages).The coloured zone represents the 95% confidence interval.

5.5.3 Particle size distribution

To evaluate the temporal variation of the particle size distribution, number concentrations per selected size class were plotted for each monitoring site (Figure 5.17 to Figure 5.20).

For Amsterdam (Figure 5.17), the temporal variation plot of the individual particle size classes shows that most particles are in the smallest size class (10-20 nm) with a daily average particle concentration of ±2500 #/cm^3, followed by the particle size class of 30-50 nm (±1700 #/cm^3) and 20-30 nm (±1500 #/cm^3). On average, the 10-20 nm size class contributes 30% of the total particle numbers, followed by the size classes of 30-50 nm (21%), 20-30 nm (18%), 50-70 nm (12%), 100-200 nm (10%) and 70-100 nm (9%). Except for the 10-20 nm size class, all classes seem to exhibit a comparable traffic-related diurnal variation with distinct morning and evening peaks. The time pattern of the PNC in the 10-20 nm class is less distinct and seems to consist of a single peak during daytime hours. Also in the weekends a similar profile is observed for the 10-20 nm particles.

As noted before, these data suggest a non-traffic related input of mainly smaller-sized particles in Amsterdam. This UFP source seems to persist throughout the weekend, as a comparable diurnal

pattern as on week days can be observed. There is no clear decrease in the average particle number concentrations throughout the weekends, neither a seasonal influence.

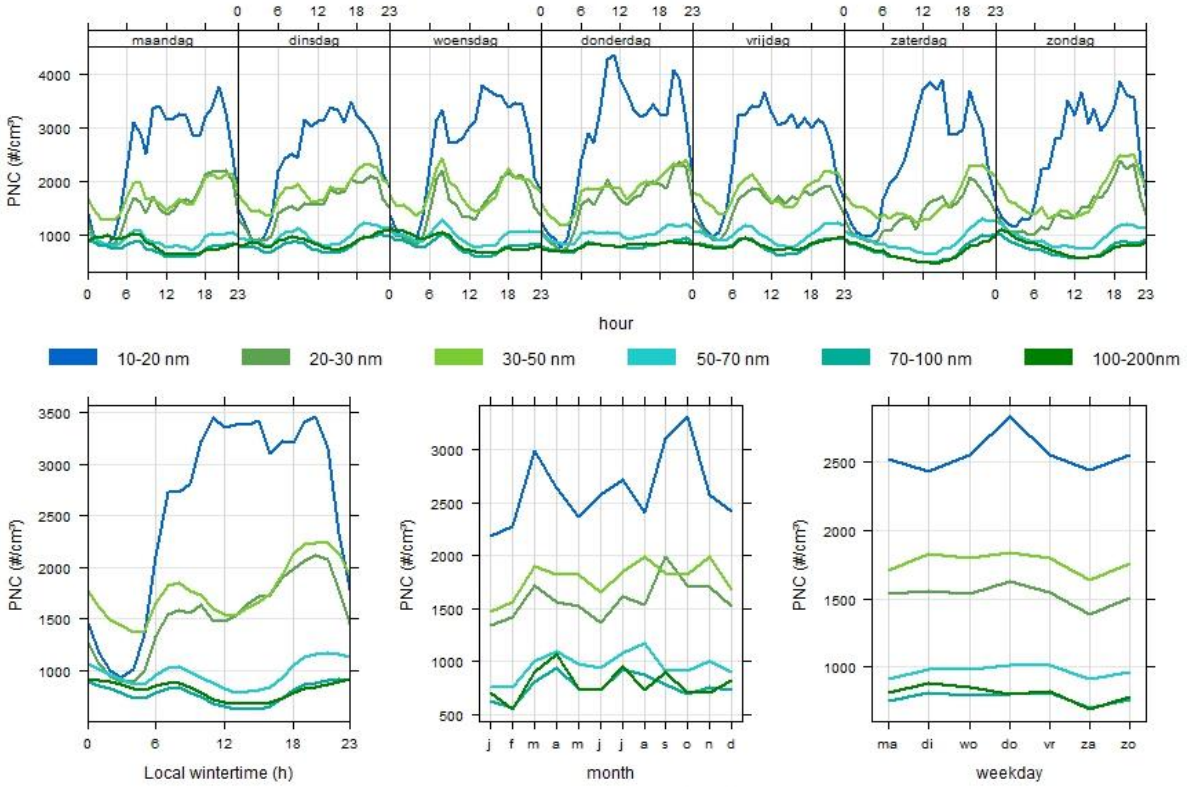

Figure 5.17: Temporal variation of the particle number concentration (# cm^{-3}) observed at the Amsterdam monitoring site (AD1S) within the 10-20 nm, 20-30 nm, 30-50 nm, 50-70 nm, 70-100 nm and 100-200 nm size classes at three different time scales (monthly, daily and hourly averages).

For the Antwerp site, the temporal variation of size-specific particle number concentrations shows a clear traffic-related diurnal variation (Figure 5.18). The average temporal variation is fairly comparable to the BC variation observed before. Clear morning and evening peaks are visible with a concentration build-up throughout the week and a decrease throughout the weekends (Figure 5.18). On weekend days only an evening peak can be observed. For all size classes, higher average particle number concentrations are measured during the winter months (October-March).

Comparable to the results for Amsterdam, the largest contribution in terms of particle number is observed in the 10-20 nm size class (on average 25% of total particle numbers), followed by the particle size class of 30-50 nm (22%), 20-30 nm (17%), 50-70 nm (13%), 100-200 nm (12%) and 70-100 nm (11%). While the relative importance of the size classes is comparable between Amsterdam and Antwerp, an increased contribution of the smallest particle size class (10-20 nm) is found in Amsterdam (30%) compared with Antwerp (25%).

For the hourly-averaged particle number concentrations in Antwerp, a small midday-peak can be observed in the 10-20 nm size class, which seems to resemble at new particle formation (nucleation) events in urban areas as formerly described (Dall'Osto et al. 2013, Pey et al. 2008, Querol et al. 2011). We tested this hypothesis by selecting for midday-early afternoon hours (11:00-15:00h) and plotting the measured 10-20 nm particle number concentrations (#/cm^3) against the solar radiation (W/m^2), temperature (T, °C) and ozone (O_3, µg/m^3). However, no relation could be observed (R^2 = 0.0099 for radiation, R^2 = 0.0051 for T and R^2 = 0.0012 for O_3). Consequently, the small peaks in 10-20 nm particles appear not be related to new particle formation events. However, further research is needed to assess the occurrence and importance of nucleation events at the Antwerp site.

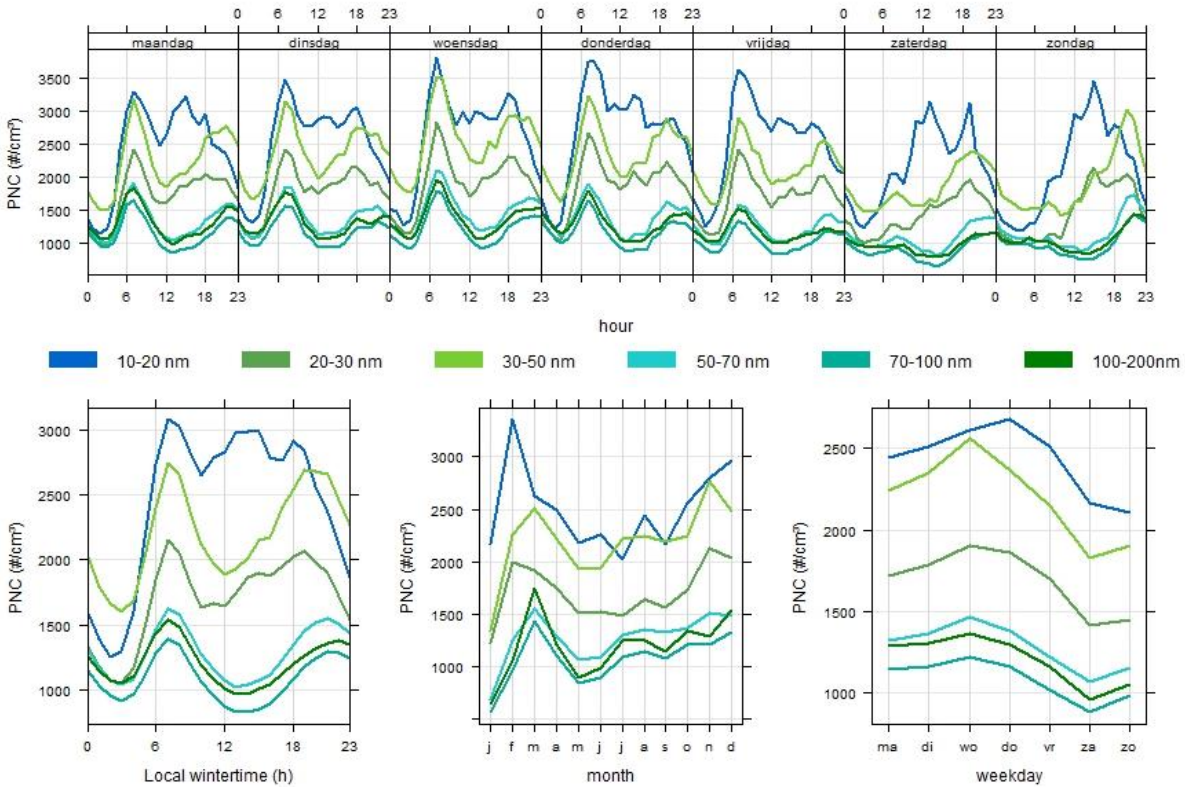

Figure 5.18: Temporal variation of the particle number concentration (# cm^{-3}) observed at the Antwerp monitoring site (AP1S) within the 10-20 nm, 20-30 nm, 30-50 nm, 50-70 nm, 70-100 nm and 100-200 nm size classes at three different time scales (monthly, daily and hourly averages).

In Leicester, the hourly, weekly and monthly variation of size-specific particle numbers shows similar patterns as observed for Antwerp (Figure 5.19). Firstly, hourly-averaged particle number concentrations show distinct morning and evening peaks during week days and only an evening peak during weekends. Secondly, a clear decline of the daily-averaged particle number is observed during weekends, which is comparable to Antwerp. Nevertheless, the daily-averaged particle concentration on week days is rather constant in Leicester instead of increasing throughout the week, like in Antwerp. Finally, a peak in monthly-averaged particle concentrations is observed during winter months (October-March), comparable to Antwerp.

It is worth noting that in Leicester a pronounced correlation seems to exist between the different particle size classes (Figure 5.19). This is likely related to the different type of monitor used in Leicester (UFPM) compared to Amsterdam and Antwerp (SMPS).

Looking at the temporal size-resolved UFP variation in London, the daily, weekly and monthly courses seem fairly capricious. This is probably due to the shorter monitoring period (April - December 2014) compared to the other monitoring sites. Nevertheless, a comparable consecution of the individual particle size classes in terms of particle number contribution can be observed (100-200 nm < 70-100 nm < 50-70 nm < 20-30 nm < 30-50 nm). In contrast to Leicester, no pronounced correlation seems to exist between the individual particle size classes. This might be due to the applied calibration factors, which are based on co-located Grimm SMPS measurements by the ECN trailer (see section 3.2.3.1 on UFPM correction). Moreover, no clear UFP decrease can be observed during the weekend. For the 20-30 and 30-50 nm size classes, the largest peak is even observed on Sunday evening.

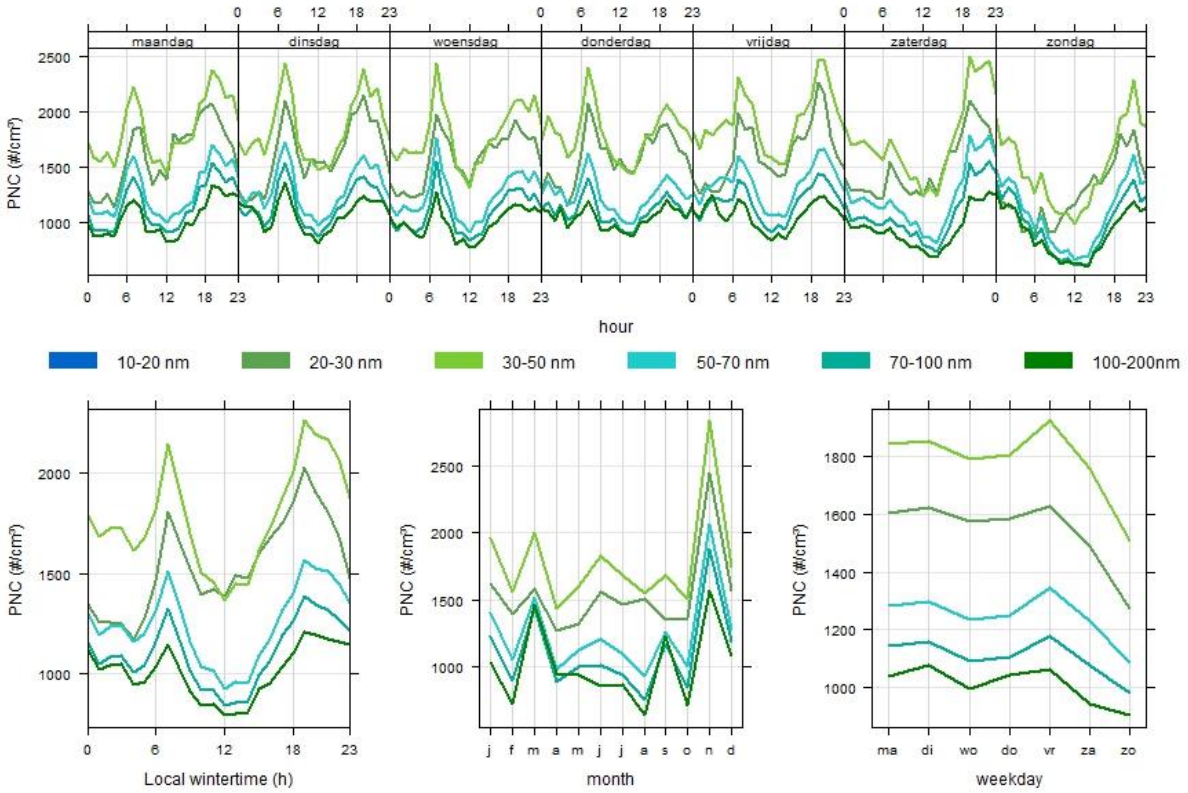

Figure 5.19: Temporal variation of the particle number concentration (# cm^{-3}) observed at the Leicester monitoring site (LE1S) within the 20-30 nm, 30-50 nm, 50-70 nm, 70-100 nm and 100-200 nm size classes at three different time scales (monthly, daily and hourly averages).

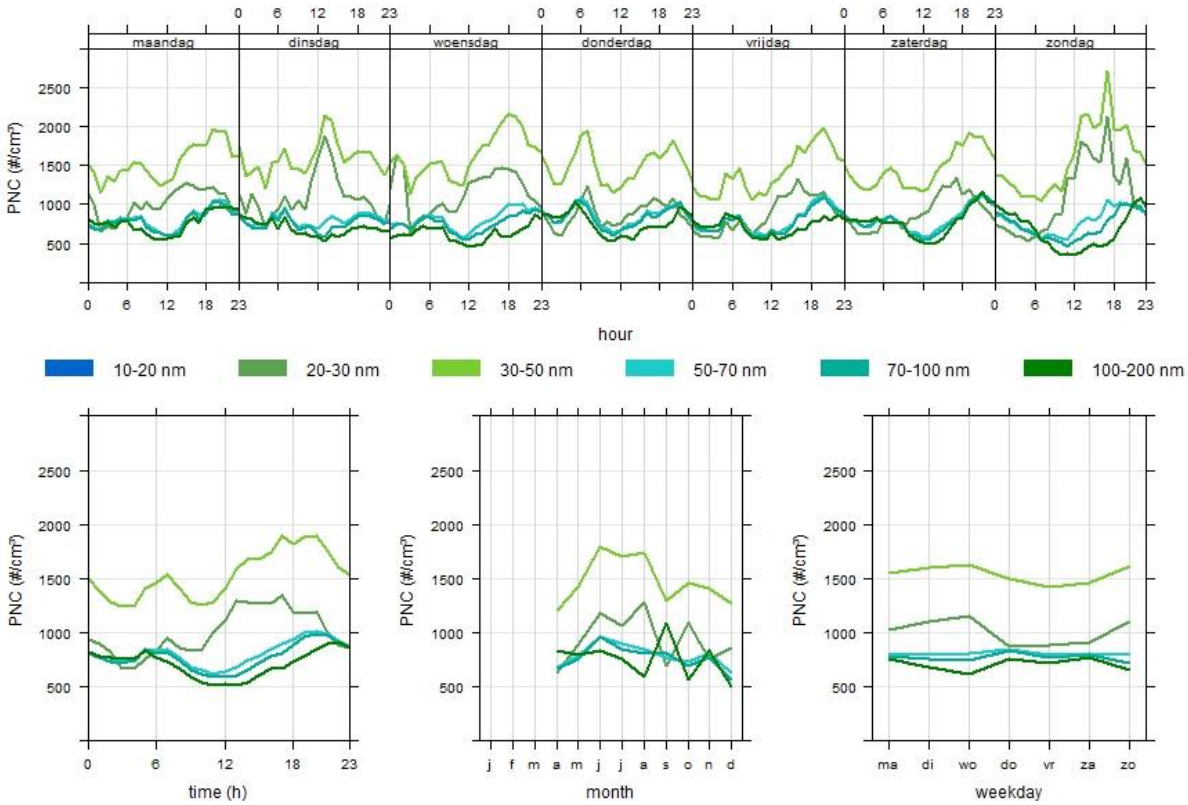

Figure 5.20: Temporal variation of the corrected particle number concentrations (# cm^{-3}) observed at the London monitoring site (LO1S) within the 20-30 nm, 30-50 nm, 50-70 nm, 70-100 nm and 100-200 nm size classes at three different time scales (monthly, daily and hourly averages). This figure is based on UFP measurements from April,2014, to December, 2014.

5.5.4 Monthly averaged size-distributions

Monthly averaged size-resolved particle number concentrations were calculated, using a 75% data threshold, to evaluate the temporal variation of the UFP size distributions throughout the considered 2-year monitoring period (Figure 5.21). Looking at the monthly-averaged size distributions, the overall size distribution appears to be fairly stable through time.

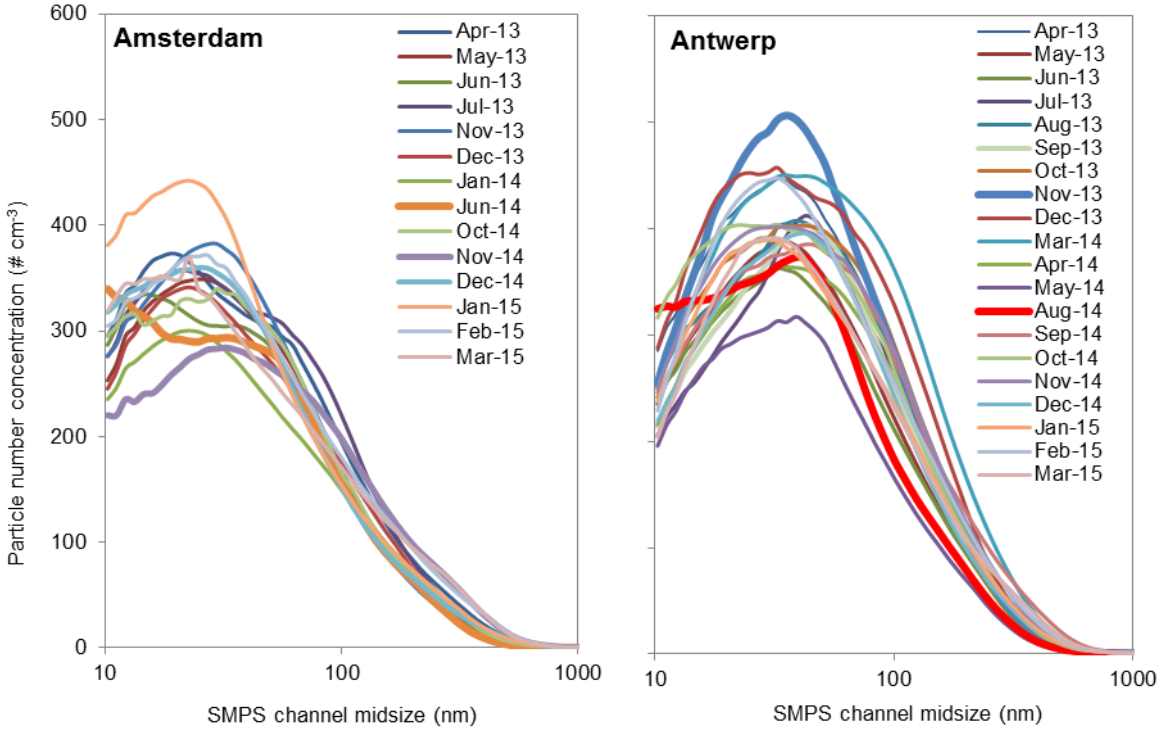

Figure 5.21: Monthly-averaged (75% data threshold) UFP size distributions, based on the 45 SMPS size bins, throughout the entire monitoring period in Amsterdam (left) and Antwerp (right). Divergent size distributions are shown in bold.

Nevertheless, shifts in particle number peaks can be observed for specific months. For Amsterdam (Figure 5.21, left) divergent size distributions are obtained for June 2014 and November 2014, shown in bold in the figure. In June 2014 there is a clear peak in the 10-20 nm size range, while in November 2014 the peak is in the 30-50 nm size range. During these months, the experienced wind field might be an explanation for the diverging size distributions. While the average wind speed is very similar for both months (3.64 m/s in June and 4.25 m/s in November), the wind blows from the SW (244°) in June and from the SE (141°) in November. As Schiphol airport is located south-west of monitoring station AD1S, at about 8 km upwind, the different wind direction may be an explanation for the observed peak in the 10-20 nm size range. Comparable results were reported in two recent studies of UFP measurements in the vicinity of international airports (Hudda et al. 2014, Keuken et al. 2015). The potential effect of Schiphol airport is discussed in section 5.7. In November 2014, the wind is blowing from the city centre resulting in a typical traffic-related UFP size distribution with peak particle number concentrations around the 30-50 nm size range.

For Antwerp (Figure 5.21, right), the most divergent size distributions are obtained in November 2013 and August 2014, with comparable peaks in the 35-39 nm size class but a higher contribution of 10-20 nm sized particles in August 2014. Monthly averaged wind fields at the meteo site used for AP1S are fairly comparable between November 2013 (3.86 m/s, 212°) and August 2014 (3.93 m/s, 209°). So Based on these data, no explanation can be found for the higher 10-20 nm contribution in August. Nevertheless, it should be noted that regional wind measurements (Luchtbal site for Antwerp) are used, which may be different from the wind experienced at the air quality station due to the local urban architecture. In contrast to the regional wind fields, the considered months differ in terms of temperature and radiation. While the average air temperature and radiation was 7 °C and 30 W/m^2 in November 2013, August 2014 experienced an average air temperature of 17 °C and 157 W/m^2. Air temperature and insolation can play an important role in new photochemical particle formation (so-

called nucleation events), in particular in urban environments where volatile organic compounds (VOCs) are present (Kulmala et al. 2004, Pey et al. 2008, Querol et al. 2011).

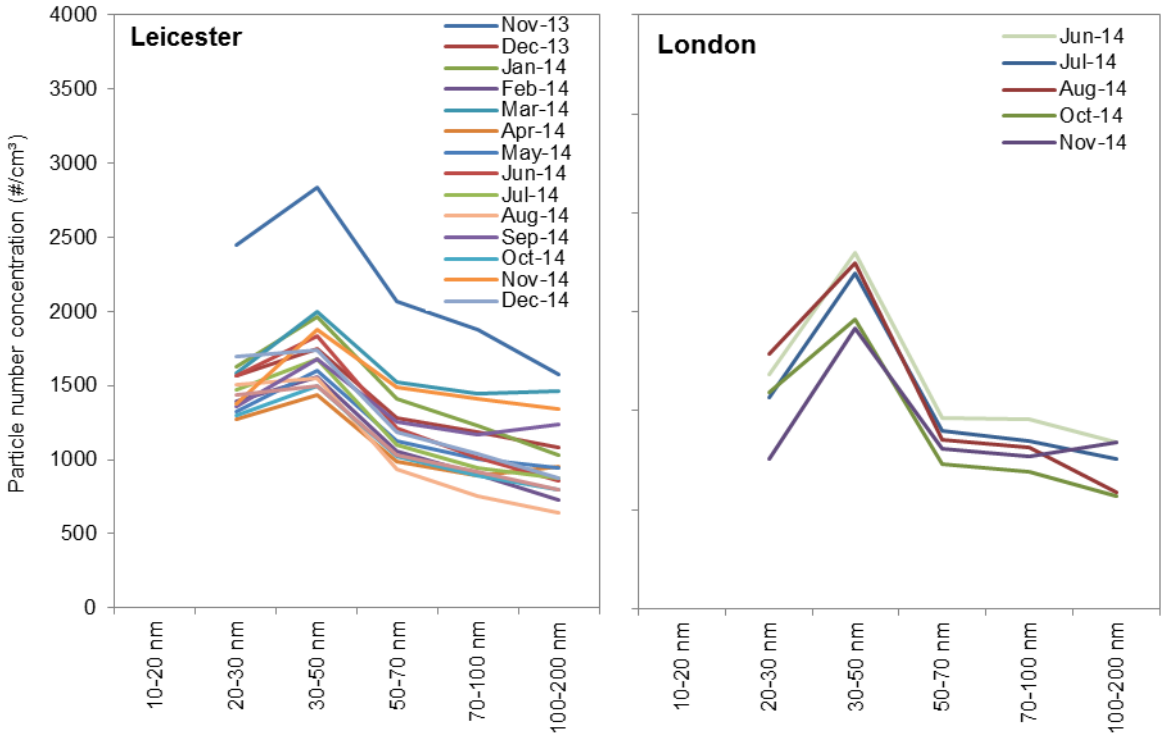

Figure 5.22: Monthly-averaged (75% data threshold) UFP size distributions, based on the five UFPM size bins, throughout the entire monitoring period in Leicester (left) and London (right).

Looking at the monthly-averaged UFP size distributions for Leicester and London (Figure 5.22), very limited temporal variation can be observed in the considered size bins. Only in Leicester, overall higher UFP concentrations are obtained for all size bins during November 2013. Although the festivities during November (Diwali, Guy Fawkes Night) and a pollution episode (see section 5.2) might explain a higher UFP concentration in the larger size classes, no direct explanation can be found as the entire UFP size distribution is distinctly elevated compared to the other months.

5.6 Relationship of UFP with more commonly monitored air pollutants

To evaluate the relation of UFP with more commonly monitored air pollutants, half-hourly and daily-averaged total number concentrations were plotted against half-hourly and daily PM_{10}, $PM_{2.5}$, NO_2, NO and BC concentrations for the considered monitoring sites (AD1S, AP1S, LE1S and LO1S). From these plots, relations could be observed between TNC on the one hand and BC (Figure 5.23), NO_2 (Figure 5.24) and NO (Figure 5.25) on the other hand.

5.6.1 TNC versus black carbon and NO_x

The strongest relation between TNC and BC at the daily interval was observed for London (R^2 = 0.50) and Antwerp (R^2 = 0.49), followed by Leicester (R^2 = 0.41). In Amsterdam, no clear relationship was observed between TNC and BC (R^2 = 0.087).

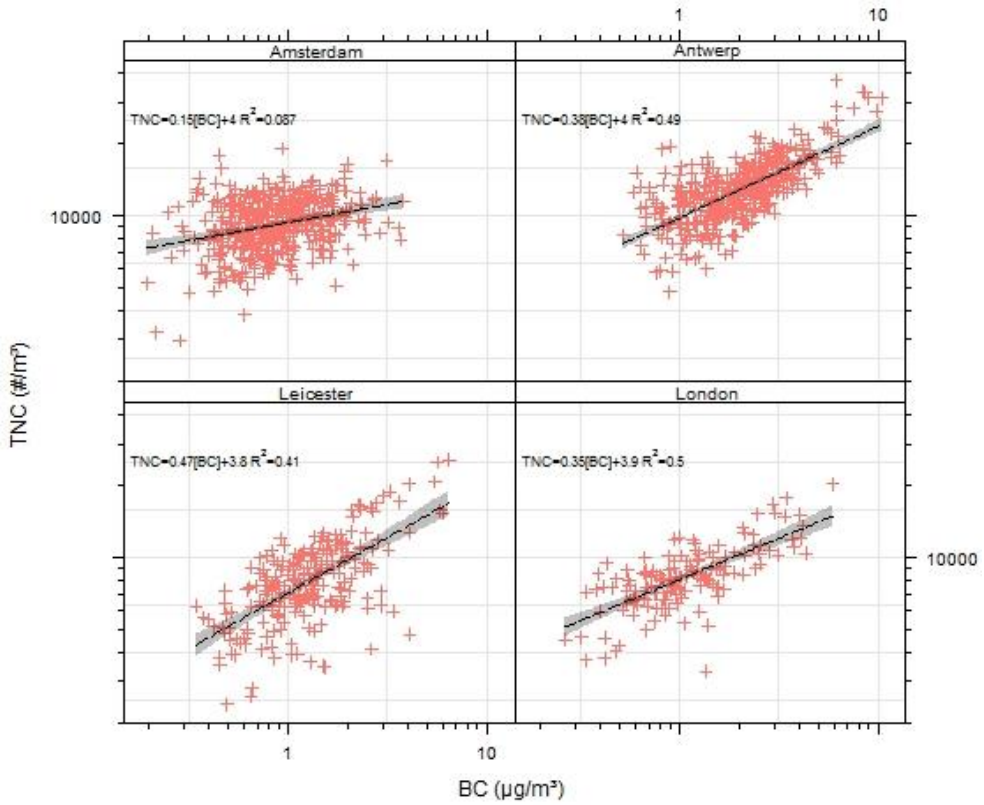

Figure 5.23: Regression plots of daily-averaged total particle number concentration (#/cm³) and BC (µg/m³) for all considered sites (AD1S, AP1S, LE1S and LO1S). Regression plots are displayed with logarithmic scales.

Daily-averaged NO_x concentrations (Figure 5.24 for NO_2 and Figure 5.25 for NO) were best related with TNC in Leicester (R^2 = 0.58 for NO_2 and R^2 = 0.58 for NO), followed by Antwerp (R^2 = 0.55 and 0.53, respectively), London (R^2 = 0.38 and 0.29, respectively) and Amsterdam (R^2 = 0.14 and 0.13, respectively). So overall, TNC shows a relationship with typical traffic-related pollutants (NO_2, NO and BC). This observation confirms that traffic is an important source of UFP in the considered urban environments.

Nevertheless, for the monitoring site in Amsterdam, no relations are observed between the typical traffic-related pollutants and TNC. Therefore, traffic may not be the dominant UFP source at the Amsterdam monitoring site. The presence of the low emission zone in Amsterdam might be a reason for the lack of relation between traffic-related pollutants and UFP and/or other UFP sources might be involved.

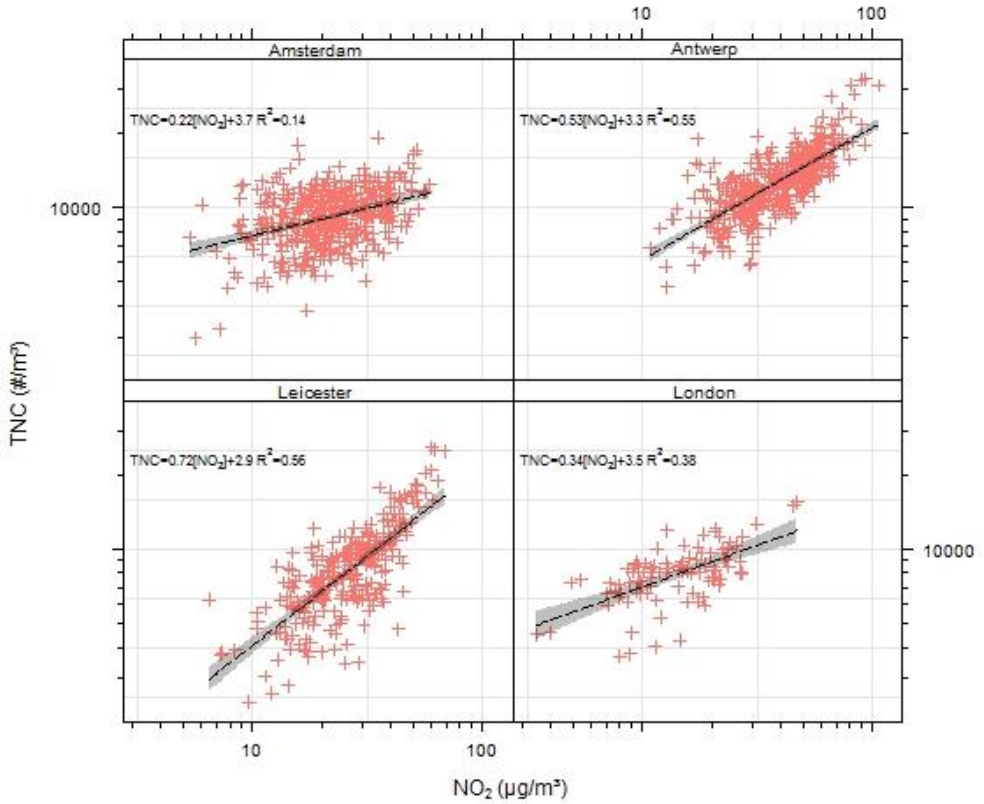

Figure 5.24: Regression plots of daily-averaged total particle number concentration (#/cm³) and NO_2 (µg/m³) for all considered sites (AD1S, AP1S, LE1S and LO1S). Regression plots are displayed with logarithmic scales.

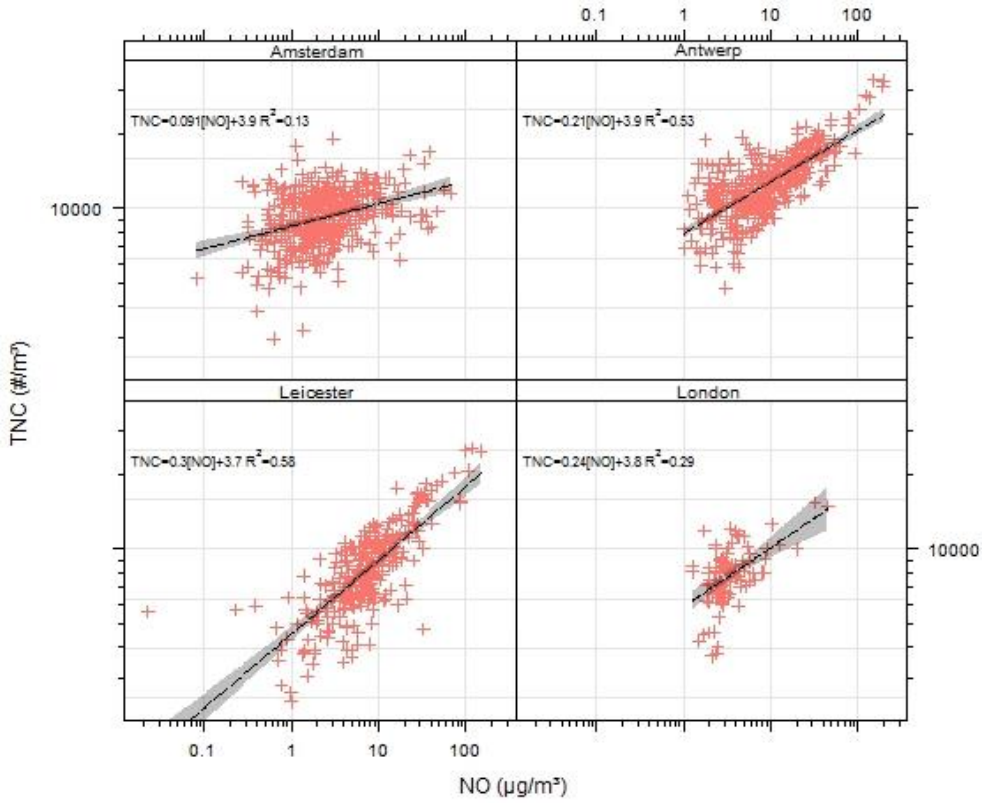

Figure 5.25: Regression plots of daily-averaged total particle number concentration (#/cm³) and NO (µg/m³) for all considered sites (AD1S, AP1S, LE1S and LO1S). Regression plots are displayed with logarithmic scales.

5.6.2 Seasonality of air pollutant relationships

As an example of the possible seasonality of the relation between air pollutants, seasonal regressions are shown for BC vs. TNC at the Antwerp site (Figure 5.26). For Antwerp, the best relation between BC and TNC is obtained during the winter season (R^2 = 0.64). The relationship was weakest in summer (June, July, August), which may suggest that in these months there is also non-traffic UFP (e.g. originating from new particle formation).

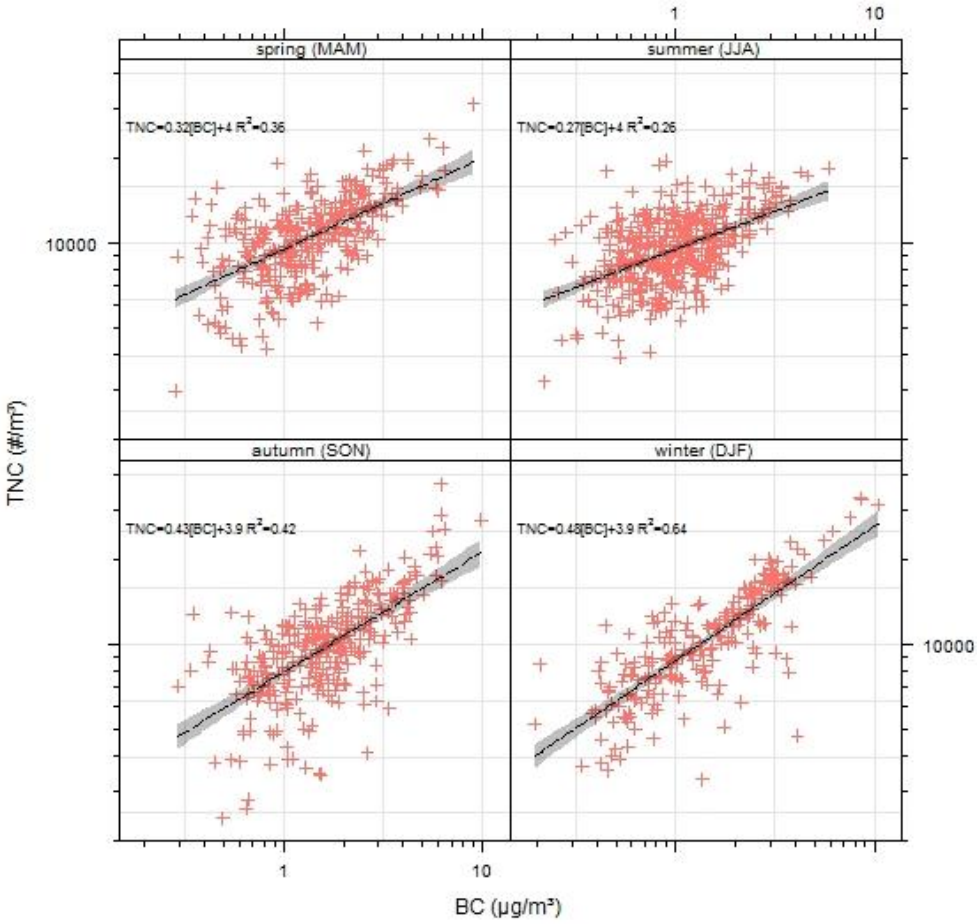

Figure 5.26: Regression plots of daily-averaged total particle number concentration (#/cm³) and BC (µg/m³) per season at the Antwerp monitoring site (AP1S). Regression plots are displayed with logarithmic scales. The months used per season are abbreviated by their first letter.

5.7 Influence of wind on the total particle number concentration and size distribution

All considered monitoring sites are classified as urban background stations. In order to assess the influence of local sources on the measured air quality variables, the potential effect of the experienced wind field on the total and size-resolved particle number concentration was evaluated. From the wind roses visualised in Figure 5.27, it is clear that Amsterdam, Antwerp, Lille and Wijk aan Zee mainly experience SW wind directions.

Average wind speeds over the entire sampling period were 4.8 m s^{-1} for Amsterdam, 4.1 m s^{-1} for Antwerp, 3.0 m s^{-1} for Leicester, 2.3 m s^{-1} for Lille, 3.8 m s^{-1} for London and 7.1 m s^{-1} for Wijk aan Zee. Highest wind speeds were thus obtained for Wijk aan Zee, which is not surprising taking into account the coast-based location of the monitoring station. Note that the wind speed is not necessarily measured at the same height in each city (see section 2.5).

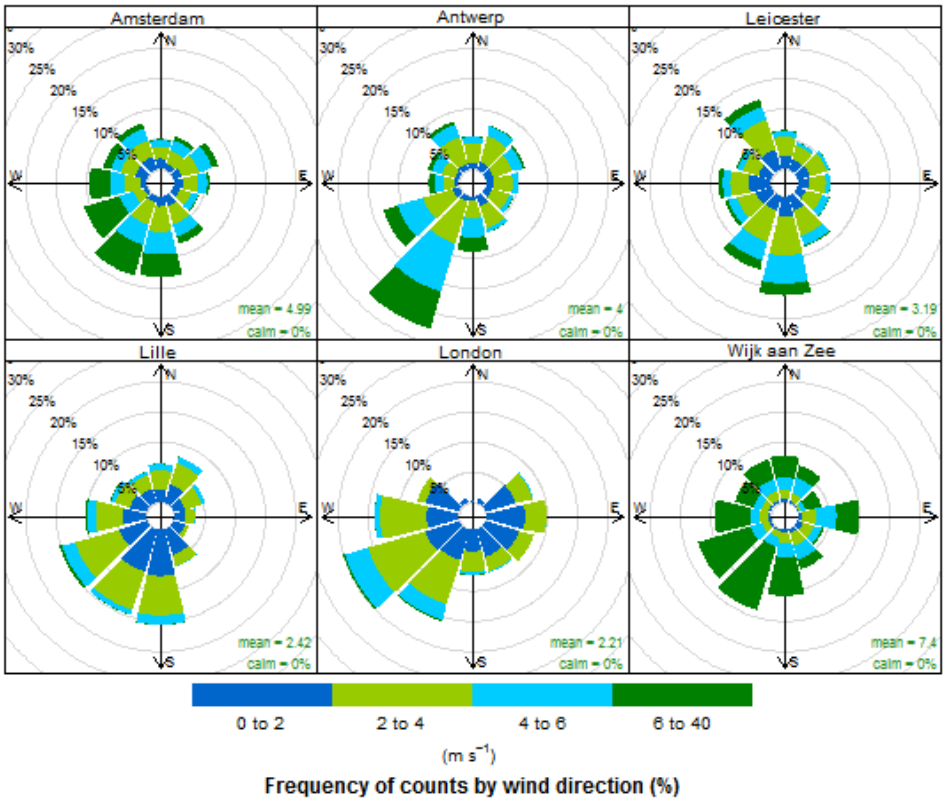

Figure 5.27: Wind roses for the considered monitoring period (April 2013 - December 2014) at all monitoring sites (AD1S, AP1S, LE1S, LL1S, LO1S and WZ1S).

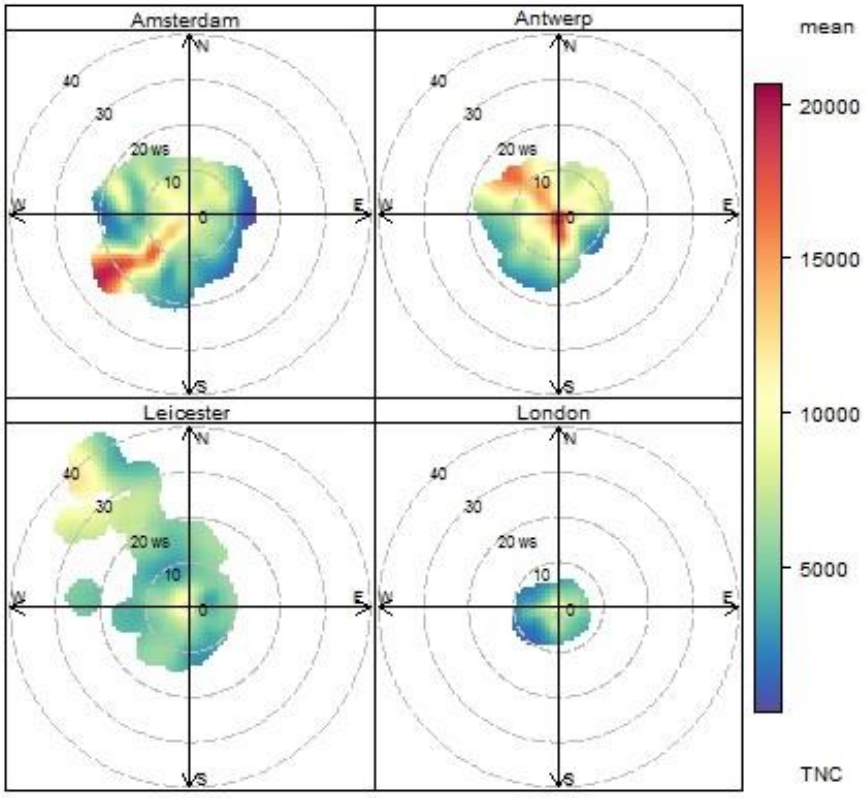

Figure 5.28: Polar plot of the wind field averaged total particle number concentration (# /cm³) for the considered monitoring stations (AD1S, AP1S, LE1S, LO1S).

When polar plots of the wind direction averaged TNC are plotted per monitoring site (Figure 5.28), clear site-dependent effects are observed. While Leicester shows a relatively homogeneous TNC concentration that is independent of wind direction and wind speed, Amsterdam, Antwerp and London show significant TNC variation depending on the experienced wind fields. Moreover, based on the considered polar plots, the location of contributing UFP sources can be derived.

The Antwerp monitoring site (Figure 5.28, top right) is clearly positioned near a southern-located UFP source, which presumably is the traffic-intensive Plantin en Moretuslei. When low wind speeds are experienced, highest UFP concentrations are obtained. At higher wind speeds, UFP emitted by the local traffic will be diluted, resulting in lower UFP concentrations. With NW wind directions, an additional UFP source is observed. Looking at the individual size classes, the source effect of the Plantin en Moretuslei is most apparent for the 20-30 and 30-50 nm size classes (results not shown). Moreover, additional 20-30 and 30-50 nm particle sized sources can be observed when wind is blowing from the NW direction. This effect was observed before at this site (see section 6.1) and might be attributed to other local sources (streets) situated at the northern side of the Antwerp monitoring site and become of importance in the UFP measurements when the wind is blowing from their direction.

For the Amsterdam site (Figure 5.28, top left), a marked increase in TNC can be observed under strong SW winds. Looking at the individual size classes, the increase in TNC for SW winds is only observed for the 10-20 and 20-30 nm size classes (not shown). This might be attributed to emissions from Schiphol airport (Figure 5.29), in line with Keuken et al. (2015), who recently reported a marked UFP increase in Amsterdam dominated by 10-20 nm sized particles for periods when the wind was blowing from Schiphol. The TNC increased by a factor of three at a monitoring station (Adamse Bos) located 7 km from Schiphol (Keuken et al., 2015). Also Hudda et al. (2014) reported on a 4- to 5-fold increase in particle number concentration at 8-10 km downwind of Los Angeles International airport.

Taking into account that (1) Schiphol Airport is located upwind at about 8 km in the SW direction from the Joaquin monitoring site (AD1S; Vondelpark), (2) a non-traffic-related temporal variation of the 10-20 nm size range was observed which persisted throughout the weekends (Figure 5.17) and (3) no clear relations were obtained between TNC and traffic-related pollutants (see 5.6), Schiphol seems to contribute to urban UFP concentrations in Amsterdam. As the wind in Amsterdam mainly blows from the SW direction (Figure 5.27), an influence on the particle number concentrations within the city centre can be expected.

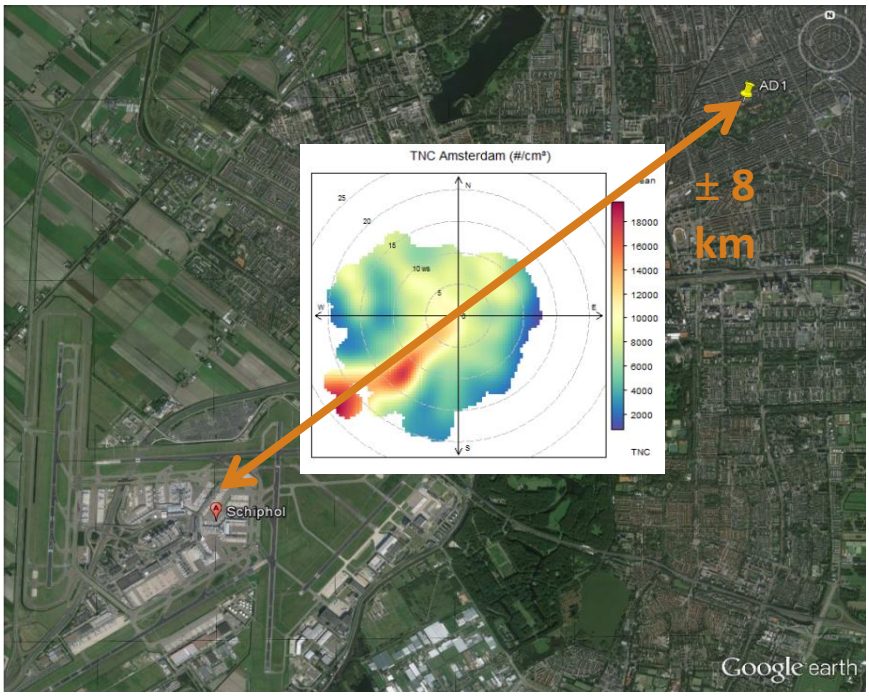

Figure 5.29: Location of the Amsterdam monitoring site (AD1) at about 8 km from Schiphol airport with a polar plot of the resulting total number concentration (TNC) at the monitoring site.

For Leicester (Figure 5.28, bottom left), a slight increase in total particle number concentration can be observed for periods in which wind was blowing from the west (NW-SW). A N-S directed main road (Welford Road) with residential areas is situated west of the Leicester monitoring station and a green area and Leicester University are situated east of the station. As the temporal variation shows a traffic-related diurnal variation, it can be assumed that the main road is contributing significantly to the observed particle number concentrations. The highest contribution in particle number concentration during western wind conditions was observed for the 20-30 nm size class (not shown).

London (Figure 5.28, bottom right) shows rather homogeneous particle number concentrations independently from the experienced wind fields. No clear effect of London Heathrow airport (± 35 km in western direction) or London city airport (± 8 km north) can be observed on the measured UFP concentrations. Only during strong and eastern wind conditions, an increase in TNC can be observed. This might be due to the Port of London, which is located at about 15 km in the eastern direction of the LO1S monitoring site. Previous studies already reported significant UFP contributions of shipping in coastal regions (Gonzalez et al. 2011, Healy et al. 2009, Querol et al. 2011).

Plotting the average TNC per wind direction (Figure 5.30), site-specific particle source contributions seem to be confirmed. Increased particle number concentrations can be observed for certain wind directions as described above.

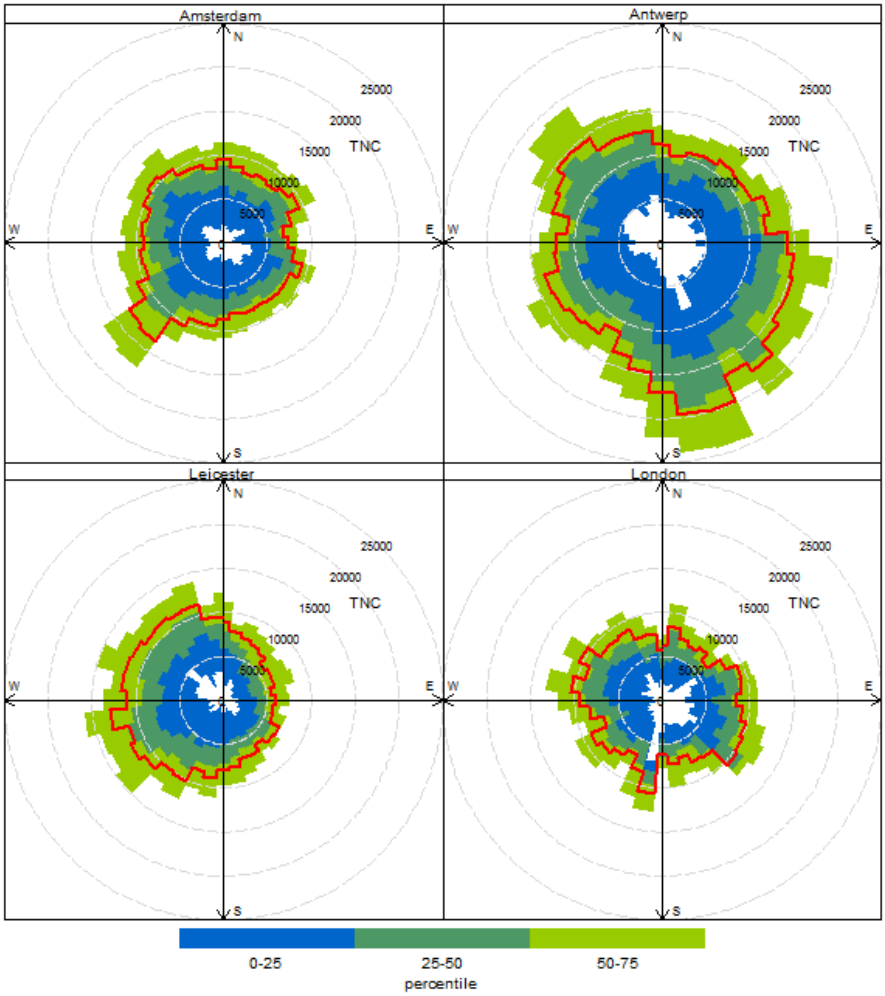

Figure 5.30: Polar plot of the wind direction averaged total particle number concentration (red) with corresponding 0-25, 25-50 and 50-75 percentiles for the considered Joaquin stations (AD1S, AP1S, LE1S and LO1S).

For Amsterdam (Figure 5.30, top left), TNC is increased by 34% when the wind is blowing from Schiphol (205-245°) compared to the other wind directions. Knowing that the city centre of Amsterdam is located downwind of Schiphol airport and south-western wind directions were experienced throughout 16% of the total monitoring period (5436 half-hourly values on a total of 34830 half-hourly

values were between 205-245°), a significant attribution of Schiphol on citizens exposure in Amsterdam can be expected. Taking into account the 34% TNC increase and 16% occurrence of 205-245° wind directions, Schiphol airport determined 5.44% of TNC at the Amsterdam monitoring station near Vondelpark (city center of Amsterdam).

By plotting the particle number concentrations of the smallest size class (10-20 nm) as a function of wind direction, the directional effect becomes much stronger for Amsterdam and Antwerp (Figure 5.31). For Amsterdam, the 10-20 nm PNC is almost doubled (99% increase) when wind is blowing from 205-245° (Figure 5.32, top). Taking into account the 16% occurrence of 205-245° wind directions, Schiphol airport accounted for 16% of the total experienced 10-20 nm particles at the Amsterdam monitoring station.

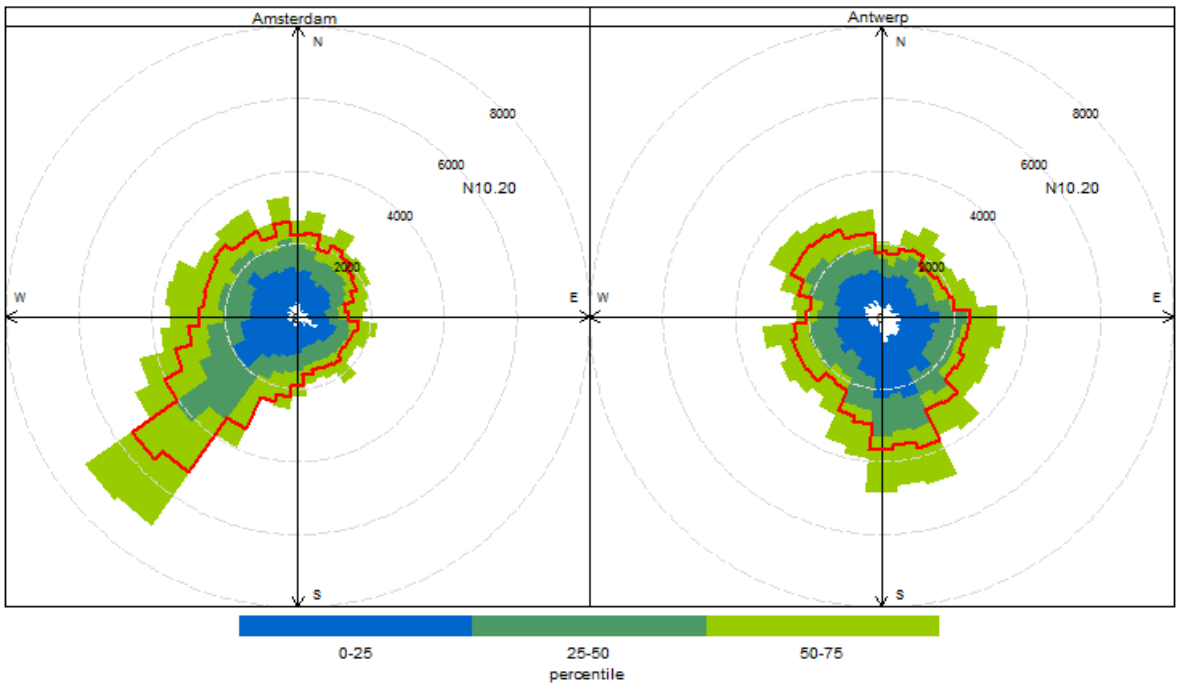

Figure 5.31: Polar plot of the wind direction averaged particle number concentration of the smallest particle size class (10-20 nm) with corresponding 0-25, 25-50 and 50-75 percentiles.

Given the apparent contribution of Schiphol airport to UFP concentrations at the Amsterdam monitoring station (AD1S), the potential effect of the number of plane movements on particle number concentrations was evaluated. Monthly-averaged flight movements (landing or take-off of an aircraft operating a scheduled or non-scheduled service) throughout the monitoring period (Apr 2013 to March 2015) were compared to monthly-averaged PNC of 10-20 nm size class obtained from the SMPS and monthly-averaged TNC obtained from the EPC (Figure 5.33). Monthly-averaged UFP concentrations were selected for 205-245° wind conditions. Based on these monthly data, no clear relation could be observed between the number of flight movements in Schiphol Airport and the particle numbers at the station AD1S. Further analyses could e.g. only look at take-offs instead of including all plane movements and evaluate the relation at a higher temporal resolution.

As Antwerp also has an airport (Antwerp International Airport) at about 2.5 km in south-eastern direction from the AP1S monitoring station (Figure 5.34), a potential influence of this (relatively small) airport on atmospheric UFP concentrations was evaluated as well. To do so, we selected UFP monitoring data during southeast wind episodes (115-155°) and compared the average UFP concentration (total number and size-resolved concentrations) to the UFP concentration measured for all other wind directions.

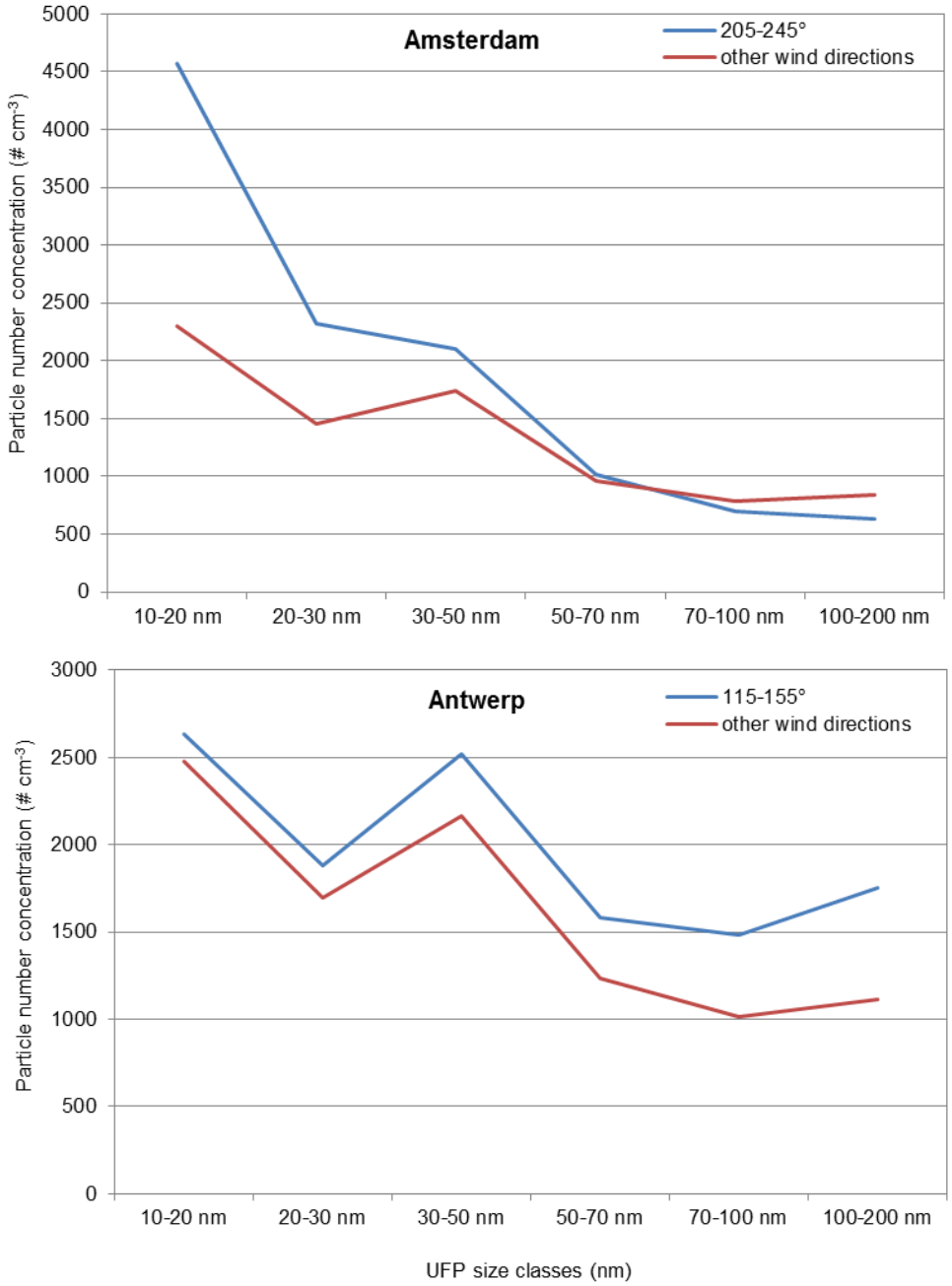

Figure 5.32: Average size distributions measured at the AD1S (Amsterdam) and AP1S (Antwerp) stations during wind conditions coming from the direction of airports (205-245° for Amsterdam and 115-155° for Antwerp; blue) and all other wind directions (red).

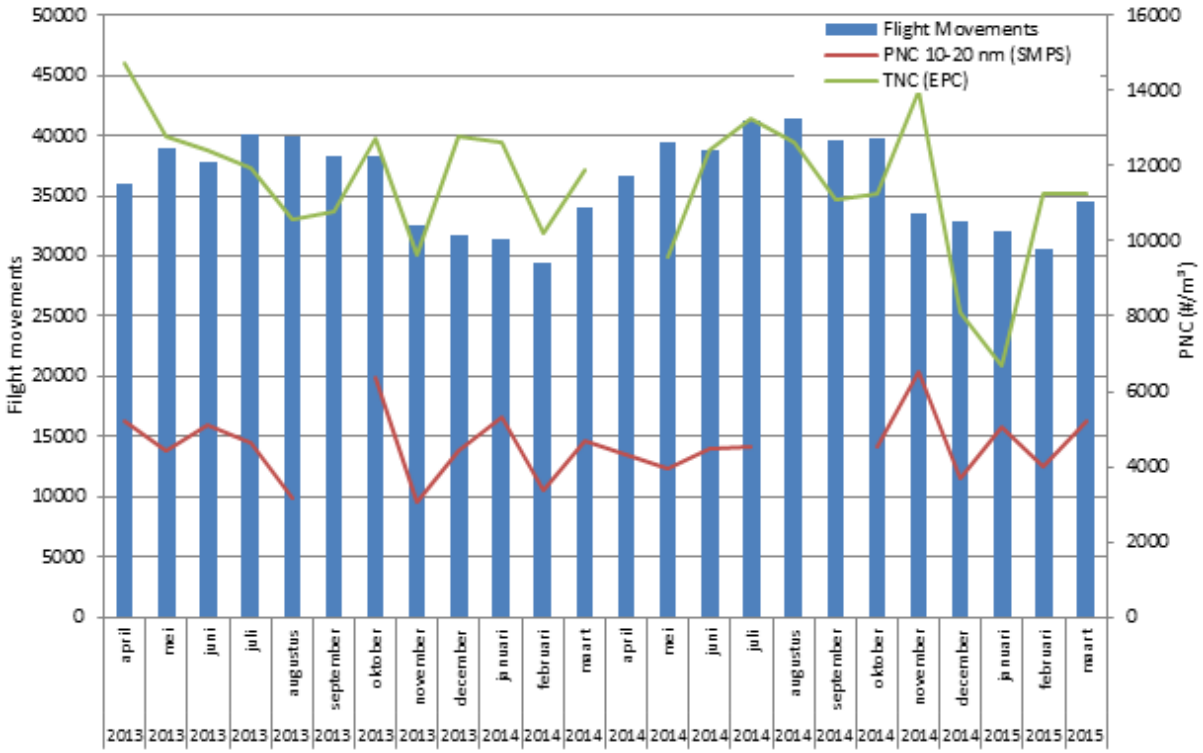

Figure 5.33: Monthly-averaged number of flight movements at Schiphol airport (blue bars), the 10-20 nm particle number concentration (red) and total particle number concentration (green) under SW wind directions for the entire sampling period (April 2013 to October 2014).

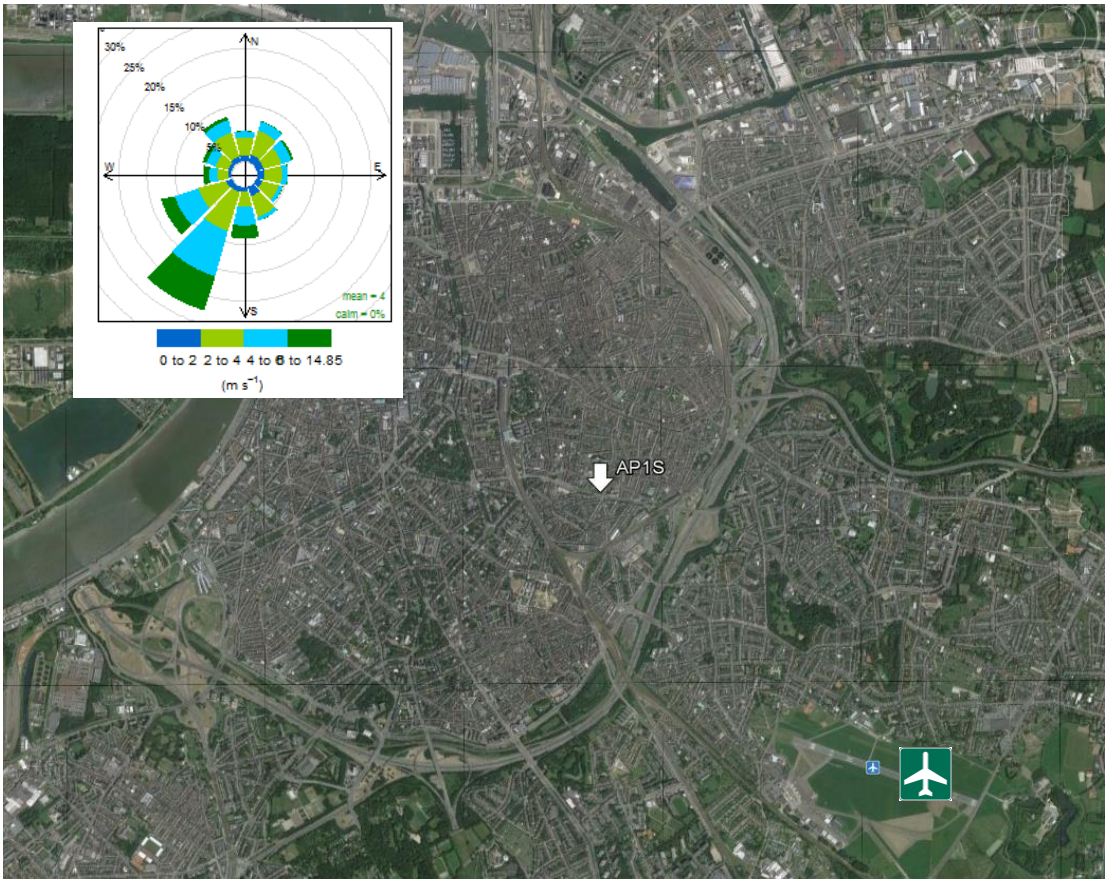

Figure 5.34: Location of Deurne airport at 2.5 km SE from the AP1S monitoring site with a windrose of the experienced wind fields throughout the considered monitoring period.

The average TNC increases with 17% when wind is blowing from the SE (115-155°), from 13432 to 15772 particles/cm^3. Also based on the polar plots in Figure 5.30 and Figure 5.31, a south-eastern emission source can be identified. Nevertheless, in contrast to Schiphol airport, the increase in size-resolved UFP numbers is observed rather evenly spread over the different particle size ranges (Figure 5.32, bottom), slightly dominated by the larger particle size ranges (>50 nm). This leads us to conclude that the observed UFP increase does not only originate from Antwerp airport but may consist of particles originating from the Antwerp ring road which is located in between the AP1S site and the Antwerp airport (Figure 5.34).

From the UFP size distribution, no clear influence of Antwerp International airport on the measured UFP concentrations at the AP1S site can be observed. Moreover, good relations are obtained with typical traffic-related pollutants (see Figure 5.24-Figure 5.26). It should be noted that the airport has about 10 times less flight movements compared to Schiphol (between 2500 and 4822 monthly flight movements in 2013 and 2014) and that the city centre of Antwerp is not located downwind of the airport (wind directions between 115 and 155° were only experienced during 7% of the half-hourly measurements (2388 of 34622 half-hourly measurements). The impact of Antwerp International Airport on the UFP exposure of local inhabitants of Antwerp seems, therefore, inferior to the emission strength of road traffic (Plantin en Moretuslei and ring road).

5.8 Lung-deposited surface area (LDSA) at an urban background site in Leicester (LE1S)

The surface area of atmospheric aerosols is an important property alongside other properties such as particle mass and number concentrations. Over recent years a number of epidemiological studies examining the health effects of particles have shown that the particle surface area may have a stronger correlation with negative health effects than particle mass and number (Oberdörster 2005, Nel et al. 2006, Singh et al. 2007, Nurkiewicz et al. 2009).

In the monitoring station in Leicester (LE1S, see section 2.2.3.1), the lung-deposited surface area (LDSA) was measured by a nanoparticle surface area monitor (NSAM, TSI 3550, see section 2.3.4). We present the LSDA measurements at station LE1S from November 2013 to April 2015 (99% data coverage) and discuss the findings in relation to other air pollutants. Furthermore, the LDSA values as measured directly by the NSAM were compared with results obtained by calculating the LDSA parameter from SMPS measurements. This comparison was possible for the short period when the mobile trailer was next to station LE1S (4 March to 4 April 2014, see 4.3).

5.8.1 Diurnal, weekly and seasonal variations of LDSA

Similarly to BC and NO_x, a clear seasonal variation was observed for the LDSA concentration. Statistics of LDSA, BC, and NO_x are shown in Table 5.8.

Table 5.8: Statistics of LDSA (µm^2/cm^3), BC (µg/m^3), and NO_x (µg/m^3) measured in Leicester (LE1S). Total period: Nov 2013 to May 2015). Cold period: Nov to Apr, warm period: May to Oct 2014.

Variable	Time period	Average	Min	Max	St. Dev.
LDSA	Total period	30	0.1	295	25
	Cold period 2013-2014	39	0.6	283	33
	Cold period 2014-2015	37	1.5	295	26
	Warm period	23	0.1	146	14
BC	Total period	1.5	0.1	16.0	1.4
	Cold period 2013-2014	1.8	0.9	13.5	1.8
	Cold period 2014-2015	1.8	0.2	16.0	1.7
	Warm period	1.3	0.1	13.0	1.0
NO_x	Total period	41	0.4	628	38
	Cold period 2013-2014	48	2.1	597	47
	Cold period 2014-2015	52	2.4	628	45
	Warm period	29	0.4	232	21

The diurnal variation of LDSA (Figure 5.35), like for BC and NO_x, depends on emission characteristics of the dominant sources and on meteorological conditions. The average daily patterns of LDSA, BC, and NO_x based on half-hourly means are quite similar. During the cold period (Nov - Apr) the impact of traffic was obvious on weekdays (Mon-Fri) when the highest LDSA concentrations were measured during morning (6:00 - 9:00) and evening (18:00 - 21:00) rush hours. This likely results from the motor vehicle emissions combined with a lower mixing layer height and lower temperature. Higher LDSA concentrations were also measured on workday morning rush hours during the warm period, but with lower LDSA values than in the cold period. This may be due increased solar radiation leading to faster atmospheric dispersion of aerosols and hence a dilution of LDSA concentration. In addition, LSDA in summer was usually lower in the evening rush hour than in the morning, which is probably related to the stronger turbulent mixing and higher mixed layer depths in the evening.

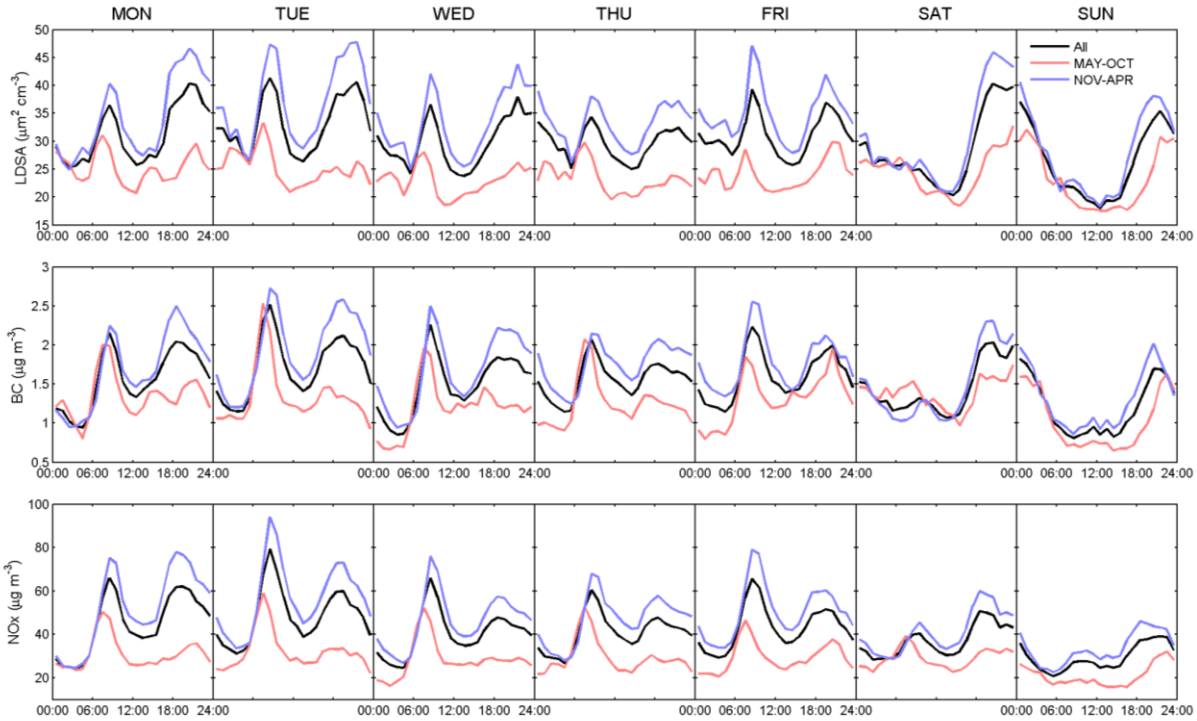

Figure 5.35: Diurnal and weekly variations of LDSA, BC, and NO_x in Leicester (LE1S) for all data (black line), the warm period (May-Oct, red line) and the cold periods (Nov-Apr, blue line).

During the weekends, the diurnal variation of LDSA was similar throughout the year, but considerably different from that on workdays. In the early morning of the weekends lower LDSA concentrations were observed whereas higher concentrations were observed in the afternoon and evening. During the cold season weekends an afternoon peak still occurs as traffic emissions are combined with the emissions from cooking and domestic heating, making it higher than the warm period afternoon peak. Additional weekend contributions occur in summer from events such as barbeques, and late night activities on Saturdays result in a longer lasting peak occurring later in the day. It is interesting to note that there was also a LDSA peak around mid-day that did not occur for BC and NO_x, which suggests that the afternoon peak might not be linked with traffic emissions. Previous studies have shown similar peaks in the diurnal variation of number concentrations at urban background sites (Jeong et al. 2004, Laakso et al. 2003) due to new particle formation (Menon et al. 2002, Kulmala et al. 2004, Kuang et al. 2008).

5.8.2 Relationship between LDSA and BC, NO_x and total number concentration

The relationship between LDSA and other pollutants (BC, NO_x, total particle number concentrations (TNC)) was examined at the seasonal level (Figure 5.36). In general, LDSA correlates well with the other pollutants. The results suggest that traffic emissions have a major impact on LDSA at this site. The correlation between half-hourly LDSA on the one hand and BC, NO_x or TNC on the other hand was significantly higher in the winter than in other seasons. This may be related to meteorological

conditions and/or indicate that the sources of particles in the winter were not the same as those in other seasons.

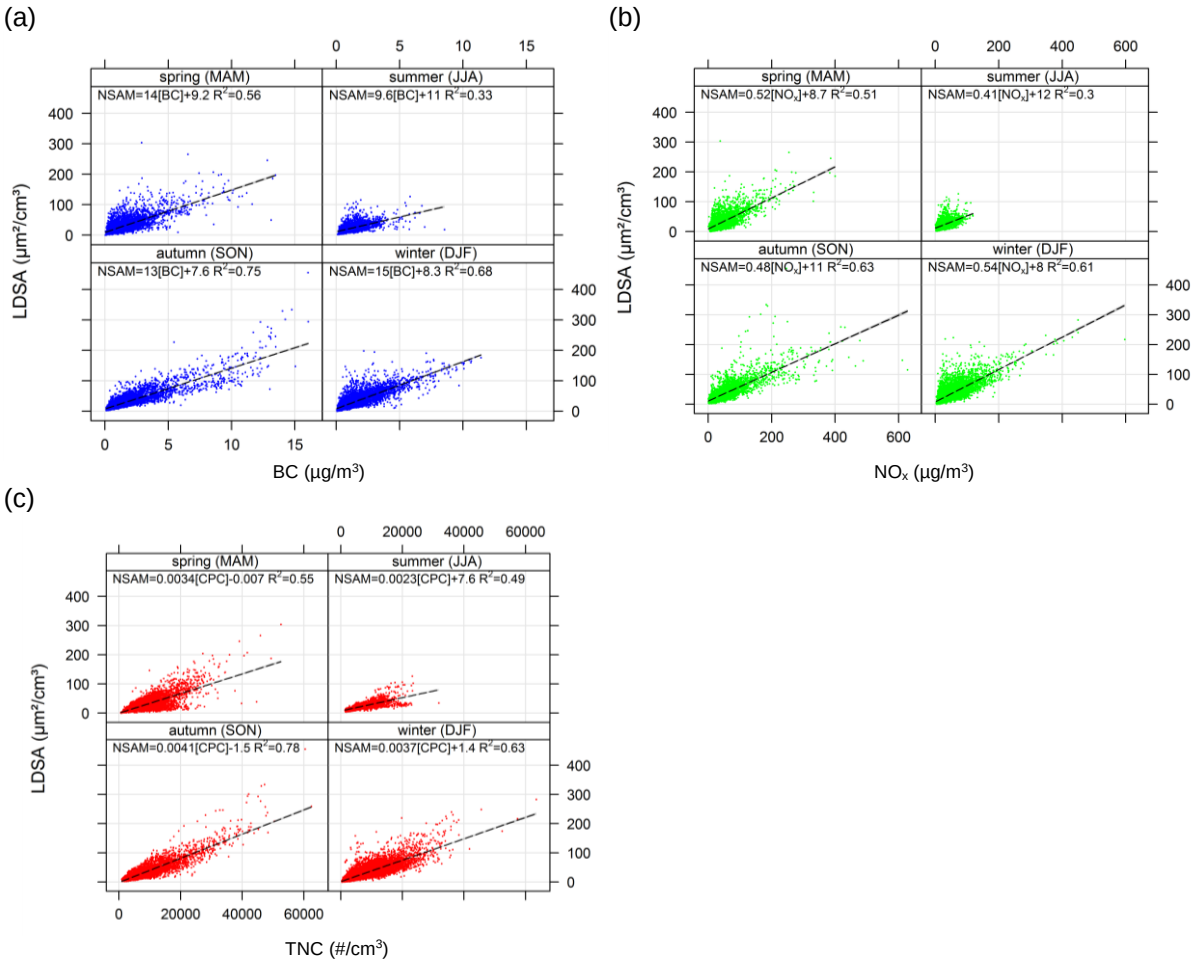

Figure 5.36: Seasonal correlations between LDSA and (a) BC, (b) NO_x, (c) total number concentration (TNC) in Leicester (LE1S) from Nov 2013 to Apr 2015.

5.8.3 Comparison of LSDA according to NSAM and SMPS

The LDSA concentration as measured directly with the NSAM was also calculated from SMPS particle size distribution data for a 1-month period in March 2014. Calculations were carried out assuming spherical particles and according to the ICRP model for a reference worker (ICRP 1994). LDSA from SMPS was calculated by converting the particle number size distribution into a total surface area size distribution (Eq. 3.1) and multiplying this distribution with the size-dependent alveolar deposition fraction as specified by the ICRP model (Eq. 3.2) (see Figure 2.18).

$$Surface\ Area(d_{pi}) = \pi \times d_{pi}^2 \times N(d_{pi}) \qquad \text{(Eq. 5.1)}$$

$$LDSA = Surface\ Area(d_{pi}) \times [ICRP]\% \qquad \text{(Eq. 5.2)}$$

with d_{pi} the central diameter of the upper and lower boundaries for a given size bin and $N(d_{pi})$ the particle number concentration. The size distributions recorded by the SMPS were weighted by the alveolar deposition curve and integrated over different size ranges of interest (10-100, 20-100, 20-400, and 400-1000 nm). The results in Figure 5.37 show that the LDSA of the NSAM and the LDSA based on the 20-400 nm size bins of the SMPS were in good agreement, with a coefficient of determination (R^2) of 0.89 and a regression slope of 1.2. Overall, it can be concluded that the LDSA measured by the NSAM appears to cover particles from 20 to 400 nm.

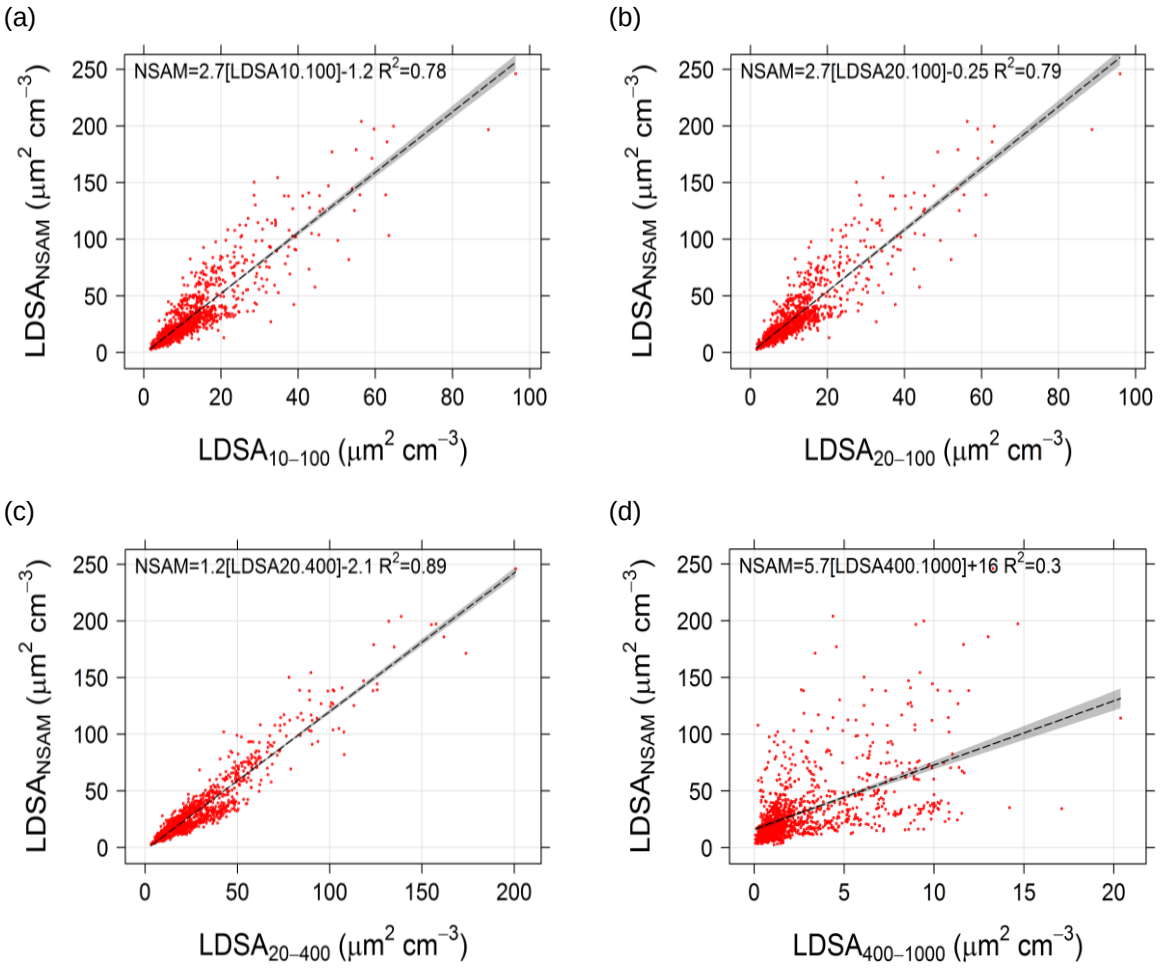

Figure 5.37: LDSA comparison between the NSAM and SMPS in Leicester (LE1S, March 2014) for the LDSA calculated from the SMPS particle size range of (a) 10-100 nm, (b) 20-100 nm, (c) 20-400 nm, (d) 400-1000 nm.

6 Intra-urban variability of UFP and BC

In epidemiological studies, UFP data from a single monitoring site are generally used as a measure of population exposure in a wider region. One reason for this is the lack of sufficient data at other sites and this may potentially result in exposure misclassification. While the variation in PM_{10} (or related particle mass parameters) is known to be quite low over an urban region, this is less obvious in the case of particle numbers.

In the Joaquin project the intra-urban variability between sites was investigated by comparing temporal and spatial variations of UFP particle number and size distributions during dedicated campaigns.

- First of all, in the city of Antwerp a gradient study near a main road and two intra-urban campaigns were carried out in 2013. In total UFP concentrations were measured simultaneously at seven different sites. The results are described in other reports and summarized in section 6.1.
- Furthermore, in three cities (Amsterdam, Antwerp and Leicester) simultaneous measurements were carried out at two sites, i.e. the fixed monitoring station and a trailer location. All six sites are classified as “urban background” with respect to measurements of PM_{10}. More details of each measurement site are given in chapter 2. The results of these campaigns are show in section 6.2.

6.1 Short-term gradient study and intra-urban campaigns in Antwerp (2013)

6.1.1 Overview of reports

In 2013, two UFP measurement campaigns were conducted in Antwerp by VITO and ISSeP under the authority of VMM. Different types of air quality locations were selected to find out (1) how the UFP concentration and distribution varies with increasing distance to a main road and (2) if one central monitoring station is representative for UFP concentrations in the Antwerp region.

The results of the first measuring campaign, carried out in February 2013, were reported by Frijns et al. (2013b). The second campaign in October 2013 was described by Frijns et al. (2014), but only data of three of the four sampling sites were included.

The report VMM (2014) combines the results of the February and October 2013 campaign in Antwerp, and additionally gives information about:

- measurements of the public park location during the October campaign;
- measurements of traffic intensity and relationships between UFP and traffic;
- comparison of the results of the February and October campaigns.

6.1.2 Conclusions (VMM 2014)

The gradient study at monitoring station in Antwerp (AP1S) in February 2013 evaluated the number concentration and the size distribution of particles at three sampling sites at 10, 30 and 55 m distance of a main road (2 x 2 lanes). The main results were:

- The total number concentration of particles < 1 µm (TNC) was higher at 10 m from the road than at 30 and 55 m. The concentration at 55 m was slightly higher than at 30 m, so that for the total 4-week measuring period no clear gradient was observed.
- For downwind conditions the TNC was on average 17% lower at 30 m from the road than at 10 m and 22% lower at 55 m from the road than at 10 m.
- For downwind conditions the number of particles <25 nm decreased with increasing distance to the road. The larger particles differed less between the three distances.

The intra-urban study in Antwerp in February and October 2013 analysed the spatial-temporal variability of the number concentration and size distribution of particles at 5 sites (February) or 4 sites (October). It was found that:

- The mean TNC varied by a factor of five between the sites and increased with an increasing traffic exposure of the site. On week days all sites showed a diurnal variation in the TNC, with traffic-related peaks during the morning and evening rush hours;

- The TNC was strongly correlated between the urban background site and the 4 other sites. However, this relationship differed between the February and October campaigns.
- The particle number in the distinguished size classes was moderately to strongly correlated between the monitoring station and the 4 other sites. The correlation was lower for particles of 20-30 and 30-50 nm and increased for the larger size classes.
- The particle size distribution generally had a similar trend for all sites and periods. The highest number concentrations were found on week days for particles <20 nm (on the average 26% of the TNC). In the weekends the size classes <20 nm and 30-50 nm contributed equally to the TNC (about 20%). Ultrafine particles dominated the TNC, accounting on the average for 87% of the TNC on week days and 81% in the weekend.
- In comparison with the urban background site, the spatial divergence in the TNC was lowest at the public park site and highest at the street canyon site.

We also examined relationships between particle numbers, 3 other air quality variables and the traffic intensity. It was found that:

- The TNC per site was correlated with PM_{10} in October, based on daily means, but the data were limited and the relationship varied per site and most likely also over time.
- The TNC per site and period was strongly correlated with BC and for all sites a maximum correlation value was found for particles of 100-200 nm. The relationship varied per site and period.
- The TNC at all sites was strongly correlated with NO_2 (weekly data), and smaller particles were more strongly correlated with NO_2 than larger particles.
- The TNC per site and period was correlated with the traffic intensity, and the highest correlations were found for small (<50 nm) particles.

From this short-term study we conclude that:

- The urban background station in Antwerp (AP1S) cannot be considered to be representative for rural background areas and more traffic-exposed sites.
- The particle number at 5 sites and during 2 periods in Antwerp was influenced by traffic intensity, but also depended on other factors such as the site characteristics, the proximity to local sources and meteorological conditions.
- During this short-term study positive relationships were found between UFP and PM_{10}, BC and NO_2, but the relationships varied by site and period.
- More data are needed to examine whether and which relationships exist on the long-term between these parameters and the number and size distribution of ambient particles.

6.2 Short-term campaigns at two sites per city in Amsterdam, Antwerp and Leicester

To evaluate the intra-urban variability of the monitored pollutants, UFP and BC measurements at the fixed monitoring sites in for Amsterdam, Antwerp and Leicester (AD1S, AP1S and LE1S) were compared to simultaneous measurements at the second trailer locations (AD2T, AP2T and LE2T) (Table 6.1). The comparison periods lasted 2 to 6 weeks, depending on the city. In London, no measurements at a second trailer location were performed.

Table 6.1: Fixed (S) and trailer (T) measurements to evaluate intra-urban pollutant variability.

Station	Location	Site	Monitoring period	Instruments*
AD1S	Vondelpark	Fixed	14/05/2013 - 30/05/2013	MAAP, EPC, SMPS
AD2T	Nieuwendammerdijk	Trailer	14/05/2013 - 30/05/2013	MAAP, EPC, UFPM, SMPS
AP1S	Borgerhout	Fixed	07/10/2013 - 04/11/2013	MAAP, EPC, SMPS
AP2T	Stadspark	Trailer	07/10/2013 - 04/11/2013	MAAP, EPC, UFPM, SMPS
LE1S	Leicester University	Fixed	05/04/2014 - 29/05/2014	MAAP, EPC, UFPM
LE2T	Brookfield	Trailer	05/04/2014 - 29/05/2014	MAAP, EPC, UFPM, SMPS

* BC was measured with a MAAP, TNC with an EPC and the UFP size distribution with an SMPS or an UFPM. More information on the instruments is given in section 2.

6.2.1 Average TNC and BC

Figure 6.1 shows the average TNC at the fixed station and trailer location per city. The averages were calculated over the respective campaigns in Amsterdam, Antwerp and Leicester and hence were not obtained simultaneously in the three cities (Table 6.1).

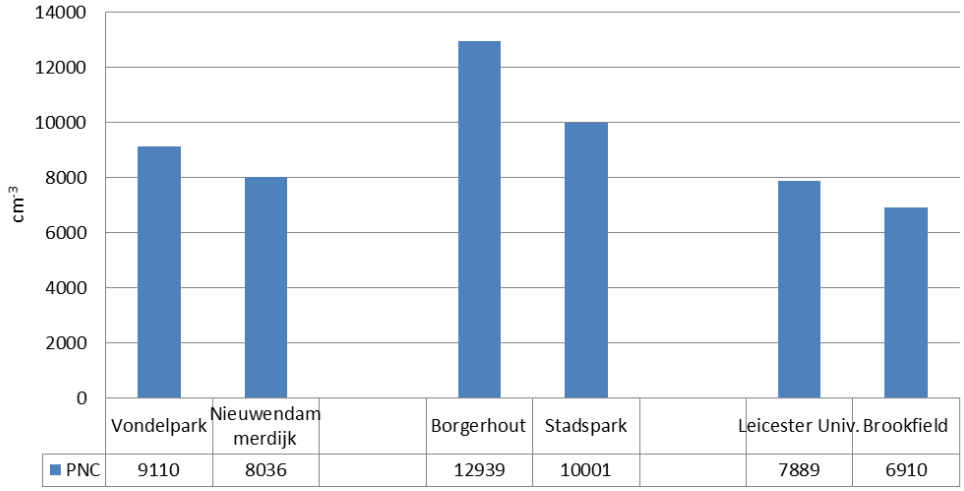

Figure 6.1: Average TNC at the monitoring station and trailer location in Amsterdam (Vondelpark and Nieuwendammerdijk), Antwerp (Borgerhout and Stadspark) and Leicester (Leicester University and Brookfield). Note: results of short-term monitoring periods that were carried out non-simultaneaously in the three cities.

The mean TNC ranges from 6820 (Brookfield, LE2) up to 12939 particles/cm^3 (Borgerhout, AP1). Patterns seen for the fixed monitoring sites during these limited campaigns were confirmed in the longer-term measurements at these sites, and mainly reflect the proximity to and intensity of road transport. For example, the Borgerhout site in Antwerp is rather close to a busy road which explains the high numbers there; the Brookfield site in Leicester is at a relatively quiet parking lot.

The spatial differences in BC are shown in Figure 6.2, again calculated as averages over the respective campaigns in Amsterdam, Antwerp and Leicester. Here, we observe a similar pattern as for UFP number concentrations, i.e. higher levels at the fixed stations. Considering the changes between the paired sites it is noted that the relative increases for BC is higher than for TNC. This is most evident in the cities of Antwerp (+75% for BC and +29% for TNC) and Leicester (38% versus 14%). Although UFP and BC have a common source (traffic), the stronger rate of change might be caused by non-exhaust road traffic emissions such as tire and brake abrasion resulting in particles constituting of BC being larger than the ultrafine diameters of particles (<100 nm) emitted by road traffic exhaust. The effect is strongest at the monitoring station in Antwerpen due to nearby vehicle emissions.

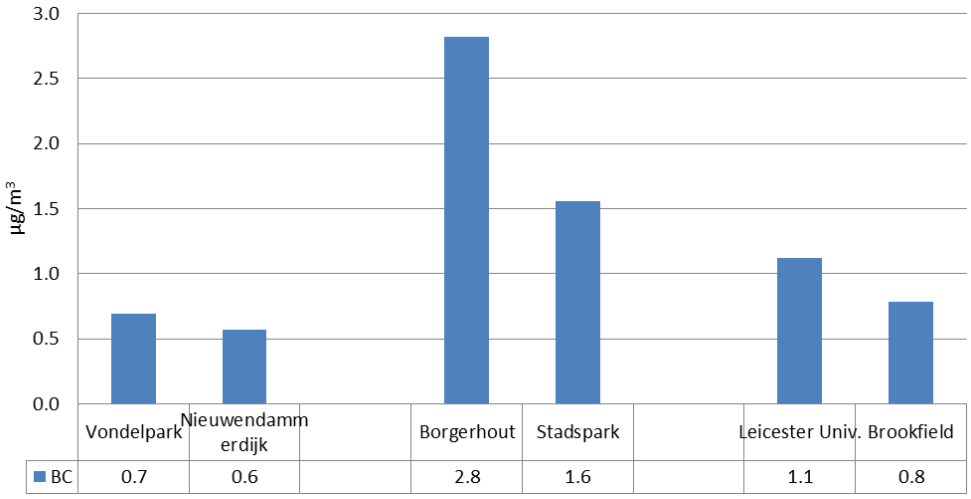

Figure 6.2: Average BC concentrations at the monitoring station and trailer location in Amsterdam (Vondelpark and Nieuwendammerdijk), Antwerp (Borgerhout and Stadspark) and Leicester (Leicester University and Brookfield). Note: results of short-term monitoring periods that were carried out non-simultaneously in the three cities.

6.2.2 Time series of TNC and BC

The half-hourly BC and UFP data at the trailer locations were averaged to hourly concentrations and plotted against the BC and UFP concentrations obtained from the fixed monitoring sites in Amsterdam (Figure 6.3), Antwerp (Figure 6.4) and Leicester (Figure 6.5).

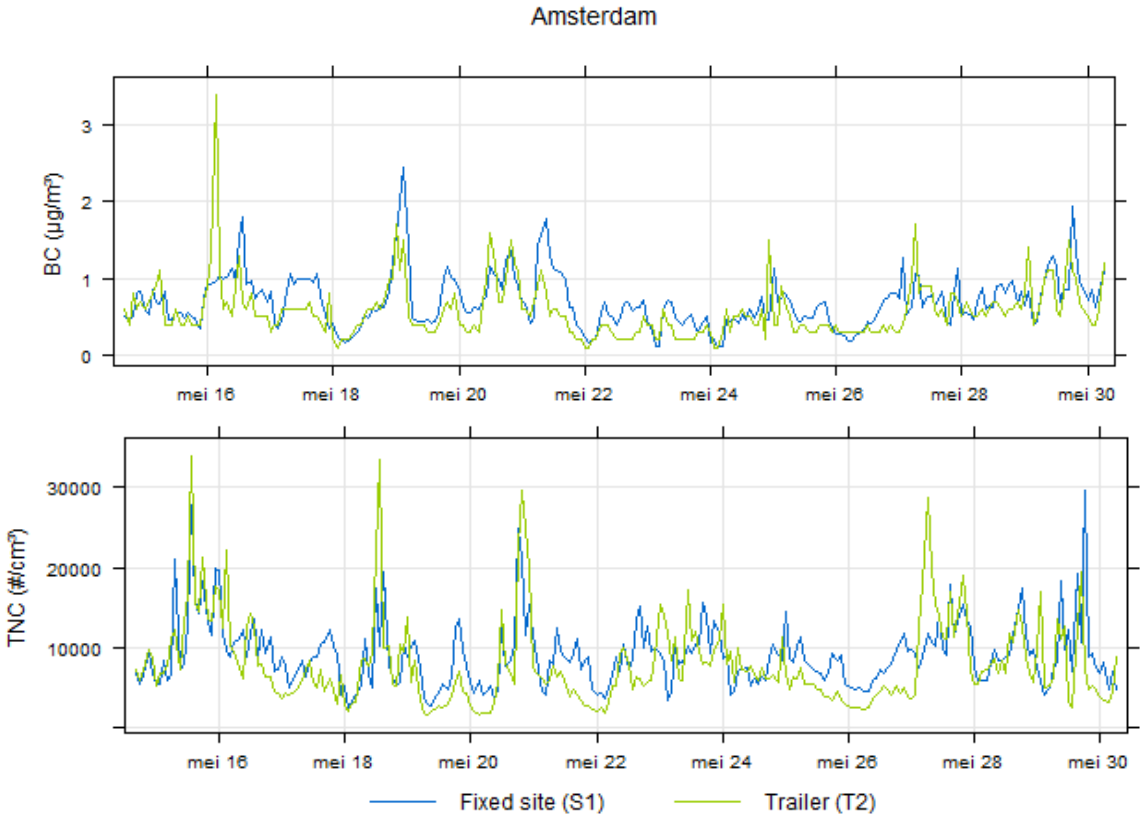

Figure 6.3: Temporal variation of the hourly black carbon (BC) and total particle number (TNC) concentration at the monitoring station (1S) and trailer (2T) locations in Amsterdam (May 2013).

The temporal variation plots show that the BC and UFP concentrations at the two considered locations per city (fixed monitoring station 1S and trailer location 2T) covariate in time. In particular for Antwerp

(Figure 6.4) and Leicester (Figure 6.5), the covariance in pollutant concentrations between both locations seems good, while for Amsterdam some deviations between the two monitoring locations is observed (Figure 6.3).

The time series show that variations of UFP levels correspond with time at the paired sites to a certain extent. First, there is a (slowly changing) base level (with lowest concentrations) which behaves roughly similar in time and magnitude at both paired sites. In particular, this is the case in Antwerp and Leicester, while in Amsterdam there is a small difference of roughly 3000 #/cm^3. It is noted that the distance between the paired sties is largest in Amsterdam (8 km) with Nieuwendammerdijk already close to the border of Amsterdam, while the sites in Leicester and Antwerp are still located in the city centre. This can be considered as the non-urban background contribution. Looking at the individual particle size classes, it can be seen that this effect is predominantly observed in the 10-20 nm size class, which may be influenced by the different distance to Schiphol.

In addition, part of the fast variation is recognizable at both sites per city. A clear example is seen in the time series for Antwerp (Figure 6.4): the peaks at the Stadspark location (AP2) usually occur at the same moment at Borgerhout (AP1) but have a different magnitude. This is also found at the Leicester sites, and to a lesser extent, at the Amsterdam sites, likely due to the different influence of a non-traffic source. This could be regarded as an overall urban contribution mostly originating from traffic emissions following a similar behaviour in time but differing in quantity depending on the distance to these emissions. Apart from these contributions, there are local effects affecting one site but not the other as can be seen in Amsterdam.

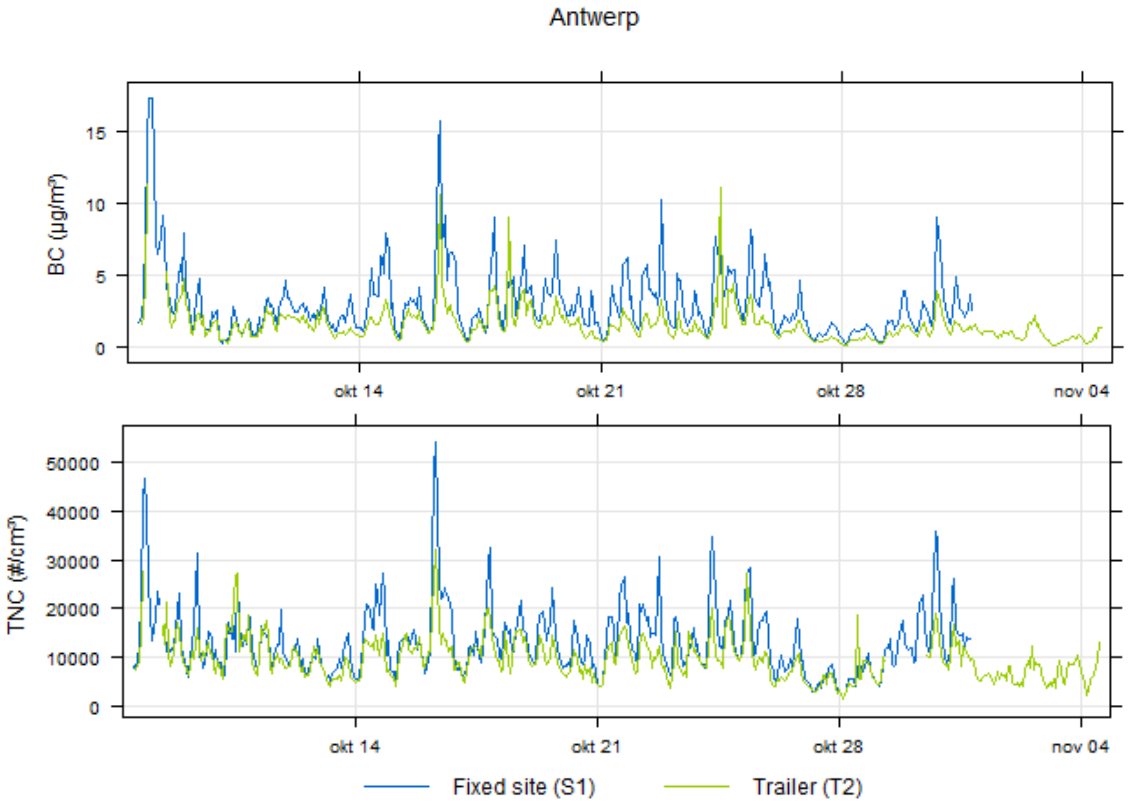

Figure 6.4: Temporal variation of the hourly black carbon (BC) and total particle number (TNC) concentration at the monitoring station (1S) and trailer (2T) locations in Antwerp (October 2013).

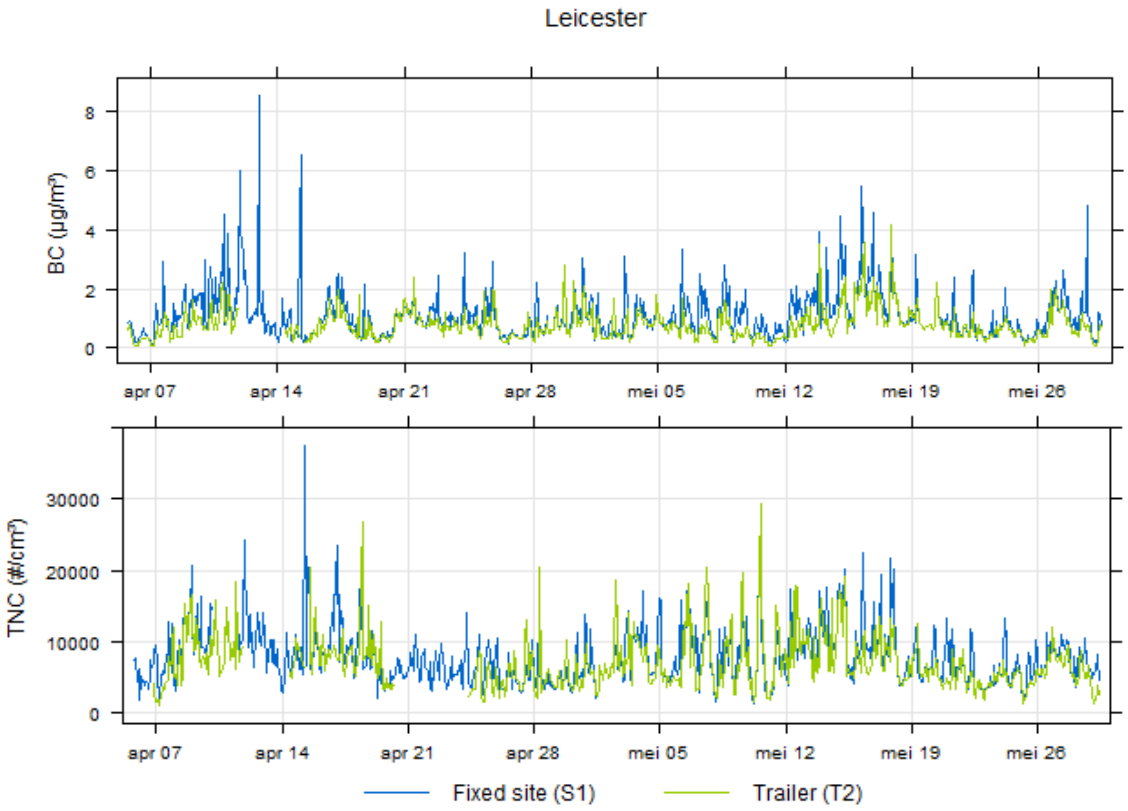

Figure 6.5: Temporal variation of the hourly black carbon (BC) and total particle number (TNC) concentration at the monitoring station (1S) and trailer (2T) locations in Leicester (May 2014).

Although the intra-urban BC and UFP concentrations covariate in time, some deviations (e.g. Amsterdam) and differences in magnitude can be observed within the individual cities. For Amsterdam, the fixed station and trailer location are located in relatively green areas. Nevertheless, the trailer location has no important local traffic sources and is located further away from Schiphol airport. This might explain the predominant lower BC and UFP concentration at the trailer location. The BC and UFP concentration in Antwerp is clearly lower at the trailer location (T2), which is not surprising as the trailer was located inside an urban green area (public park) while the fixed monitoring site is located near a busy access road of Antwerp. For Leicester, no clear deviations between the fixed station and the trailer site can be observed. Both locations are relatively quiet, and at a comparable distances from a main road, respectively Welford road (22500 vehicles/day in 2013) and London Road (20500 vehicles/day in 2013) as documented in section 2.

6.2.3 Association between the TNC and BC at the two sites per city

To evaluate the intra-urban variability of BC and total UFP concentration (TNC), regressions of the measured BC and TNC concentrations at the considered locations (fixed-trailer) were plotted for each city (Figure 6.6). In line with the interpretation of the time series, the correlation of the TNC between the two sites per city is highest in Antwerp (r = 0.70) and Leicester (r = 0.61), in contrast to the lower correlation for Amsterdam (r = 0.44).

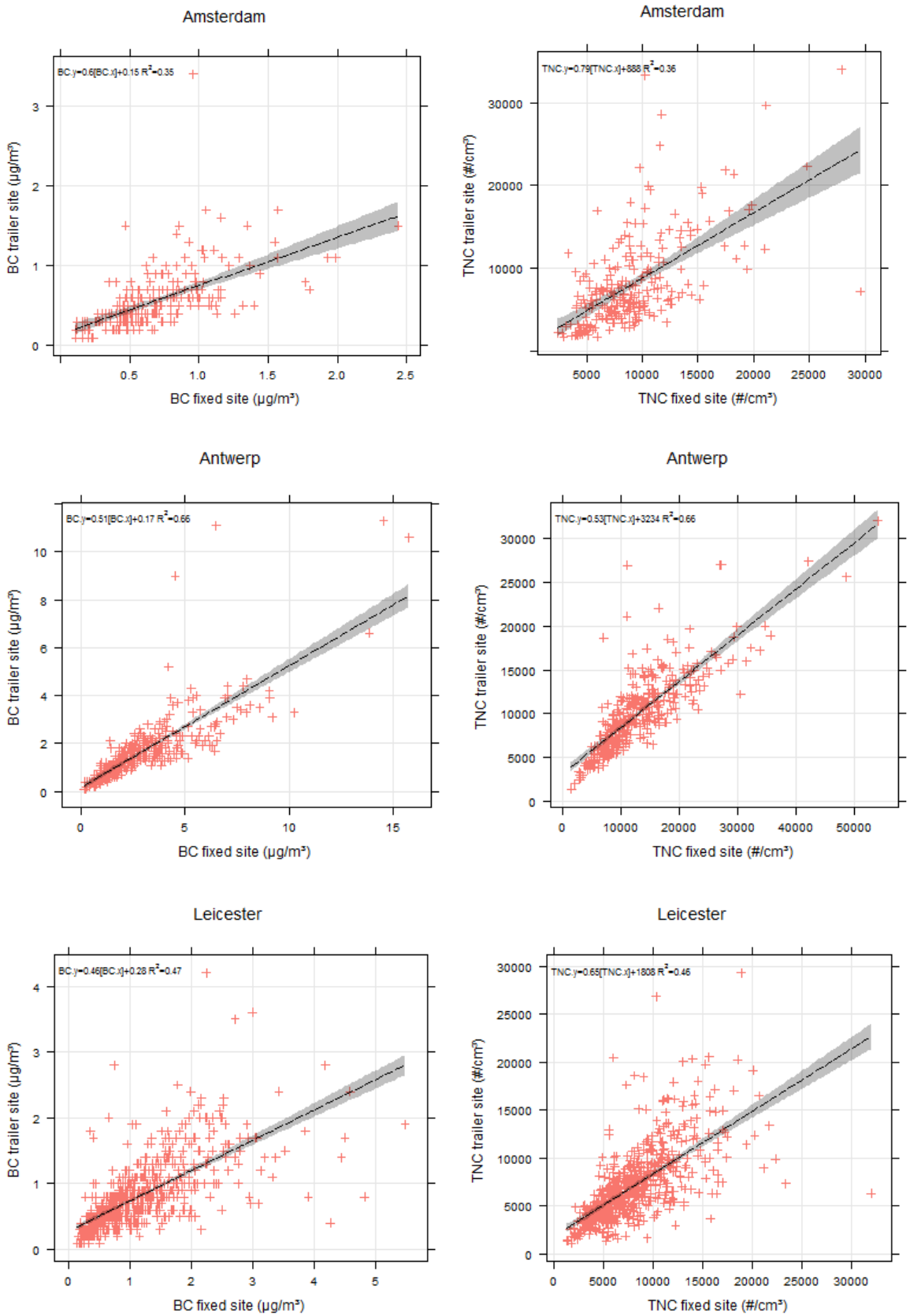

Figure 6.6: Scatterplots of the half-hourly BC (left) and TNC (right) concentrations at the trailer location vs. the fixed monitoring station in Amsterdam (top), Antwerp (middle) and Leicester (bottom).

Studying the time series for Amsterdam in more detail (Figure 6.3) it is seen that occasionally much higher (peak) values at the second site have been measured. Looking at the individual size classes (not shown) indicates that the peaks are mainly caused by 10-20 nm particles. Further insight for these unusual peak events can be derived by plotting the (half-hourly) differences in concentrations as a function of the prevailing wind direction (Figure 6.7):

- For the wind directions between 50° and 200° no systematic deviation is observed. Both sites then show similar numbers largely due to the dominance of long-range transport over Europe in these directions. Particle numbers also appear low (in contrast to the mass contribution) for this wind sector.
- For wind directions between 200° and 270° there is an extra contribution of particles, most likely originating from emissions southwest of Nieuwendammerdijk, which may be from the city area and/or Schiphol, resulting in the higher number concentrations.
- For wind directions between 270° and 50° (W to NE) the Vondelpark station shows higher numbers probably due to industrial activity in the Amsterdam harbour and busy motorways (A10, A8) which does not influence the second site Nieuwendammerdijk in a similar manner. A very local contribution might arise from the Overtoom itself. Traffic emissions in this street might reach the station by the open passage between this street and the station (located ~60 m south of the Overtoom).

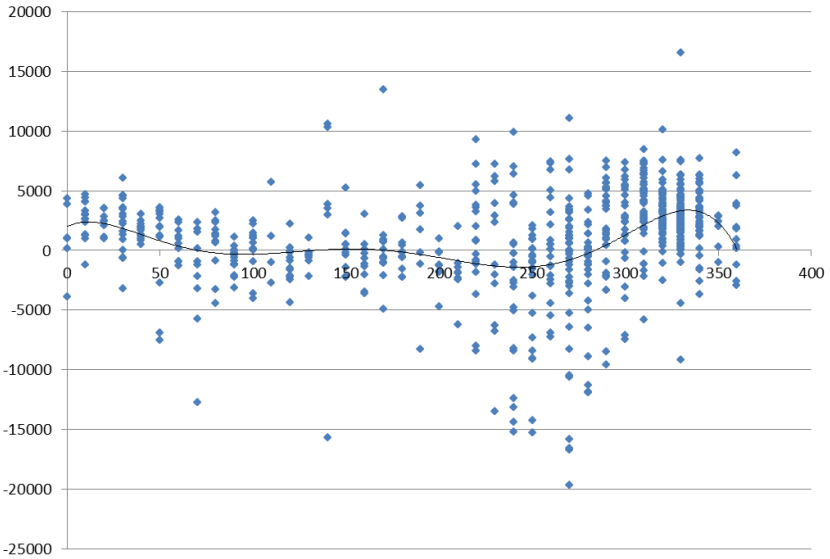

Figure 6.7: Difference in (half-hourly) TNC between Amsterdam Vondelpark (ADS1) and Nieuwendammerdijk (AD2T) as a function of the prevailing wind direction with a best (polynomial) fit.

In addition to the scatterplots, the coefficients of divergence (COD) and Spearman rank correlation coefficients (r_s) between the two sites per city were calculated for BC and TNC (Table 6.2).

Table 6.2: Coefficient of divergence (COD) and Spearman rank correlation coefficients (r_s) for black carbon (BC) and UFP total number concentration (TNC) between the fixed and trailer locations within Amsterdam, Antwerp and Leicester.

	BC		TNC	
	COD	Spearman rank (r_s)	COD	Spearman rank (r_s)
Amsterdam	0.23	0.69	0.25	0.59
Antwerp	0.30	0.89	0.16	0.85
Leicester	0.25	0.77	0.18	0.77

As already suggested by the time series plots, the weakest association (highest COD and lowest r_s) is obtained between the two sites in Amsterdam, while the highest correlations are obtained between the sites in Antwerp (Figure 6.6 and Table 6.2). Nevertheless, the differences in BC and UFP concentrations between the two sites is largest for Antwerp, which is not surprising as the fixed site is located near a busy access road while the trailer was located in an urban park area.

6.2.4 Size distribution at the two sites per city

Pearson correlations and CODs were also calculated for aggregated size distributions. The analysis shows clear differences between the concurrently sampled sites in Amsterdam (Figure 6.8), Antwerp (Figure 6.9) and Leicester (Figure 6.10). The calculated COD values show a decrease in COD with increasing particle size in Amsterdam, and to a lesser extent in Leicester, but not in Antwerp.

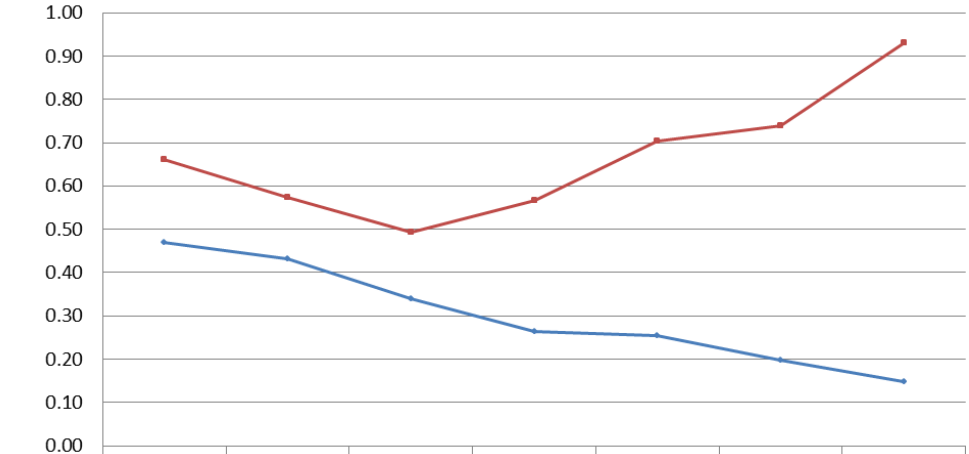

	N10-20_S	N20-30_S	N30-50_S	N50-70_S	N70-100_S	N100-200_S	N200_S
COD	0.47	0.43	0.34	0.26	0.26	0.20	0.15
r	0.66	0.57	0.49	0.57	0.70	0.74	0.93

Figure 6.8: Coefficient of divergence (COD) and Pearson correlation (r) between the particle number concentration per size class in Amsterdam Vondelpark (ADS1) and Nieuwendammerdijk (AD2T).

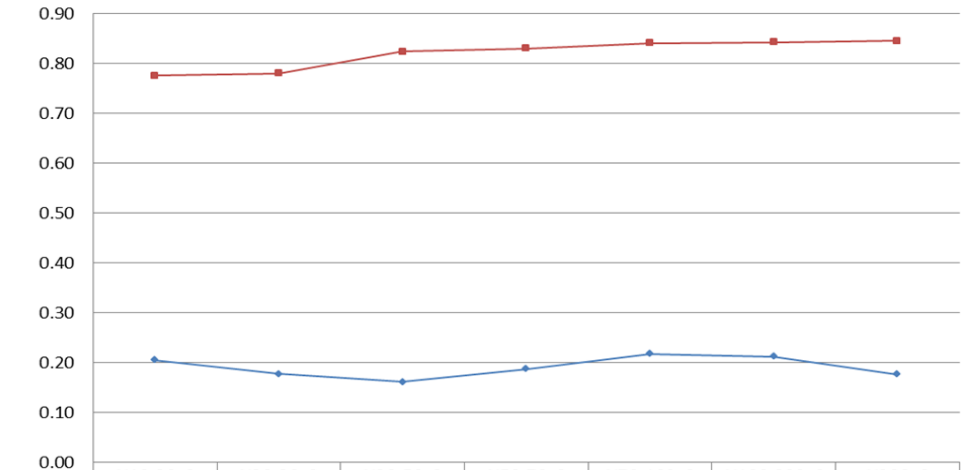

	N10-20_S	N20-30_S	N30-50_S	N50-70_S	N70-100_S	N100-200_S	N200_S
COD	0.20	0.18	0.16	0.19	0.22	0.21	0.18
r	0.78	0.78	0.82	0.83	0.84	0.84	0.84

Figure 6.9: Coefficient of divergence (COD) and Pearson correlation (r) between the particle number concentration per size class in Antwerp Borgerhout (ADS1) and Stadspark (AD2T).

In general, low spatial divergence and high correlation coefficients can be expected for sites separated by a relatively short distance and impacted by similar PM emission sources. Clearly, this is the case in Antwerp with COD values in the order of 0.20 and (Pearson) correlation coefficients around 0.80 (Figure 6.9). Here, the distance between the paired sites is roughly 1250 m and vehicular emissions are dominant at both sites.

The distance between the two sites in Amsterdam is about 8 km. The spatial variability analysis for these sites shows an inverse relationship between particle size and COD value (Figure 6.8): the highest spatial divergence is observed for the smallest particles, and the COD decreases with increasing particle size. Heterogeneity exists up to 100 nm (COD > 0.25). Overall, this implies that

number concentrations of particles less than 100 nm differs from site to site (due to direct emissions of traffic nearby) whereas particles greater than 100 nm tend to have more similar concentrations at the two sampling sites, probably originating from sources further away and influencing both sites. It is important to note that the variation in Pearson correlation coefficients as a function of particle size is not consistent with the variation in CODs. Combined with the heterogeneity existing for particles below 100 nm, correlations of UFP number concentrations are moderate (0.50-0.65) in this size range.

For Leicester, the spatial analysis shows an inverse relationship between particle size and COD value (Figure 6.10), but less pronounced than for Amsterdam. For the largest size class (>200 nm), the COD value is much larger and the Pearson correlation is lower compared to smaller particles. This is most likely caused by inaccurate particle number measurements for this size class by the UFPM devices, as shown by earlier comparison campaigns during the Joaquin project (see e.g. section 3.2).

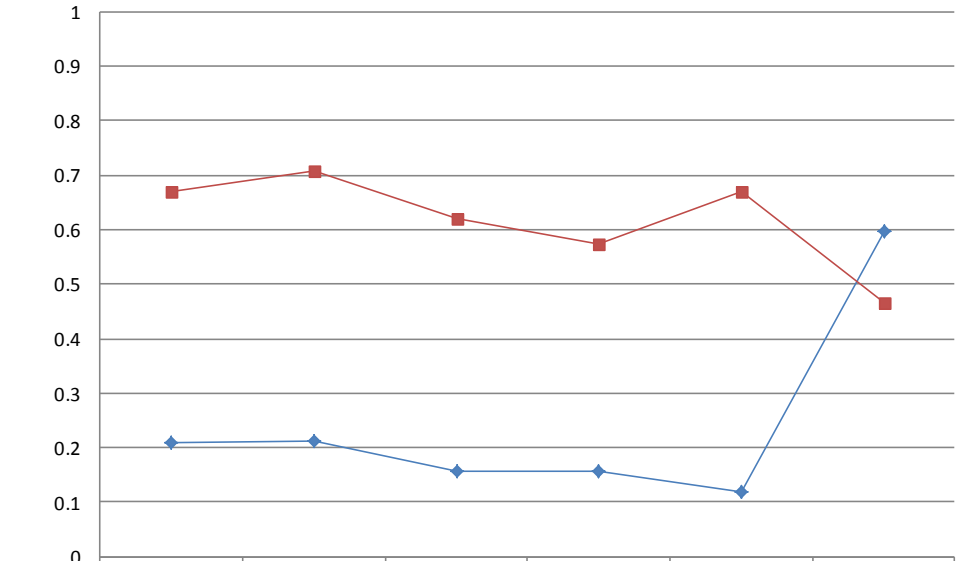

	N20-30_U	N30-50_U	N50-70_U	N70-100_U	N100-200_U	N200_U
COD	0.207552217	0.210350416	0.156769259	0.155768996	0.118368842	0.596202585
r	0.669148073	0.706740181	0.621683597	0.572728117	0.669335643	0.46619889

Figure 6.10: Coefficient of divergence (COD) and Pearson correlation (r) between the particle number concentration per size class in Leicester University (LES1) and Brookfield (AD2T). The deviating values for N200 (>200 nm) are likely due to inaccurate UFPM measurements for this size class.

6.2.5 Relative differences in size distribution

To evaluate potential intra-urban differences in UFP size distribution, the simultaneous average size distributions for both monitoring sites were plotted for Amsterdam, Antwerp and Leicester (Figure 6.11).

Based on the size distributions (Figure 6.11), we can conclude that large proportional differences in number concentration can be observed, depending on the considered particle size class. On average, the largest intra-urban variation in TNC was observed in Antwerp (38%), followed by Amsterdam (24%) and Leicester (20%). For Amsterdam, the 10-20 nm particle number concentration was 48% lower at the trailer location (AD2, Nieuwendammerdijk), compared to the fixed monitoring station (AD1, Vondelpark). For Antwerp, the largest difference was observed in the largest particle size range (100-200 nm), with a 49% lower particle number concentration at the trailer location (AP2, Stadspark), compared to the fixed monitoring station (AD1, Borgerhout). In Leicester, the largest difference was observed in the 70-100 nm size range, with 30% lower particle number concentrations at the trailer location (LE2, Brookfield), compared to the fixed monitoring site (LE1, Leicester University).

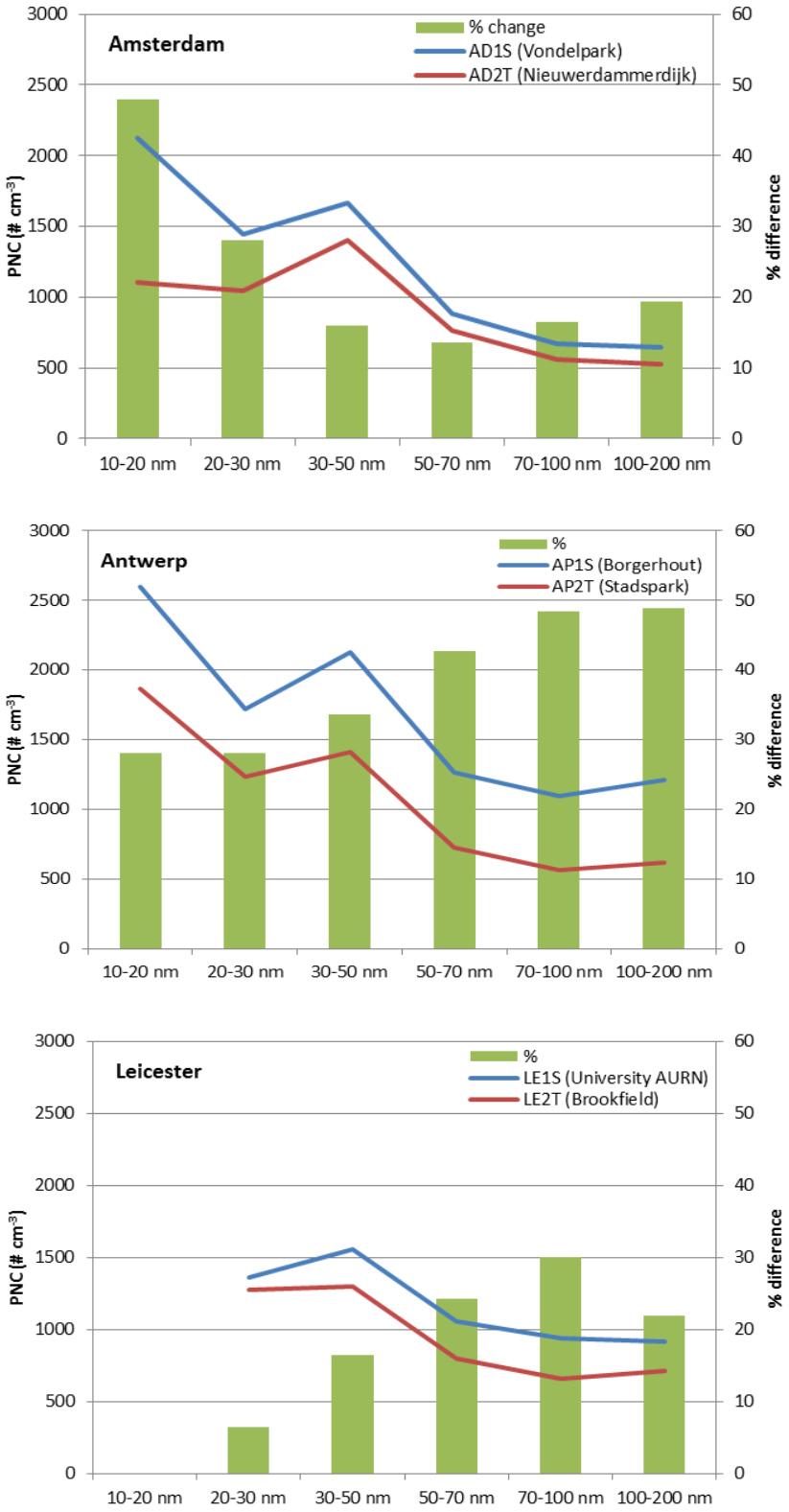

Figure 6.11: Average UFP size distribution and percentage difference between the fixed (S) and trailer (T) locations in Amsterdam, Antwerp and Leicester.

So, although the considered pollutants covariate fairly well in time at the different locations, proportional differences in particle number concentration are found between the individual intra-urban sites, as influenced by their proximity to urban UFP sources. This implies that the location of the UFP monitoring station is of primordial importance when evaluating citizen's exposure to UFP in urban environments.

Comparing the SMPS trailer data for all available trailer locations (same instrument, but different time and location (Figure 6.12)), an overall similar size distribution can be observed for the individual cities and sites with a general concentration peak of ~30 nm particles. Slightly deviating distributions are observed for the monitoring stations in Amsterdam (AD1T) and Leicester (LE1T) with a shift in particle number concentrations towards the <20 nm (AD1T) or 70 nm (LE1T) size class.

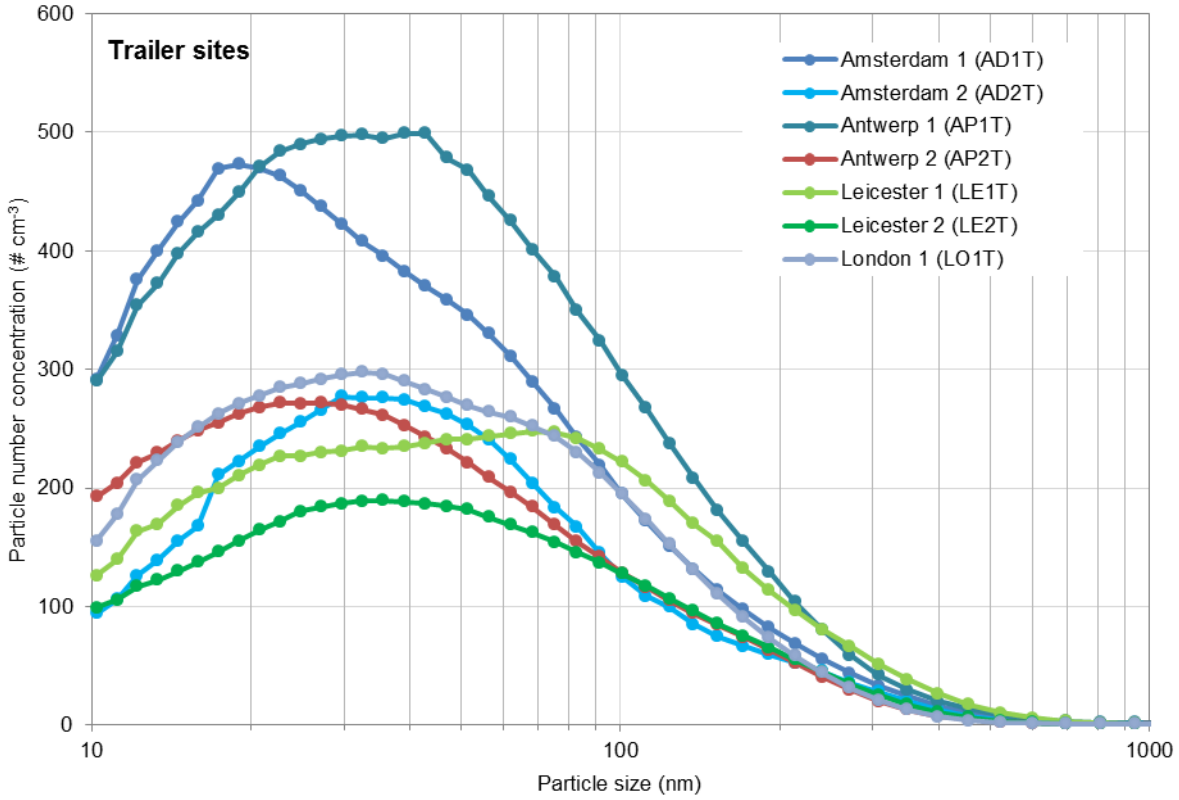

Figure 6.12: Normalized (dN/dlog D_p) UFP size distributions at all trailer locations in Amsterdam (AD1), Antwerp (AP1), Leicester (LE1) and London (LO1), based on SMPS measurements (45 size bins). Site 1T is the trailer location next to the fixed monitoring station, while 2T is the second trailer location in the considered cities. Note: data of short-term and non-simultaneous monitoring periods (see section 2.1 for the exact dates).

7 Conclusions

Action 1 (WP1A1) of the Joaquin project aimed at obtaining novel time series of simultaneous UFP measurements in four NW-European cities (Amsterdam, Antwerp, Leicester and London), both in terms of total and size-resolved particle number concentrations. From this explorative dataset, collected by this continuous UFP monitoring network, the objective was to investigate the temporal variation in UFP number concentration and size distribution, to assess the added value of UFP data in addition to more common parameters such as nitrogen oxides (NO_x) and black carbon (BC) and to evaluate the feasibility of long-term UFP measurements within air quality monitoring networks.

To evaluate instrument comparability, there was an initial measurement campaign in Antwerp and follow-up comparisons at the four sites using a mobile trailer. The agreement between devices of the same type was good (<10% difference), but the total PNC was underestimated by the size-resolved devices compared with the particle counters.

Due to initial regulatory problems in the setup of the UFP network, measurements started later in Leicester and London. Nevertheless a fairly long-term time series of UFP measurements was obtained (2 years for Amsterdam and Antwerp and ~1 year for Leicester and London). Data coverage of the UFP measurements was comparable with (but lower than) the coverage of more common pollutants (PM, NO_x).

The considered Joaquin cities showed comparable UFP size distributions with similar proportional contributions of the individual particle size classes (100-200 < 70-100 < 50-70 < 20-30 < 30-50 < 10-20 nm). Moreover, the quantified UFP size distributions showed to be fairly stable in time. Nevertheless, quantification of the separate UFP size classes enabled us to identify different contributing emission sources on different spatial scales. Comparing the UFP size distribution between the monitoring sites, a better association was obtained between the large UFP size classes. Larger particles, therefore, seem to be more uniform in space, which confirms the regional nature of these aerosols. In comparison to the other monitoring sites, Antwerp had a large proportional contribution of 30-50 nm particles, which can be considered as typical traffic-related particles, while Amsterdam had a larger contribution of 10-20 nm particles.

Compared to the other monitoring sites, the site in Antwerp showed a significantly higher particle number concentration due to its proximity to the Plantin en Moretuslei, a busy access road of Antwerp. Ambient UFP concentrations, in line with BC and NO_2, showed a clear traffic-related diurnal variation with distinct morning and evening rush hour peaks on week days, but only a clear evening peak in the weekends. Together with the high UFP concentrations in Antwerp, these observations confirm road traffic as an important UFP source in urban environments.

Compared to Antwerp, Leicester and London, UFP measurements in Amsterdam showed some aberrations with (1) a high and continuous (non-diurnal) 10-20 nm contribution which persists during the weekends, (2) a significant input of (mainly 10-20 nm sized) UFP when the wind comes from the governing SW direction and (3) no clear relation of the total and size-resolved UFPs with traffic-related pollutants. This leads us to believe that Schiphol airport acts as a source of ultrafine particles, which contributes to atmospheric UFP concentrations in the city centre of Amsterdam. Taking into account the frequency of (governing) SW wind fields, and the proportional increase of total and 10-20 nm sized UFP, Schiphol airport was estimated to contribute to respectively 5% of TNC and 16% of 10-20 nm particles measured at the Vondelpark monitoring station.

Finally, the intra-urban spatial variation of UFP and BC was evaluated using the trailer measurements conducted within the scope of Joaquin Action 3 (WP1A3). Although the temporal variation of BC and UFP at the two intra-urban monitoring sites is correlated ($r = 0.69$ to 0.89 for BC and $r_s = 0.59$ to 0.85), the absolute difference assessed by the coefficient of divergence (COD) can be considerable. On average, the largest difference in total PNC between the two sites was observed for Antwerp (38%), followed by Amsterdam (24%) and Leicester (20%). For the individual particle size classes, the differences can be much larger (e.g. up to 48% in the 10-20 nm size class in Amsterdam and 49% in the 100-200 nm size class in Antwerp). This intra-urban variation is influenced by the proximity of UFP sources. This implies that the location of the UFP monitoring station is of primordial importance in order to evaluate the citizen's exposure to UFPs in urban environments.

We can conclude that all applied UFP instrumentation performed fairly well and reliably. The observed intra-urban spatial variation and influence of individual UFP sources (e.g. in Antwerp) suggests that one monitoring site will not be representative for an entire city in term of absolute numbers. On the other hand, the urban temporal UFP variation seems to be reflected sufficiently by a single urban monitoring site. Although monitoring of the total PNC (e.g. by a total particle number counter) already provides reliable information on atmospheric UFP levels, additional size-resolved UFP measurements (e.g. by SMPS or TSI3031) provide valuable information on contributing emission sources and aerosol formation and transformation processes. Moreover, by combining both total and size-resolved UFP instruments, instrument anomalies can be easily detected.

With regard to urban UFP monitoring, this long-term monitoring dataset has provided important insights into the spatiotemporal variation of total and size-resolved ultrafine particles and the feasibility of long-term monitoring networks. All Joaquin sites were considered as urban background locations. Nevertheless, the UFP concentration measured at e.g. the Antwerp site was considerable influenced by the nearby Plantin en Moretuslei. Therefore, it is relevant to ask "what is a good background location"? Should an urban background site not reflect the minimal UFP number concentration experienced throughout the entire city? According to the European Environment Agency (EEA), an urban background station is "*not determined significantly by any single source or street, but by the integrated contribution from all sources upwind of the station*". Overall the goal should be to obtain representative air quality data for the city under consideration.

The degree of correlation between UFP and other traffic-related pollutants shows that traffic is a significant, but not exclusive, UFP source at all the sites investigated. Due to the short atmospheric lifetime of UFP and their strong dependence on local sources, total and size-specific PNC can vary meaningfully on short spatial and temporal scales. Therefore, UFP monitoring at a single site may not be indicative of the actual exposure in the communities surrounding the site. This pleads for thoughtful consideration when selecting urban background stations for UFP measurements in heterogeneous urban environments. To more accurately estimate human exposure and subsequent health impacts of UFP, measurements and/or modelling on finer spatial scales is valuable.

References

Asbach H., Fissan B., Stahlmecke B., Kuhlbusch T.A.J., Pui D.Y.H. (2009). Conceptual limitations and extensions of lung-deposited Nanoparticle Surface Area Monitor (NSAM). Journal of Nanoparticle Research 11, 101-109.

Carslaw D.C., Ropkins K. (2012). openair - an R package for air quality data analysis. Environmental Modelling and Software 27-28, 52-61.

Carslaw D.C., Ropkins K. (2015). openair: Open-source tools for the analysis of air pollution data. R package version 1.1-5, www.open-airproject.org.

Cordell R.L., White I.R., Monks P.S. (2014). Validation of an assay for the determination of levoglucosan and associated monosaccharide anhydrides for the quantification of wood smoke in atmospheric aerosol. Analytical and Bioanalytical Chemistry 406, 5283-5292.

Dall'Osto M., Querol X., Alastuey A., O'Dowd C., Harrison R.M., Wenger J., Gomez-Moreno F.J. (2013). On the spatial distribution and evolution of ultrafine particles in Barcelona. Atmospheric Chemistry and Physics 13, 741-759.

Fissan H., Neumann S., Trampe A., Pui D.Y.H., Shin W.G. (2007). Rationale and principle of an instrument measuring lung deposited nanoparticle surface area Journal of Nanoparticle Research 9, 53-59.

Frijns E., van Laer J. (2013). Interim report. SOP Environmental Particle Counter (EPC) 3783.

Frijns E., Van Laer J., Aerts W., Brabers B., Berghmans P. (2013a). UFP instrument comparison at an urban background location in Antwerp. Study accomplished under the authority of VMM. VITO report 2013/MRG/R/172. Flemish Institute for Technological Research, Mol, Belgium. Available at http://www.joaquin.eu.

Frijns E., Van Laer J., Berghmans P. (2013b). Short-term intra-urban variability of UFP number concentration and size distribution. Study accomplished under the authority of VMM. VITO report 2013/MRG/R/173. Flemish Institute for Technological Research, Mol, Belgium. Available at http://www.joaquin.eu.

Frijns E., Van Laer J., Berghmans P., Bergmans B., Lenartz F. (2014). Short-term intra-urban variability of UFP number concentration and size distribution - October 2013 campaign. Study accomplished under the authority of VMM. VITO report 2014/MRG/R/59. Flemish Institute for Technological Research, Mol, Belgium. Available at http://www.joaquin.eu.

Gonzalez Y., Rodríguez S., García J. C. G., Trujillo J. L., García R. (2011). Ultrafine particles pollution in urban coastal air due to ship emissions. Atmospheric Environment 45, 4907-4914.

Healy R. M., O'Connor I. P. , Hellebust S. , Allanic A., Sodeau J. R., Wenger J. C. (2009). Characterisation of single particles from in-port ship emissions. Atmospheric Environment 43, 6408-6414.

Hudda N., Gould T., Hartin K., Larson T.V., Fruin, S. (2014). Emissions from an International Airport increase particle number concentrations 4-fold at 10 km downwind. Environmental Science and Technology 48, 6628-6635.

ICRP (1994). Human respiratory tract model for radiological protection. ICRP Publication 66. Ann. ICRP 24 (1-3).

ISO 15900 (2009). Determination of particle size distribution – differential electrical mobility analysis for aerosol particles. www.iso.org, Geneva, Switzerland.

Jeong C.H., Hopke P.K., Chalupa D., Utell M. (2004). Characteristics of nucleation and growth events of ultrafine particles measured in Rochester, NY. Environmental Science and Technology 38, 1933-1940.

Joaquin (2015). Composition and source apportionment of PM_{10}. Joint Air Quality Initiative, Work Package 1 Action 2 and 3. Flanders Environment Agency, Aalst. Available at http://www.joaquin.eu.

Keuken M.P., Moerman M., Zandveld P., Henzing J.S., Hoek G. (2015). Total and size-resolved particle number and black carbon concentrations in urban areas near Schiphol airport (the Netherlands). Atmospheric Environment 104, 132-142.

Krudysz, M., Moore, K., Geller, M., Sioutas, C., and Froines, J. (2009). Intra-community spatial variability of particulate matter size distributions in Southern California/Los Angeles, Atmospheric Chemistry and Physics 9, 1061-1075.

Kuang C., McMurry P.H., McCormick A.V., Eisele F.L. (2008). Dependence of nucleation rates on sulfuric acid vapor concentration in diverse atmospheric locations. Journal of Geophysical Research 113, D10209.

Kulmala, M., Vehkamaki, H., Petaja, T., Dal Maso, M., Lauri, A., Kerminen, V.M., Birmili, W. & McMurry, P.H. (2004) Formation and growth rates of ultrafine atmospheric particles: a review of observations, Journal of Aerosol Science 35, 143-175.

Laakso L., Hussein T., Aarnio P., Kompulla M., Hiltunen V., Viisanen Y., Kulmala M. (2003). Diurnal and annual characteristics of particle mass and number concentrations in urban, rural, and Arctic environments in Finland. Atmospheric Environment 37, 2629-2641.

Maenhaut W., Vermeylen R., Claeys M., Vercauteren J., Matheeussen C., Roekens E. (2012). Assessment of the contribution from wood burning to the PM_{10} aerosol in Flanders, Belgium. Science of the Total Environment 437, 226-236.

Menon S., Saxena V.K., Durkee P., Wenny B.N., Nielsen K. (2002). Role of sulfate aerosols in modifying the cloud albedo: a closure experiment. Atmospheric Research 61, 169-187.

Minguillón M.C., Brines M., Pérez N., Reche C., Pandolfi M., Fonseca A.S., Amato F., Alastuey A., Lyasota A., Codina B., Lee H.K., Eun H.R., Ahn K.H., Querol X. (2015). New particle formation at ground level and in the vertical column over the Barcelona area, Atmospheric Research 164-165, 118-130.

Mishra V.K., Kumar P., Van Poppel M., Bleux N., Frijns E., Reggente M., Berghmans P., Panis L.I., Samson R. (2012). Wintertime spatio-temporal variation of ultrafine particles in a Belgian city. Science of the Total Environment 431, 307-313.

Nel A., Xia T., Mädler L., Li,N. (2006). Toxic potential of materials at the nanolevel. Science 311, 622-627.

Nurkiewicz T., Porter D., Hubbs A., Stone S., Chen B., Frazer D., Boegehold M., Castranova V. (2009). Pulmonary nanoparticle exposure disrupts systemic microvascular nitric oxide signaling. Journal of Toxicological Science 110, 191-203.

Oberdörster G., Maynard A., Donaldson K., Castranova V., Fitzpatrick J., Ausman K., Carter J., Karn B., Kreyling W., Lai D., Olin S., Monteiro-Riviere N., Warheit D., Yang H. (2005). Principles for characterizing the potential human health effects from exposure to nanomaterials: elements of a screening strategy. Particle and Fibre Toxicology 2:8.

Petzold A., Kramer H., Schönlinner M. (2002). Continuous measurement of atmospheric black carbon using a Multi-angle absorption photometer. Environmental Science and Pollution Research Sp. Iss. 4, 78-82.

Pey J, Rodríguez S., Querol X., Alastuey A., Moreno T., Putaud J.P. & Van Dingenen R. (2008). Variations of urban aerosols in the Western Mediterranean, Atmospheric Environment 42, 9052-9062.

Querol X., Alastuey A., Pey J, Viana M, Moreno T, Minguillón MC, Amato F, Pandolfi M, Pérez N, Cusack M, Reche C, Dall'Osto M, Ripoll A, Karanasiou A (2011). Nanoparticles in the atmosphere. Seminarios SEM 8, p. 24-39.

R Development Core Team (2014). R: A language and environment for statistical computing. R Foundation for Statistical Computing, Vienna, Austria, www.R-project.org.

Singh S., Shi T., Duffin R., Albrecht C., van Berlo D., Hohr D., Fubini B., Martra G., Fenoglio I., Borm P.J.A., Schins R.P.F. (2007). Endocytosis, oxidative stress and IL-8 expression in human lung epithelial cells upon treatment with fine and ultrafine TiO_2: Role of the specific surface area and of surface methylation of the particles. Toxicology and Applied Pharmacology 222, 141-151.

Titos G., Lyamani H., Sorribos M., Foyo-Moreno I., Alados-Arboledas L. (2012). Monitoring of ultrafine particles at an urban environment in southern Europe. Abstract of poster B-WG02S2P25, European Aerosol Conference, 2-7 Sep 2012, Granada,

Vercauteren J., Matheeussen C., Wauters E., Roekens E., van Grieken R., Krata A., Makarovska Y., Maenhaut M., Chi X., Geypens B. (2011). Chemkar PM_{10}: An extensive look at the local differences in chemical composition of PM10 in Flanders, Belgium. Atmospheric Environment 45, 108-116.

VMM (2012). Bedieningsvoorschrift voor monsteringneming met Leckel SEQ 47/50, BDV-021.

VMM (2014). Intra-urban variability of ultrafine particles in Antwerp (February and October 2013). Flemish Environment Agency, Erembodegem. Available at http://www.vmm.be.

Wilson J.G., Kingham S., Pearce J., Sturman A. (2005). A review of intra urban variations in particulate air pollution: implications for epidemiological research. Atmospheric Environmont 39, 6444-6462.

Yang A., Jedynska A., Hellack B., Kooter I., Hoek G., Brunekreef B., Kuhlbusch T.A.J., Cassee F.R., Janssen N.A.H. (2014). Measurement of the oxidative potential of $PM_{2.5}$ and its constituents: the effect of extraction solvent and filter type. Atmospheric Environment 83, 35-42.

Zhu Y., Hinds W.C., Kim S., Shen S., Sioutas C. (2002). Study of ultrafine particles near a major highway with heavy-duty diesel traffic. Atmospheric Environment 36, 4323-4335.

Annex 1: Detailed site descriptions

1.1 Amsterdam (the Netherlands)

1.1.1 Vondelpark (AD1)

The Joaquin sampling site in Amsterdam is an urban background station of the air quality monitoring network of GGD Amsterdam. The station is located at the northern edge of the public park 'Vondelpark (Figure 1).

Website information: http://www.luchtmetingen.amsterdam.nl/DetailPage.aspx?SID=014

At a distance of 64 m to the north there is a main road (Overtoom) with a mean traffic intensity of about 17000 vehicles/day (http://www.verkeersprognoses.amsterdam.nl for 2015). The Overtoom road has two lanes, one in each direction plus two bus/tram lanes in the centre of the road and has relatively high buildings on both sides ('street canyon').

Between the site and the Overtoom there is a six-storey building. A small passage connects the Overtoom with the site. The measuring station is located in the courtyard of a revalidation centre. The site is close to tennis courts and a public park (in the south). The gravel tennis court can be a source of coarse dust particles. In the Vondelpark, barbecue activities are allowed at specific locations, except during dry periods.

Description per wind direction:

- N: main road (Overtoom at 64 m);
- E: private parking and green area;
- S: tennis court and public park (Vondelpark);
- W: six-storey building (Figure 2).

Figure 1: Detail of the location of site AD1 (Amsterdam Vondelpark).

Figure 2: Measuring station AD1S.

The harbour of Amsterdam is located north-northwest of AD1 (Figure 3). Typical activities in the harbour are road and shipping traffic, storage and transhipment of petrochemical products, ore and coal. In the harbour, there is a coal-fuelled electricity plant (Hemwegcentrale) 5.2 km north of AD1.

Schiphol airport is located about 8.7 km southwest of AD1.

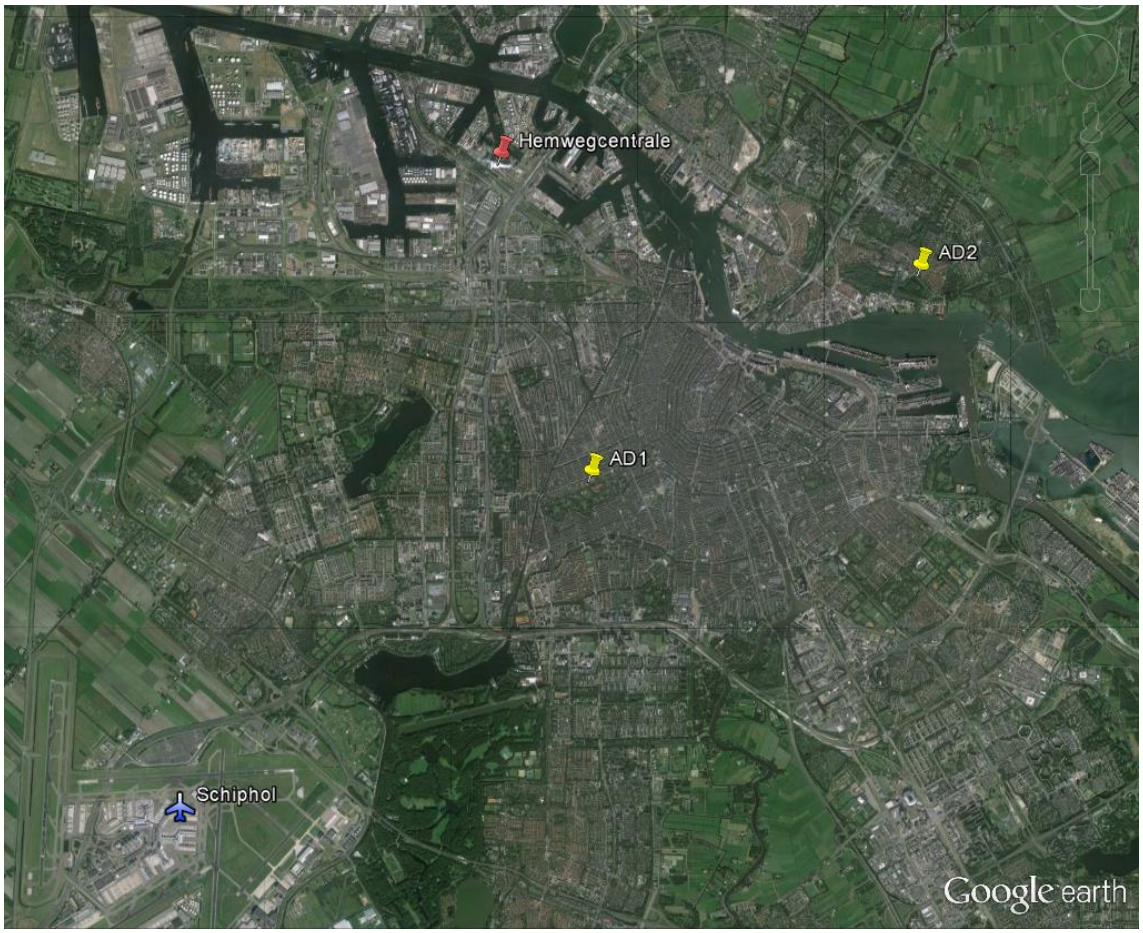

Figure 3: Location of site AD1 and AD2 in the city of Amsterdam. Schiphol airport and a power plant (Hemwegcentrale) in the harbour are also shown.

1.1.2 Nieuwendammerdijk (AD2)

The temporary Joaquin site in Amsterdam is an urban background station of the air quality monitoring network of GGD Amsterdam (Figure 4). The station is located at Nieuwendammerdijk, at about 6.2 km from site AD1 (Figure 3).

Website information: http://www.luchtmetingen.amsterdam.nl/DetailPage.aspx?SID=003

The nearest road (Nieuwendammerdijk) is at a distance of 20 m and is only used by local residents. The traffic intensity is estimated to be less than 300 vehicles per day (**Fout! De hyperlinkverwijzing is ongeldig.** for 2015). Site AD2 is a typical background location surrounded by grass fields without any specific sources nearby. Further to the south is a water connection to the North Sea used by inland shipping vessels and sea vessels for bulk transportation.

Per wind direction:

- NE: local road at 20 m (Nieuwendammerdijk);
- SE and NW: grass;
- SW: lake.

For south-eastern wind directions there may be an influence of the AKZO site (production of catalysts and formerly also sulfuric acid).

Schiphol airport is located about 15 km southwest of AD1.

Figure 4: Detail of the location of site AD2 (Amsterdam Nieuwendammerdijk).

1.2 Antwerp (Belgium)

1.2.1 Borgerhout (AP1)

The Joaquin sampling site in Antwerp is an urban background station that is part of the VMM air quality monitoring network. The station is located in Borgerhout (VMM station code 42R801).

Website information: http://luchtkwaliteit.vmm.be/details.php?station=42R801

Site AP1 is located 30 m from a major access road (Plantin en Moretuslei) (Figure 5). The station is set on a terrain of a primary school, next to the playground.

The Plantin en Moretuslei connects the inner city with a major highway eastwards (E313). The road is east-west orientated and has four lanes (two in each direction). There is a bus stop in front of the entrance to AP1.

In February 2010, daily traffic volume on the Plantin en Moretuslei was 37000 vehicles on weekdays and 25000 vehicles in the weekend (Misha et al., 2012; based on video counting), or a time-weighted average of 33500 vehicles/ day. The reported fraction of heavy duty vehicles was 7% (week) and 3% (weekend) (Misha et al., 2012). In February and October 2013, the mean traffic intensity was 32000 vehicles on week days and 23500 vehicles in the weekend (VMM, 2014; based on counting loops), or a time-weigted average of 29500 vehicles/day.

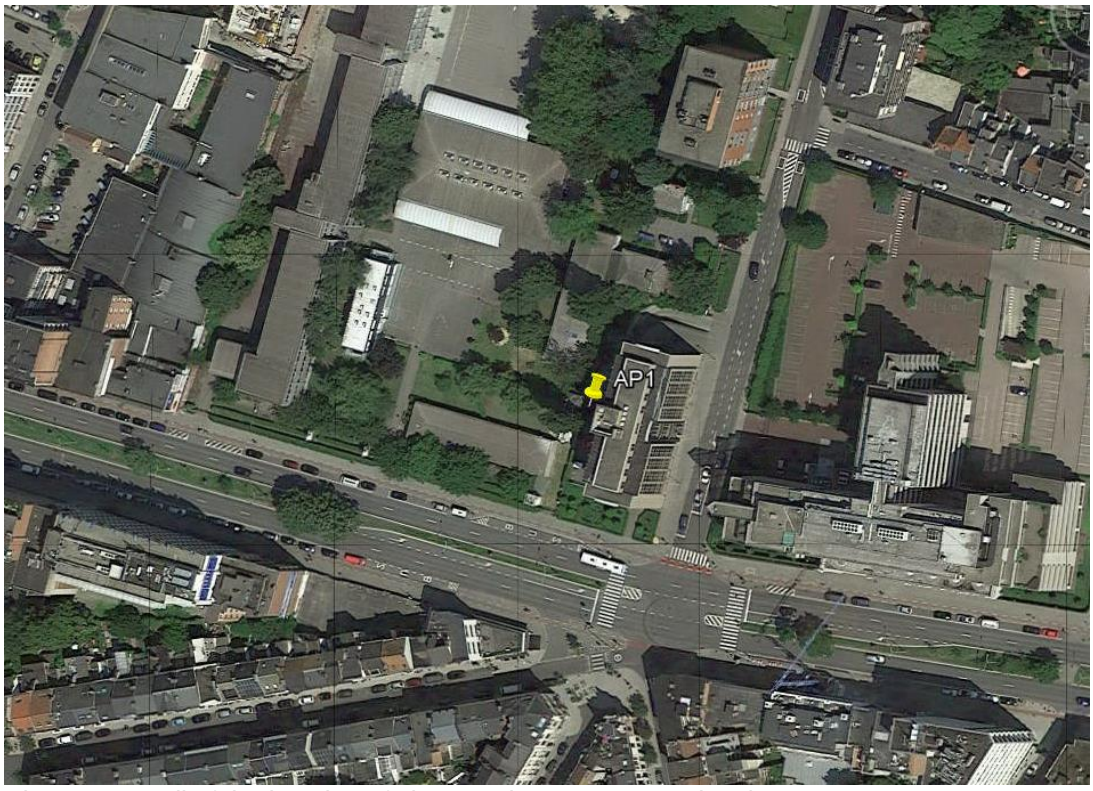

Figure 5: Detail of the location of site AP1 (Antwerp Borgerhout).

Per wind direction

- N: school area (grass and trees);
- E: first a small parking area, then a 6-storey office, then a smaller street;
- S: main road (Plantin and Moretuslei) with a bus stop in front of the entrance to the station;
- W: playground of the school (pavement and artificial grass mat).

Site AP1 is located in a densely populated neighbourhood and within the major ring road around Antwerp. The closest distance to the ring is ~700 m in E-SE direction. The closest distance to a rail road is ~500 in W-SW direction.

Figure 6: Street view of station AP1S (red arrow) seen from the other side of the Plantin en Moretuslei.

At the regional scale, a potential source of air pollution is the harbour of Antwerp (N-NW, >4 km distance), with power plants and important (petro)chemical and other industrial activities. In the SW direction at about 8 km from the station, there is an industrial site (Umicore) with metal processing (e.g. As, Cd, and Pb).

Antwerp airport is located 3 km SE of site AP1. In 2014 there were about 44000 flight movements (= departures and arrivals) at this airport (http://www.antwerp-airport.be).

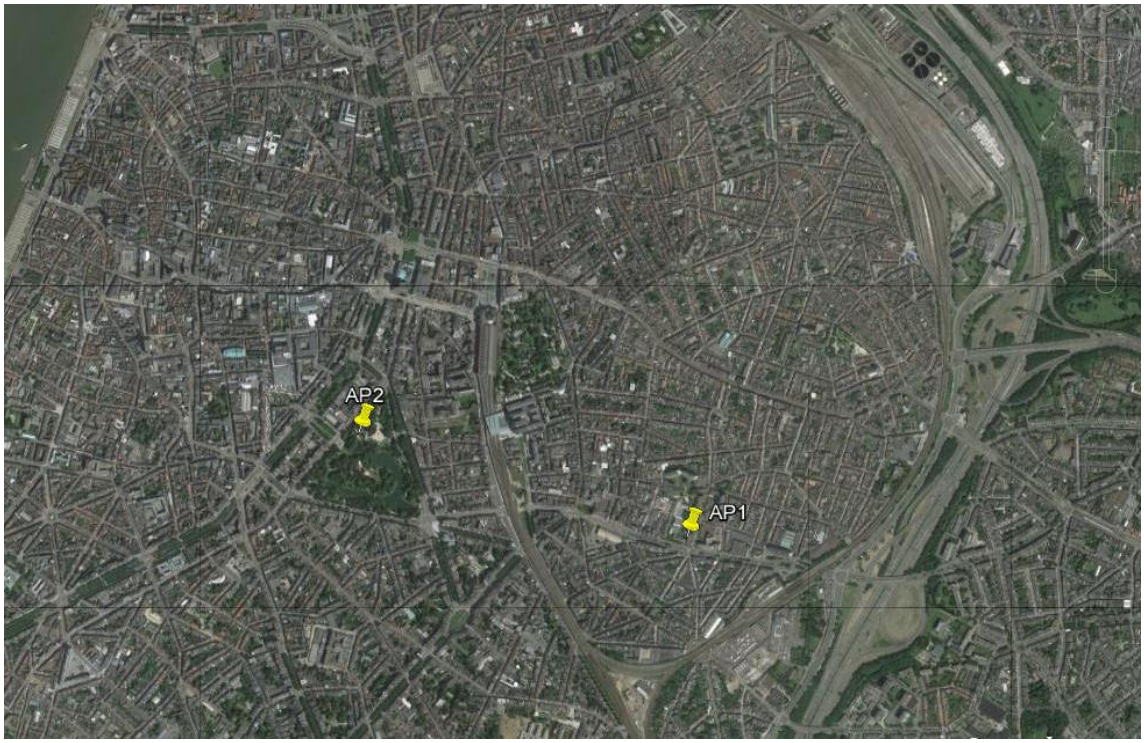

Figure 7: Location of site AP1 and AP2 in the city of Antwerp.

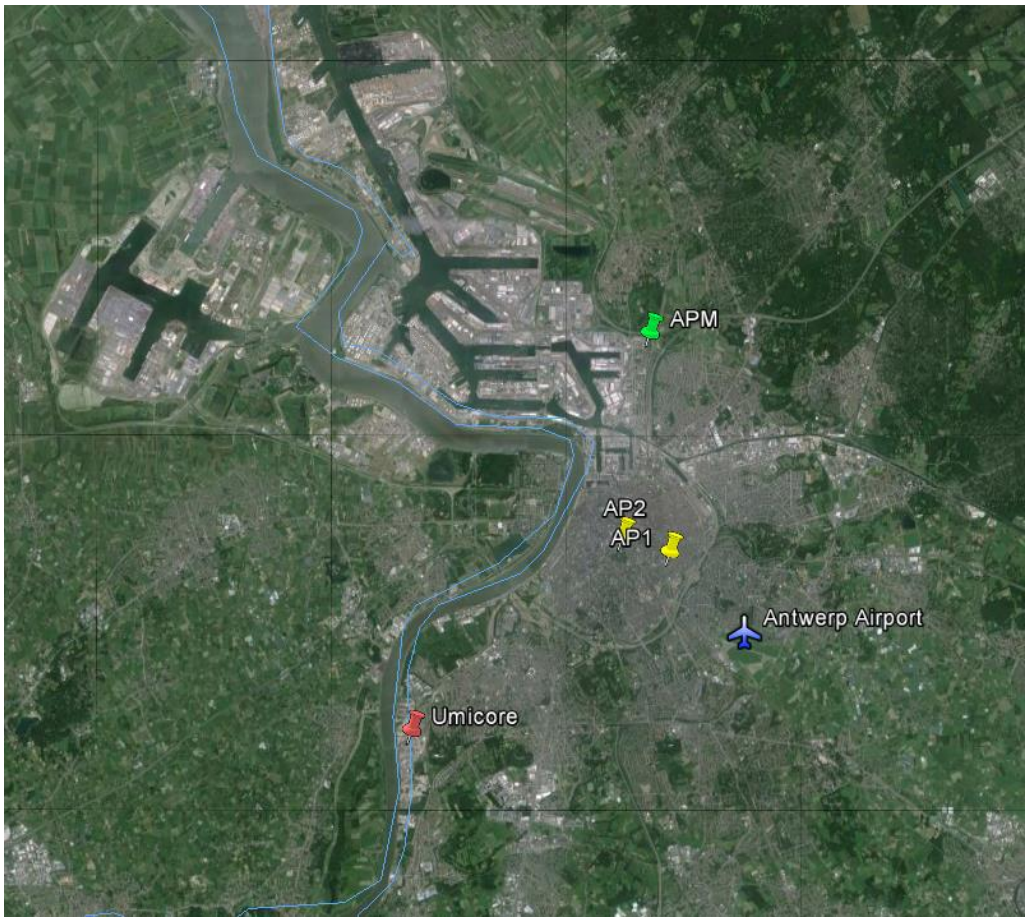

Figure 8: Region of Antwerp with air quality monitoring sites AP1 and AP2, meteorological monitoring site APM (Luchtbal), an industrial site (Umicore), Antwerp airport and the harbour of Antwerp NW of the city.

1.2.2 Stadspark (AP2)

Site AP2 is a temporary sampling location in a public parc with mature (mainly deciduous) trees (Figure 9). Site AP2 is located at a distance of 1.3 km to the northwest from site AP1 (Figure 7).

The closest road to site AP2, at distance of 45 m, is the Rubenslei with 2x1 lanes. In February and October 2013, the mean traffic intensity at the Rubenslei was 8500 vehicles on week days and 6000 vehicles in the weekend (VMM, 2014; based on counting loops), or a time-weighted average of 7800 vehicles/day.

Parallel to the Rubenslei there is a busier road (Frankrijklei). This road has 2x3 lanes plus 2 central bus and tram lines. Traffic intensity data are not available for this road.

Per wind direction:
- NW: local road (Rubenslei) at 45 m and main road (Frankrijklei) at ~170 m;
- E: 1-storey building;
- S: open area;
- W: deciduous trees.

Site AP2 is located further away from the main ring road around Antwerp than AP1, but it is closer to the River Scheldt (1.5 km in western direction) (Figure 7).

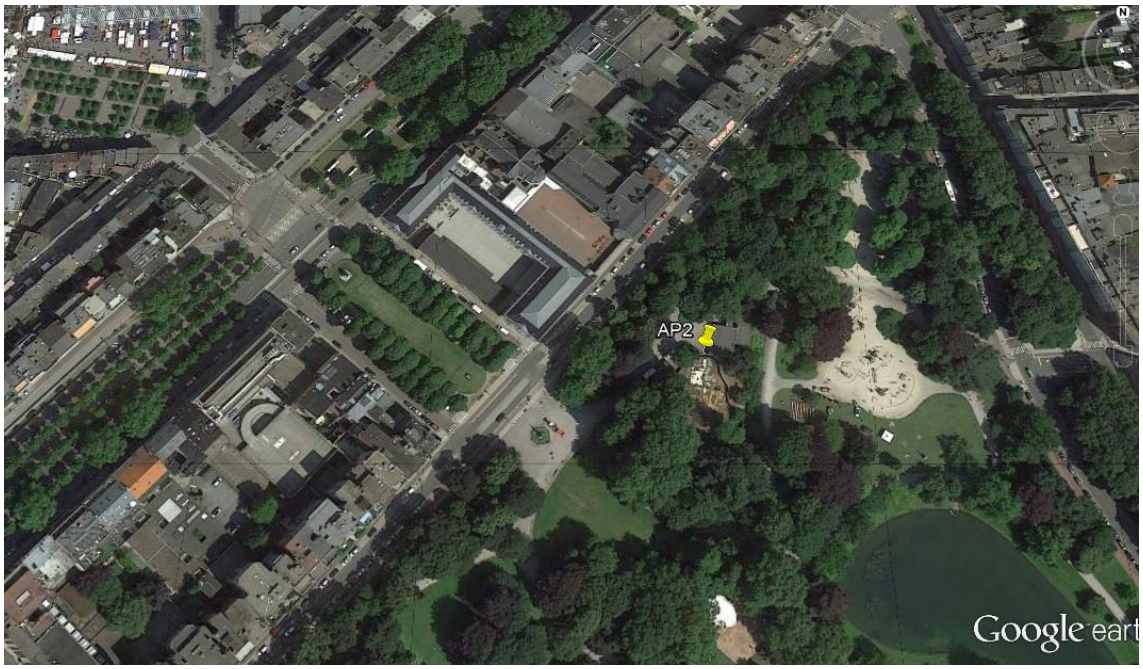

Figure 9: Detail of the location of site AP2 (Antwerp Stadspark).

1.2.3 Six extra sites in Antwerp

Next to AP1 (Borgerhout) and AP2 (Stadspark), within the Joaquin project the UPF number concentration and size distribution have been measured at six extra sites in Antwerp. An initial instrument comparison was carried out at an urban background site in Wilrijk (Vuurkruisenplein) in December 2012 and January 2013. The site is described by Frijns et al. (2013a).

In February 2013, UFP measurements were carried out seven sites in Antwerp: the sites AP1 and AP2 described above, two sites near site AP1, a suburban site (Frederik Van Eedenplein), an urban street canyon site (Turnhoutsebaan) and a ring road site (Noordersingel). In October 2013, measurements occurred at four sites in Antwerp: AP1, AP2, the suburban site and the ring road site. These sites are described by VMM (2014).

1.3 Leicester (United Kingdom)

1.3.1 Leicester University (LE1)

The Joaquin sampling site in Leicester is an urban background station of the AURN network. The station is located on the campus of the University of Leicester near Welford Road (Figure 10).

Website information: http://uk-air.defra.gov.uk/networks/site-info?uka_id=UKA00573

The nearest road is the University Road (20 m NW). The nearest main road is Welford Road (140 m S-SW) with 2x1 lanes. According to traffic counts by the Department for Transport, the traffic intensity on the Wellington Road was about 22500 vehicles/day in 2013 (http://www.dft.gov.uk/traffic-counts, count point 36549). The majority of the vehicles were cars and taxis (87%), followed by light goods vehicles (10%), heavy goods vehicles (1.1%), buses and coaches (0.9%) and motorcycles (0.9%).

Figure 10: Detail of the location of site LE1 (Leicester University).

Per wind direction

- N: university buildings;
- E: two-storey building (sports centre);
- S: grass, Welford Road (140 m);
- W: park area.


Figure 11: Measuring station LE1S.

East Midland airport is at a distance of 27 km north-northwest of site LE1 (Figure 14).
There are also several power stations in the region:

- Ratcliffe Soar power station (EON), the biggest one in the region (29 km N-NW of LE1)
- Corby power station (33 km E-SE of LE1)
- Stamford power plant (46 km E-NE of LE1)
- Spalding power station (70 miles E-NE of LE1)

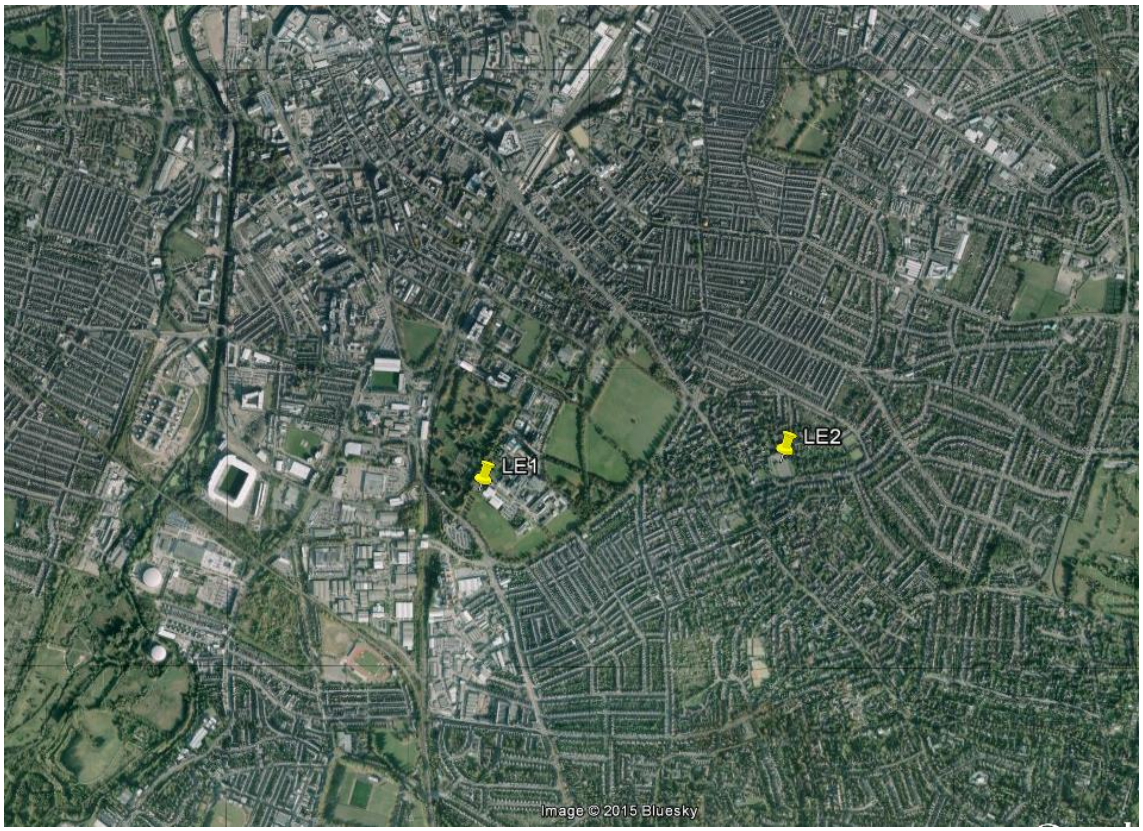

Figure 12: Site LE1 and LE2 in the city of Leicester.

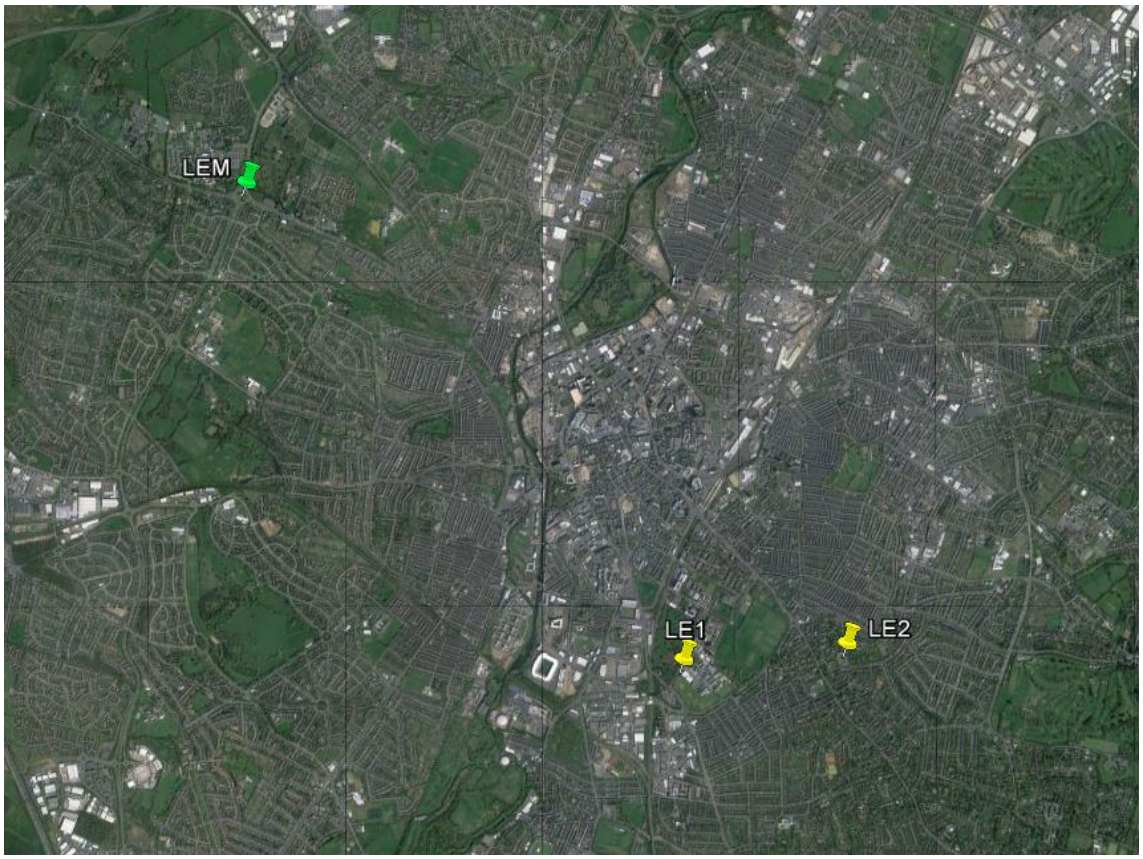

Figure 13: Region of Leicester with air quality monitoring sites LE1 and LE2 and meteorological monitoring site LEM (Groby road Traffic Island).

Figure 14: Site LE1 and LE2 in the region of Leicester with indication of East Midlands airport and four power stations.

1.3.2 Brookfield (LE2)

The temporary Joaquin site in Leicester is an urban background site in Brookfield, at a distance of about 1.2 km east from LE1 (Figure 12).

The trailer was located on a large and frequently-used parking lot (Figure 15; Figure 16). The nearest roads are Ashfield Road (90 m in the north) and Holmfield Road (90 m south). The nearest main road is London Road, at 190 m west of LE2.

According to traffic counts by the Department for Transport, the traffic intensity on London Road was about 20500 vehicles/day in 2013 (http://www.dft.gov.uk/traffic-counts, count point 56147). The majority of the vehicles were cars and taxis (87%), followed by light goods vehicles (9%), buses and coaches (2%), heavy goods vehicles (1.4%) and motorcycles (0.6%).

Per wind direction:

- N: residences, Ashfield Road at 90 m;
- E: residential gardens;
- S: Holmfield Road at 90 m;
- W: London Road at 190 m.

Figure 15: Detail of the location of site LE2 (Leicester Brookfield).


Figure 16: Measuring trailer at site LE2 (Leicester Brookfield).

1.4 Lille-Fives (LL1, Lille, France)

The Joaquin sampling site in Lille is an urban background site that is part of the air quality monitoring network of atmo Nord-Pas-de-Calais. The station is located in Lille-Fives (Figure 17).

Website information:
http://www.atmo-npdc.fr/mesures-et-previsions/mesures-en-direct/carte-d-identite-des-stations.html

Site LL1 is set on the campus of a school (Groupe Scolaire Lakanal). The nearest road is at 35 m (rue du Vieux Moulin). This is a local street with 2x1 lanes that is located east, south-east and south of the site. No traffic data is available for this street.

Per wind direction
- N and E: one-storey building (Figure 18);
- E, SE and S: nearest street;
- S and W: grass.

Figure 17: Detail of the location of LL1 (Lille-Fives).

Site LL1 is located ~230 m from a large number of railroads.

Power plants (Figure 19):

- Centrale thermique du Mont de Terre-Resonor (~750 m S);
- Chaufferie de Lille-Hellemmes (~1.5 km E);
- Chaufferie des Beaux-Arts (~1.9 km W);
- Mons Energie (~2.7 km NW).

The Centrale thermique du Mont de Terre-Resonor is a power plant that uses gas and, from time to time, also coal. In 2013 no wood has been used as fuel, there is no declaration for wood burning.

Other industrial sites are (Figure 19):

- Brasserie Heineken de Mons / G Goossens (~ 3 km NE): brewery;
- H2D (~1.1 km E-SE): "surface treatment, mechanics";
- Haghebaert et Fremaux (~2.5 km E-SE): chemicals;
- Technicentre SNCF D'Hellemmes (~1.3 km SE), main activity: surface treatment, mechanics;
- ECL - Electrification Charpente Levage (~2.3 km S);
- LFB Biomédicaments (~1.1 km SW).

A study has been carried out (BASIC study in 2012) on the heating fuels used in the region of Nord-Pas-de-Calais. This study shows that the inhabitants of Lille use more wood as heating fuel than the inhabitants of other large cities in the region (wood use in Lille = 305 kWh/inhabitant).

The report is not public, but the main results can be found in an online presentation:
http://www.observatoire-climat-npdc.org/fr/ressources-documentaires/etude-du-chauffage-dans-la-r%C3%A9gion-nord-pas-de-calais

Figure 18: Measuring station LL1S.

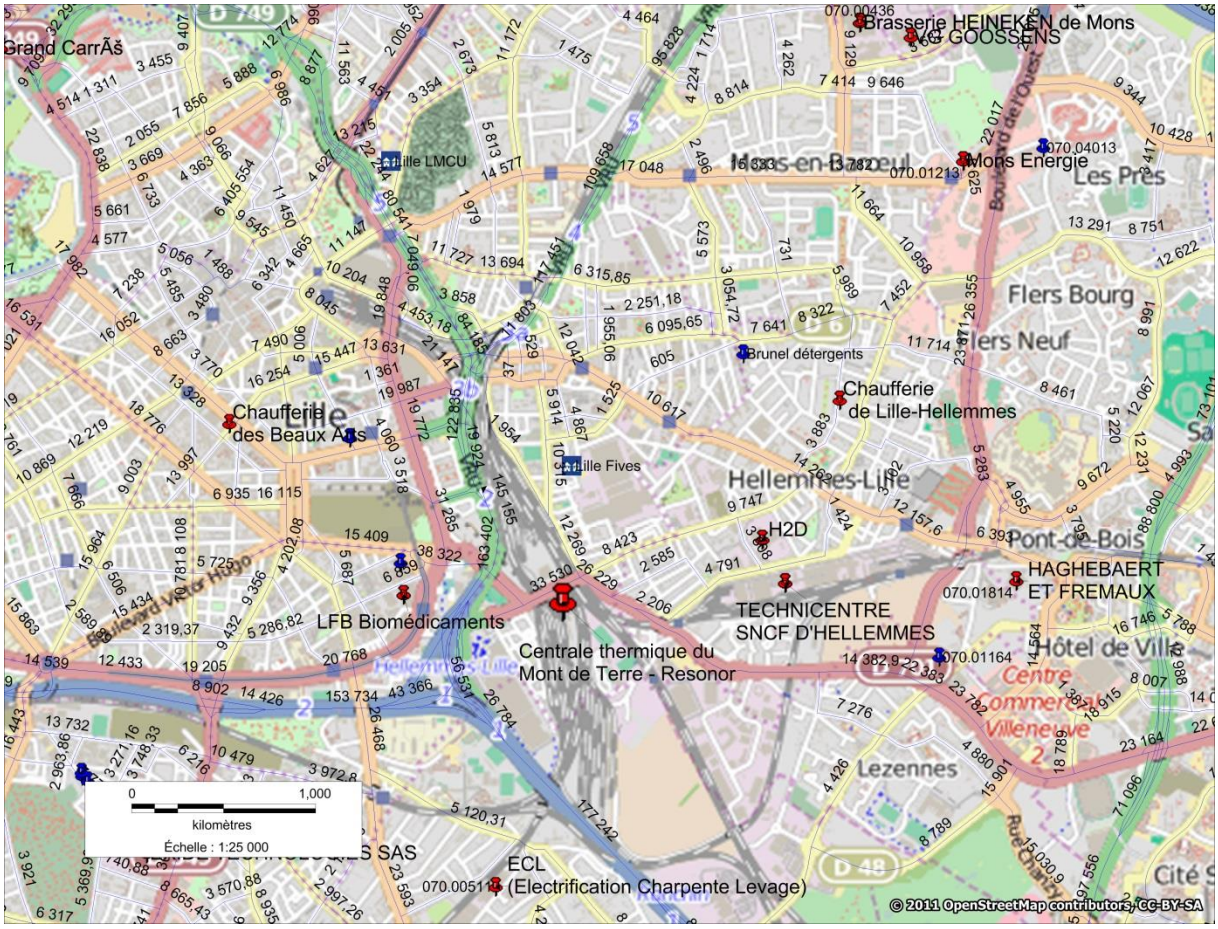

Figure 19: Location of LL1 (blue square "Lille Fives" in the centre of the map) in the city of Lille. Red symbols indicate the location of power plants and industrial sites.

The quarter Lille-Fives is located east from the main city of Lille.

Lille airport is at about 7 km south of site LL1.

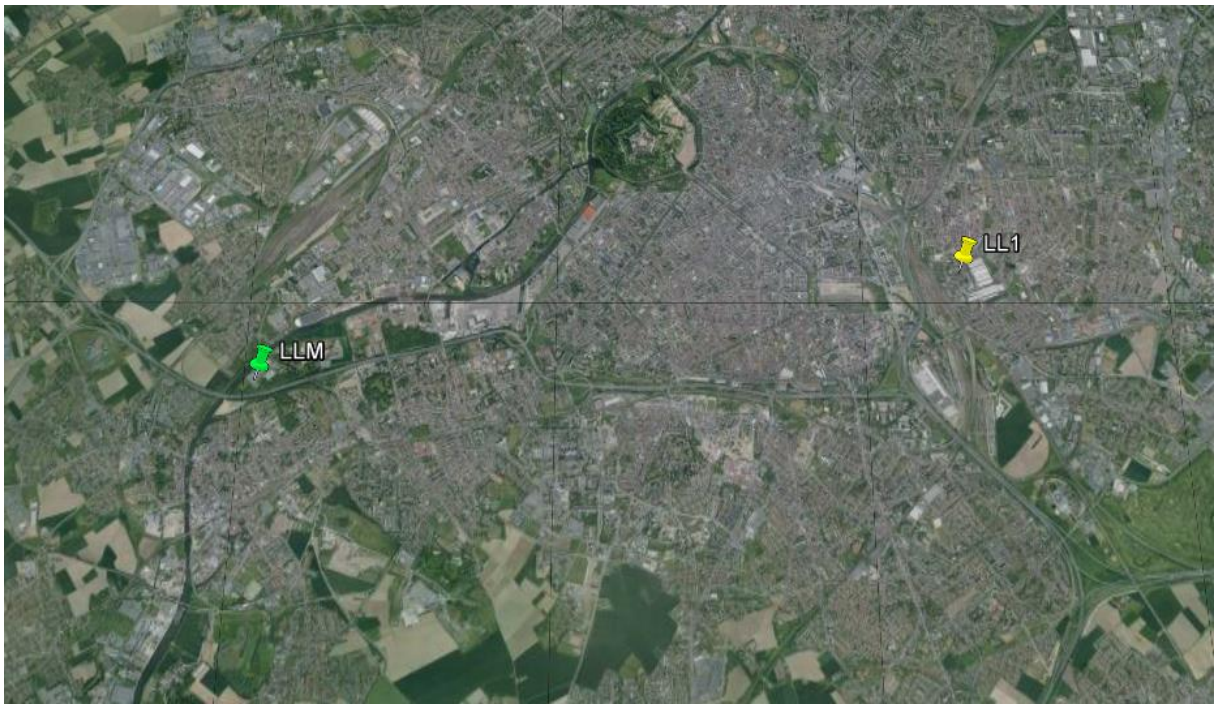

Figure 20: Region of Lille with air quality monitoring site LL1 and meteorological monitoring site LLM (Sequedin).

1.5 Eltham (LO1, London, United Kingdom)

The Joaquin sampling site in London (LO1) is an urban background station that is part of the Defra Air Quality Network. The station is located in Eltham, a suburban district of South East London.

Website information: http://uk-air.defra.gov.uk/networks/site-info?site_id=LON6

Site LO1 is in an existing building on the grounds of an environmental education centre in Eltham (Figure 21). The surroundings consist of a mixture of habitats including trees, areas of grass, ponds, a golf course and housing. The University of Greenwich is opposite the site.

The nearest road (A210 Bexley Road) is approximately 60 m to the south of the site. The A210 is a feeder road into and out of the centre of London and a local high street for the neighbourhood with a lively shopping area.

According to traffic counts by the Department for Transport, the annual traffic intensity on the A210 is about 16500 vehicles/day (mean ± SD = 16414 ± 1205 for 2001-2013; http://www.dft.gov.uk/traffic-counts, count point 36808). The majority of the vehicles are cars and taxis (75%), followed by buses and coaches (10%), light goods vehicles (10%), heavy goods vehicles (2%) and motorcycles (2%).

Per wind direction:
- N and W: trees and grass;
- E: one-storey building (Figure 22);
- S: building, Bexley road at 60 m.

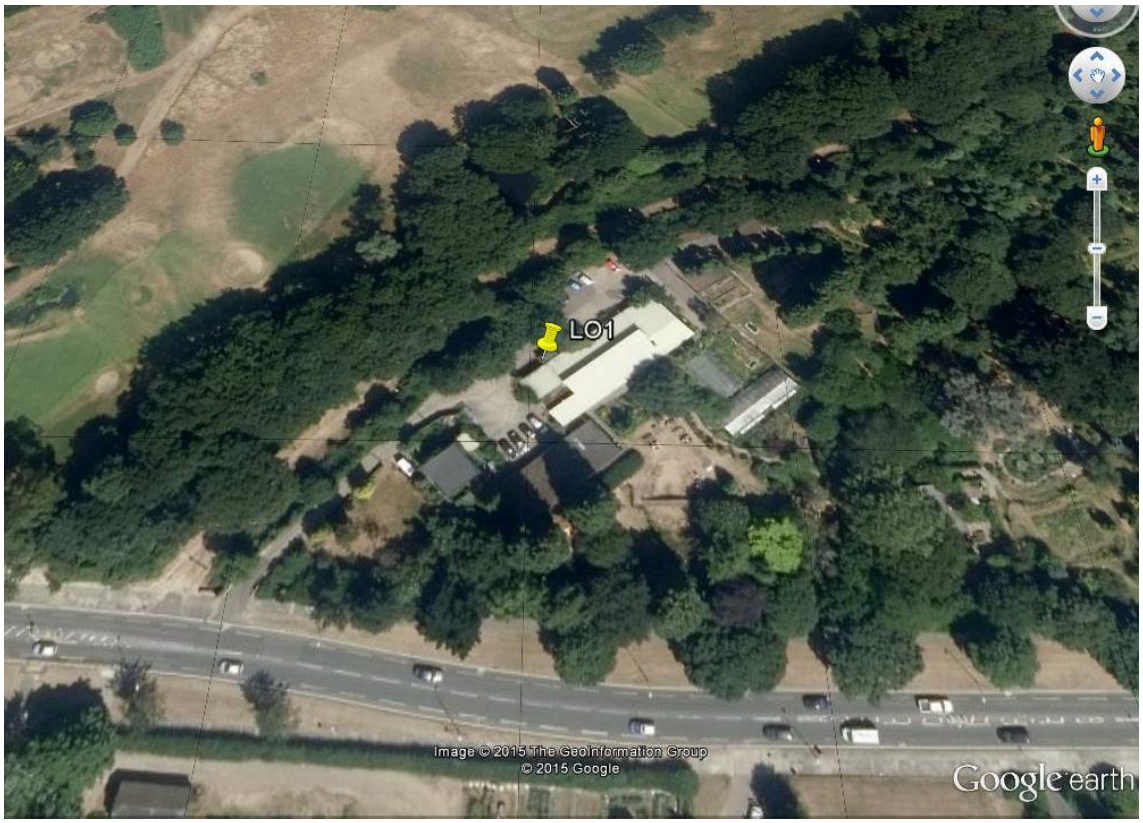

Figure 21: Detail of the location of LO1 (London Eltham).


Figure 22: Measuring station LO1S.

At the urban scale the Highway A2 is about 560 m to the north of LO1 (Figure 23). This is a major route into and out of London from the south east.

For the A2 section near site LO1 the annual traffic intensity is about 77000 vehicles/day (mean ± SD = 76479 ± 6492 for 2001-2013, http://www.dft.gov.uk/traffic-counts, count point 38664). The majority of the vehicles are cars and taxis (75%), followed by light goods vehicles (16%), heavy goods vehicles (6%), motorcycles (3%) and buses and coaches (1%).

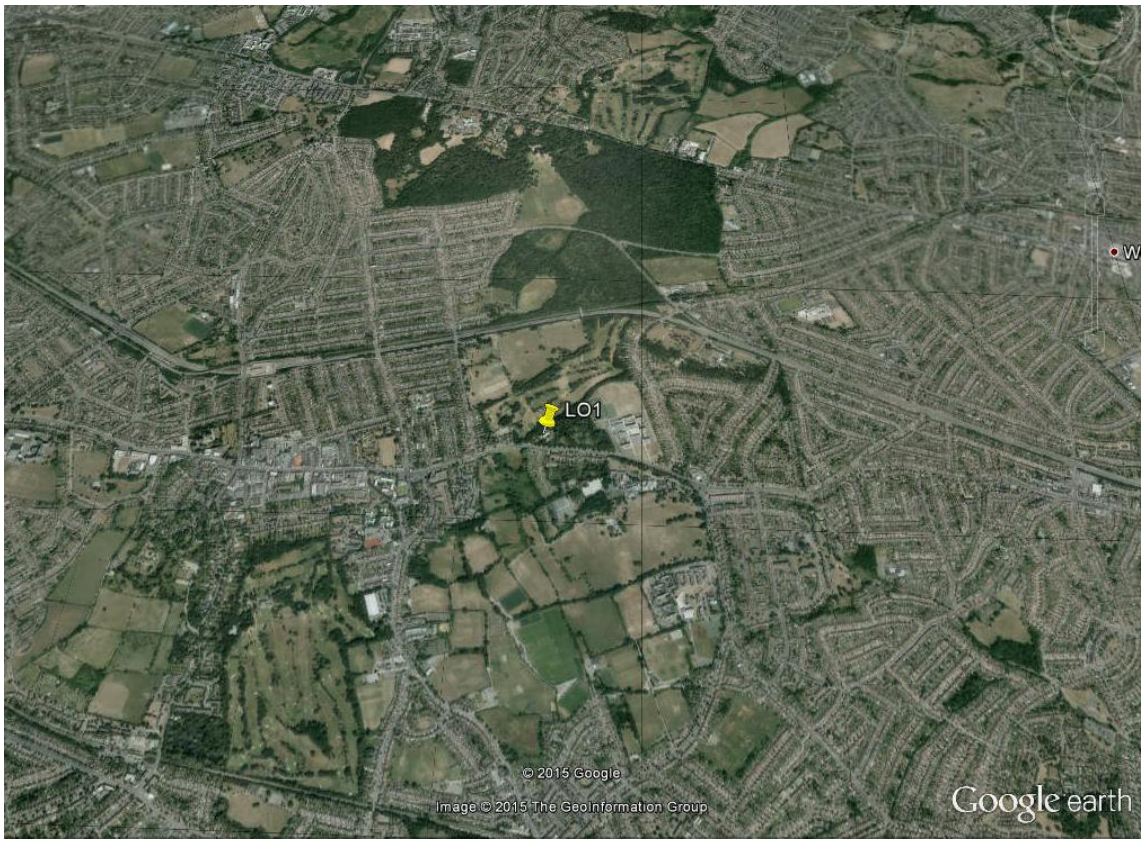

Figure 23: Location of LO1 in Eltham.

Site LO1 is located at approximately 13 km south east from the city centre of London. The A2 and A20 are major route ways into and out of London, while the M25 (motorway) which encircles London is 11 km away at its nearest point. There are two airports in the vicinity, London City airport is 6 km away (north-northeast) while Biggin Hill aerodrome is 14 km away (south). London Heathrow airport is 38 km away (west). There is some industry in the regional area; however the biggest source of pollution will be from transport emissions.

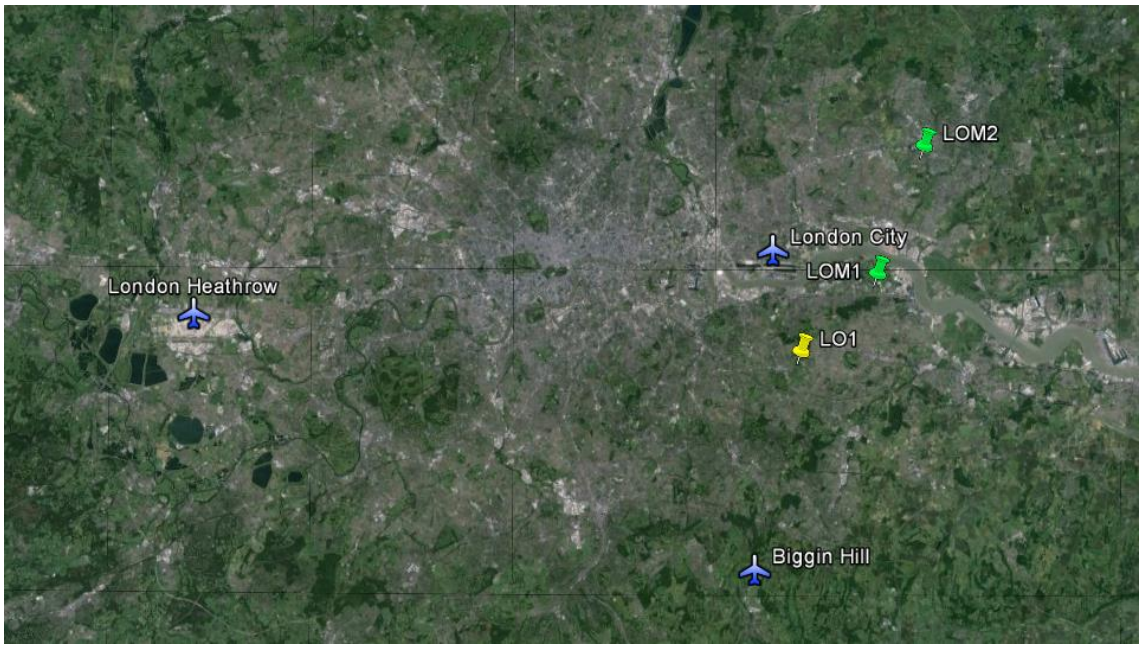

Figure 24: Region of London with air quality monitoring site LO1 (southeast of the city centre), the meteorological monitoring sites LOM1 (Bexley - Belvedere West) and LOM2 (Barking and Dagenham - Rush Green) and the airports of London City, Biggin Hill and London Heathrow.

1.6 Wijk aan Zee (WZ1, the Netherlands)

The Joaquin sampling site in Wijk aan Zee is an industrial monitoring site of Province North Holland. Site WZ1 is located approximately 30 km west from Amsterdam.

Website information: http://www.luchtmetingen.noord-holland.nl/DetailPage.aspx?SID=553

Figure 25: Detail of the location of WZ1 (Wijk aan Zee).


Figure 26: Wijk-aan-Zee measuring station.

Site WZ1 is located at the north side of a parking lot used by visitors of a camping site (Banjaert). Residences of Wijk aan Zee inhabitants are present at a distance of approximately 40 m. The nearest road (Burgemeester Rothestraat) is at a distance of 70-80 m to the south and west. The nearest main road (Verlengde Voorstraat) is at 175 m.

Per wind direction
- N and E: camping area (Banjaert);
- S and W: parking lot and residences (40 m), local road (70-80 m).

The industrial zone of IJmond is located east (750 m) and south (1-2 km) of site WZ1. The main activities in the industrial zone are the production of steel (Tata Steel, south of WZ1) and energy (NUON).

Figure 27: Location of WZ1 in the city of Wijk aan Zee.

Figure 28: IJmond region with air quality monitoring site WZ1, meteorological monitoring site WZM (KNMI IJmuiden) and the industrial harbour area south of WZ1.

Annex 2: Daily-averaged PM concentrations (April 2013 - March 2015)

PM$_{10}$ in monitoring station Amsterdam Vondelpark (AD1S)

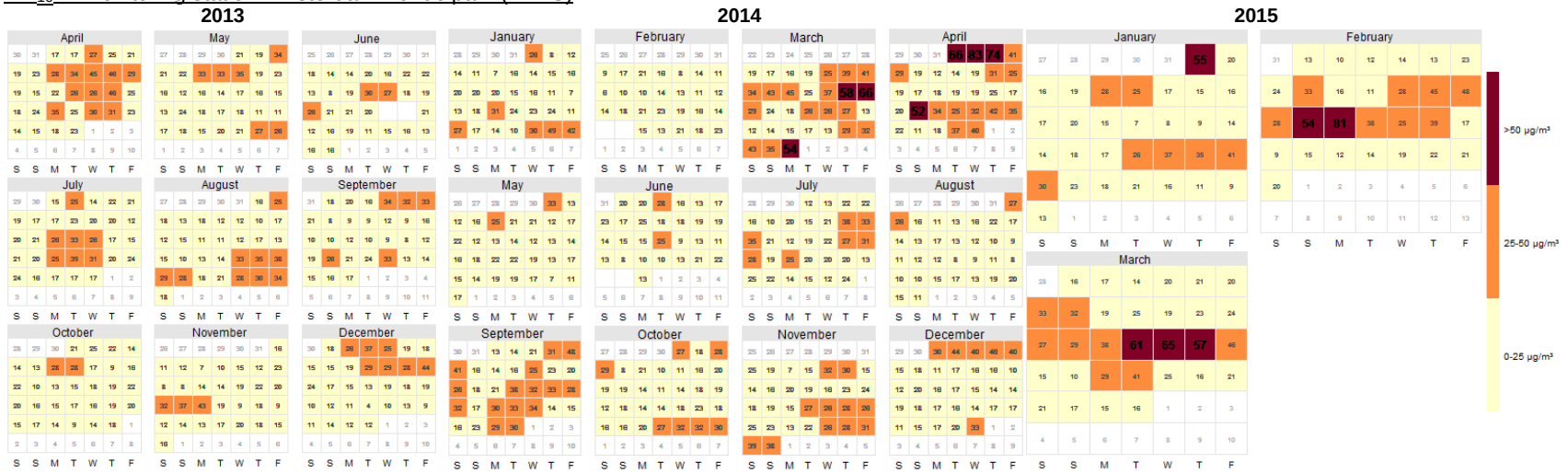

PM$_{10}$ in monitoring station Antwerp Borgerhout (AP1S)

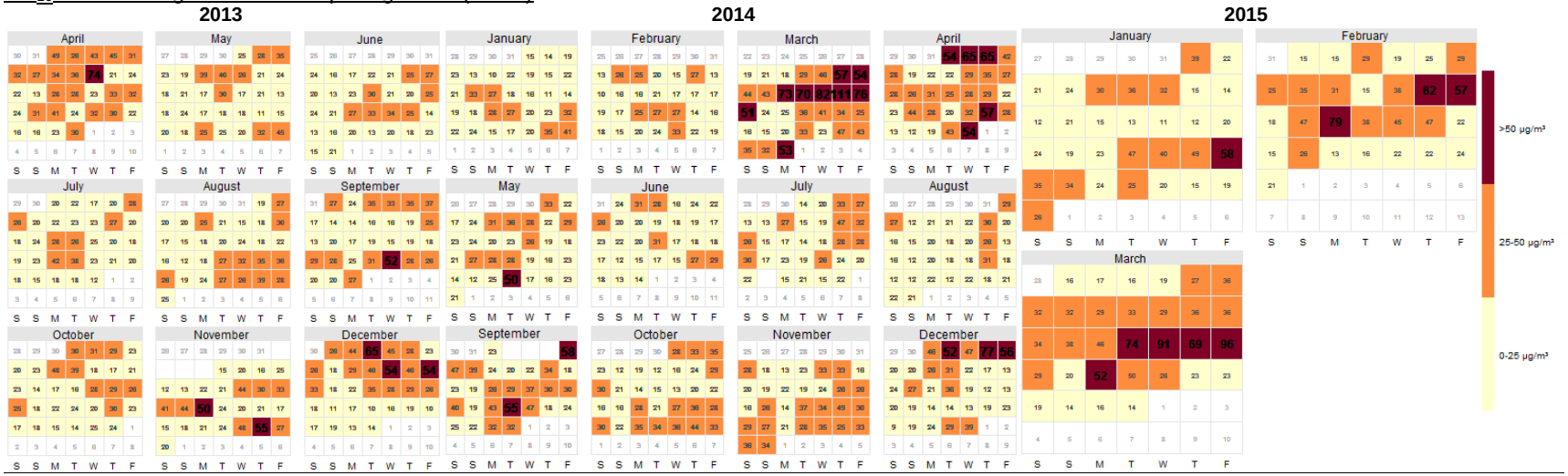

$PM_{2.5}$ in monitoring station Leicester University (LE1S)

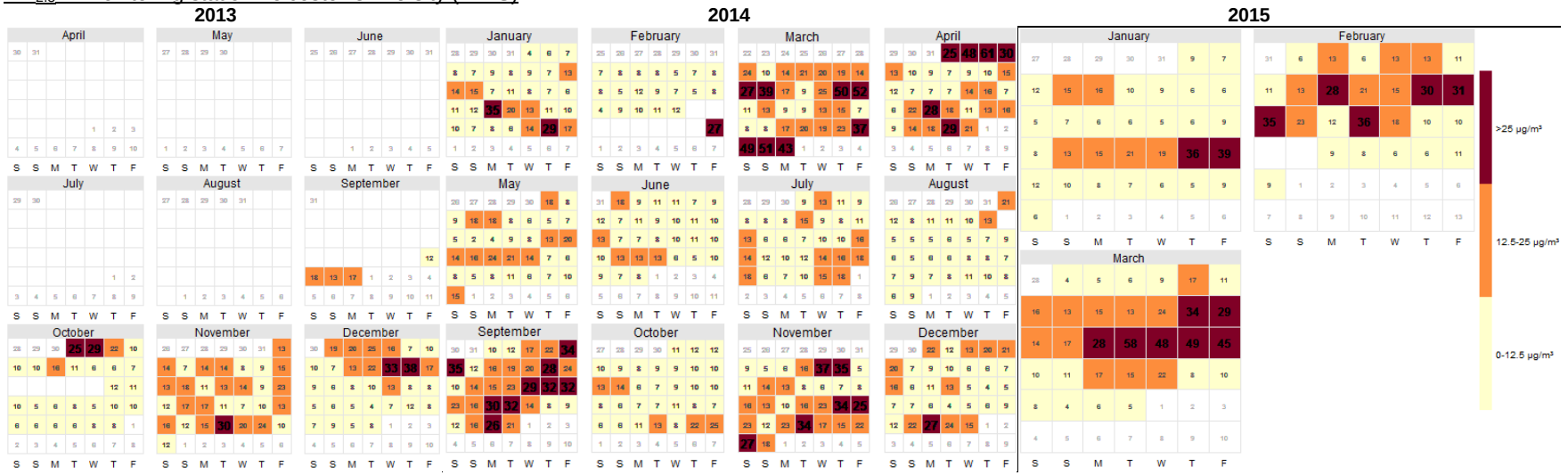

PM_{10} in monitoring station London New Eltham (LO1S)